



University of  
**Salford**  
MANCHESTER

Descaling Petroleum Production Tubing Using Multiple Circular High-  
Pressure Nozzles.

Kabir Hassan Yaradua

School of Science, Engineering and Environment  
University of Salford, Salford, UK

Submitted in Partial Fulfilment of the Requirement of the Degree of Doctor  
of Philosophy, February 2020

# List of Contents

List of Contents .....	ii
List of Figures .....	vii
List of Tables.....	xii
Acknowledgements .....	xiii
Declaration .....	xiv
List of Publications.....	xv
Nomenclature .....	xvi
Abstract .....	xvii
Chapter 1 .....	1
Introduction .....	1
1.1 Preamble .....	1
1.2 Scales problems in oil production .....	2
1.3 Scale control .....	3
1.4 Research problem statement.....	4
1.5 Research motivations.....	6
1.6 Research contributions .....	7
1.7 Research aim.....	7
1.8 Research objectives .....	7
1.9 Structure of the research thesis.....	8
1.9.1 Chapter 1: Introduction .....	8
1.9.2 Chapter 2: Petroleum production challenges .....	8
1.9.3 Chapter 3: Multiple spray characterization.....	9
1.9.4 Chapter 4: Experimental set up.....	9
1.9.5 Chapter 5: Results and discussion.....	10
1.9.6 Chapter 7: Conclusions and recommendations.....	10

Chapter 2 .....	11
Petroleum Production Challenges .....	11
2.1 Overview.....	11
2.1.1 Petroleum production associated problems .....	11
2.1.2 Flow assurance problems in production tubing .....	13
2.2 Kinetics of scale formation.....	14
2.2.1 Factors influencing scale formation.....	19
2.2.2 Scale classifications .....	20
2.2.3 Scale compositional analysis .....	22
2.2.4 Scale chemistry .....	23
2.3 Scale management .....	38
2.3.1 Scale prediction/monitoring.....	39
2.3.2 Scale prevention.....	40
2.3.3 Economics of scale management .....	42
2.4 Scale removal techniques .....	42
2.4.1 Effective descaling operations .....	43
2.5 Chemical descaling method.....	45
2.5.1 Limitations of chemical descaling approach.....	47
2.5.2 Successful chemical descaling operation around the world .....	48
2.5.3 Chelating agent.....	52
2.5.4 Factors effecting chelating agents.....	55
2.6 Mechanical descaling technique .....	56
2.6.1 Types of mechanical descaling techniques .....	57
2.6.2 Successful mechanical descaling operation. ....	61
2.7 Summary .....	67
Chapter 3 .....	68
Jet Spray Dynamics and Mechanism .....	68

3.1	Overview.....	68
3.2	Nozzle performance.....	68
3.2.1	Spray system .....	68
3.2.2	Nozzle characterization.....	69
3.2.3	Spray performance summary .....	73
3.3	Atomization .....	74
3.3.1	Spray jet break up.....	74
3.3.2	Spray characterisations /atomizers.....	78
3.4	Spray analysis .....	85
3.4.1	Drop size .....	86
3.4.2	Drop size distribution (DSD) .....	86
3.4.3	Spray angle.....	91
3.4.4	Droplet velocity.....	92
3.4.5	Spray impact pressure .....	92
3.4.6	Spray pattern .....	93
3.5	Spray jet cleaning .....	96
3.5.1	Mechanism for jetting technique.....	99
3.6	Descaling Operations.....	107
3.6.1	Spray overlap.....	108
3.6.2	Pressure drop (multiple nozzle) .....	109
3.7	Summary.....	109
Chapter 4	.....	111
Experimental Set-up and Procedure	.....	111
4.1	Overview.....	111
Phase One	.....	113
4.2	Descaling rig design and assembly.....	113
4.2.1	Descaling rig assembly .....	113

4.2.2	Descaling chamber design, construction and set up .....	116
4.2.3	Descaling Chamber component .....	117
4.2.4	Scale holder .....	122
4.3	Soft scale production .....	124
4.3.1	Wax moulder design .....	124
4.3.2	Wax scale preparation .....	125
4.4	Scale characterization .....	127
4.4.1	Soft Scale compositional & chemical analysis .....	127
4.4.2	Hard scale compositional & chemical analysis .....	130
4.4.3	Hard scale compositional analysis .....	130
Phase Two .....		134
Descaling Experiment .....		134
4.5	Scale removal experimental design procedure .....	134
4.5.1	Descaling experiment preparations .....	135
4.5.2	Experimental procedures for scale removal.....	139
4.5.3	Safety precaution measure .....	144
4.5.4	Source of errors in the scale removal test .....	144
4.5.5	Scale removal error mitigation measures.....	145
4.5.6	Experimental error analysis.....	145
4.6	Summary .....	147
Chapter 5 .....		149
Results and Discussion.....		149
5.1	Overview.....	149
PHASE 1 .....		150
Pre-descaling Experiment .....		150
5.2	Scale characterization .....	150
5.2.1	Chemical/compositional analysis.....	150

5.2.2	Soft scale compositional & chemical analysis.....	150
5.2.3	Hard Scale compositional & chemical analysis.....	153
PHASE TWO	.....	157
Descaling Experiment	.....	157
5.3	Scale removal experiment .....	157
5.3.1	Ambient decaling experiment .....	157
5.3.2	Compressed descaling experiments .....	167
5.3.3	Vacuum descaling trials .....	176
5.3.4	Chamber pressure comparison .....	186
5.3.5	Optimum descaling requirement.....	195
5.3.6	Summary .....	206
Chapter 6	.....	207
Conclusion and Recommendations	.....	207
6.1	Conclusions.....	207
6.2	Recommendations.....	209
Reference	.....	210
Appendices	.....	217
Appendix A	.....	217
APPENDIX B	.....	225
APPENDIX C	.....	226
APPENDIX D	.....	239
APPENDIX E	.....	242

# List of Figures

<b>Figure 2.1:</b> Scale deposit (a) in production tubing, (b) schematics of scale inflicted production tubing by (Slumberger, 2013).....	14
<b>Figure 2.2:</b> Calcium carbonate deposit (a) in production tubing, (b) SEM image (Okocha et al 2014) .....	25
<b>Figure 2.3:</b> Effect of temperature to different types of calcium Carbonate (Guan H. et al 2015) .....	25
<b>Figure 2.4:</b> Calcium sulphate deposit (a) in production tubing, (b) SEM images (Esbai et al., 2016).....	27
<b>Figure 2.5:</b> Effect of Temperature on solubility of CaSO <sub>4</sub> (Johnson et al. 1999) ...	28
<b>Figure 2.6:</b> Barium Sulphide deposit (a) in production tubing, (b) SEM images (Meeham, 2010) .....	28
<b>Figure 2.7:</b> Effect of Temperature on solubility of Barium Sulphate (Meehan 2010). .....	29
<b>Figure 2.8:</b> Strontium sulphide deposit (a) in production tubing, (b) SEM Images (Al Mubarak et al, 2017) .....	30
<b>Figure 2.9:</b> Iron sulphide deposit (a) in production tubing, (b)SEM Images (Mahmoud et al., 2015) .....	32
<b>Figure 2.10:</b> Scale deposit composition in X Sour Gas (a),(b) stability of various iron Sulphide in respect to pH (Al-Bauli et al. 2015).....	34
<b>Figure 2.11:</b> Chemical structures of common aminopolycarboxylic acids (Almubarak et al., 2017) .....	55
<b>Figure 3.1</b> Specific gravity versus conversion factor graph (Spraying system 2015) .....	70
<b>Figure 3.2:</b> Spray angle Vs spray coverage (BETE 2018).....	71
<b>Figure 3.3:</b> Atomization (droplet size and distribution) (Spraying system 2015) ...	72
<b>Figure 3.4:</b> Sheet disintegration breaks up proposed by (Dombrowski et al. 1962)	74
<b>Figure 3.5:</b> Forces acting along spray jet (Rajendran et al. 2012). .....	75
<b>Figure 3.6:</b> Break-up length behaviour of liquid jet (Arai et al., 1995).....	76
<b>Figure 3.7:</b> Liquid atomisation mechanisms (Liu H 2000).....	76
<b>Figure 3.8:</b> Classification of atomisers (Yule &Dunkley 1994 ; Abuhesa M . 2010). .....	79

<b>Figure 3.9:</b> spill returns atomiser (BETE 2018).....	81
<b>Figure 3.10:</b> Hollow Cone Atomiser spray (BETE, 2014) .....	82
<b>Figure 3.11:</b> Full cone Atomiser spray (BETE 2018).....	83
<b>Figure 3.12:</b> Flat Spray Pattern atomiser (BET 2014) .....	84
<b>Figure 3.13:</b> Flat Spray Atomiser.....	85
<b>Figure 3.14:</b> Typical drop size distribution (Nasr et al. 2002).....	87
<b>Figure 3.15:</b> Drop size bars based on number and volume (Lefbvre 1989) .....	87
<b>Figure 3.16:</b> Usual drop size frequency distribution curves (number and volume)	88
<b>Figure 3.17:</b> Usual shape of cumulative drop size.....	88
<b>Figure 3.18:</b> Particle distribution median, mode and mean (Malvern instrument limited 2015) .....	89
<b>Figure 3.19:</b> Relative drop sizes by nozzle series (Spraying System 2017).....	91
<b>Figure 3.20:</b> Spray angle (Naber et al 1996).....	91
<b>Figure 3.21:</b> Spray impact pressure (Naber et al 1996) .....	92
<b>Figure 3.22:</b> Scale deposit in a production tubing .....	96
Figure 3.23: Schlumberger Jetting Technique (Schlumberger 2013).....	97
<b>Figure 3.24:</b> Classification of cavitation (Lauterborn 1980) .....	103
<b>Figure 3.25:</b> Cavitation regimes along Francis turbine (Brennen., 1995) .....	103
<b>Figure 3.26:</b> Light emitted by a trapped cavitation bubble (Zhang Y 2013).....	104
<b>Figure 3.27:</b> Electro optic shock created by laser plasma (D.F Gardon 2008).....	104
<b>Figure 3.28:</b> particle cavitation (DFD 2015).....	105
<b>Figure 3.29:</b> Typical flows through a nozzle (Martynov et al. 2006).....	106
<b>Figure 3.30 :</b> Arrangement of nozzles on descaling header (spray overlap) (Nasr et al 2002).....	108
<b>Figure 3.31:</b> Nozzle pressure difference Vs flow rates of different numbers of nozzles (Tian, Li, Huang, Niu, & Xia, 2009).....	109
<b>Figure 4.1:</b> Descaling rig components, (a) Compressed air system, (b) Vacuum pump & (c) high pressure water pump.....	113

<b>Figure 4.2:</b> Picture of the assembled control board .....	114
<b>Figure 4.3:</b> Descaling rig set-up .....	115
<b>Figure 4.4:</b> Design of the chamber .....	116
<b>Figure 4.5:</b> Interior section .....	116
<b>Figure 4.6:</b> metal plate (a) 3D image and (b) picture with O ring seal .....	117
<b>Figure 4.7:</b> (a) Top plate (outside view) (b) Bottom plate (inside view) and (c) Assembled views of metallic top cover .....	118
<b>Figure 4.8:</b> Scale sample assembly (without chamber tube) .....	118
<b>Figure 4.9:</b> Multiple nozzle header, (a) picture, (b) operational cross-section.....	121
<b>Figure 4.10:</b> High-pressure nozzle, (a) picture, (b) operational cross-section.....	121
<b>Figure 4.11:</b> Assemble nozzle header, (a) Arial & (b)side view.....	121
<b>Figure 4.12:</b> Scale holder (a) & (b) component and (c) assembly .....	122
<b>Figure 4.13:</b> Complete assembled descaling rig. ....	123
<b>Figure 4.14:</b> 3D Pictures of wax moulder (a) component and (b) assembled.....	124
<b>Figure 4.15:</b> Prepared wax scale samples preparation and after cooling.....	126
<b>Figure 4.16:</b> Constructed soft scale (a) hollow shape, (b) solid shaped samples ..	127
<b>Figure 4.17:</b> Thermo Scientific Nicolet iS10 Fourier-transform infrared spectroscopy (a) ATR sample drop window (b) complete FTIR system .....	129
<b>Figure 4.18:</b> Hard Scale samples (a) CaCO <sub>3</sub> , (b) SrSO <sub>4</sub> .....	130
<b>Figure 4.19:</b> Experimental design process .....	134
<b>Figure 4.20:</b> Scale deposits .....	136
<b>Figure 4.21:</b> Stand-off distance arrangement .....	137
<b>Figure 4.22:</b> Header and nozzles configurations.....	138
<b>Figure 5.1:</b> NMR result of soft scale sample .....	151
<b>Figure 5.2:</b> Infrared analysis compared to paraffin flakes from NIST data base ..	152
<b>Figure 5.3:</b> Infrared analysis compared to liquid paraffin .....	152
<b>Figure 5.4:</b> SEM Results of Sample A at (a) 1 mn, (b) 40 μm and (c) 100 μm magnifications .....	153

<b>Figure 5.5:</b> SEM Results of Sample B at (a) 1 mn, (b) 30 $\mu\text{m}$ , (c) 40 $\mu\text{m}$ and (d) 100 $\mu\text{m}$ , magnifications.....	153
<b>Figure 5.6:</b> EDX Result Sample A at (a) 0.1, (b) 0.2 spectrums .....	154
<b>Figure 5.7:</b> EDX Result for Sample B at (a) 0.1 (b) 0.2, (c) 0.3 spectrums .....	155
<b>Figure 5.8:</b> XRD result Sample A.....	156
<b>Figure 5.9:</b> XRD results sample B .....	156
<b>Figure 5.10:</b> Ambient descaling results for hollow soft scale at 25mm-distance..	160
<b>Figure 5.11:</b> Ambient descaling results for solid soft scale at 25mm-distance ....	162
<b>Figure 5.12:</b> Ambient descaling results for $\text{SrSO}_4$ scale deposit at 25mm-distance .....	164
<b>Figure 5.13:</b> Ambient descaling results for $\text{CaCO}_3$ scale deposit at 25mm-distance .....	166
<b>Figure 5.14:</b> Compressed descaling results for hollow soft scale at 25mm-distance .....	169
<b>Figure 5.15:</b> Compressed descaling results for hollow soft scale at 25mm-distance .....	171
<b>Figure 5.16:</b> Compressed descaling results for $\text{SrSO}_4$ scale deposit at 25mm-distance .....	173
<b>Figure 5.17:</b> Compressed descaling results for $\text{CaCO}_3$ scale at deposit 25mm-distance .....	175
<b>Figure 5.18:</b> Vacuumed descaling results for hollow soft scale at 25mm-distance .....	178
<b>Figure 5.19:</b> Vacuumed descaling results for solid soft scale at 25mm-distance..	181
<b>Figure 5.20:</b> Vacuumed descaling results $\text{SrSO}_4$ scale deposit at 25mm-distance	183
<b>Figure 5.21:</b> Vacuumed descaling results for $\text{CaCO}_3$ scale deposits at 25mm-distance .....	185
<b>Figure 5.22:</b> Chamber pressure impact comprising for descaling hollow soft scale at 25mm-distance .....	188
<b>Figure 5.23:</b> Chamber pressure impact comprising for descaling solid soft scale at 25mm-distance .....	190
<b>Figure 5.24:</b> Chamber pressure impact comprising for descaling $\text{SrSO}_4$ scale deposit at 25mm-distance .....	192

**Figure 5.25:** Chamber pressure impact comprising for descaling  $\text{CaCO}_3$  scale deposit at 25mm-distance ..... 194

**Figure 5.26:** Descaling impact of non-hydro-connected parameters for respective deposits..... 198

**Figure 5.27:** Descaling impact of hydro-connected parameters for respective deposits ..... 201

**Figure 5.28:** Descaling impact of chamber pressure and its efficiency for respective deposits..... 204

## List of Tables

<b>Table 2.1:</b> Summary of Scale chemistry .....	35
<b>Table 2.2:</b> Pre and post descaling results of the six wells (Ramones et al., 2015) ..	50
<b>Table 2.3:</b> Pre and Post Descaling results of Kuff well(Mirza et al., 1999) .....	51
<b>Table 2.4:</b> Pre and Post Descaling Results for five Kuff Gas wells (Bolarinwa et al., 2012).....	63
<b>Table 2.5:</b> Pre-and post-descaling result of field (EW 873) Golf of Mexico (Clameto et al. 2003).....	65
<b>Table 2.6:</b> Post descaling and simulation result of Ghwar field (Alabdulmohsin et al., 2016).....	66
<b>Table 3.1 :</b> Spray Performance Summary .....	73
<b>Table 3.2:</b> Mean diameters across and their applications (Nasr et al. 2002) .....	89
<b>Table 4.1:</b> Error analysis of 3 nozzles ambient descaling results .....	146
<b>Table 4.2:</b> Error analysis of 3 nozzles compressed descaling results .....	146
<b>Table 4.3:</b> Error analysis of 3 nozzles vacuumed descaling results.....	147
<b>Table 5.1:</b> Multiple High-Pressure Circular Nozzle Descaling Operations Guide	205

# Acknowledgements

I would like to use this medium to express my deep gratitude to Almighty Allah for the gift of life, faith, strength and health. To my parent (Hafsat & Kabir Yaradua) for their everlasting and unconditional support including Mr Bello Yusuf and my subliming's Mohammed, Bello, Umar, Fatima, Hafsat, Aisha and Zainab Kabir. Also, to my lovely wife and child (Zainab-Abu & Bello-Ammar) that contributed physically and spiritually tremendously toward realising this dream. It will not be possible to finish this program without the support of my very best friend and Supervisor Dr. Abuabakar Abbas who have been there for me for long and my Co-supervisor Dr Amir Nuorian for his eminent support. So also, our wonderful research team of Prof G.G Nasir, Dr Godpower Enyi, Dr Martins Bubby, Dr. Babbaie Mesiam, and Mr Mapins Alans for bringing out the best out of me. Most importantly to Petroleum Technology Development Fund (**PTDF**) and their staffs especially Mr Ahmed Galadima and Mr Bako for sponsoring this PhD program.

I wish to express my heartfelt gratitude to my friends and colleagues, most especially Engr. Ahmadu Abdullahi, Engr Salihu Maiwalimah, Dr. Mohammed Abba, Engr Shehu Ushau, Mr Chalasani Kiran, Dr Aminu Abba and Yusuf Bashir for their marvellous contribution toward putting this Thesis together. To my MSC research members like Engr Joyce, Jose, John and Hamid for their patience and contributions during the experiment hard times. In addition to, Dr Umar Ilyas, Mr Farooq Bello, Mr Hamis Bichi, Mubarak Aliyu, Abdullatif Yusuf, Farooq Idris, Abubakar Ibrahim and Sadiq Abdallah for their calls and prayers that made me feel at home despite the geographical distance between us during the duration of this programme. Last but not the list is all those that were there for me knowingly and unknowingly for their encouragement and guidance throughout the period of this research and during the preparation of this thesis.

# Declaration

I, Kabir Hassan Yaradua, declare that this dissertation report is my original work, and has not been submitted elsewhere for any award. Any section, part or phrasing that has been used or copied from other literature or documents copied has been clearly referenced at the point of use as well as in the reference section of the thesis work.

.....

Signature

.....

Date

.....

.....

Approved by

Dr. Abubakar Abbas  
(Supervisor)

.....

Signature

.....

Date

.....

.....

Approved by

Dr. Amir Nourian  
(CO-Supervisor)

# List of Publications

1. K. H. Yaradua, A. Abbas, A Nourian (2020) Experimental removal of paraffin scale from petroleum production tubing using multiple high-pressure spray., *ILASS 2019 Conference* (Submitted)
2. K. H. Yaradua, A. Abbas, A Nourian (2020) Investigating the effect of varying tubing air concentration during the descaling petroleum production tubing using multiple high-pressure nozzles *Journal of Petroleum Engineering* (Submitted)
3. K. H. Yaradua, A Abbas, A Norian, (2020) Determining the optimum descaling requirement for decaling of production tubing effected by different types of scale using multiple high-pressure spray, *Journal of Petroleum Engineering* (on Progress)
4. K. H. Yaradua , A Nourian A Abbas, A Norian, S. Maiwalima (2020) Investigating the impact of non-hydrodynamic connected descaling parameters (Nozzle configuration & Stand-off distance) in removing different stages of scale deposits from petroleum production tubing with multiple high-pressure spray, *Journal of Petroleum Engineering* (on Progress)
5. K. H. Yaradua, A Abbas, A Norian, S. Maiwalima, I.John (2020) Investigating the impact of hydrodynamic connected descaling parameters (injection pressure and number of nozzles) in removing different stages of scale deposit from petroleum production tubing with multiple high-pressure spray, *Journal of Petroleum Engineering* (on Progress)
6. K. H. Yaradua A Abbas, A Norian, A.Ahmadu(2020) Characterization and Mimicking of paraffin scale deposit from household candle wax *Journal of Petroleum Engineering* (on Progress)
7. H.Bashir, S. Maiwalimah, K S. Maiwalima, K Hassan (2020) Experimental Analysis of Methane Adsorption Potential in Cored Clay-Rich Sandstones., *Adsorption Science and Technology ADT-19-0136* (Under Review)
8. S. Maiwalimah, A Abbas, S. Maiwalima, K, Hassan (2019) Effect of temperature and salt concentration on rheological behaviour of surfactants *SPE-NAICE 2019 Conference*
9. K. H. Yaradua A. Abbas, A Nourian (2019) Determining the Efficiency of Using Multiple High-Pressure Nozzles in Removing Different Types of Scale Deposit from Production Tubing *SPARC-2019 Conference*
10. K. H. Yaradua, A. Abbas, A Nourian Petroleum production enhancement solutions *SPARC -2018 Conference*

# Nomenclature

$\sigma$	Surface tension, kg/ s <sup>2</sup>
A	Surface area(m <sup>2</sup> )
$\pi$	3.14
U	velocity, m/s
D <sub>2</sub>	droplet diameter
$\rho$	liquid density, kg/ m <sup>3</sup>
t	Time [sec]
F	Force
l/min	Litres per minute
$\delta_i$	Middle diameter of droplet sizes in range (m)
$f_D$	Doppler frequency
R	Radius
Re	Reynolds number (= $\rho_L U_o d_o / \mu_L$ )
D	Droplet diameter ( $\mu\text{m}$ )
$\chi$	Downstream distance (mm)
P	Pressure (MPa)
O	Orifice diameter (mm)
Q	Liquid volume flow rate (l/min)
$\nu$	Liquid viscosity
$\theta$	Angle of spray (degrees)
$\lambda$	Wavelength (m)
d	Droplet
M	Mass
D <sub>30</sub>	Volume mean diameter ( $\mu\text{m}$ )
D <sub>20</sub>	Surface mean diameter ( $\mu\text{m}$ )
D <sub>32</sub>	Sauter Mean Diameter (SMD) ( $\mu\text{m}$ )
PDA	Phase Doppler Anemometry
LDA	Laser Doppler Anemometry
RR	Rosin Rammler
Nu	Nusselt Number
Gr	Grashof Number
CFD	Computational Fluid Dynamics
n	Constant
MIC	Minimum Inhibition Concentration
CTU	Coiled Tubing Unit
NCN	Non-Centre Nozzle Arrangement
CN	Centre Nozzle Arrangement
CNO	Centre Nozzle Overlap Arrangement
HWP	High Pressure Water Pump
ESPS	Electric Submersible Pump System
WO	Rig Workover
Capex	Capital expenditure
Opex	Operational expenditure
SEM	Scanning Electron Microscope
EDs	Energy Dispersive X-ray Analysis
XRD	X-ray Diffraction Technique
FTIR	Fourier-Transform Infrared Spectroscopy
NMR	Nuclear Magnetic Spectroscopy

# Abstract

The mechanical approach of utilizing high-pressure water for scale removal has gained wider acceptance by multinational despite facing poor downhole performance challenges (cavitation) that need abrasion compensation (sand). Although sand particles have side effect of jeopardize the integrity of the well completion. Replacement of sand with steaming beads was excellent with good post descaling well completion integrity at the expense of environmental complexity. While the recent single nozzle, solid free aerated jetting descaling technique was characterised with poor scale coverage and high descaling time.

This novel experimental scale removal technique utilises multiple high-pressure spray of up to 10MPa and low flow rate of 12 l/m from multiple flat fan nozzles of different arrangement and stand-off distance. Housed in a constructed simulated production tubing chamber with vacuum and compression capacities to remove hard scale deposits of  $\text{SrSO}_4$  and  $\text{CaCO}_3$ . In addition to the constructed wax deposit (paraffin) of different shapes signifying different growth stages of paraffin in production tubing.

Generally, the performance of each or combination of the descaling parameters during the experiment depends on the shape and type of the scale deposit in question, most especially the chamber air concentration and nozzles arrangements. Also, the amount removed of all the respective scale deposit was found to increase with increase in injection pressure and reduction in number of nozzles. Likewise, the effect of stand-off distance toward the erosion rate of all the four respective descaling candidates was found to reduce with increase in downhole jetting position from 25mm to 50mm and 75mm, even though could be compensated with the right choice of nozzles arrangement.

Injecting at 10 MPa with 5nozzles combination at ambient air concentration removed 49g, 32g, 3.2g & 1.8g of paraffin of hollow & solid shape,  $\text{SrSO}_4$  &  $\text{CaCO}_3$  deposits respectively, that cumulatively increases by a factor 1.6 after altering the nozzle configuration to 4nozzles. Subsequently reducing the numbers of nozzles to 3nozzles further increase the initial cumulative removal by a factor of 4.3 across the respective deposits at 25mm stand-off distance. Also utilising 3nozzles configuration at ambient chamber pressure removed 43g, 5.2g, 2g, & 1.7g of the respective deposits at 4.8 MPa injection pressure that cumulatively increased by a factor of 2 after throttling further to 6.0 MPa injection pressure. Further increasing the injection pressure to 10 MPa cumulatively increase the initial removal of the respective deposits by a factor of 7.2.

While nozzle configuration (header arrangement) that depends on the size and shape of the sample, was found to remove 7% & 13% with CN arrangement more than CN and CNO configuration when descaling hollow shape scale at the best of other parameters in ambient condition. Whereas removing of solid,  $\text{SrSO}_4$  and  $\text{CaCO}_3$  deposit respectively, the CN arrangement removed 6%, 4% & 0.1%, more than the CNO arrangement and 0.08% & 0.1%, 0.02% more than NCN arrangement under the same descaling conditions.

Varying the tubing air concentration from ambient to compressed and later vacuum was found to have direct impact on the resultant spray impact and aids erosion and hoops stress for the first condition. In addition to cyclin stress & abrasion for the second and cavitation jetting mechanism for the last air concentration. Likewise, 254g, 104g, 6.5g & 4.4g of the respective deposits was removed at ambient chamber pressure at optimised descaling parameters that as a result of introducing 0.2 MPa compressed air into the chamber increases by a factor of 1.5. Impressively, a better cumulative removal factor of 1.7 across all the respective deposits was archived after suction the chamber by -0.08 MPa.

Prior to the descaling experiment some descaling preparational experiment of chemical and compositional analysis of the hard scale samples were conducted through the combination SEM, EDX and XRD and found to be  $\text{CaCO}_3$  &  $\text{SrSO}_4$  deposit respectively. While the constructed soft scale sample were confirmed to be paraffin through NMR & FITR analysis.

# Chapter 1

## Introduction

### 1.1 Preamble

Flow assurance is one of the most vital economic features of crude production. Define as the ability to economically produce petroleum product up to the top surface production /processing facility from the reservoir during the lifetime of an oil field (Jordan, Sjuraether, Collins, Feasey, & Emmons, 2001), with scale control as its integral pillar. Up to date, scale deposit in production tubing's remain the most troublesome flow assurance problem throughout the production life of a well. Scale deposition hinder flow assurance not only by dramatically declining oil production rate but by limiting well accessibility for well integrity and performance programs (Alabdulmohsin, El-zefzafy, Al-malki, Al-mulhim, & Ali, 2016). All well flow channels from reservoir, wellbore & near-well bore, downhole & downhole equipment, production tubular, wellhead to topside production. Including processing facilities (e.g. pump, separators, heat exchangers, etc.) are prone to scale deposit when in contact with water during water production from the field (Guan, 2015). These possess a stargedic challenges to to acheiveing global energy security.

Among the few to mention of noticeable oilfield around the world that have recorded scale problems are: *Kuff* Gas well in Bahrain that exhibit scale deposit problem 7,000 inch from the tubing lower section and production casing down to the perforation intervals. Limiting its flow assurance by reducing wellbore accessibility and well deliverability (Mirza, Prasad, & Company, 1999). In addition to surface production/processing facilities suffering erosion damages from produce scale particle encountered due to the scale problems. Another case can be that of *Fadhili* wells with an average daily gross production rate of 1500 BOPD and over 90% water cut, which was halved by production within four month (Esbaei et al., 2016). This was due to calcium carbonate scale deposited along the tubing and other flow line, approximately a 20 to 30 BOPD drop per well. Operator data from North Sea shows almost 75% had been plugged by scale and/or fines combination (Jordan et al. 2001) . The results of the plugging frequency of the Statoil data is 0.02 in per well-year suggested relationship between failure due to (scale and/or fines) plugging and the number of well-years, to be mostly caused by scale problems.

Scale cases can be instantaneous such as that of North Sea *Miller* field, were a 30,000 barrels of oil per day (BOPD) production capacity well was halted to zero production capacity due to scale growth with 24 hours (Brown 1998). Likewise, scale problem has been proven to be one of the reasons *Statjord* Oil field in North Sea operated by Statoil oil has fallen below the production decline curve, with 60% of its stock tank original oil in place (STOOIP) recovered via secondary recovery techniques for the past 23

year (Børeng, Skinnemoen, Vigen, Vikane, Andrews, Asa, & Hauptmann 2002). Consequently, leaving composite distributions of circumvented oil reserves, water and gas.

## 1.2 Scales problems in oil production

Petroleum reservoir formation are made up of different type of salt originating from different source with different fluid constituent naturally forming together with oil and gas in same reservoir environs. Though difficult to quarantine but can rather be identify and mitigated. Effects like nucleation in reservoir downhole completion equipment, production tubing, casing and surface production/processing equipment can be mitigated.

This unfortunate petroleum problem affecting large oil fields in North Sea, Canada, Saudi Arabia and the rest. Threatened flow assurance by creating high pressure drop along the tubing due to reduction in tubing flow cross section area that can instantaneously reduce or even halt production to zero if care is not taken.

However, among the available oil recovery techniques (water injection) found to be effective in agitating reservoir suffering from production decline but related to side effect of water incompatibility problems. Usually when injection water (sea water is rich in carbonate and sulphate ions) mix with produce water (rich in barium, magnesium, calcium etc. depending on type of formation). This leads to the precipitation of various type of scales such as  $BaSO_4$ ,  $MgSO_4$ ,  $CaSO_4$ , etc. Although many scholars such as (Ahmad, 2006) believe to some extent during water injection scale formation can simply be due to reaction of fresh water, formation and the mineral in the rock creating mineral deposit in produce water.

Predominant scales in oil field are formed either through precipitation of natural water from reservoir rock or oversaturated produce water (with scale component), due to mixture of incompatible water downhole. Its more problematic in the case of sea water injection breakthrough with Barium, or Strontium Sulphate both highly insoluble (Gholinezhad, 2006).

Among the most serious oil field problems today is scale deposition, a product of two incompatible water usually formed during water injection operations (Merdhah & Yassin, 2009). Also Change in pressure, partial pressure, temperature, pH,  $CO_2$ ,  $H_2S$  can be major drivers of scale formation. For instance, the change in temperature and pressure of water flowing from one point to another can aid the production of sulphate scale (Jordan & Mackay, 2015), which is mostly formed due to incompatible mixture of injected water (rich in sulphate ions) and formation water (high in concentration of calcium, barium and strontium ions). Same process can lead to formation of calcium carbonate precipitation which together with calcium sulphate are problematic type of scale creating operational issue such as tubing, open hole section and flow line blockage (Alabdulmohsin et al., 2016). The formation of the earlier mention type

of hard scale dramatically reduce porosity, permeability, production rate, case is worsen when deposited on pay zone (Farrokhrouz & Asef, 2010). Hence, it can now be clear that scale problems are mostly associated with the later life of a well.

### 1.3 Scale control

The quest for continues improvement in scale management strategies and control cannot be overemphasis keeping in mind the threat scale formation is posing on global energy security. Since the discovery of scale formation problems different techniques, tools and technology have been developed to manage scale problem from prevention to removal stage, through the entire production system both on and offshore. Though the prevention techniques (prediction ,monitoring and mitigating the risk of scale formation) in the capital expenditure (CAPEX) phase of the field life, is always better than confrontational measure of cure (scale removal techniques/solution) at the operating expenditure (OPEX) phase (Jordan et al., 2001) as has since been emphasise by many scholars.

A tremendous cost savings can be achieved if the current scale control/management techniques have been in place during the CAPEX phase. For example, the utilisation of gas lift to aid well clean-up will reduce cost of coiled tubing operations and production decline. Scale cause by water cut rise can be avoided through scale squeeze treatment before water breakthrough (Jordan et al., 2001). Another technique can be the commencement of reservoir treatment prior to production to arrest any scale formation tendency near the wellbore by deployment of solids and fluid system inhibitors. So also, the utilizing continuous injections such as gas lift and capillary to control downhole scale and subsequently squeeze treatment within the production circle and water cut rise of a producing well.

Despite the evolution of tools and techniques in the field of scale management, no single tool/technique has proven to be universally applicable to all scale type, formations or oil wells, leaving the tools selection to be determine by their pros and cons, before the development of recent technique (Gholinezhad, 2006). Therefore, the fact as mention by (Alabdulmohsin et al., 2016) is choosing a scale removal techniques for each well is govern by knowledge of the type, quantity, texture, composition and location of the scale to be removed.

Even though the cost of scale removal can be high, but differing treatment might cost higher (Gholinezhad, 2006). Hence, scale control remains centre for attraction for flow assurance. Its clear that the rate of increase in production index and revenue generation will always outweigh the cost of scale control (Alashhab et al., 2006). Considering some succelull after descaling senerios discussed below.

In the case of *Duri* field in Indonesia an increase in revenue by \$3.6MM in 90 days within 18 days payback period was achieved after successful  $\text{CaCO}_3$  scale removal (Schlumberger, 2013). A Scale

inflicted oil well in *Ghawar* field, the world largest most prolific was return to full well accessibility status. A 30% increase in production and more than \$1 MM of cost saving after a successful descaling operation (Alabdulmohsin et al., 2016). Similarly, *Statjord* Oil field in North Sea operated by Statoil oil despite fallen below the production decline curve with history of recovering 60% of its STOOIP via secondary recovery techniques for the past 23 year (Børeng et al., 2002). Return to stream with approximately 700-1000 sm<sup>3</sup>/d of oil after performing a successful scale removing job.

A new descaling solution has been found promising by systematically descaling both type of scales deposits on electric submersible pump system (ESPS) resulting in eradication of rigs work over (WO) requirement as reported by (Ramonés, Rachid, Flor, Gutierrez, & Milne, 2015). Increasing their average run life from 40 to 140 days, 6 day per well average rig cost saving and \$1.5 MM average savings in delayed production. Likewise post-descaling and simulation nodal analysis results to asses post descaling performance of a carbonate (sour) gas reservoir well in Saudi Arabia shows a significantly increase from 6 MMSCFD well flow at buttonhole pressure of 3,715 psi to 10.2 MSCFD well flow at 3,825 psi bottom hole pressure (Mukhliss et al., 2014). Matching a 0.27 md permeability and (-5) skin effect improvement corresponding to almost 80% improvement and a better AOF. Proven to have effectively remove the damage and the reservoir is responding

## **1.4 Research problem statement**

Proper planning by integrating scale control into asset life cycle management of a well in CAPEX phase such as good water injection strategies or incorporating the appropriate technology during well completion. Instead of confronting scaling problems during OPEX Phase (development/production stage) will be more effective and economical (Jordan et al., 2001). While in the case of discovered scale problem during OPEX phases of a well due to failed, poor preventive measures or expiration of inhibition life, scale removal remains the only solution. Usually chemical or mechanical techniques or even combination of the two are used for effectively removal of the scale in order to regain the flow assurance of a well. The core principles of a successful scale removal approach depend on regaining well accessibility and increasing production rate of the well. In an economic (cost of scale removal to revenue generation after descaling operation), efficient (descaling time), simple (non -complex with few steps), safe (safety of rig personnel), integrity (well completion equipment conditions) environment friendly (environment of well and vicinity) approach. Although, seem difficult to achieved since inception/revolution of scale removal techniques/tools.

The application of high-water jet in numerous industrial applications has been on record for a long time for demolition, cutting different materials. Most importantly used for scale cleaning in oil and gas

production tubing invaded by organic or inorganic scales like paraffin, asphalt, calcium and magnesium compound respectively. Especially the later among listed that prove to be difficult to remove through chemical method (Aslam et al., 2000). Makes mechanical approach as the best removal option

Even though jetting technique under mechanical descaling method have recently gained wider acceptance by multinational companies (Bajammal et al., 2013) like Saudi Aramco, Shell, Slumberger and the rest. Despite, suffering serious setback due to its ability to only effective clean scale at ambient condition, while backward pressure reduce its cleaning ability as it moves downhole (Crabtree & Johnson, 1996) which is attributed to cavitation effect.

Cavitation can be defined, as phenomenon where due to decrease in pressure across the jetting atomizer cavities are formed in the liquid jet (void or bubbles). Resulting from liquid change in phase to vapour or equal to vapour pressure of water. Cavitation effect in solid free jetting led to the introduction of abrasive (sand particles) to compensate low jetting performance downhole which end up jeopardising the integrity of well completion. Posing a lot of threat to the integrity of the tubing itself, other well completion and top surface facilities in addition to the environment.

Replacement of sand particles with sterling beads proves to be effective at the expense of environmental complexity. Sterling beads side effect are not just limited to tubing damage but the complicated delivery pump requirement for pumping the high-density suspension (liquid and solid). The slurry may end up being deposited on the tubing or other bottom-hole completion equipment (Mahmoud, Kamal, & Geri, 2015) leading serious operation problems

Just as cavitation negative effect toward reduction in performance of high-water jet down hole prompts multinationals to introduce sterling bead (liquid and solid). The environmental and well integrity negative effect of using sterling bead motivated the introduction solid free jetting descaling technique research. A pure water jetting approach that will not be affected by cavitation effect, combining both erosion and stress cycling mechanism, by utilizing aerated chamber with incorporated single high pressure flat fan nozzles (Abbas, 2014). The noble research was not only able to increase solid free jetting performance down the production tubing, but answer question related to cavitation such as cavitation suppression distance (stand off distance), relationship between aeration and suppression of cavitation. In addition to the relationship between air concentration in the aerated chamber and cavitation bubble length.

Despite the tremendous achievement made by the single high pressure aerated flat fan nozzle technique some identified research gap, and room for improvement will not be neglected (Abbas, 2014). Notwithstanding, the calls for improvement by many researchers and quest of developing an effective scale removal technique by the multinational companies. The spray research group decided to extend

the single nozzle research by introducing a state-of-the-art technique that will include the use of multiple high-pressure nozzles in a compressed and/or vacuum chamber this time.

The multiple high-pressure nozzle will utilize at least two of the four jetting mechanism at the same time. Either by firstly compressing (pressuring the chamber and suppressing cavitation to archive erosion, cyclin stress and likely abrasion mechanism). Secondly, suctioning (extending cavies by vacuuming the chamber to achieve erosion, cavitation and abrasion jetting mechanism). Regardless of the high achievement in scale removal recorded by the single nozzle research, the following research problem remained un-answered.

- High rig time (descaling time) required when using single nozzles
- In adequate scale circumference coverage by using single nozzle leading to non-uniform scale destruction that can lead to tubing blockage
- Utilizing and extending cavities flare (cavitation) instead of suppression might lead to better well cleaning downhole since erosion, cyclin stress and abrasion effect might be archive
- Aeration effect on real oil and gas well in respect to environment, rig personnel and the integrity of well completions
- Ambiguous cost implication of the techniques

## **1.5 Research motivations**

Combining the above listed un-answered question from the existing aerated single high-pressure flat fan techniques. Couple with the expected challenges from the proposed multiple high-pressure nozzles with option of compression or cavitation. This research may likely have to answer the following question too.

- Pumping requirement needed to effectively operate multiple high-pressure atomizers
- The challenge of generating uniform descaling impact across the scale circumference due to spray overlap region
- Rate of compression required to supress cavitation product from multiple nozzles
- Optimization of number of nozzles in order to reduce high risk of tubing overflow
- Selection of number of nozzles, type (same or combination of different type of atomizers to couple into multiple nozzle header) for effective descaling operations

## 1.6 Research contributions

- Develop an operational guide for the selection of optimum descaling parameter/techniques required for effective removal of different types of scales from petroleum production tubing using multiple high-pressure nozzles.

## 1.7 Research aim

- Enhancing the rate of scale removal in petroleum production tubing using multiple high-pressure nozzles header in different air conditions

## 1.8 Research objectives

The prime objectives of this work are the hydrodynamic characterisation of multiple high-pressure nozzles to remove scale from production tubing with the following goals in mind.

- To design, construct & assemble the upgraded descaling rig including the descaling chamber (ambient, compressed and vacuumed condition), in simulation of ideal descaling conditions
- To design/fabricate a wax scale moulder and utilizing it in producing soft scale samples candidate of different sizes and shape that can simulate different scale growth stages in production tubing.
- To characterize both scale samples, through chemical and compositionally analysing the hard scale candidate using the combination of scanning electron microscope (SEM), energy dispersive X-ray analysis (EDX) and X-ray diffraction (XRD) technique. In addition to nuclear magnetic resonance (NMR) spectroscopy and Fourier-transform infrared spectroscopy (FTIR) techniques for the constructed soft scale sample.
- To study the effect of descaling parameters, such as chamber air concentration, numbers of nozzles and injection pressures, standoff distance and header arrangement towards the rate of scale removal for different scale samples in different chamber pressure.
- To investigate the impact of air water concentration in descaling chamber to the rate of scale removal when using multiple HP nozzles at different chamber pressure (ambient, compressed and vacuum) and different descaling parameters.
- To determine the optimal descaling requirement for the effective scale removal of different types scale deposit in petroleum production tubing.

## **1.9 Structure of the research thesis**

This thesis is structured in form of chapters, and each chapter to contain and explain relative acquired knowledge and activities that took place during the research work.

### **1.9.1 Chapter 1: Introduction**

This chapter introduce the concept of scale problem in flow assurance before narrowing the issue to production tubing with example of recorded cases around the world. Followed by the brief chemistry of scale formations coupled with life examples of scale inflicted oil well across the globe. Then scale control and its economics with real life scenario of successful post descaling dividend across the world. Before briefly highlighting the history/evolution of scale removal techniques, pros & cons and limitation of application of the techniques so far. Finally narrate what conspired the introduction of single spray aerated nozzle by Spray and Petroleum Research Group (SPRG).

In addition to what motivated the introduction of latest state of the art propose approach that involve the utilization of multiple high-pressure nozzles in simulated chamber of different chamber pressure. Coupled with its research motivation, contribution aims and objective of the research.

### **1.9.2 Chapter 2: Petroleum production challenges**

The chapter elaborated in detail scale problem starting with the overview of flow assurance and production tubing deposit problems. Followed by dynamic of scale formation, implication to flow assurance (scale deposit) with cited examples around the world.

Further discuss the chemistry of scale formation including classification, categorization and chemical analysis of scale sample (via SEM, EDX, XRD & XRF) as recommended in the single nozzle approach. Scale control/management in terms of prediction and prevention (Inhibition), its economics, and brief history on the evaluation of scale removal and control equipment's/medium. Subsequently introduce descaling approach in terms of its core principle, types, (chemical or mechanical), and examples of live effective and successful combine (chemical and mechanical technique) scale operation across the globe were later discussed. Chemical descaling technique with its limitations, followed by chelating agent with it type, influencing factors and example of successful solo chemical descaling operation across the globe were cited. Closing the chapter with discussion on mechanical descaling technique, type and tools. While giving emphasis on jetting technique history, evaluation, mechanism and citing successful lone mechanical descaling operation across the globe and wrapping all point with a summary of the whole chapter.

### **1.9.3 Chapter 3: Multiple spray characterization**

This chapter provide the fundamental and advantage of high-pressure water jet over others. Starting with explanation on the performance of a nozzle or spraying system in terms of parameters and factors that affect the performance of a spray system. Followed by discussion on atomization process in respect of types and classification of atomisers, patternation and liquid break up process. Then analyses flow behaviour, spray characterization of multiple nozzle spray focusing investigations on essential parameters like droplet velocity, droplet size, distribution, and spray overlap region under ambient condition. Highlight advantage and benefit of adopting multiple nozzles over single nozzle and ability of solid free jet to effectively perform downhole without the use of starling bead. Subsequently introduce mechanical descaling techniques by concentrating on it jetting mechanism aspect (erosion, abrasion, cyclin stress and cavitation). Closing with their description, influencing factors, uses, operative mechanism, relationship to fundamental parameters when utilizing multiple spray system and benefit toward effective descaling operations.

### **1.9.4 Chapter 4: Experimental set up**

The chapter focused on detailed experimental set up narrative, theories and strategies. Driven across, the research, sketches, design, construction and assemblies of the experimental rig, which will be used under ambient, pressurized and vacuum condition. The chapter is divided in to two phases of pre descaling and descaling experiment.

The pre-descaling activities which were conducted outside the descaling chamber in preparation of the descaling trials as further classified into two sections too. The first section covers the design, construction and assembly of the declining rig, in addition to design/construction of wax moulder and its further utilization to produce soft scale sample of various shapes. While the second phase includes chemical and compositional characterization of both the available hard and constructed soft scale sample through the combination of EDX, SEM & XRD technique and NMR & Infrared techniques respectively.

The second phase term the descaling trials (carried inside the assembled descaling chamber) covers three sections: The first section studied the effect of descaling parameters like injection pressure, numbers of nozzles, stand-off distance and header configurations toward the rate of scale removal. While the second section investigated the effect chamber water/air concentration i.e. ambient, compressed and vacuum air condition toward the rate of scale removal. Finally, the third section concentrated on determining the optimum descaling requirement for the effective scale removal of different types scale deposit in petroleum production tubing.

### **1.9.5 Chapter 5: Results and discussion**

The chapter extensively discuss and analyse result obtained from all the set of tests conducted in chapter (4) four. Highlighting and comparing the significant of the findings with unlimited comparison of the result to recent industrial application by multinational and existing SPGR techniques within the effective descaling operation threshold.

### **1.9.6 Chapter 7: Conclusions and recommendations**

The final chapter furnish and conclude all findings and values drawn from the research. Provides recommendation that will improve descaling operations and last but not the least identify research gaps that could be basis for future descaling research.

# Chapter 2

## Petroleum Production Challenges

### 2.1 Overview

The chapter elaborated in detail scale deposition challenges starting with the scariest of all flow assurance problems (scale deposit). Followed by discussion on scale deposit problems in production tubing, kinetics of scale formation, scale formation influencing factors and its implication toward flow assurance with examples around the world. Furthermore, discusses both scale composition and chemistry for scale formation, in the attempt of classification and categorization of scale types. Couple with scale compositional analysis (Via SEM, EDX, XRD) as recommended in the single nozzle research approach.

After highlight of scale problems and details of scale control management, the in depth of scale removal technique came to board by discussing types of scale removal techniques (chemical & mechanical). subsequently defining successful descaling programme wrapping up with few examples of combine (chemical & mechanical) successful descaling operations around the globe. Discussion on chemical descaling approach, limitations coupling with chelating agent, types, influence factors and examples from some successful chemical descaling approach around the globe.

Mechanical descaling approaches were detailed and in addition are thorough on types of mechanical approach (milling, string shoot, ultrasonic and jetting technique), Jetting technique/tools evolution and mechanism (erosion, cycling stress, abrasion and cavitation). Together with examples from some successful mechanical descaling operation around the globe. Finally, the whole chapter was summarised.

#### 2.1.1 Petroleum production associated problems

Flow assurance as the ability of a well to economically produce fluid from reservoir to the surface production facility remains threaten by production associated problem. Mostly caused by poor planning at CAPEX phase of field development leading to avoidable remedial and work over at OPEX phase of the field by the production technologies. This preventable and curable production technologist nightmare does not only hinder the economy of petroleum production by production drop, limiting well accessibility, rig integrity, personnel and environment safety, cost of preventing and curing the menace. But also, a technical quagmire because some of the associated production problems can be trigger effect to others. Example is the case of asphaltene precipitation aiding nuclei for paraffin precipitation (Wang et al., 2016) or as tubular corrosion is attributed to be the primary source of iron sulphides scales

production. Possibility of conversion of siderite to iron sulphite scale is high been unstable in presence of H<sub>2</sub>S (Coleman et al., 1993). Also, (Richard,1968) reported that the reactions of siderite with sodium sulphite in aqueous solution at 25°C will produce smythite.

While some of the associated production problems treatment can be cause for others. Scale inhibitor contains corrosion triggers just like how iron sulphate reacts to HCl to release high concentration of H<sub>2</sub>S during chemical scale removal process forming a hazardous corrosive mixture (Wang et al., 2013). Attributed with side effects on the metallurgies of down-hole completion particularly in high temperature sour gas well.

The associated production problems can even occur simultaneously like combination of organic and inorganic scale deposit at same location as recorded in Saudi Aramco well (Al-Taq et al., 2015). Also, analysis result of collected bailer sample from wells reported by (Ali et al., 2015) indicated the combination of organic materials like paraffin, asphaltene and inorganic deposit like ankerite, anhydrite and insignificant presence of halite and quartz. Fortunately, some of the petroleum production associated problems may even share solution.

The history of most of the associated petroleum production problems can be rooted to dynamic nature of hydrocarbon production process. Resulting to physiochemical changes like reduction of pressure and temperature during the flow of fluid from reservoir to production facility causing deposition of heavy hydrocarbon materials like Asphaltene. The petroleum production associated problems include:

Asphaltene is an associated production problem identified as the heaviest polar component of crude oil with aggregate molecular weight of 103 to 105 moles higher than risen and aromatic with no definite structures. Presences in colloidal particles or micelles usually stabilize by risen. For easy definition oil fraction that are insoluble in n-heptane but soluble in benzene cause by physiochemical changes (temperature, pressure, chemical), their combination and can be agitated by the presence of positively charged calcite scale and that of CaCl<sub>2</sub> & MgCl<sub>2</sub> salt (Soheil et al., 2013; Al-Taq et al., 2015). Been a surface-active component of crude oil with interaction/absorption properties on different rock surface. It can easily restrict flow in production tubing, absorb on rock surface to block pore throat or even change its wettability (Ring J.N., 1996). Sometimes asphaltene form sludge in the presence of iron during simulations by stabilizing water-in-oil interface (Jacop et al., 1986; Figuerow Ortiz, et al., 1996; Kokal et al., 1998) or even tight emulsions with increase asphaltene fraction in the water-oil-interface.

Another production associated problem caused by change in physiochemical properties is Paraffin. With density around 900 kg/m<sup>3</sup>, soluble in benzene and some esters and insoluble in water with 46 and 68 °C range of melting point usually tasteless and odourless. It can deposit at any part of the production system

(Armacanqui, Eyzaguirre, Flores, Zavaleta, & Camacho, 2016). Including wellbore, pumps, production tubing, and top surface production facilities.

Hydrate is another physiochemical change related production associated problem. Found in natural gas and oil pipeline together with other heavy carbon deposition problems like wax and asphaltenes. This usually, agitated by hydrate forming gas molecules supply change in physiochemical parameters (high pressure and low temperature) and water supply accessibility. (Kalland, 2006) attributed it to consequential effects like blockage, while in deep water an ingress of gas into the umbilical may form due to decreases in pressure and increase in temperature

Corrosion the deterioration of metal and its properties is another production associated problem. It can attack any component of the production system at any stage during the lifetime of a well due to metallic nature of production system component and or inheritance nature of hydrocarbon system component term acidic corrosion. So, as hydrogen Sulphide ( $H_2S$ ) and other component use for in formation damage reduction and scale inhibition. Finally, oxygen from oxygen itself, carbon dioxide ( $CO_2$ ), chloride ions which are introduce through contaminated drilling fluid, injected and produce water can cause corrosion. Denis et al. (1994) narrated that corrosion problem is estimated to cost united state industries about \$170 billion a year.

Other petroleum production problems may be related to mechanical and geological causes. Like production of fluid with sand (clumps and grain) attributed to formation breakdown or wellbore and reservoir plugins from production of fluid with siliceous or fine clay.

Packing and rapping our point with the scariest among all the production problems (Scale). This is caused by fluid incompatibility, though not overruling the change in the physiochemical property's fluid (temperature, pressure, pH, and  $CO_2/H_2S$ ) which are difficult to arrest. Due to the quest for energy drive or production agitation from depleted reservoir throughout the lifetime of a field. Scholar like (Guan, 2015) believe the entire production system is prone to scale deposition so far its water contact

### **2.1.2 Flow assurance problems in production tubing**

Production string does not just serve as the flow assurance gate way because it's the main production conduit or well access for remedial and maintenance programmes like login and the rest. But their places were the highest percentage of the total pressure losses of the production system occurs. So, for the production technologist to identify and treat any production ailment located from production tubing down to the wellbore reservoir or reservoir in a cheap, effective, safe, and environmentally friendly way. He must have a safe passage plan along the tubing that will not at any cost harm to the tubing and other tubing string completion integrity.

This is because the effect of scale deposition in production tubing are not limited to decline in production rate but preventing well integrity and performance assurance programmes (Yusuf et al. 2016). Most record on scale afflicted well around the world tip production tubing among the entire production system to be most scale venerable because some scale grow all the way up to production tubing from other lower production system. If not arrested in time, end up blocking it like the case reported of a well suffering from poor deliverability, erosion damage at surface production facility and well bore restriction. This is as a result of scale deposit in the 7000-inch lower section of the tubing and production casing all the way to the perforation intervals (Mohamed et al 1999). Not underrating the dangers like desolation/hydration process and other surface facilities cause by suspended mobile scale in water, although more dangerous and difficult to treat if it's adhered to the wall of the tubing (Salami, Monem, Development, & Zadco, 2010). Making it difficult even in presence of improves reservoir placement technology and intelligence fluid system to archive a quick and non-damaging solution. Due to the verse chemical composition of scale layers adhering to the inside of the production tubing (El Hajj, Pal, & Zoghbi, 2015). A typical schematics of scale deposition in production tubing is elaborated in Figure 2.1

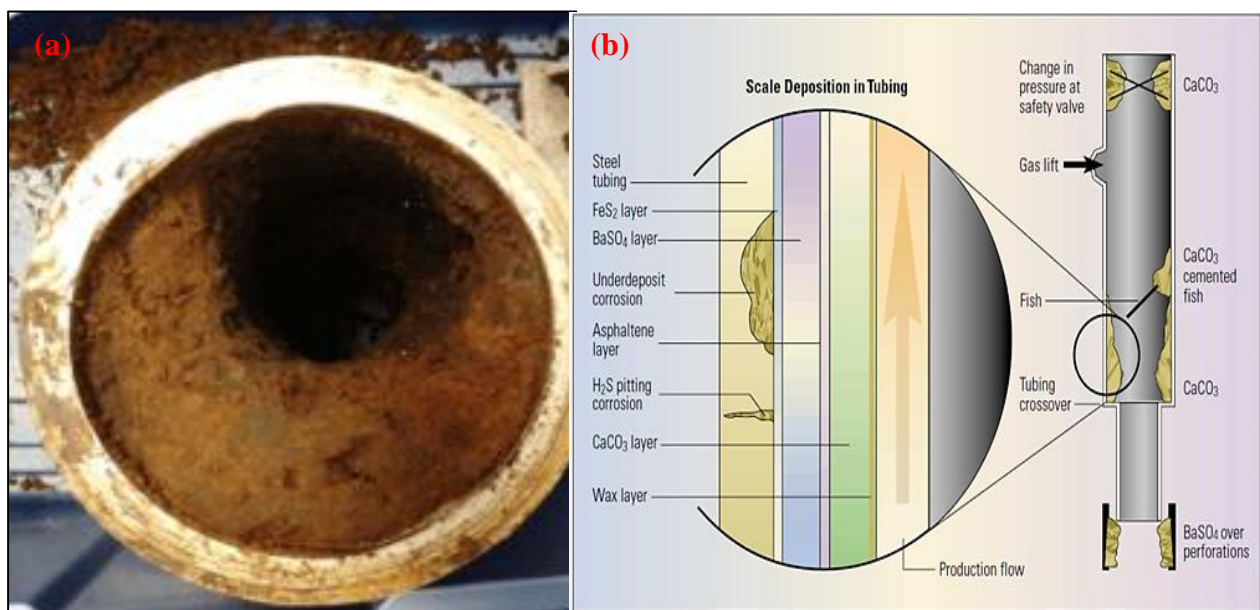


**Figure 2.1:** Scale deposit (a) in production tubing, (b) schematics of scale inflicted production tubing by (Slumberger, 2013)

## 2.2 Kinetics of scale formation

Scale deposition problem is non-racial and non-boundary flow assurance and energy security threat, that had cut and inflected almost all the oil and gas field across the entire globe.

Starting with few cases from Gulf nations of the Asian continent like *Kuff* Gas well in Bahrain that suffers from poor well deliverability, wellbore poor accessibility and erosional damages at the top surface production/processing facility. Attributed to scale deposition from production interval up the way to 7000 inch of the lower section of the production tubing and production casing (Mirza et al., 1999). *Fadhili* field in the Eastern Saudi Arabian was half to its production capacity (150BOD and 90% water cut) within four months. Estimated to be around 20 to 30 BOD drop per well as a result of calcium carbonate deposited along both production tubing and other flow lines. World most prolific oil field (*Gwahar*) approximately 225km length by 30km width in the same Saudi Arabia has been suffering from Iron scale problems (Leal et al 2009). Among other Gulf oil fields afflicted with scale deposition problems are *Zakum* field in Abu-Dhabi, the world 4<sup>th</sup> largest oilfield (Al-Ashhabet al. 2006). *Fateh* field Dubai, UAE (Ringin J and Read P 1982). While in the cases of deep Asia: *South Sumatra* oil field in Indonesia (Mitchel. et al 1980) and *Miono* gas field 350km north of Karachi Pakistan (Field et al. 2013). These are few from the many oilfields in Asia that have been experiencing production decline associated to water influx restricting fluids flow along the production tubing due to carbonate deposit.

In the European continents, North Sea oil fields like *statjoft* oil field, which has fallen below production decline curve with 60% of its STOIP recovered via secondary techniques for the past 23 years due to scale problems (Børeng et al., 2002). *Statoil* oilfield where scale was proven as the major cause from operator data showing 75% plugged by scale, fine or their combination and a plugging frequency of 0.02 int/well-year (Jordan et al., 2001). More dangerous and instantaneous is the case of *Miller* field where a 30,000bopd production capacity well was halted to zero within 24 hours (Crabtree et al., 1999). The case of *Gyda* field north eastern part of Norwegian continental shelf of North Sea (Mackay, Jordan, & Torabi, 2003). *Alba* field in UK continental shelf (Farrelet al., 2013). In addition, some prolific wells in USSR (Cowan et al., 1975) are among many fields suffering from severe scale plugging.

In the African continent, an African oil field like *Gmasa* oil field in Egypt which has suffered a production decline approximately one tenth of its normal production capacity due to hard scale deposit (Cowan et al., 1976). Strontium and calcium sulphate were found in surface and sub-surface production facilities of *Al Morgan* field in Egypt (El-hattab, 1985). The three-water flooded field operated by GUPCO in the Gulf of Suez area (Lico et al., 1980) and also (Khelil et al., 1979) mentioned some water flooded oilfield in Algeria

Wrapping my points with few cases from the American fields are: *Ew 873* of the Gulf of Mexico, well with chronic near wellbore formation damage and tubular restriction due to barium sulphate (BaSO<sub>4</sub>) scale build up. As a result of incompatible mixture of formation water and biocide inhibited sea water well (Sopngwi et al., 2014). So also, (Quiroga et al., 2003) reported about Petrobras operated oil field

in the Brazilian offshore that have live in the history of severe hard scale problems mostly due to the nature of the offshore field

Scale formation is a product of many production operation factors depending on the type of scales in question, physiochemical, kinetic and thermodynamic properties of produce fluid. Like (chemical composition & concentration, temperature, pressure, pH, salinity, CO<sub>2</sub>/H<sub>2</sub>S liberation and outgassing, time). Similarly, the age of the well and the oil recovery technique on ground (water incompatibility mixture between formation water and poorly treated injected water will be inevitable when using some secondary recovery techniques).

Mineralogy and lithology of the formation (Sandstone reservoir will contain high concentration of strontium (Sr<sup>2+</sup>) and (Ba<sup>2+</sup>) cations). Also, while carbonate and calcite cement sandstone will be rich in magnesium (Mg<sup>2+</sup>) and divalent calcium (Ca<sup>2+</sup>) cations. In addition, complexity of equipment and completion design, type of well (vertical, multi mingling or even horizontal associated with low drawdown being the ability lift carbonate scale up hole) or onshore /offshore and the type of the field (Gas or Oil field). Lastly, level of scale preventive commitment at the CAPEX phases of the fields even though some factors are more outweighing.

Most disturbing flow assurance problems are kinetics of crystal growth of mineral with poor solubility (scale) which main cause can be grouped into three core-factors: Geological factors like mineral composition, ground water circulations. Engineering related parameters like well pressure, pumping rate, introduce fluids to the oil-bearing formation. So as physical /chemical factors like change temperature, pressure PH and the rest (Nancollas and Reddy 1974) that are more peculiar in oilfield scale deposition

Many petroleum/flow assurance concern scholars have tried to justify or streamline the core course of scale production to be: Reduction in solubility as a result of physiochemical changes like increase in temperature or decrease in pressure. Precipitation as a result of mixture of incompatible waters (sea water rich in SO<sub>4</sub> anion and formation water containing C<sup>2+</sup> or Ba<sup>2+</sup>cations forming mineral scale). Increase in concentration above solubility range from the result of brine evaporation are the three suggested mechanism for mineral scale formation by (Mackay et al., 2003) and also concurred by (Abbas, 2014) among many scholars.

While change in temperature and pressure drop, water break through impact, like increase in sea water mixing ratio, increase in pH level. Which can increase CaCO<sub>2</sub> potential once the pressure fall below the CO<sub>2</sub> bubble point leading to liberation of carbon dioxide (Salami et al., 2010). Reductions in solubility of salt as a result of increase in temperature or decrease in pressure of brine (contributing to the precipitation of calcium carbonate or carbonate scales). The mixture of two in compactable fluids (precipitation of sulphate scales BaSO<sub>4</sub> from incompatible mixture of cation rich formation water and

sulphate rich sea water). The case of organic- deposit on submersible pump can be due to crude oil cooling and the separation of volatile/light fraction near the pump intake (Ramones et al., 2015). While in organic scale deposit can be attributed to high water cut and high pressure drop in the wellbore

Salt precipitation is as a result of increase in salt concentration above solubility limit due to brine evaporation. (Scale precipitations like NaCl can occur as a result of dehydration from mixture of dry gas stream with low brine stream in high pressure/high temperature well) (Bowman et al., 2010). Oil and Gas are produced alongside produce water, which is as a result of change in pressure and temperature in production tubing and can agitate the liberation of CO<sub>2</sub> with the consequences of increasing the pH level of the produce water. This leads to precipitation of calcium carbonate (Crabtree et al., 1999). Factors behind the precipitation of scale are mixing of in compactable brines or change in PH or physical conditions like pressure and temperature (Wang et al., 2013). While (Moghadasi et al., 2003) relate it to the adverse effect of temperature because the higher temperature the higher the scaling tendency of some oilfield scales (sulphate and calcium carbonate). Organic scale is usually deposited outside crude oil and plugging the formation due to variation of temperature and pressure in oil and gas reservoir during production is (Dale et al. 2014) thought. While the organic scale deposition and growth on surface is agitated by both hydrodynamic of the system and the nature of the surface. Also (Heydrich, Hammami, Choudhary, Mockel, & Ratulowski, 2019) highlighted the important of the oil and gas water volume fraction, flow regime, shear at the surface, surface energy & roughness.

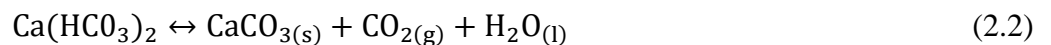
Even though water is basic reason for forming oilfield scale and so is drop in partial pressure of CO<sub>2</sub> a defining factor too. Temperature, variation in hydrogen ion concentration, ionic concentration, additional stripping due to gas lift operations, water flooding or reservoir communication cannot be under emphasize. If partial pressure of CO<sub>2</sub> drop occurs at the well head, scale is expected to form at flow line with the potential of progressing down to the wellbore all the way to the reservoir. Also, if low enough, at production separator scale may deposit there (Khalaf 2001). *Awali* field can serve as a good example were pressure, temperature and gas stripping are the primary source of scale formation (Esbai et al., 2016). Brine production from different formation can occur due to high rate of gas production in a well leading mixing of incompatible brines of different saturations that can easily precipitate salt and plug well (Farrokhrouz & Asef, 2010). Still CO<sub>2</sub> stripping might be the major reason of calcium carbonate scaling since formation water at reservoir condition is in aqueous (bicarbonate). Therefore, any disturbance of it equilibrium by under equilibrium and CO<sub>2</sub> stripped from it will lead to calcite scaling due to pressure reduction (Esbai et al., 2016). As expressed in equation 2.1



Despite the scholar's consensus on primary scale agitators is to be temperature and pressure fluctuations, water incompatibility, outgassing and shift in pressure. Quite a lot of cases of oversaturated produce water meeting all scale formation requirements refuse to form scale (Crabtree et al. 1999). It's then establish that another core requirement outside all the above mention is the essential growth from its solution with creation of less stable atoms (Abbas, 2014). Through the development of unsteady bunch of atoms (seed crystals) during homogenous nucleation process. So, lonely depending on these three sequential requisite stages of super saturation, nucleation and precipitation

First stage is super saturation: Usually as a result of mineral concentration of brine exceeding it equilibrium concentration, forcing salt to precipitate out of solution and form scale. Supersaturated is aided by variation in temperature and pressure, increase in mineral concentration, thermodynamic variation, particle sizes, hydrodynamics' (agitation & velocity), kinetics (time). In addition to pH and other environmental factors leading to the birth of small particle called Nuclei (El-Hattab, 1985). Since solubility limit can be exceeded once the natural state of fluid is altered, thereby leading to scale formation with a temperature and pressure complex tendency. Therefore, water solubility of mineral will increase with increase in temperature and will decrease with decrease in pressure. Related to the role of thumb that predicted by (Cabtree et al., 1999) the solubility of most minerals to decrease by a factor of two for every pressure decreases of 48 MPa (7000 psi) with the exception calcium carbonate which solubility in water increases with decrease in temperature.

Super saturation can occur once the solubility limit of a fluid is disturbed (Scale can form once the thermodynamic of one or more component is exceeded). Temperature and pressure are the major functions of the kinetic reaction that form scale. Despite, it has been well established that mixing two in compatible water is reasons for scale formation, changing the kinetics of single water can generate scale too (Moghadasi et al., 2003), (El Hajj et al., 2015). It can also be established that the higher the degree of super saturations of water the higher the rate of precipitation causing more decline in permeability (Al-Taq et al., 2015). Like the way decrease in pressure or temperature surely decrease ionic solubility of salt (basis for carbonate scale precipitation  $\text{CaCO}_3$ )



Second stage of scale formation begins after the birth of nuclei. As a result of the mention scale driver's couple with its ability to grow out of solution formation of unstable cluster of atoms from over saturated fluids during homogenous nucleation processes. Then proceed to form seed crystal as a result of local fluctuation in the equilibrium of the ionic concentration of the supersaturated solution (Cabtree et al., 1999). The seed crystal increases in size as a result adsorption of ions on to the defect of the face of the crystal. Likewise, the enlarge crystals grows in energy driven from decrease in surface free energy of

the crystal. Then, after the increase in radius exceed the critical radius free energy decrease rapidly. Subsequently, leading to continues growth of the large crystal and dissolving of smaller seeds again. Seed crystal serving as catalyst for scale formation means seed crystal formation will result to growth of scale deposit if given large enough degree of saturation.

Thus, in heterogeneous nucleation crystal growth is expected to start on pre-existing fluid boundary surface (Yousef et al. 2014). Defect on pipe surface like perforation, roughness in liners, joint steam in pipelines, or production tubing are cantered to be the major site for heterogeneous nucleation process. High degree of turbulence is another scale formation catalyst, since scale accumulation occurs at the bobble point pressure of the flow system making it good reasons for the rapid deposition of scale on down-hole equipment's (Toyloret al. 2013). Similarly, (Mackey et al., 2019) added that the formation of iron-oxyhydroxide form steel corrosion can create sites for heterogenous nucleation and aid additional scale growth

After the formation of nuclei, a reasonable quantity of molecules must agglomerate and position in fix crystal lattice. Pre-existing mineral or metal surface like weld, corroded surface, scratch or nicks on a pipe, foreign crystal maters, sand & clay particles are favourable nucleation locations. Another requisite for scale formation is adequate contact time between the supersaturated solution and the nucleation site. There by nuclei creating a location for additional mineral deposition to form crystal that continues to growth and adherence to form scale (El-Hattab, 1985). In conclusion is that scale forms when the kinetic factor that inhabit the mineral growth are overwhelm by its thermodynamic driven force.

### **2.2.1 Factors influencing scale formation**

The formation of mineral crystalline deposit (oiled filed scale) is attributed to the precipitation of solid brine present in the production and the reservoir flow system (Abbas, 2014). Injection of incompatible water have been single as major cause of calcium and carbonate scale formation inflicting damage in both injection and producing well (Almubarak, Ng, Nasr-el-din, & Texas, 2017). Sulphate scales like barium sulphate ( $BaSO_4$ ) and the rest are formed as a result of mixture of two in compactable brines because formation water containing cations of barium, calcium & strontium and that of sea water are containing sulphate compounds. Result from twenty four well brine samples from brine chemistry test suggested acid treatment as main cause of scaling in 2009 (Farrokhrouz & Asef, 2010) linking the precipitation of calcium sulphate to the detrimental of acidization.

Scale formation depends on water production in a well. Complex fluid rich in ions or close to saturation limit are easily formed when water wash, dissolve and carry some of the mineral component from natural environment by-products of marine life and water evaporation enrich sea water with ion. While water

associated with oil gas well are chemically different from that of ground and near ground surface. The deeper, the more ionic concentrations due to alteration of sedimentary minerals (sandstone reservoir will contain high concentration of strontium ( $\text{Sr}^{2+}$ ) and ( $\text{Ba}^{2+}$ ) cations. While carbonate and calcite cemented sandstone will be rich in magnesium ( $\text{Mg}^{2+}$ ) and divalent calcium ( $\text{Ca}^{2+}$  cations) (Abbas, 2014). Water quality continuously varies through the life of a well and can be counted as one of the causes of scale formation. Particularly when injection water is used in sustaining the driver aquifer scale build up in well (Clameto et al., 2004). This situation became even tougher with injected seawater breakthrough resulting to deposition barium or strontium sulphate which absolutely insoluble

*Gwawar* onshore fields can be good case scenario with Gulf sea water as its primary sources of floodwater (with over 4,700mg/l of sulphate and salinity 15000 mg/l near Kuwait and over 55000 mg/l near southern parts of Saudi Arabia). Before recognising low saline aquifer water (5000 mg/l to over 70000 mg/l) as an alternative (Raju 2009). The mixture of the high sulphate concentrated Gulf sea water and in compactable *Gwawar* field formation water increase scaling potential of the field

A non-universal solution has been attempted by field reservoir modelling and reservoir engineers with the intention of lowering in-compatible water scale problem. Through the creation of a buffer bank to serve as barrier that will separate the formation water from freshly injected water (Alabdulmohsin et al., 2016). Though the solution depends on good knowledge of reservoir floor regime and good cooperation between production chemistry and reservoir engineering.

The process of iron sulphide is more complex because despite factors like temperature, pH, water composition,  $\text{H}_2\text{S}$  level, variety of minerals will play a vital role in determining the final mineral phase of the product (Benning et al. 2000). Iron can easily be introduced in to the formation during corrosion acidization, especially if the acid is not equipped with enough corrosion inhibitors (Ramachandran, Al-Muntasheri, Leal, & Wang, 2015). Since, in deep sour wells, iron sulphite has always been found in well tabular after acid treatment (Nasr-El-Din and Al-Humaidan 2001, Kasnick and Engen 1989). Dissolution of reservoir rocks that have small amount of iron, sour corrosion, drilling fluid loss and tabular corrosion during acidization process can be considered as main source of irons (Ramachandran et al., 2015). Also (Merdhah and Yassin 2009) believes injection systems can easily get inflicted with scale problems when two incompatible waters are involved

### **2.2.2 Scale classifications**

Chemical composition, solubility, cause of precipitation and physical properties like hardness and density are the basis adopted by many scholars on their attempt to classified or categorize type of scale in oil and gas production.

Organic/inorganic are the most used classification term for solid scale type. Referring to the two type of mutual inclusive simultaneous occurring scale (mixed scale) that are classified based on their formation factors and chemical compositions. Organic scale are hydrocarbons of high molecular weight, that are not easily dissolve, but easily form sludge when in contact with acid. Comprising of asphaltene, paraffin, wax and soap that usually forms as a result of change in production environment i.e. significant pressure drop expose viscous oil will surely form organic scale (Mucchi, 2007). While the crystalline deposit type containing mineral salt like  $\text{CaCO}_3$  and  $\text{BaSO}_4$  are term inorganic (Sobie et al. 2006). These usually form as a result of salt precipitation from brine present in production flow system. Mostly due to incompatible mixture of brines, change in equilibrium state of reservoir fluid & ionic concentration, change in pressure, temperature and pH. sulphate, carbonate, sulphide and chloride are most encountered (Abbas, 2014). Both the two scale types can occur simultaneously making it more difficult to dissolve and impeding the ESP system (Ramonés et al., 2015). Saudi Aramco wells have recorded combination of organic and inorganic scale deposit at same location (Al-Taq et al., 2015). Analysis of some collected bailer sample from wells (Al-Taq et al., 2015): indicate combination of organic materials like paraffin and asphaltene and inorganic deposit like ankerite, anhydrite and insignificant presence of halite and quartz.

Another classification basis can be tied to their solubility in acid. Like calcium carbonate called calcite ( $\text{CaCO}_3$ ), Iron carbonate known as siderite ( $\text{FeCO}_3$ ), Iron sulphide term Pyrite ( $\text{FeS}$ ,  $\text{FeS}_2$ ) and Iron oxide ( $\text{Fe}(\text{OH})$ ,  $\text{Fe}_2\text{O}_3$ ,  $\text{Fe}_3\text{O}_4$ ) are grouped under acid soluble scale type because of their solubility in acid. While Strontium sulphide known as Celestite ( $\text{SrSO}_4$ ), Barium sulphide called Barite ( $\text{BaSO}_4$ ). In addition to calcium sulphate which appear in two forms of anhydrite( $\text{CaSO}_4$ ) at relatively high temperature and Gypsum ( $\text{CaSO}_4 \cdot 2\text{H}_2\text{O}$ ) at relatively low temperature (Merdhah and Yassin 2009) are grouped under acid insoluble scale type (Salami et al., 2010) due to their insolubility in acid.

To some extent scale deposit are classified in to hard medium and soft scale base on their physical mineral hardness and density guided by Mohs scale (ability of harder minerals to scratch soft material). Most of the organic scales are classified under the soft scale categories. While the inorganic or mineral scale crossing through medium to hard scale range (Abbas, 2014). Were soft scale being peg with hardness value of 1.0-3.0 on the Mohs scale, while medium has a hardness value of 0.3-0.5, and hard scale is within the hardness value of 0.5-10 on the scale.

A crystalline organic mineral salt deposit usually cause by supersaturation of produce water that are affected by physiochemical changes depending on the type of field are term oilfield scales and further iron scale. Among most common oilfield scale encountered are: Sulphate compound like calcium sulphate (anhydrite & gypsum), strontium sulphate (celestite), barium sulphate (barite), and calcium carbonate. While iron compound like iron sulphate, iron oxide and iron carbonate related to high

temperature gas wells (Yassin et al. 2008) (Mahmoud et al., 2015). Sulphate scales like barium and strontium sulphate in particular are the most troublesome scale species among the oilfield (Bedrikovetskiy et al. 2005) due to their thermodynamic stability (M. M. Jordan et al., 2001). Usually when water rich in calcium ion comes in contact with another water with carbonate as its basic medium common oilfield scale like calcium carbonate. So as  $(CaCO_3)$ , barium sulphate known as barite  $(BaSO_4)$ , gypsum  $(CaSO_4)$  and strontium sulphate  $(SrSO_4)$  are expected to form (Moghadasi et al., 2003). The inorganic crystalline deposits in oilfield are formed as a result of salt precipitation from brine that are present in both reservoir and production system. Factors that drive scale formation include changes in ionic concentration, temperature, pressure, pH,  $CO_2$  and the rest.

### **2.2.3 Scale compositional analysis**

Complete understanding of chemistry and mineralogy of scale. In terms of analysing their compositional constituents can be achieved using standard analytical techniques like SEM/EDX, XRD and XRF. More precise results can be achieved by their combination. While NMR and FTIR is recommended for organic scale analysis.

Scanning electron microscopy with energy dispersive X-ray (SEM/EDX) are chemical analysis tools and techniques. That utilise surface analytical techniques through high resolution images of surface topography, with excellent depth of field. To determine and identify elemental and quantitative composition of a compound.

X-ray fluorescence (XRF) is a non-destructive analysis technique carried out with (XRF) spectrometer. Utilised in determining the elemental composition of material or routine chemical analysis of rocks, minerals, fluids and sediments. It basically operates on wavelength - dispersive spectroscopic principle like that of electron microprobe (EPMA). Which simply measures the fluorescent (or secondary) X-ray emitted from a sample when it is excited by a primary X-ray source.

X-ray powder diffraction (XRD) is a fast-analytical technique. Basically, used for phase identification of crystalline material (mineralogy) like scale deposit, shale core, catalyst, cement, formation core and the rest. Achieved by differentiating numerous forms of compounds with same chemical formula (Chung 1974, 1975; Klug and Alexander 1974; O'Conner et al. 1991; Sitepu et al. 2005). So, the average bulk composition of the finely ground, homogenized analysis material can then be determined. This sole application is characterized with constraints in ability to provide complete information due to peak pattern.

Therefore, to have an effective analysis and detailed scale characterization for crystalline, semi-crystalline, and non-crystalline material. A solubility testing and extra analysis tool like XRF elemental

analysis are needed (El Hajj et al., 2015). An example of the publisher suggestion is a result from combine analysis (XRD and XRF test respectively) for calcium carbonate scale. The result indicates the presence of calcite, sodium feldspar, and calcium feldspar. The XRD still shows halite, quartz, and magnetite while the XRF result suggests high percentage of dolomite and calcite. In addition, 82% of the sample was readily soluble in HCl acid, while 93.11% as observed from the spot acid solubility test.

The Nuclear Magnetic Resonance (NMR) Spectroscopy is well known for revealing compounds unique structures by identifying carbon-hydrogen framework of organic compounds.

Additionally, Infrared Spectroscopy is another tool for analysing organic substance that lies around the interaction of infrared light and molecules either by measuring it emission, absorption or deflection for analysing and identification of chemical substance, functional group in a compound and other applications.

## 2.2.4 Scale chemistry

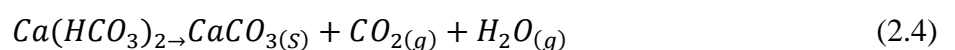
### 2.2.4.1 Calcium carbonate scale (CaCO<sub>3</sub>)

Calcium carbonate is mostly found in oil field operation due to limestone region abundance (Okocha et al. 2014), its soluble in acid and produces white effervescence. Exist in distinct crystal geographical forms like calcite, aragonite and vaterite with different solubility and the earliest mention exhibiting greatest stability in respect to strength particular for oilfield situations (El Hajj et al., 2015). Equation 2.3 demonstrates calcium carbonate deposition as a result of calcium carbonate precipitation.



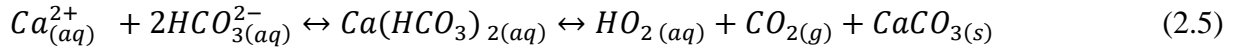
Calcium carbonate deposition is normally attributed to severe pressure drop between reservoirs and well bore, along the production string (tubing, safety valves & chokes etc.) (Moghadasi et al., 2003). Sometimes even further away from well up to the top surface facilities (M. Jordan & Mackay, 2015) such as heat exchanger, separator etc.

Carbonate scale formation is instigated as a result of pressure drop during production leading to supersaturating of formation water with calcium carbonate (Mackay et al., 2006). Therefore, the pressure reduction liberating CO<sub>2</sub> in to gas phase leaving the solution supersaturated in calcium carbonate (Moghadasi et al., 2003). Furthermore, it can occur due to evolution of carbon dioxide as a result of aquifer or connate water exceeding their bobbles point. Henceforth decreasing the carbonate solubility and forming precipice of divalent ions like iron, calcium, and the rest (Jordan et al 2015) as outline by the equation 2.4.

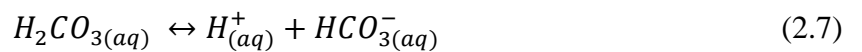


The dissolution of CO<sub>2</sub> and Ca<sup>2+</sup> in brines during production is prime in calcium carbonate precipitation. If the reservoir is static (non-flowing condition) the entire fluid system is expected to be in thermodynamic equilibrium. Continues drop in pressure result to degassing of carbon dioxide, raising the pH in the produce water and calcium carbonate precipitation (Yassin et al., 2006). Also, loss of CO<sub>2</sub> produce fluid in pre-seawater breakthrough age can be another cause of CaCO<sub>3</sub> precipitation.

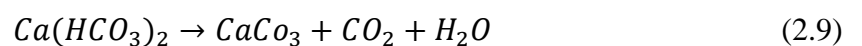
It can also be proven that calcium carbonate solubility is primarily affected by the CO<sub>2</sub> content of water. Since bicarbonate formation increase with carbon dioxide concentration and decrease of carbon dioxide content in an equilibrium system leading to the formation calcium carbonate (Kamari et al. 2014) as illustrated in equation 2.5. Combination of calcium and bicarbonate ion is another likely cause of calcium carbonate scale formation. As a result of some insignificant quantity of ions bicarbonate detach at that pH value equivalent most of injection well to form H<sup>+</sup> and CO<sub>3</sub> CO<sub>3</sub><sup>2-</sup> (Kazemiet al., 2014). Mixture of waters containing real carbonate ions will have high scaling possibilities due calcium carbonate decomposition.



The effect of carbon dioxide partial pressure toward carbonate scale formation should not be neglected because in-depth understanding of brine and CO<sub>2</sub> (in gas phase) chemical reactivity is vital. As most carbonate reservoirs contain the compositions of mineral cement and carbon dioxide. At reservoir condition (high temperature up to 200 °C and high pressure up to 30 MPa) the formation water is calcium carbonate saturated. The equations bellow illustrates CO<sub>2</sub> in contact with water dissolving to form carbonic acid



The decomposition is as a result of pressure reduction leading to liberation of carbon dioxide by increasing the pH (shift in equilibrium of the reaction to the right).Causing precipitation of calcium carbonate once the amount of calcium carbonate out weight that of water (El Hajj et al., 2015) as illustrated in the equation 2.19. While Figure 2.2 illustrates a CaCO<sub>3</sub> inflicted production tubing with different SEM topographical magnifications.



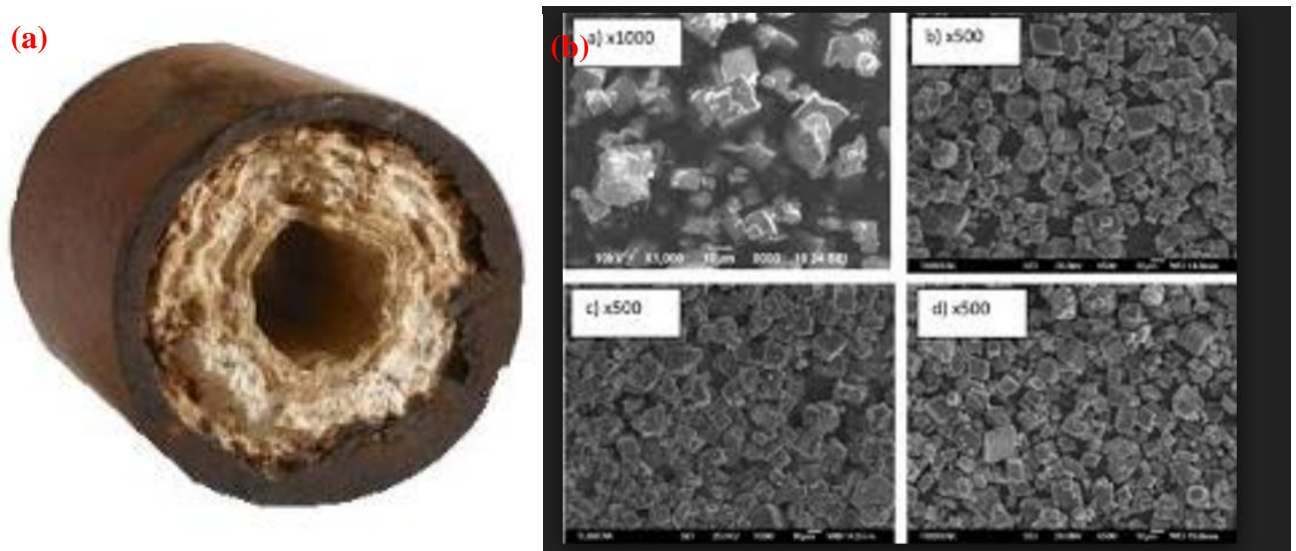


**Figure 2.2:** Calcium carbonate deposit (a) in production tubing, (b) SEM image (Okocha et al 2014)

The side effect of some secondary recovery techniques can be key to carbonate scale formation like the case of geochemical challenges introduce at both producer and injector well due to CO<sub>2</sub> injection. Even thou the geochemical risks attach to the injector well are more attributed to the dissolution of calcite cement or of the rock being weakening by carbonate matrix than calcite precipitation (Jordan M., et al., 2015). Acidification of brine occur with decrease in pH of the brine as a result of CO<sub>2</sub> dissolving it and Figure 2.4 demonstrate the effect of temperature to the three types of CaCO<sub>3</sub> deposits.

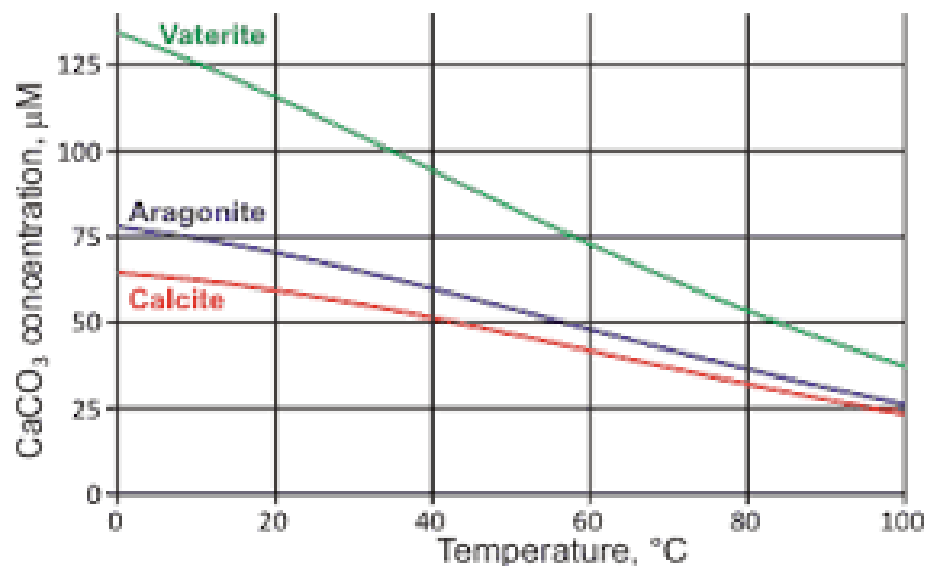


**Figure 2.3:** Effect of temperature to different types of calcium Carbonate (Guan H. et al 2015)

#### 2.2.4.2 Calcium sulphate scale (CaSO<sub>4</sub>)

Calcium Sulphate (CaSO<sub>4</sub>) is mostly made up of calcium and sulphate ion and or traces of other ions if deposited from composite poly-metallic solutions or traces of wax silt and rust if precipitate from oilfield fluid. Even forms solid solution when it co-precipitated with strontium sulphate (Yassin et al., 2006).

It's believed to be one of the most troublesome of the other scale specie, been difficult to remove due to its thermodynamic stability (Bedrikovetski et al., 2005). Limiting its solubility when used in typical organic acid for simulation treatment (Odo et al., 1991) since it is pH independent, it can freely precipitate in an acid environment (post acid simulation treatment). Thereby restricting the chemical removal technique to only when deposited at the reservoir (El-din et al., 2004). Calcium sulphate can cause operational problems at both injector and oil/gas production well (Al-Muntari et al., 2001). Since it can severely damage permeability or damage down-hole equipment due to the impermeable hardness of the scale deposit.

Many scholars have streamlined the major influencing factors in calcium sulphate scale formation to be supersaturation, pressure, temperature, evaporation, ionic strength, pH agitation and contact time. Nonetheless still emphasize is given more to chemical incompatible mixture of two fluids due to water injection, acid simulations as highlighted by many publishers (Al Muntari et al., 2001). For instance the deposition of  $\text{CaSO}_4$  in oil pipes is typically attributed to incompatible mixture of waters at the subsurface during flooding of the producing well (Singh-Gaur, 2019). So also, mixture of incompatible fluid in case of injection (aquifer and sea water) containing sulphate ions  $\text{Ca}^{2+} + \text{SO}_4^{2-} = \text{CaSO}_4$  commonly calcium sulphate (Jordan et al., 2001). Yet still chemical factors were not ruled out as the principle cause of scaling by (Vetter and Phillips 1970). Acidization treatment of lime stone/dolomite in Kangan and Dagan formation were outlined by (Farrokhrouz & Asef, 2010) as the reasons for calcium sulphate formation because of pH increase of the solution.

It has since been established that the solubility of calcium sulphate is critically affected by ion concentration (Abbas 2014). Since  $\text{CaSO}_4$  solubility decreases with temperature increase due to scale mineral deposit being favoured by higher ambient down hole temperature. Calcium sulphate complication may arise due to its polymorph stability under different temperature and ionic strength conditions (stable or unstable polymorphs). As a result of the transition zone between dehydrate, hemihydrate and anhydrite (Vetter and Phillips 1970). Therefore, keeping phase equilibrium into account, solubility will decrease with increase in temperature (Nancollas and Reddy 1974). Even though up to date petroleum engineers remain keen on  $\text{CaSO}_4$  growth at high temperature.

Among the calcium sulphate species gypsum remains the most common and difficult to remove due to its low solubility in water (almost 2.36 kg in  $1\text{m}^3$  of water at  $25^\circ\text{C}$ ). The insolubility of calcium sulphate can increase with increase in temperature (as low as 1.69 kg in  $1\text{m}^3$  of water at  $90^\circ\text{C}$ ) making it more difficult to remove (Delorey et al., 1996, Carlberg and Matthews 1973). This is easily expressed by equation 2.10.



Main influencing factor for gypsum solubility include temperature as the key, pressure and PH value of the solution. The solubility of calcium sulphate is more aided by low pH value and high pressure (Kashib et al., 2014). Pressure drop have been priorities over temperature as cause of gypsum or anhydrite deposition under down-hole condition. Conditional to temperature or ionic strength of the compound can be stable with-it solubility decreasing with increase in temperature (Kazemi et al., 2014). In hotter and dipper wells anhydrite is the most favoured form of calcium sulphate due to it less solubility than gypsum which can be found at temperature up to 100°C and above 100°C. Anhydrite would precipitate straight from solution or dehydrate to form anhydrite in the case of gypsum (Okocha et al., 2014). Seem clear from equation 2.11 ironically express that  $\text{CaSO}_4$  solubility in water increase with increase in pressure and Figure 2.5 elaborates  $\text{CaSO}_4$  inflicted production tubing.

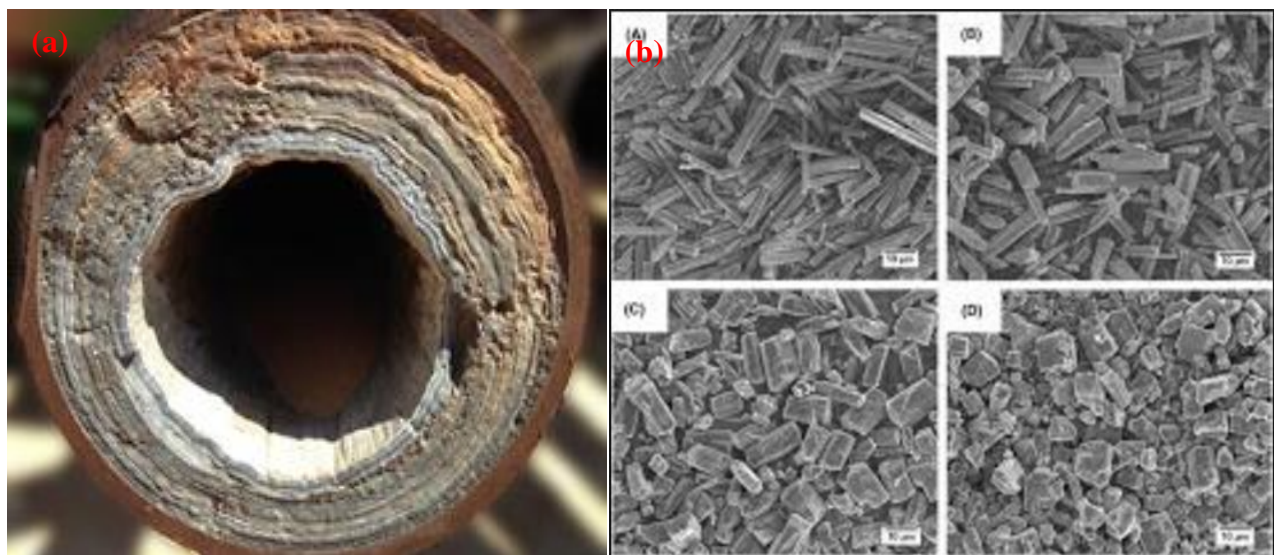
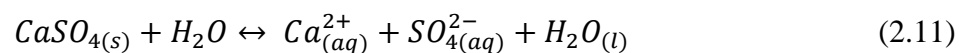


**Figure 2.4:** Calcium sulphate deposit (a) in production tubing, (b) SEM images (Esbaei et al., 2016)

Calcium sulphate saturation index can be complicated for the salt under consideration. Gypsum the most common scale of the three different phases of calcium sulphate occurs at a low temperature (<100°C). While at higher temperature anhydrite the most stable of them is anticipated (>100°C) and hemihydrate around (212°C). In brine solution at temperature below (176°C) gypsum is most likely and any of the three phases is expected to form with gypsum and anhydrite at high end and gypsum at low end if temperature range is between (176-250°C). (Oddo et al. 1994). For the case of hemihydrate is mostly found in no turbulence system with high ionic strength. Therefore, its scaling tendency is not much when using prediction equation of less soluble anhydrite above 250 °F, making anhydrite scale easily ascertain (Moghadas et al., 2003) and the effect of temperature on  $\text{CaSO}_4$  solubility is illustrated in Figure 2.6.

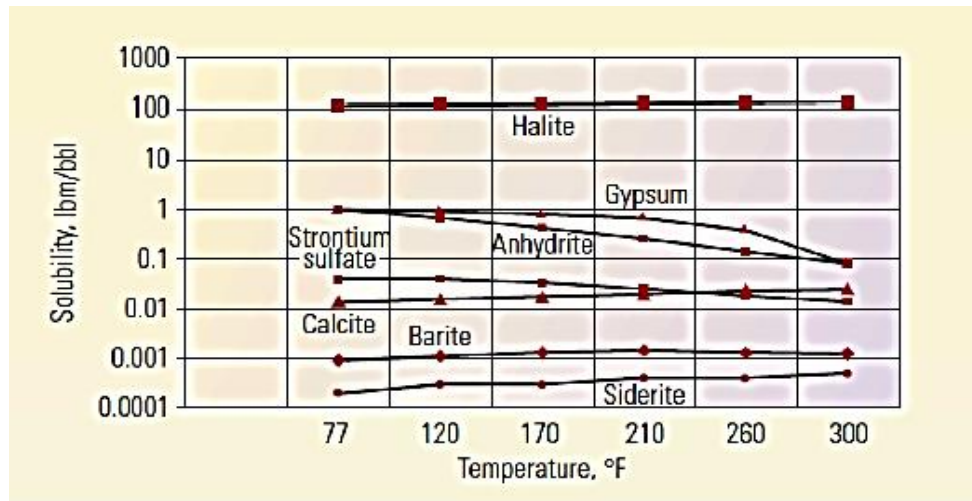


Figure 2.5: Effect of Temperature on solubility of  $\text{CaSO}_4$  (Johnson et al. 1999)

### 2.2.4.3 Barium sulphate scale ( $\text{BaSO}_4$ )

Barium sulphate scale is the second member of the sulphate scale species, have since been term most annoying, costly and insoluble of all alkaline earth sulphate encountered in oilfield operations, which are distance from been solved (Vetta, 1975). This is because its presence in water agitate huge precipitation and serve as catalyst for the formation of the two other sulphate scale species (calcium sulphate and strontium sulphate). Also results show that barite scale may precipitates out of hydraulic fracturing fluid in absence of reservoir mineralogy and sulphate radical formation due to degradation of ammonium persulfate breakers within the fluid (Mackey et al., 2019). Finally, it's not just been the most insoluble oilfield praecipe, its thousand time less soluble than calcium sulphate at surface condition (Abbas 2014) and schematics of  $\text{BaSO}_4$  inflicted production tubing is shown in Figure 2.7

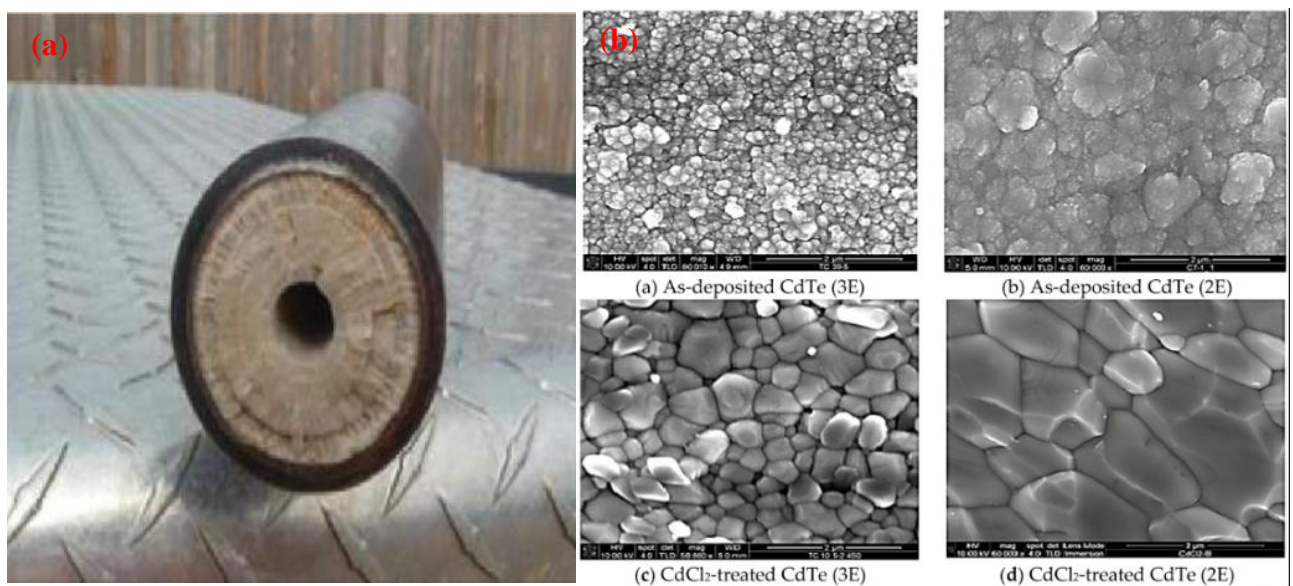
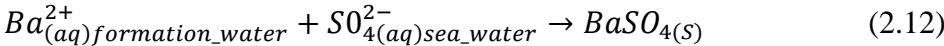
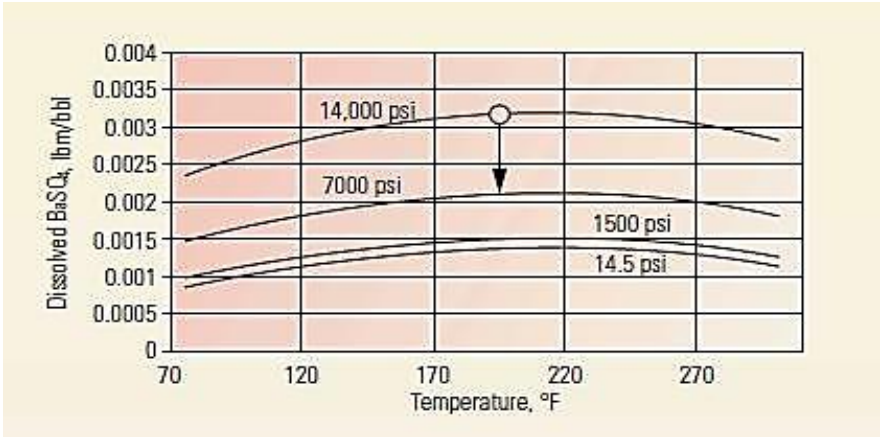


Figure 2.6: Barium Sulphide deposit (a) in production tubing, (b) SEM images (Meeham, 2010)

Formation of barium sulphide scale depends on several sources, composition changes in factors like pressure, temperature, salinity, pH and mixture of two incompatible waters of different compositions. For instance, SO<sub>4</sub> anion of 200mg/l (around 0.02ppg) concentration and above from seawater during injection and diluted water from ground and near ground water environment together with chemically contaminated deep subsurface water associated with oil and gas (Franca et al 2007). Barium sulphate scale remains the principle risk for flow assurance so far seawater is injected into a formation contains barium ions. Its believe to be lower in solubility than calcium carbonate and the other sulphate scale species (Mackay et al., 2003). Once the natural state of the fluids is disturbed leading to the solubility limit of one or more of the components been exceeded barium sulphate will begin to precipitate. Its solubility is found to decreases with factor of two for higher temperature around 200°C and increase by same factor of two with 25°C-100°C temperature range (Franca et al., 2007). Equation 2.12 demonstrates barium sulphate formation based on the source of ionic constituent component:



Barium sulphate scale precipitation prediction parameters are pressure drop, salt content and temperature. Depending on it scaling severity which is tied to rate of scaling and efficiency of chemical inhibitors used (Abbas A 2014). The two ways for barium sulphate scale tendency prediction are analysis of the scale material sample (with poor preventive masseur limitation) and water sample analysis. For examples a strong scaling tendency is assumed when product of Ba<sub>++</sub> and SO<sub>4-</sub> ion concentrations is near BaSO<sub>4</sub> solubility value as suggested by (Vetta 1975). Another prediction basis can be thermodynamic condition related information's (Vetter J., et al, 1975) and kinetics of precipitations (Colins et al, 1956). While the complete scale prediction deposition model will require solubility data of the compound (Gilbart 1982). Its precipitation is more affected by temperature and its solubility increase with increase in temperature, ionic concentration of the brine and pressure (Davis et al., 1971). While the effect of temperature on BaSO<sub>4</sub> solubility is demonstrated in Figure 2.8



**Figure 2.7:** Effect of Temperature on solubility of Barium Sulphate (Meehan 2010).

In the case of saturation index of Barium sulphate, its behaviour is similar to strontium sulphate even though it's less soluble than strontium sulphate under same condition. As most of barium sulphate scale are found containing strontium sulphate (celisite) (Cowan et al. 1967) making it difficult to exist alone.

#### 2.2.4.4 Strontium sulphate scales ( $\text{SrSO}_4$ )

Strontium sulphate scale is the third of the sulphate scale species, more identical to barium sulphate than calcium sulphate, a white crystalline powder and a salt of strontium. Only of recent pure strontium sulphate scale precipitation came to record because it mostly precipitates together with barium sulphate scale (MacMillan et al., 2002). Its principle precipitating factors are similar to that of barium sulphate due to shared behaviour only with more emphasis to mixture of incompatible waters and  $\text{SrSO}_4$  supersaturate produce water. (Yassin et al 2008). A schematic  $\text{SrSO}_4$  inflicted production tubing is shown in Figure 2.9.

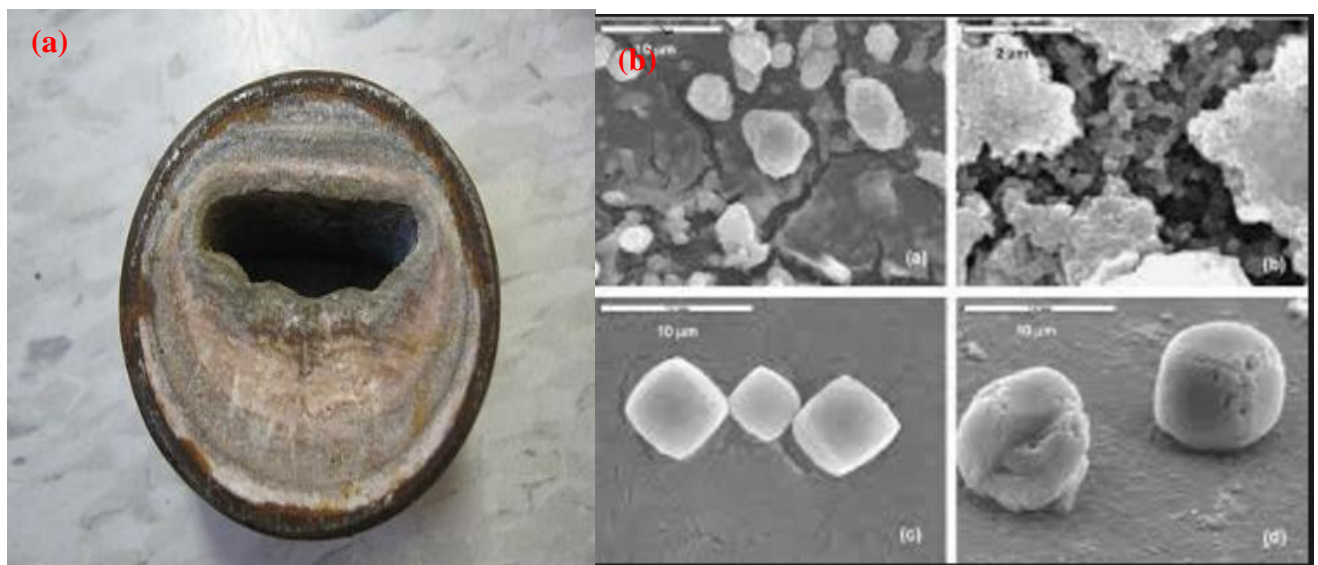


**Figure 2.8:** Strontium sulphide deposit (a) in production tubing, (b) SEM Images (Al Mubarak et al, 2017)

Strontium scale Saturation index is very similar to that of barium sulphate. Even though more soluble than  $\text{BaSO}_4$  with poor water solubility and better solubility in HCl, nitric acid and sodium chloride (Shen et al., 1983), making it presence in most of the barium calcium oilfield scale as celisite.

#### 2.2.4.5 Iron sulphide scale

These common oil and gas problem are more peculiar to sour oil and gas well with iron sulphide ratio as a basis for classification. That decrease as the formed scale comes closer to the well head (i.e. the soft type which is easily removes by acid e.g. pyrrhotite and the hard type not easily remove by acid e.g. Pyrite). It exist in various crystalline forms due to difference content of it sulphur to iron ratio, since iron sulphide is formed as a result of iron and hydrogen sulphide reaction (Mahmoud et al., 2015).

Deposition is inclined toward stabilizing oil water emulsion during secondary recovery (Nasr-El-Din and Al Humaidan 2001). Its physical properties range in various forms, from viscous fluid to oil coated mass or dry powder. Depending on functions like temperature, pressure, pH and age of scale (Taylor et al., 1999) and is mostly present in +2 oxidation state in normal reservoir conditions or +3 oxidation state when at equilibrium most case in the surface facilities

The deposition of water oil absorbing amorphous solid particle (iron sulphide scale) due to presence of hydrogen and sulphide can cause serious operational problems at producer and injection well (Kasinck and Engen, 1989; Nasr-El-Din et al. 2000; Chen et al. 2009). The characterization of the dense and black material that resulted to from the synthetisation of iron sulphide was in good agreement with literature (Jack et al. 2000),(Hafiz, Hoegerl, Alsuwajj, Almathami, & Hughes, 2017). Also Iron sulphide formation is not just tied to changes in temperature, pressure, fluid composition (hydrocarbons, salt and water), iron and sulphide concentration/ratio but the reaction condition under which it forms (Hafiz et al., 2017). It can either be due to injection of high sulphate seawater or production of hydrogen as free gas in sour gas wells (Seto and Beliveau 2000). Even as a result of formation containing iron minerals, iron carbonate compound, other source like chlorite clay minerals and the rest (Taylor et al. 1999). Also, contaminated acid due to mixture with dissolve rust from production tabular and surface storage tank (large amount of iron solution can be produced from desolation of corrosion product and mile scale in acid). While (Hall and Dill 1988) outlines iron (II) and Iron (III) mixture to be, due to mixture rust dissolving in acid during acidization process leading iron scale deposit in both wellbore and formation

Reaction between steel tabular and produce  $H_2S$  as a result of sulphate reducing bacteria (SRB) subject to factors like: pressure, age of scale and temperature of the environment can lead to the formation of different type of iron scale of different properties, crystalline structure and iron to sulphate ratio (X. Wang et al., 2013). So also (Q. Wang et al., 2016) assumes produce  $H_2S$  gas, corrosion of down-hole tabular and fluid from formation with iron mineral content to be the combine effect for iron scale formation .

Iron sulphate under different condition and concentration is more soluble in inorganic acid like HCl but can create environmental safety hazard by releasing high concentration of  $H_2S$ . Increase corrosion tendency for down-hole metallurgies especially in high temperature well (Wang et al., 2013). Not easily soluble or remove by organic acids like gluconic, glutamic, succinic and maleic acid and better removed by chelating agent like EDTA and DTPA at PH value of 6 and 25W% concentration can yield a 40 g/litre solubility of iron sulphide. Though the mixture acid and chelating agent have been proven inefficient (Elkatatny & Fahd, 2017). While of recent (Hafiz et al., 2017) have proven otherwise through the polymer-based and THPS dissolvers using synthetic iron sulphide.

The seven-solid phase of Fe-s system is used in presenting solubility state of iron sulphate since each of them is characterized by different solubility behaviour. The bisulfide ion as given in equation 2.13: chosen to be a better method of presenting the solubility product of iron sulphide due to the uncertainty of the second ionization constant (Rickard & Luther 2007). Also Figure 2.10 illustrated sulphide inflicted production tubing.

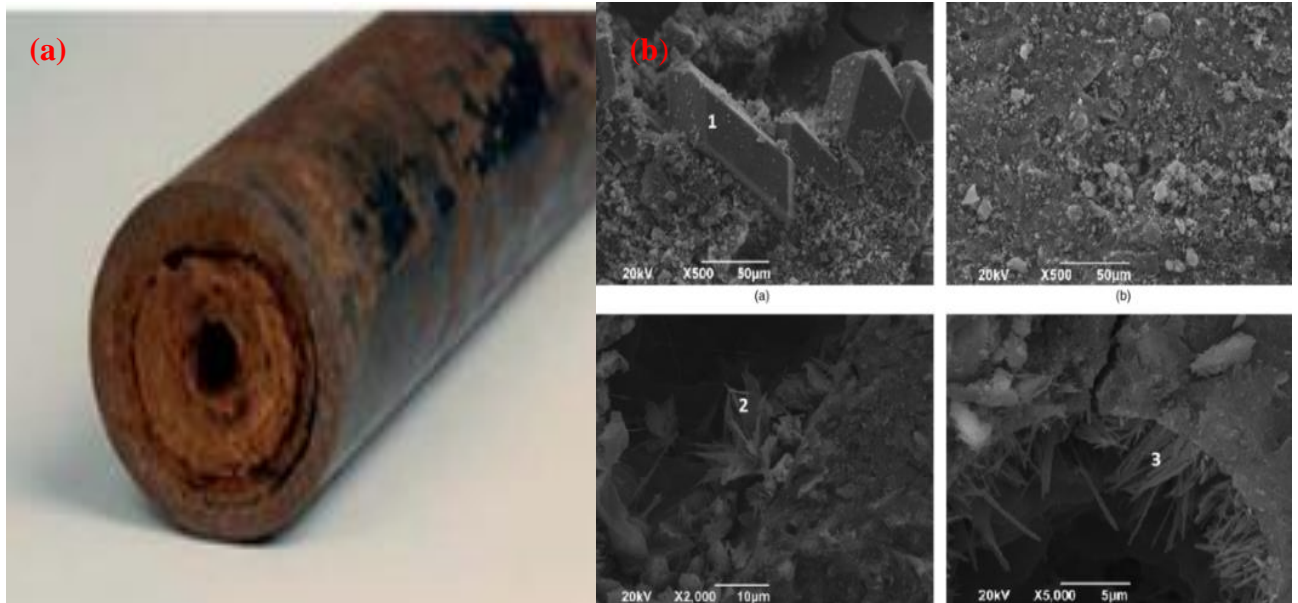


**Figure 2.9:** Iron sulphide deposit (a) in production tubing, (b)SEM Images (Mahmoud et al., 2015)

Pyrite ( $FeS_2$ ): Is the most stable of iron sulphide scale and has weak solubility in HCl acid. Possibly generated as a result of secondary reaction of non-stoichiometric iron sulphide (Ford et al. 1992), such as Pyrrhotite in a wet gas environ.

Pyrrhotite ( $Fe_{1-x}S$ ): Mostly associated to  $H_2S$  and high temperature (Shoesmith et al. 1980). Been a non-stoichiometric group of iron sulphides makes their classification more difficult (Vaughan & Craig 1978). With number of poly types of hexagonal or mono-clinic crystal symmetry with numerous poly types occurring with same spacemen (Buali et al., 2014) Also terms as magnetic pyrite, due to it colour similarities to pyrite.

Troilite ( $Fe_{1-x}S$ ): Known to be the stoichiometric end-member phase of monoclinic pyrrhotite group, without vacancies in its atomic structure (X is 0 to 0.2). It's mainly found in meteorites, and can basically be categorize as a subset of pyrrhotite

Marcasite ( $FeS_2$ ): Basically, known to be the intermediate disulphide between pyrite and nonstoichiometric iron sulphides with iron sulphide of cubic crystal structure been the major physical and crystal difference with pyrite. Simply polymer of pyrite with an orthorhombic crystal structure and

oxidization, acid condition and anoxic condition at high temperature of 220°C can be the agent of the transformation (Qian et al. 2011). White iron pyrite as sometimes referred to though physically and crystallographically different from pyrite.

Mackinawite (FeS): lone crystalize result from H<sub>2</sub>S by ferrous iron precipitation or it salt at temperature lower than 100°C without oxidant (Berner, 1964). Describe as a low temperature preferential iron shilphide scale, normally occurring in low temperature aqueous solution (Morse et al, 1987; Richard and Luther, 2007). In order words described as a distorted, close packed, cubic array of S atoms with some of the gaps filled with Fe.

Greigite (Fe<sub>3</sub>S<sub>4</sub>): Serve the intermediary role in the formation of mackinawite or pyrite (Benning et al. 2000). Since it cannot directly form from solution but transform from pre-existing mackinawite (Hunger and Benning, 2007). Though with time transform to more stable marcasite or pyrite (Schoonen and Barnes, 1991). The formation of marcasite is not only pH dependant but attaining the intermediate sulphide species critical concentration threshold (Qian et al 2011). Either oxic or anaerobic conditions through dissolution-precipitation mechanism can aid the formation of both marcasite and pyrite.

#### **2.2.4.6 Ferric compound scale**

Ferric iron are usually introduce to the well through either drilling fluid or simulation acid (Almubarak et al., 2017) . Which only occur during spent acid flow back at the presence of H<sub>2</sub>S by reducing ferric ions **into** ferrous ions (Lovley, 1991; Pyzik and Sommer, 1981) with iron sulphide believed to be the product of the precipitation by (Richard and Luther, 2007). It's clear that large chloride irons from combination of high chloride concentration at low pH and will encourage crystal structural stability and formation of akaganeite (Cornell and Schwertmann, 2003). Additionally, (Vella 1997) cautions that the high amount of heat generated from the oxidation of dry sulphide can cause explosion

Since sulphide is vulnerable and liable to both oxidation and swift reaction between atmospheric oxygen and fresh mackinawite. Just as proven by some lab work forming a thin layered mill scale during builds up process consisting of magnetite, hematite and wüstite (Benchiheub et al. 2010). So, the absence of H<sub>2</sub>S can aid the transformation of a less stable one to a more stable one over time (Murad 1983). Also, through two distinct mechanism ferrihydrite can generate either goethite in a solution from dissolve Fe (III) ions through the dissolution of ferrihydrite or internal dehydration and re-arrangement within ferrihydrite aggregate to produce hematite.

Ferrous compound scale: FeS most known as iron (II) or ferrous sulphide are iron-deficient non-stoichiometric. Black or brown leading to colour of sludge, insoluble in water. Produce from hypoxic conditions like dead zone of lakes and swamp due to presence of sulphide reducing bacteria (SRB) in the water most time reacting with metal ion to form metal sulphide. Figure 2.11 illustrates the pH effect

on the stability of various iron sulphide and scale composition deposit in sour gas well. Also, the summary of the entire scale compositional chemistry is presented in Table 2.1.

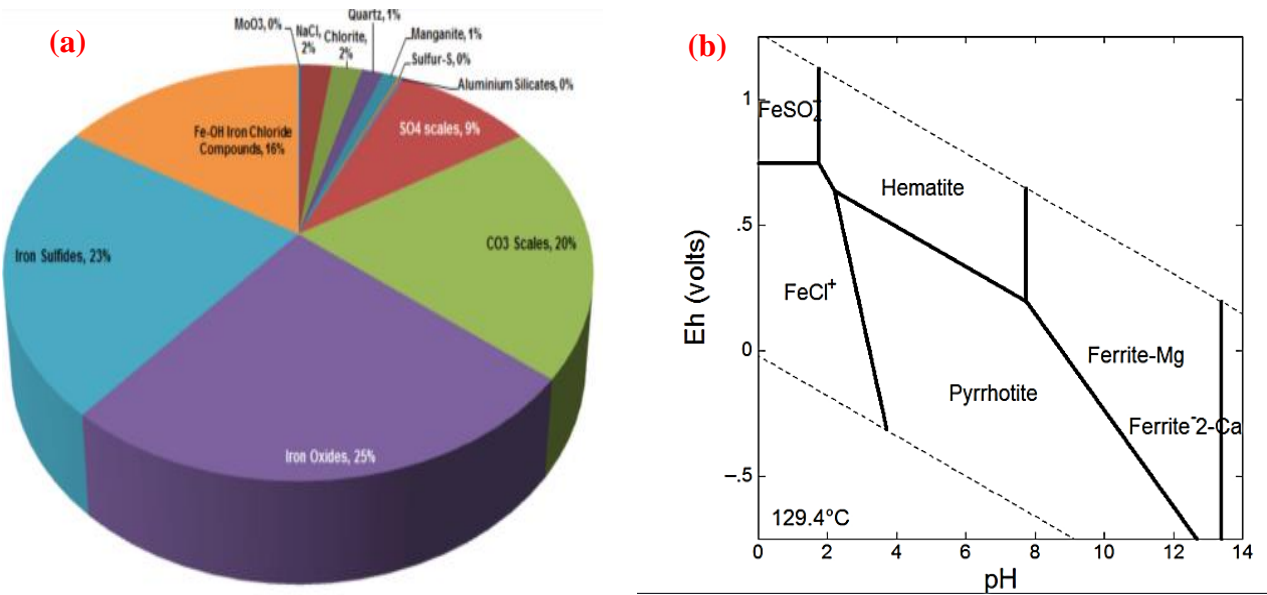


**Figure 2.10:** Scale deposit composition in X Sour Gas (a),(b) stability of various iron Sulphide in respect to pH (Al-Bauli et al. 2015)

## 2.2.4.7 Summary of scale chemistry

**Table 2.1:** Summary of Scale chemistry

Summary of oilfield scales type				
Organic scales				
Name	Chemical Formula	Mechanical Properties	Principle variables	Abundance
Asphalten	Asphalten are normally Polycyclic aromatic hydrocarbons, that may include many substituents like alkyl groups & heteroatoms (e.g. N, O, or S)	Are molecular substances that are found in crude oil, along with resins, aromatic hydrocarbons, and saturates	Physio-chemical properties of fluid Like increase in temperature differential, residual time and decrease in flow rate	Deposited at borehole near formation, the downhole pump, the tubing, surface flow lines, separators, storage tanks and pipelines and submerse pump
Hydrate	Compound containing water with definite mas in H <sub>2</sub> O form and transform to anhydrite when it loses it water molecules	Water evolution when subjected to heating, also solubility of its anhydrous residue in water and when dissolved in water the residual hydrate colour is reverse to the colour of the hydrate	Agitated by hydrate forming gas molecules supply, change physiochemical parameters (high pressure and low temperature) and water supply accessibility	Associated problem found in natural gas and oil pipeline together with other heavy carbon deposition problems like wax and asphatenes
Paraffin	C <sub>n</sub> H <sub>2n+2</sub> Since in chemistry it used Synonymously with alkaline	A white tasteless colourless solid product of petroleum product with 20-40 carbon atoms of hydrocarbon molecules with density around 900 kg/m <sup>3</sup> , soluble in benzene and some esters and insoluble in water with 46 and 68 °C range of melting point	Increase in temperature differential, residual time and decrease in flow rate	Deposited at borehole near formation, the downhole pump, the tubing, surface flow lines, separators, storage tanks and pipelines and submerse pump

Most common oilfield scale / inorganic scale				
Name	Chemical Formula	Properties	Principle variables	Abundance
Calcium Carbonate	CaCO <sub>3</sub>	It's an odourless, fine white powder with 2.71 g/mL density and 1,339°C melting point at its calcite form. Aragonite, been most common form that has a density of 2.83 g/mL and melting point of 825 °C.	Partial pressure of CO <sub>2</sub> , temperature, total dissolved salts, pH	Found in Limestone formations and deposited along reservoir, borehole and production conduits
Calcium Sulphate: Gypsum Hemihydrate Anhydrite	CaSO <sub>4</sub> .2H <sub>2</sub> O CaSO <sub>4</sub> .1/2H <sub>2</sub> O CaSO <sub>4</sub>	A white to offwhite powder with 2,525° C melting point and 2.5 g/cm <sup>3</sup> density that is insoluble in water	Total dissolve salt, pressure and temperature	Product of mixture of injected sea water and calcium contain formation that can deposit at reservoir, borehole and production conduits
Barium Sulphate	BaSO <sub>4</sub>	Decomposing white solid with 4.25 g/cm <sup>3</sup> density and 2,235 °C melting point	Temperature, pressure & dissolved salt	Product of injecting sea water containing sulphate into sandstone formation and most deposited from down production system all the way the production conduct
Strontium Sulphate	SrSO <sub>4</sub>	Coexist with barium sulphide almost all the time	Pressure, temperature and total dissolve salt	Share same properties with barium sulphide
Iron sulphide scale				
mackinawite	FeS	Its bronze to grey-white colour tabular crystals of mineral sulphite and anhedral masses. With 2.5 Mohs hardness value and 4.17 a specific gravity.	precipitate from aqueous solutions with metastable material as its main constituent	Mostly found in mineral of low temperature aqueous environments
Cubic	FeS	A blue-black or pinkish chemical compound of iron and sulphur with 4.049 g/cm <sup>3</sup> density and 295.805 molar mass	Highly unstable	not found in natural sate
Troilite	Fe <sub>1-x</sub> S	An Opaque material of bronze brown and grey brown colour with 4.61 average density	Stoichiometric end member of the Fe <sub>1-x</sub> S group. x is between 0 to 0	Normally found in meteorites

pyrrhotite	Fe <sub>1-x</sub> S	A nonstoichiometric variant troilite. Also known as magnetic pyrite due their similarities in colour thou less magnetic	Approximated in two forms Fe <sub>7</sub> S <sub>8</sub> for the Monoclinic while the hexagonal has Fe <sub>10</sub> S <sub>11</sub>	Most abundant iron sulphide in the entire solar system, Earth even though rare in marine systems
smythite	Fe <sub>9</sub> S <sub>11</sub>	An Opaque brownish black, bronze-yellow Metallic compound. Brittle with 4½ on Mohs scale value	Metastable phase associated to the Fe <sub>1-x</sub> S group	Mostly found in hydrothermal system and more associated to carbonate though very scarce
Greigite	Fe <sub>3</sub> S <sub>4</sub>	Sulphur equivalent of the iron oxide magnetite with 4 to 4.5 Mohs scale hardness index and 4.049 specific gravity	Metastable Fe <sup>II</sup> Fe <sup>III</sup> sulphide; named the thiospinel of iron	More peculiar to freshwater system and its fairly widespread
pyrite	FeS <sub>2</sub>	A greenish black streak compound with 6 to 6.5 Mohs scale hardness index and 4.9 to 5.2 specific gravity.	Nick named the Fools Gold and a stable Iron (II) disulphide	Most dominating and abundant mineral on the surface of the Earth
marcasite	FeS <sub>2</sub>	Also known as white iron pyrite with orthorhombic crystal structure of Pale bronze yellow to silvery yellow on fresh surface with Dark grey to black streak	Metastable iron (II) disulphide	Locally found in mineral present in hydrothermal systems and in sedimentary rock

**Iron compound Ferric Compound Scale**

Name	Formula	Properties	Principle variables	Abundance
Ferrous Carbonate Ferrous Sulphide Ferrous Hydroxide Ferrous Hydroxide	FeCO <sub>3</sub> FeS Fe(OH) <sub>2</sub> Fe(OH) <sub>3</sub>	The fourth most common element in the Earth's crust with wide range of oxidation state of -2 to +7 characterise with high pressure and temperature and atomic number of 26.	Corrosion dissolve gases and PH	Mostly found across the entire earth crust by weight and also the sun and star. Usually deposited in tabular of sour high temperature wells.

## 2.3 Scale management

Scale management strategy have for long remained at the centre of attraction of flow assurance having direct implications across all the production technologist basic responsibilities. Ranging from well productivity, well completion, well simulation, associated production problems, remedial and, artificial lift/productivity enhancement and surface processing cutting throughout workover of the life of a field. Hence (Farrokhrouz & Asef, 2010) believe that proper adaption of scale management plan will enhance production index and assure safe and easy production of a well for a long time.

Effective scale management strategy has been based on treatment philosophy of prevention is better than cure. ‘‘The right motto of preventing the re-occurrence of scale’’ (Ghouri, Ali, Shah, Ejaz, & Haider, 2018). Putting to consideration economic, production, time and safety of rig component, personnel and well environment. These comprises of two vital processes of risk assessment and economic evaluations that are applied throughout the field life cycle. Risk assessment allows the prediction of possibility of mineral scale production, location and severity to be reviewed against current and future field development alternative. Through allowing existing and near market scales control techniques to be justifiably evaluated for effective scale control strategy identification. While the second process (economic evaluation) is all about using modest economic models to compare, justify and identify the most cost effective scale management solutions from does identified during the risk assessment process phase at the CAPEX Phase of the field (M.Jordan et al., 2001). Lastly identify situation and stages were scale control can be uneconomical like the case of some marginal field were cost of treatment might exceed lifting cost (Mackay et al., 2003). Un-doubtfully over estimating threat can lead to installation of unnecessary completion that can be economic burden to the CAPEX cost and potential maintenance issues in the OPEX phase. Since (Graham et al. 2002) has generalized that the far away the scale deposition is from surface facility the more difficult it’s to manage

In cooperating scale control as part of asset life cycle management is vital. For instance, developing a scale control treatment strategy at the project development stage rather than plateau, decline or decommission development stage. Since scale control in life cycle management is subject to various challenges attributed to rise in water cut, as well transit from dry production to high water cut production. This more preferred approach by (Mackay et al., 2003) because it permit the choice of suitable economic technology and incorporation of appropriate remedial technology in both completion design and installations.

Predicting, assessing the severity and location of scale problem in a new field that can be done by calculating the mass of expected scale deposit using thermodynamic and kinetic calculation. Even though, the case of location of scale formation are still lagging. It can aid the selection of preventives majors like inhibition treatment in reservoir or near wellbore infiltration modelling brine mixing and stripping of scaling ions before the production/injection fluid reaches the wellbore in more severe case (Jordan & Mackay, 2015). Which are both are attributed to CAPEX phase (e.g. in cooperation of desulphation plant) and OPEX (e.g. scale squeeze treatment)

### **2.3.1 Scale prediction/monitoring**

The area of scale risk evaluation or prediction has improved over time. Evolving from simple empirical thermodynamics calculations and limited solubility data to predicting potential of scale formation by Stiff and Davis (1952a, 1952b), Oddo and Tomson (1981), Vaone and Skillern (1982). Recently, Oddo and Tomson (1997) (Moghadasi et al., 2003). Then the introduction of commercial software prediction tools like, MultiScale<sup>†</sup>4 (PetroTech<sup>†</sup>), ScaleSoftPitzer<sup>†</sup> (Rice Brine Chemistry Consortium<sup>†</sup>), and Scale Chem<sup>†</sup> (OLI Systems<sup>†</sup>). Utilise for predicting expected type of scale to be formed, probability of scale formation and maximum scale amount. Working on the principles of thermodynamic only instead of kinetic equation (only few models incorporate kinetic parameters) which is not satisfactory. Since factors like nucleation, adhesion, kinetic of crystal growth and other important factors are not considered. Lately scale prediction tools are combining with other simulators for more accurate scale risk prediction result. Examples include Eclipse<sup>†</sup>, Streamline/Frontsim<sup>†</sup> (Wahid et al., 2011), statistical models like principal component analysis<sup>†</sup> (Skeck et al., 2008). Also scholars like (Guan, 2015) reported geochemical models such as Ion Reaction<sup>†</sup> model from Heriot-Watt University and combination of models with hydrodynamic prediction tools like PIPESIM<sup>†</sup> and computational fluid dynamics (CFD)

The latest development is not limited to considering the thermodynamic, kinetic and hydrodynamic conditions that leads to precipitation of scale forming compound. For accurate scale prediction method, but in addition consider all conditions that will leads to adherence of the precipitate or precipitating compound. The area of squeeze inhibitor placement was taken care of by the introduction of Squeeze V/VI<sup>†</sup> series software manufactured by Heriot-Watt University widely used by the industries today (Guan 2015). While the existing gap in reactive transport modelling for calculating the impact on pH of reservoir geo-chemicals reactions toward producer well for effective development of scale management programme have finally been solved. Through the introduction of numerous 1D reactive transport models like PHREEQC and Geochemist's Workbench and for the important of brine rock and brine mixing interaction been affected by 3D flow in complex reservoir system. 3D Simulation and reactive transport codes like GEM, STARS, Reveal, UTChem and TOUGHReact are utilize for EOR (ASP and

CO<sub>2</sub>-WAG) flooding chemistry predictions (M. Jordan & Mackay, 2015). Advancement in the area of subsea scale prediction includes laboratorial, analytical, modelling and hardware technology has been archived through introduction of MARS system, and CIMV technologies (Gaun 2015). For the effective scale management like identifying where exactly scaling water is coming from (formation zone), expected location for scale deposition and most effective ways of managing it.

### **2.3.2 Scale prevention**

Oilfield scale inhibition is a preventive measure or process of avoiding or mitigating scale deposition from hindering flow assurance at any location of the entire production system. Using special class of chemicals to slow or poisoning the scale process of growth in water system. It's not just the key integral of the scale management system but for both flow assurance and production economics. Likewise, suggested by (Jordan et al., 2001) that the pre-production treatment of reservoir to avoid scale formation near the well bore, the utilization of continues injection (capillary & gas lift) to control down-hole scale. In additional with adhering to squeeze treatment strategy as the production well transit within their life cycle and water cut rises will eliminate unnecessary economic burden at the OPEX phase will have a tremendous impact toward the economy of field.

Chemical inhibitors (solid or chemical in soluble or emulsified form) are special chemical of either organic or inorganic set of chemicals: Like organo-phosphorus compounds (phosphoric acid salts and organic phosphate ester), phosphates (sodium tripolyphosphate and sodium hexametaphosphate) and phosphates (sodium tripolyphosphate and sodium hexametaphosphate) (Weintri et al., 1979). That could be applied as preventive major in a form of squeeze treatment prior to water breakthrough. Since water break through onset will increase both mass and severity of the scale by increasing the required minimum inhibitory concentration (MIC) and amount of inhibition to control the scale. The solid scale inhibitor is usually applied through the rat hole or retained with in the propped fracture and utilising scale impregnated proppant. While the liquid type scale inhibitors utilise the conventional squeeze treatment method of enhance adsorption (Colinset al. 1997). Either precipitation (Yuan et al., 1995) or even emulsion droplet entrapment (Williams G et al., 2001) & (Kelly R et al., 1992) deployed with fracturing fluid during fracture operation

Also, liquid system subsequent to 'data' fracture or even as squeeze treatment during well clean up or post fractures operation prior to water breakthrough (Collins et al. 2001). Gas lift, inlet of electric submersible pump and capillary string run above the packer are main medium of deploying liquid inhibitors (Jodan M et al., 2001). Bypass feeder cane are used to deploy the solid controlled-solubility phosphates (Cowan J et al., 1976). Bottom hole well packs (Sloat1963), baskets and filter packs,

(pattonet al., 1977) and formation squeeze-fracturing. (Timsley et al.,1967) are additional inhibition deployment mediums.

The most renowned method of pumping or applying scale inhibitor in the oil industries today are either by pumping inhibitors into the system through squeeze and bullhead method. The first is considered as the simplest or continues chemical injection through capillary string or gas lift method (Esbai et al., 2016) and only effective in the absence residual scale in the system because the inhibited formation fluid can further deposit scale on existing scale surface.

Of recent, the case of *Fadili* reservoir of *Alwali* field were utilizing only treatment pressure, quantity of the residual acid volume and wire line dummy runs detected calcium carbonate deposition along the tubing and flow line. With tendency of halving production of 1500BPD and over 90% water cut in four months approximately 20 to 30 BOPD drop per well for the five *fadili* horizontal inflicted wells. After the application of continues scale inhibitor injection through gas lift method and adhering to extensive product selection process by chosen the product with the best chemistry that can endure the expected harsh application at good economic cost. Through series of testing protocols like compatibility, gunging tendency, temperature stability, compatibility with other treating chemicals and effective performance at lower MIC. It successfully resulted to the optimization of volume of acid used compared to the amount of scale measured by reducing both risk and cost. Likewise permit the conversion of the three of the wells to annular gas lift producers and return production to 240 BOPD (Esbai et al., 2016). These can serve as our first successful post inhibition scenario.

Most amazing is the combination of scale removal and scale inhibition treatment at once. It demonstrates numerous opportunities of reducing the well intervention cost through single intervention operation that will offer both economic benefit and reduction in well intervention risk. The risk of precipitation during simulation treatment is reducing by assurance of inhibition of simulated zone. Through pumping combine treatment which directly protect value added by the scale removal treatment (Smith et al., 2000). Since the options of choosing inhibition or regular simulation are cost driven and attributed to high operational cost. Although, it's had since been established that despite planned inhibition scale can be deposited before scale inhibition deployment or at the end of the treatment life of the scale inhibition. Therefore, the requirement for simulation treatment in many wells to remove calcium scale is deem necessary.

Challenges like optimizing economic benefit of the combine treatment in comparing with the cost of sequential treatment and inhibition treatment. Also, corrosion control assurance by avoiding significant altering of the corrosively of the simulation system by the scale inhibitors, its compatibility to the formation fluid and the simulation system in both live and spent. So, the adverse effects of combine flow

back of combine scale removal and inhibition treatment (live and spent) toward the surface processing system. Finally, the effective adsorb onto the formation within the entire potential pH ranges of the simulation system (live and spent) are attributed to operations conditions.

Since despite the identification of HCl to be effective in calcium scale removal inhibition adsorption and system compatibility remain difficult in combine treatment. Contrariwise chelating agent-based scale dissolvers proves better in corrosion control and scale inhibitors when spent with consequences of higher cost. Than the organic acid which offer a compromise that allows most of the system requirement to be meet (Smith et al., 2000). Thereby tying the success of formulating a combing scale inhibitor and removal system to the tailoring of scale inhibition selection to the simulation system requirement. The availabilities of calcium carbonate scale inhibitors with effective adsorption under high acid conditions. The inability of preventing the precipitation of calcium salt of a wide range of scales inhibitors with calcium chelation by scale dissolvers and the threshold scale inhibitor concentration above which corrosion control in HCl acid system was lost.

### **2.3.3 Economics of scale management**

The economics of scale control is more subject to how well scale prevention strategies are incorporated in CAPEX phase of a field to reduce removal and inhibition cost during the OPEX phase. While the case of existing scales is the comparison of the cost of descaling to the expected increase in production or cost of lifting in monetary aspect. The adaption of simple economic models to assess available scale management options during the field life by quantifying the value of the treatment in terms of \$/bbl. of oil protected to prevent the cost of treatment from exceeding the cost of lifting. This is achieve by considering and ranking various cost of scale related intervention against the development type (Jordan et al., 2001). Since in highly severe scaling environment, the cost of production loss cause by scale damage combine price of scales prevention is projected to cost more than \$15/bbl produce oil making scale control to be more than a critical issue. (Mackay et al., 2003). Similarly (Nasr & Burby, 2006) reported that British Petroleum groups (BP) spent over £2M per annum on mineral scale control budget for it North sea managed wells which 20% of the losses were attributed to scale removal and inhibition .

## **2.4 Scale removal techniques**

Scale management have been based on the prevention is better than cure philosophy. Like mineral concentration control in water and acidizing management for scale prevention still considered most economical way of scale avoidance. Nevertheless in the case of already deposited scale, emergency and

rapid techniques response (cure) is the only option (Farrokhrouz & Asef, 2010). Since it's clear that even with proper plan scales management strategy in the CAPEX phase of fields scale can be deposited either before inhibition deployment or at the end of the inhibition treatment life (Smith et al., 2000). Thereby limiting the solution to the OPEX phase removal techniques (Mechanical or chemical descaling techniques). Worst case in the past a full rig work over to replace the production tubing contrary to the prevention is better than cure scale management philosophy.

The choice of the descaling techniques and tools have been govern by the knowledge of type, texture , quantity and composition of the scale to be remove (Alabdulmohsin et al., 2016). Both mechanical and chemical removal approach are effective and truly depending on physical property of the scale and it location (Salami et al., 2010). For instance chemical (dissolution) or mechanical (milling or jetting) or rig workover when the cost of pulling and drilling out the deposit is relatively cheaper (easily assessable and shallow land deposit location) (Alabdulmohsin et al., 2016).This leaves tools and techniques selection on the hands of operational limitation of the tools and techniques in question. As at up till now, no tool or technique have proven universally applicable to all scale types, formation or fields (Gholinezhad, 2006).Sometime conflicting success and failure result from same tool or techniques run in two similar cases can be attributed to unknown, unwanted or unpredictable problems and the diversity of parameters and down-hole governing criteria. Therefore, the idea of imposing absolute ranking of the tools through comparison will be difficult due to range of applicability of each tool. Even though, factors like deploying unit, cost, and application area, available diameters and potential of removing hard scale can be considered (Gholinezhad, 2006). For instance, chemical HCl approach will be effective for scales like calcium carbonate and mechanical approach (mill by utilizing oscillator) the best solution for completely plugged well since it might take jetting approach longer time

### **2.4.1 Effective descaling operations**

A descaling approach is considered successful or effective only if it capable of regain the inflicted well accessibility with corresponding increase in production; In an economical (total cost associated to scale removal in comparison to the rate of revenue generation from post descaling result) efficient (descaling time), safe (safety of the personnel). In addition to integrity of (the well and its completion/equipment condition) simple (uncomplicated with less job) environmentally friendly way (to the well and its environment). However, this proves difficult to achieve since the inception/revolution of scale removal techniques/tools. Despite the suggestions of a quick and non-damaging to any of the production system remedial approach by (Alabdulmohsin et al., 2016). Another key for a successful descaling approach is design and execution of effective descaling operation program (Mukhliss et al., 2014) which depend on:

- i. Scale in question (type, size, texture composition and location of scale)

- ii. Well conditions (pressure limitation conditions of the well i.e. integrity and well control: underbalance, overbalance or balance determining the need of well isolations)
- iii. Well architecture, completion design and location (determine the selection of descaling down-hole tool and conveying equipment such as CT size)
- iv. Operational condition (rate limitations for effective scale debris transfer to surface i.e. solved by the introduction of enhance transportation fluid)
- v. HSE policy (content of H<sub>2</sub>S encountered during operation and surface handling of flow back materials i.e. PFMS availability)
- vi. Budget and project economic viability of the operations (the enhancement of project payback time alongside projected production increase, logistics and associated cost of mobilizing and deploying tools and equipment and technical risk of executing the program).

Only few among the successful combine treatment (mechanical and chemical) result including situation and limitation. In addition to program design/execution and post descaling result of some notable scale inflicted wells around the globe will be discuss in these junctions. Keeping the reaming successful solo approach (mechanical or chemical) for discussion in their forth coming subheads.

Starting by singling out the case of Saudi Aramco operated sour gas production field in Saudi Arabia. This is among many carbon steels wells whit history of producing gas with mole percentage ratio of H<sub>2</sub>S at high temperature around the globe. Also, similar field scenarios such as Canada (Milligan 1982, Dougherty et al 1994, Teevens 1987), United States (Place 1992, Smith and Pakalapati 2004, Kapusta et al. 2008). Saudi Arabia (Kasnick and Engen 1989; Nasr-El-Din et al. 2007), France (Guiraudet 1974), United Arab Emirates (Morsi 1994) and Iran (Yeganeh 1979). All Attributed with extreme conditions such as 256-320°F buttonhole temperature, 1-23 of H<sub>2</sub>S mole percentage in gas and a scale composition that corresponded with as function of depth (Al-Muntasheri G et al., 2015). This was due to successful post descaling operational result that lead to the recovery of 316 kg of solid at the surface in one instance. Subsequently (Buali et al. 2014, Mukhliss et al. 2014) reported an increase in the well gas production and overall obtainable gas reserves

Chemical approach: Inhibition difficulties and freely occurrence of iron sulphide in sour environment makes FeS scale prevention and removal tedious. Also, by utilising iron sulphide dispersant to keep iron sulphide in produce water and avoid iron sulphide precipitation. Further complications like rapid generation of H<sub>2</sub>S from the result of strong mineral acid utilization (X. Wang et al., 2013).The interference of the dissolving power of HCl acid by both hydrogen sulphide scavengers and iron control agent (Nasr El-din et al., 2000) prompt the introduction of mechanical techniques in to the descaling programme flow chart.

Mechanical approach: Begins by the utilization of a zero-formation damage temporary reservoir isolation technique (Buali et al. 2014, Mukhliss et al., 2014). Followed by that of fluidic oscillation technology cleaning device (Webb et al. 2006, Leal et al. 2007, Buali et al. 2014). Together with a high pressure-jetting tool with a down-hole motor or turbine attached to mills lead to effective iron sulphide scale removal (Bolarinwa et al. 2012, Mukhliss et al. 2014). (Leal et al. 2007; Buali et al, 2014) had reported the current utilization of mechanical method in southern area.

The second scenario is still a Saudi Aramco operated gas well, *Kuff* gas wells to be specific. Were many of the wells are suffering from combine organic and inorganic scale deposit (iron sulphide, iron oxide and calcium carbonate) resulting to poor well bore accessibility and weak production. The concurrent history of failed combine descaling operations (mechanical through coiled tubing and chemical dissolves through CT or Bull heading) between the years 2007 to middle of 2010 lead to suspension of the approach. Leading to the introduction of newly innovated integrated mechanical descaling procedures that lead to successful descaling result like production restoration and wellbore accessibility (Bolarinwa et al., 2012). In addition to changing unsafe and complex interventional operation to safe and conventional CT Intervention by eliminating rig work-over requirement

First stage includes temporary reservoir isolations to eradicate H<sub>2</sub>S return to surface followed by cleaning with safe solid handling at low choke pressure to enable a close system and minimum surface testing equipment's. While the second stage focuses on eliminating the long soaking time and/or H<sub>2</sub>S generation during chemical dissolution through a mechanical approach consisting of a design high pressure jetting tool conveyed on CT for hard scale removal purpose. That optimizes the utilization of large outside CT string diameter for clean out and combine with special high temperature gel for sufficient lift and reducing the risk of stuck pipe (Bolarinwa et al., 2012). Which resulted in the control and enhancement of scale removal treatment.

## **2.5 Chemical descaling method**

Chemical scale removal method: Are descaling approaches that are based on the utilization of dissolutions mechanism of inorganic (mineral) acid like HCL/HF, organic like maleic, glutamic, succinic, and gluconic. Likewise, challenging agent like EDTA, HEDTA and the rest. In order to effectively remove scale in any part of the production system. Most time considered the cheapest, first and conventional solution for non-easily access scale deposit were mechanical intervention are deemed non economical and ineffective to deployed.

The technical knowhow of how treating chemicals access the scale surface in term of surface to volume ratio or surface to mass ratio are the governing factors for archiving successful chemical treatment.

Reason why the small surface area for large total deposit mass in case of production tubing scaling considering a very small chemical reactivity made (Schlumberger. 2013) (Spe et al., 2013) tips chemical treatment as good removal technique. Although it unsafe for both completion, personals and well environment.

Chemical treatment depends on dissolution: a kinetic process quantified by it rate while dynamic equilibrium state is attained when rate of dissolution is equal to rate of precipitation. Precipitation is quantified by solubility of a chemical property refers to ability of a substance (the solute) to dissolve in a solvent or the quantity of solute dissolvable in a given solvent under specific physical conditions. The chemical species of interest are ions present in aqueous solution in this case which combination is responsible for the formation of low soluble compound. Also, once the said compound solubility is exceeded, they will precipitate from the solution in solid form a phenomenon known as precipitation define as state of return of dissolved specie to a dissolved state. The composition of dissolve solid in a known amount of solvent is constant with time and a solution can be in an equilibrium state when the solution is saturated. While the solubility of any solute in a given solvent as the same concentration of a saturated solution. A solution can be considered unsaturated if it contains solute composition that is less than its saturation requirement. Super saturated if solute composition is higher than the saturation solution requirement due to factors like change species concentration or temperature and the rest (Abbas 2014). Hence this can lead to increase, decrease or constant solubility depending on the type of system involved

Solubility of selected compound in water is quite different with that in acid and so in different descaling chemical classes (i.e. in organic acid like HCL/HF, organic acid like maleic, glutamic, succinic and chelating agents like EDTA, HEDTA and the rest). So also, kinetic and dynamic conditions like the case of increase in mineral solubility in water as a result of increase in temperature and pressure leading to dissolution of greater number of ions. Even though not all mineral conforms to the temperature trend because the solubility of barium sulphate increases by a factor of two for temperature ranging from 25°C to 100°C and decrease by same magnitude once the temperature approaches 200°C. Which is believes to be influence by the brine salinity background (Crabtree et al., 1999). Also increase in acidity of the fluid from supplied acidity from CO<sub>2</sub> and H<sub>2</sub>S at high pressure increases mineral solubility. The difference in solubility rate of different compounds in water is as a result of combination of ions present in aqueous solution which from onset is made up of different species. The precipitation of solid minerals from solution can be due to change in physical conditions or water composition (Yassin et al., 2008). Similarly (Al-Khalidi et al., 2011) reported that dissolved magnesium ions in EDTA solutions could re-precipitate as magnesium sulphate due to dissolution of gypsum especially at low pH EDTA solutions.

Iron sulphide chemical treatment seems more complicated than other organic scales. Therefore, justifying the choice of organic and chelating agent over mineral acid due to amount of risk it poses on personnel, well environment and integrity of the well completion (Evans, 2015). While increase in hydrocarbon demand, more emphasis on HSE policy implementation with co- existence of production facilities getting closer to residential communities nowadays. Prompt the need for effective scavengers of all sour gas component and environmental friendly descaling treatment (Chakraborty et al., 2017). Contrary to conventional mineral acid approach (HCl) which is effective in removing soft scale type of FeS with the consequence of generating high corrosion rate. In addition to high amount of H<sub>2</sub>S gas especially at high temperature well increasing the operational risk at surface facility and well integrity been jeopardization (Mahmoud et al., 2015). Since high dissolving power, low corrosion and safe for usage are the optimum in achieving effective iron sulphide treatment.

Finally, a recently conducted lab experiment on iron sulphide scale removal suggests the weakness of organic acid in the removal of iron sulphide at different pH, concentration and solubility. A solubility of 40g/l of iron sulphide when using chelating agent like EDTA and DTPA at 25W% concentration with pH value of 6 was archived. Even though the mixture of organic acid and chelating agent for iron sulphide removal has been discourage. Though (Elkatatny & Fahd, 2017) reported a case were the combination of organic and mineral acid was found promising by removing 78g/l of iron sulphide at 100°C with emphasis of keeping the temperature up to 100°C and 0.014 lb/ft<sup>3</sup> corrosion rate

### **2.5.1 Limitations of chemical descaling approach**

Severe corrosion, H<sub>2</sub>S generation, lack of penetration and slugging characteristic of conventional chemical treatment (HCl) at high temperature. Couple with very low solubility of sulphate scale in mineral acid have been the major setback for chemical treatment (Almubarak et al., 2017). Even though the advancement of oil chemistry field has led to the introduction of innovative types of chemicals for different oil application like advance chelating agent for scale treatment. These innovated approaches have the opportunity of utilizing a multi-purpose chemical for removal of paraffin, asphaltenes , corrosion prevention and handling of scale & solid, based on properties of the chemical in use (Armacanqui et al., 2016). Though operation and well integrity problem are still far from been solved. In cases like that of paraffin that may contain resins, silt, gums, salt crystals, scale, sand and clay couple with restriction of treatment test to only direct field test are not as flexible as under laboratory conditions. Meanwhile the use of effective descaling chemicals such as Xylene have been discouraged due to recorded eye, fertility, skin and nervous system problem. This is as a result of its exposure through inhalation, the skin and indigestion making it difficult to handle. In addition, issues like well integrity, personnel, HSE and low solubility in respect of some types of scales like barium sulphide. Similarly, the

improvement generated from adding depressants (PPDs) to the production stream to tackle wax deposit was discouraged (Xiu et al., 2019). This was due to the utilised PPDs been organic solvent -based polymers that require large quantities of organic hazardous solvent like xylene and toluene.

## **2.5.2 Successful chemical descaling operation around the world**

The first scenario will be that of a five *fadili* wells of carbonate reservoir in active water drive in *Fadili* formation located in Bahrain. Their initial oil production rate of 1500 BOPD was halved within four month and the water cut increases to over 90% approximately 20 to 30 BOPD drop per well as a result of calcium carbonate deposit in both production tubing and other flow lines. This subsequently lower production, damage vales and flow line resulting to casing tubing communication leak due to frequent descaling operations. Utilizing only treatment pressure, quantity of the residual acid volume and wire line dummy runs detected calcium carbonate deposition along the tubing. Then continues application of chemical scale inhibitor injection through gas lift method and adhering to extensive product selection process by choosing the product with the best chemistry that can endure the expected harsh application at good economic cost. Although, recommended series of testing protocols like compatibility, gunging tendency, temperature stability, compatibility with other treating chemicals and effective performance at lower MIC makes it more complex. It successfully resulted to the optimization of volume of acid used compared to the amount of scale removed by reducing both risk and cost (Esbai et al., 2016). Also permit the conversion of the three of the wells to annular gas lift producers and return production to 240 BOPD.

Second Scenario will be that of *Gamsa* field in Egypt that have been suffering from in-organic hard scale problem for over four years due to incompatible mixture of injection water with *Nukhul* formation. The eight well production lines were clean back to their original diameter after recovering 2500 drums of deposit from the production through the operation. The production increase by almost 2,000 BOPD with 350 psi launcher pressure drop and a corresponding back pressure decrease at the producing well (Bakr et al., 2012). Couple with additional producing well into the production and efficient cost/bbl. (economic) was achieved after implementation of the following well planned descaling program.

Stage one involves the use of an organic solvent (Kerosene & Xylene with recommended mixing ratio of 1:1). A powerful gypsum scale dissolver to remove hydrocarbon materials impregnated in the scale. Follow by a thorough flushing with injection water.

Stage two is the main treatment that utilises 68,502-Gal line volume capacity of solution of SAG-01 (24.6%) to make the insoluble calcium sulphite soluble form that it can easily be pump by water. After soaking the pipe for 24 hours the line was displaced to water injection.

Third and final stage was to flush the reaction product outside the pipeline using water injection as a post flush stage. Even though many scholars like (Xiu et al., 2019) had since discourage the use of Xylene due to recorded eye, fertility, skin and nervous system problem.

Third scenario still divert to in organic scale removal due to operational challenges like inefficient dissolution of deposit pose by the simultaneous occurrence of organic and inorganic scales deposit consecutively. Similarly, is a situation where cooling regime near the intake of ESP lead to deposition of heavy oil like asphaltene coating the inorganic scale (calcium carbonate) and preventing contact between the chemical treatment and the scale.

Another situation were carbonate and sandstorm reservoir are producing heavy crude that coat their face of natural fracture/fissure or surface of the pore space respectively which can limit treatment fluid to formation contact. Heavy crude viscosity reducer solution has been proposed over many solutions by numerous researchers. Due to its various advantages like reduction of apparent viscosity of crude by several orders of magnitude, good compatibility with brine and acid based (including acidizing fluid itself). Couple with ability to work with variety of heavy viscos reducer, wide range of applicability like matrix treatment to steam assisted gravity drainage well (SAGD). Squeeze treatment to allow heavy oil reservoirs to be tested with the need for steam or additional surface equipment, simulating heavy oil reservoirs. This is by enabling adequate treatment fluid to formation reaction through the removal of crude from formation surface. In addition, use as flush fluid for easily after treatment flow back of the treatment fluid (Ramonés M et al., 2015). Although the need for laboratory testing protocols like desorption test to measure the crude desorption from the rock surface when treating with solution containing HCVR. Slipperiness test to measure the time taken for HCVR mixed solution to flow through a small diameter glass funnel. Also scale dissolution test to determine the percentage of scale that can be dissolve when solid sample is immersed in an acid solution are recommended for effective utilization of the HCVR solution. Makes it very complex and unsafe operation.

The field application program for removal of inorganic scale from ESP. Started by pumping 2% of ammonium chloride ( $\text{NH}_4\text{Cl}$ ) brine of heavy crude viscosity reducer (HCVR) mixture to initially remove the heavy oil coating on the ESP flowed by 13 bbl of solvent subsequent pumping of 10 bbl of HCl 5%, for treating the inorganic scale  $\text{CaCO}_3$  (terms main treatment). Finally post flushing by pumping 8 bbl 2%  $\text{NH}_4\text{Cl}$  brine and after pulling the CTU out of the hole. The operation successfully restarted well through the CTU rig less intervention by eliminates work over, extend the ESP run life from 40 to 140 days. Average rig cost servings of 6 days per well and an average serving of USD 1.5 million in deferred production was achieved (Ramonés et al., 2015) as shown in Table 2.2. This experiment open door for further research on the efficiency of matrix treatment in heavy oil environment.

**Table 2.2:** Pre and post descaling results of the six wells (Ramonés et al., 2015)

Well	Pre-clean out production rate (bbl/d)	post-clean out production rate (bbl/d)
A	280	500
B	200	230
C	500	520
D	420	400
E	200	220
F	260	250

The Bahraini *Kuff* Gas well producing from twenty-five gas well with 60 MMSCFD production capacities that tremendously drop as a result carbonate/iron sulphide scale infliction. Is attributed to poor corrosion inhibition and acid attack leading to work over of three of the wells to eliminate casing to tubing communication (Well # 17 and 18 were limited to 30MM SCFD before work over) is our fourth case scenario. A CT conveyed chemical descaling technique using HCl despite its disadvantages like potential of sulphide stress cracking the tubular. In addition to perpetuation of iron sulphide deposition as a result of loss of iron rich acid to the formation was chosen over mechanical methods. Mechanical approach like mill/bit drill out or jetting tools were discouraged, because with the well death, jetting performance for hard scale slows from 7,000 inch to 10,000-inch depth. Also, so, below the 7-inch casing due to coiled tubing pressure limitations and standoff distance increase between the jet and the pipe wall respectively.

The operation starts by pumping one well bore volume of 2% KCl water to reduce the 4000psi shut in well head pressure to safe and workable pressure of 800-1000psi. Then using the 1.5' or 1.75' rig up conventional CT to run the jetting nozzles down the hole to the point of obstruction or target to pump 2% KCl water at low rate to maintain positive pressure. Followed by 100 times repeated jetting of pre blended 5000gal of 15% HCl to ensure fresh acid. Also provide agitation with 2 hour coiled tubing pull out requirement to give enough soaking time for the acid and using the choke manifold to unload the well as soon as the CT is out of the hole. The Operation cautiously ended by close monitoring of the choke during flow back to avoid dissolve solid scale from causing erosion problems and slick line gauge was continuously run to determine the rate of scale clean out. The operation lead to successful running of a clipper survey through the entire length of the production tubing with the following post descaling result presented in Table 2.3. Although, negative post descaling result of high metal loss and seep pitting across the entire tubing still were inevitable.

**Table 2.3:** Pre and Post Descaling results of Kuff well(Mirza et al., 1999)

Descaling job result in kuff well				
Well	Estimated scale in Cuft/lbs	Acid Used US Gallons	Pre –Treatment Deliverability MMSCFD	After Treatment Deliverability MMSCFD
7	68.6/15,397	15,000	72	95
4	63.6/14,286	12,000	65	90
19	37.4/8,402	12,000	67	74
10	39.2/8,794	10,200	59	71
18	27.9/6,262	12,000	45	62*
11	93/20,880	10,000	58	70*
17	28.5/6,387	17,000	73	77*
14	31.7/7,126	12,000	47	Well Still SI**
13	48.4/10,872	7,000	70	63***

The fifth chemical successful descaling scenario is still organic /inorganic scale deposition in carbonate reservoirs and asphaltene making descaling operations difficult. Even with numerous solutions like mechanical, heat dispersant and aromatic based solvent like xylene or toluene (Abdul Fatah et al. 2010). Same xylene (acid emulsion xylene) effectively removes asphaltene deposition and enhances well productivity (Nasr-El-Din 2007). Also (Ibrahim et al., 2011) reported the removal of organic deposit in and around wellbore (skin), production enhancement and production tubing scale clean out using the two-chemical pack.

Since most HSE favourable solvent lack salvation power to treat asphaltene as the conventional solvent adapting recommendations like pre flushing with solvent system. Flowed by acidizing acid (HCl at 15w%) to remove the damage obstruction materials. Secondly to include iron control agent into the acid recipe to account for release iron due to acid to ankerite reaction from obstruction material and anticipate corrosion product in the production tubing. Also prevent the precipitation of asphaltene or the formation of tight emulsion through pre flushing with asphaltene solvent prior to SIS treatment (Ibrahim et al., 2011). Also, establishing a SIS monitoring program in order to optimize the number of treatments as a

function of time could tremendously help out but makes the work more complex in addition to the risk poses from utilisation of hazardous substance like xylene and the rest.

Our last and final scenario in the list of chemical descaling programs that recorded success around the world. Is the case of utilizing chelating agent to remove pyrite and different type of iron sulphide scale in oil-gas well without H<sub>2</sub>S generation which prove stubborn in the past for many approaches. Like the used of strong acid such as HCl as 10-20WT% considered effective in the dissolution of pyrite (FeS<sub>2</sub>) and marcasite form of iron sulphide scale but constrains by amount of large volume of H<sub>2</sub>S generated and its corrosive tendency toward the production strings and equipment's. Since the age of scale determine its level of solubility with the older scale been less soluble in mineral acid. Mechanical approach like milling and water jetting with excess pressure up to 140 MPa with or without abrasive was used to break the scale by making slurry of hard particle that need special gelled for transportation. Therefore, the requirement of treating each pipe or equipment with significant level of manual intervention is expensive and time consuming (Mahmoud et al., 2015). So also ineffective for complete descaling of sulphide scale deposit must especially unexposed area.

The solubility tendency of freshly formed iron sulphide mineral acid as in this case leads to the choice of chemical mitigation (chelating agent) to be experimented. Executed by pouring chelating agent like diethylenetriaminepentaacetic acid (DTPA) and converting agent such as potassium carbonate (K<sub>2</sub>CO<sub>3</sub>) along with iron sulphide into a closed flask. Then kept at fixed string speed of 70°C temperature for varying time period. Determining the solubility of the sample at 24 hours, 48 hours and 72 hours soaking time respectively. In addition to calculating the solubility of formulation for a specific sample by taking the percentage difference between initial weight and final weight of the samples. The result concluded that a maximum of 85% was achieved using combine potassium carbonate and diethylenetriaminepentaacetic acid. With economic impact of eradicating corrosion inhibition cost and H<sub>2</sub>S scavengers as no H<sub>2</sub>S was generated during the removal process. Serving as multi propose solution due to its ability to work in both oil and gas field with minimum safety consideration. It should be noted that the conversion of pyrite to iron carbonate which is soluble in DTPA by the formulation system is key in the pyrite removal .So also (Mahmoud et al., 2015) added that the high pH medium permit the transformation of FeS<sub>2</sub> to FeCO<sub>3</sub> due to ability of potassium ions to occupy and substitute the irons because of its small size compared to iron ions

### **2.5.3 Chelating agent**

Chelation is the formation of two or more distinct coordinate bonds between single central atom and polydentate (multiple bonded) ligand which are mostly organic compound. This refers to as sequestering agent, chelators, chelants or chelating agent. Chelating agent is defined as group of

compounds that contain two or more electrons donating groups functioning as Lewis base that form coordinate bonding through electron donating with central metal atom. The formation of multiple coordinate bonds from single molecules leading to the formation of more heterocyclic rings or chelate rings still refers to chelating agent. A specific subgroup of chelating agent called aminopolycarboxylic acids referring to subgroup of chelating agents contains one or more nitrogen groups as well as multiple carboxylic acid functional groups. Its strength is measured by stability constant with ion of interest (Almubarak et al., 2017). Chelating agent have since been utilize through various applications in oil and gas industries like iron control, standalone simulation fluid and scale treatment due to its ability to effectively remove scale without causing damage. This is as a result of it good dissolving power, low corrosion, and excellent iron control, low slugging tendency and mostly highly degradable and environmentally friendly. Its ability to lock the metallic ions of the scale within their closed ring structure makes it preferable chemical treatment information matrix and acid resistance scale (Abbas 2014). Some of the most re-known chelating agent are summarised below.

### **2.5.3.1 Ethylene diaminetetraacetic acid (EDTA)**

EDTA is a hexadentateaminopolycarboxylic patented in the year 1935 by a German in the name of Munz F. It has applications variety ranging from detergent, textile, oil and gas industries in simulation and iron control (Oviedo and Rodriguez, 2003). A good dissolver for calcium sulphate (Shaughnessy and Kline 1983, Cikes et al.1993) and most favourable candidate for improved chemical treatment (Crabtree M et al 1999). Nevertheless, associated to challenges like not been readily biodegradable, decrease in solubility in acid solutions. Due to its ampholytic nature or low solubility at low pH (Martell & Calvin 1952) also (Crabtree et al., 1999) characterise it to be expensive and slower in comprising with HCl

### **2.5.3.2 Hydroxyethyl ethylene diaminetriacetic acid (HEDTA)**

HEDTA is another aminopolycarboxylic acid that on the quest for finding a more effective alternative for EDTA came to board as a replacement suggested by (Frenier et al. 2000, 2003). Have since been use as simulation fluid, iron control and scale removal solution in the oil and gas industries. Structurally like HDTA with the placement of a hydroxyethyl group on one acetic acid group as it measures difference with EDTA. Even though (Frenier 1986. 2001) believes that the addition of the hydroxyethyl group improves the solubility of HEDTA, but lowers its stability constant,

### **2.5.3.3 Hydroxyethyliminodiaceticacid (HEIDA or HIDA)**

It's a tridentate chelating agent with a structure similar to nitrilotriacetic acid (NTA) except that it has only two acetate groups and a hydroxyethyl group. Mostly used for scale removal and acidizing (Frenier

2001; Frenier et al. 2004). Numerous advantages like biodegradability, solubility and been a thermal degradation product of EDTA makes it a good candidate to replace EDTA.

#### **2.5.3.4 L-Glutamic acid N, N-diacetic (GLDA)**

L-Glutamic acid N, N-diacetic acid is a new generation chelating agent (Heus et al. 2008) that been utilize in the area of simulation of carbon, sandstorm reservoir and iron control. Highly soluble in both water and high concentrated solution acid (LePage et al. 2011) due to attachment of lager group to iminodiacetic acid that reduce crystallization tendency and increase solubility (De Wolf et al. 2014). Additionally (Begum et al. 2012a, 2012b) believes that been made from L-glutamic acid or monosodium glutamate made it more biodegradable and lower in terms of stability constant compared to EDTA and HEDTA

#### **2.5.3.5 Diethylenetriaminepentaacetic acid (DTPA)**

DTPA is an octadentate chelating agent with the highest stability constant among the most commonly used chelating agent in petroleum industry. This is used in removing hard scale like BaSO<sub>4</sub> and SrSO<sub>4</sub> (Putnis et al. 1995). Even though scholars like (Sykora et al. 2001) characterised it with low solubility in water and not readily degradable challenges.

#### **2.5.3.6 Tetraazacyclododecane (DOTA)**

1, 4, 7, 10-tetraazacyclododecane: - 1, 4, 7, 10-tetraacetic acid can be best describe as a macrocyclic, octa dentate. First discovered in the year 1976 and is synthesized using cyclen and bromoacetic acid. It has been used in medical industry in aspect like magnetic resonance imaging (MRI) scans as an imaging agent and a radiopharmaceutical (De León-Rodríguez et al. 2008). A chelate lanthanides due to the high thermal stability and kinetic inertness of the complex formed.

#### **2.5.3.7 Trans-1, 2-cyclohexylenediaminetetraacetic acid (CDTA)**

Trans-1, 2-cyclohexylenediaminetetraacetic acid: - is a hexadentate chelating agent also normally used in the medical industry alongside DOTA. Though have been tested as an alternate acidizing fluid for carbonate formations in the petroleum industry (Fredd and Fogler 1997). Also (Misra et al. 1988) considered lipophilic. In addition to being hydrophilic due to the cyclohexane group making it more effective at alleviating nickel-induced alterations in the body than other chelating agents that are only hydrophilic.

#### **2.5.3.8 Methylglycinediacetic acid (MGDA)**

Methylglycinediacetic acid: - is a quadridentate chelating agent that is prepared by reacting glycine with formaldehyde and alkali metal cyanide in an alkaline medium (Schneider, et al. 1999). Also developed

based on iminodiacetic acid (IDA) with a similar chemical structure to NTA (Heldman et al. 2007). Its main advantages over the remaining chelating agent are ability to degrade in the absence of adapted bacteria at standard conditions and to maintain stability despite the effect of pH and temperature (Kolodynska 2011). Mostly found in chelating agent, dishwashing liquids and detergents.

The chemical structure of the fore listed chelating agents is presented in Figure 2.11.

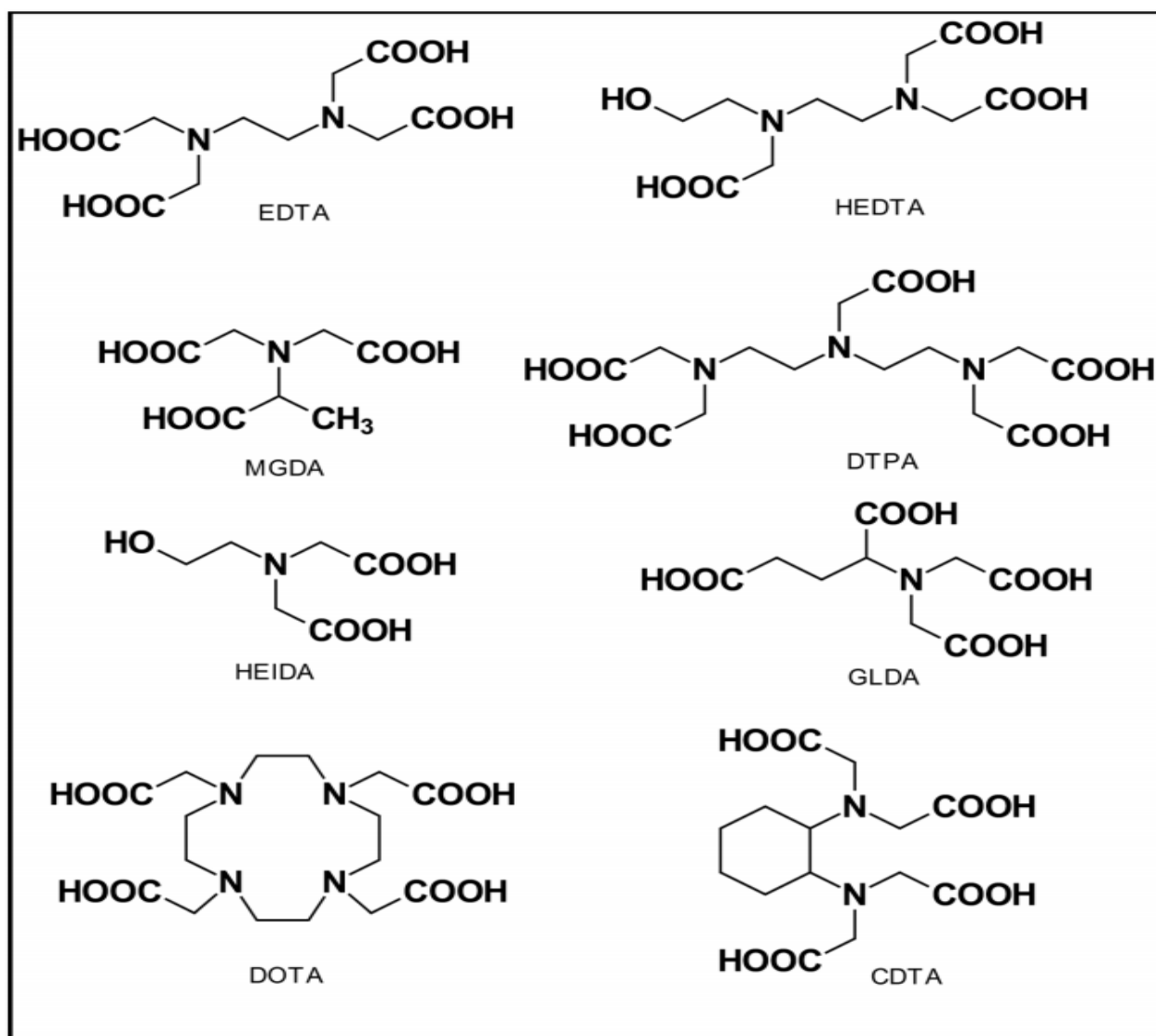


**Figure 2.11:** Chemical structures of common aminopolycarboxylic acids (Almubarak et al., 2017)

#### 2.5.4 Factors effecting chelating agents

Many parameters have impact toward the performance of chelating agent in the dissolution of specific scale. Like the way barite dissolution in DTPA increase from 0-212°F demonstrating a thermal activated process (Putnis et al., 1995; Dunn and Yen 1999; Putnis et al., 2008). Similar to the thermal unstableness demonstrated by mixture of EDTA/DTPA after been age for 24 hours at 350°F from a research toward the impact of high temperature on sulphate scale dissolvers (M. Jordan & Mackay, 2015). While studies

on impact of concentration toward the chelating agent performances shows that some of the chelating agent performance decrease with increase in concentration (Lakatos et al., 2005). Attributed to the decrease in solubility of the scale dissolvers with increase in their concentration. As a result of firstly fewer free acetic acid sites on the chelating agent (Lakatos et al., 2005). Secondly, increased steric hindrance caused by a larger number of chelating agent molecules (there will be more crowding on the path to the bulk solution and at the barite surface because of increased steric effect) (Putnis et al., 2008). Through consequences of slowing down the surface chelating process, therefore recommending the application of multi-cycling injection technique with dilute chelating agent solution (Putnis et al. 1995; Lakatos et al., 2002a). Another key function effecting the performance of chelating agent is pH value, for instance in the case of gypsum where the dissolving power was found to be increasing with increase in pH value when trying to compare solubility of gypsum in EDTA and acidic solution (Al-muntar et al., 2001). At high pH value of (>12) and highly diluted solution of pentapotassium DTPA showed the most prominent results in barium sulphate dissolution (Putnis et al. 1995; Blanco et al. 1997; Lakatos et al. 2005, Lakatos et al. (2002b)). While organic acid (maleic, glutamic, succinic, and gluconic) were found to be very weak in iron sulphide scale removal at different pH and concentration condition. On the contrary (EDTA, DTPA) at a concentration of 25 wt.% and pH of 6 had a solubility of 40 g/liter of iron sulphide from the solubility result (Elkatatny & Fahd, 2017). So, compatibility in mixing different type of chelating agent can interfere with its performance like the combination of DTPA/GLDA or DTPA/MGDA has lower performance than DTPA alone. Due to the barite dissolution been inhibited by the physical presence of other chelating agent molecules (Shende 2012). Also the mixture of chelating agent and organic acid was discouraged by (Elkatatny & Fahd, 2017) because it reduces its efficiency of removing iron sulphide.

## **2.6 Mechanical descaling technique**

The mechanical descaling approaches are preferable over chemical approach though depending on the nature, type, age and location of the scale. More considerable for non-acid tolerance scales and other poor soluble scales (Coats and Tatarski 1993). Even for the soluble scale like calcium carbonate, the advantage of solubility in HCl was accompanied by burdens like: Additional inhibition to avoid tubing damage and post treatment well clean out making mechanical method approach a better option. Mechanical descaling is achieved either by positive displacement motor and mill, liquid jetting or impact hammer with a mill. Varieties of mechanical descaling tool have been on ground for selection that can effectively remove scale at any part or location of the production system, most especially for scale inflicted production tubing through the utilization of techniques like: Abrasive slurries, sterling beads abrasives, scale blasting technique depending on nature, type and location of the scale deposit (Eltaib et

al., 2012). While due to nature of tubing deposited scales mostly very thick, too strong to be removed with explosives with low porosity (Kamari et al., 2014), making chemical treatment ineffective within a reasonable time frame.

Despite some identify mechanical descaling approach flops like poor accessibility for scale deposited in deep formation or proppant pack and high cost due to additional CTU or work over deployment. Its effectiveness in removing thick scale deposit in tubing make it preferable to the chemical approach that highly depend on type and location of scale. Couple with ineffectiveness in dissolving some scale species like sulphate scale and deep in formation deposit (Harms et al., 1988) (far from well bore).

Among many descaling operations were mechanical descaling approach triumph chemical descaling approach during descaling technique selections are: The case of extensive FeS scale deposit in *Gwahr* field carbonate producing zone facing challenges of low pressure, high temperature, open-hole completion and scale with high specific gravity. Case were work over was knocked out of options due to high cost, time and production lost. So also chemical approach due to weak dissolution of FeS, safety concern from high amount of H<sub>2</sub>S generated while using HCl and potential corrosion leaving CT deployed mechanical approach as the only economical and safe option (Buali et al., 2014). Another case can be that of Saudi Arabian carbonate reservoir suffering from scale deposit (mainly iron sulphide characterized with low solubility). The initial adapted low intervention chemical approach which success is highly attach to precise understanding of scale composition to modify the dissolver recipes and large contact area for dissolver to react with, had since been suspended. Due to its negative impact on productivity, the dissolution of by-product losses into the formation and replace. While Mechanical option which despite challenges like lifting in-efficiency due to complex wellbore geometry, pipe fatigue due to frequent CT trips. In addition to possible reservoir damage during temporary isolation was able to successfully put the well back to production with 25 MMSCFD at 2,750 psi FWHP (Mukhliss et al., 2014). Even though at the beginning the team had a consensus to intervene with jetting nozzle instead of a complete descaling work scope.

### **2.6.1 Types of mechanical descaling techniques**

Scale deposit can be effectively removed through mechanical approach by milling, ultrasonic waves, explosives, water jetting with or without abrasion and the rest. Depending on type of scale, location of deposit, well architecture and completions, descaling technique and scope/stage of operations (well accessibility for operation, scale destruction or damage removal) (Bakr et al., 2012). Conditional to the type of scale, its solubility in acid, acid tolerance of the well, completion integrity and post treatment cleaning can be solve using conventional mechanical approach (Tatarski, 1993). Either by a positive displacement motor and mill, an impact hammers with a mill or pure liquid jetting techniques

- i. Milling operations are preferably chosen over others in the case of: Thick scale, tabular located, too strong for explosive with poor permeability for effective and reasonable time chemical treatment and case for creating well access for down-hole tool in blocked tubular (Jordan et al., 2001). Using motors and cutters to penetrate and cut through scale deposit that are rarely evenly distributed on tubing wall will always limit its efficiency to the type of scale and applications like the reduction in motor stall frequency. Faster cutting can be achieved by selection of small-tooth, less aggressive mill compared to other. Challenges like the integrity of the tubing string and operational problems like high torque consumption on mud motor, frequent mill stalling, slowed ROP (Gholinezhad, 2006). In addition to more intervention time and inefficiency in removing long depth hard scale interval are inevitable
- ii. Explosives or wire line conveyed string shot are good choice for short interval located scale and other petroleum operations like perforation operations using guns, scale and corrosion deposit removal in tubular. Through explosive shock generated by pre-determined quantity of detonating cord, though reduces with increase in depth (<2000 mm) and referable for short interval not long continues scale deposit. The explosive strength calculation must consider size and type of tabular, depth to be initiated and wellbore fluid type. It deems time consuming due to the need for multiple run for given zone and frequent pulling out of tool to analysis the result and the re design of the amount of explosive for next run. In order to avoid tubing damage due to incorrect amount of design explosives and allow simulation at will (avoid gas and water bearing reservoir simulation). Therefore even with its high frequency wave generating ability, (Gholinezhad, 2006) believes that the choice of explosive for effective decaling will always be disqualified by poor hard scale removal and both completion and tool destruction.
- iii. Ultra-sonic wave technology has been used in various engineering applications like measurement, cleaning, plastic welding and also for sono-chemistry with 20 to 100kHz ultrasound power (Mason & Lorimer, 2002). The quest for transforming from chemical to physical cleaning process to increase cost saving and reduce environmental problems leads to series of laboratory experiment that prove the successful removal of gypsum. With ultrasonic wave with amplitude and vibration as key parameters couple with +sonification in a borehole. For example, could take place in free-flowing wells during production as long as the flow rates and the velocities at the point of sonification are not too high.
- iv. Jetting: -High pressure water jetting application in household and industries had been on record for a very long time. Petroleum application like high-pressure jet-assisted rock drilling system. Patented in the year 1963 by the US #3112800 while some of the earliest jetting tools were patented as back as 1940S (Gholinezhad, 2006). Also reported by (Bajammal et al., 2013) that

high pressure jetting has been recently gaining wider acceptance by multinational companies like Saudi Aramco, Schlumberger and the rest in scale removal applications

High pressure jetting is easily achieved by focusing the kinetic energy of the high velocity of a fluid (with or without abrasion) on the target surface to achieve the desired results. It has proven to be simple, economical (material and equipment requirement), safe, and the only option for non-chemical soluble scales. It can increase performance without acidization in case of high enough permeability formation and multi-purpose oil and also a gas applications (Aslam et al., 2000). The inexpensive and non-hazardous nature of water (required material) (Charles et al., 1985), coupled with the ability to combine chemical jetting to produce synergy prove to be 50% more effective than pure water or chemical treatment solely

Despite limitations like: Ineffectiveness of pure water jetting to clean medium and hard scales in tubing (Abbas 2014). In addition to the need of special friction reducers to allow higher fluid rates through the jet, without increasing the fluid viscosity (Charles et al. 1985). Coupled with down-hole challenges like high ambient pressure, confined operating space and remoteness of the tool from the pump are formidable and inability to remove large amount of scale have been recognized (Gholinezhad, 2006). All these can be tackled through proper detailed engineering design and considering factors like:

Firstly, standoff distance, which has been experimentally proven that it increases lead to reduction of the jet force impact. For instance, is a rule of thumb for removing moderate to hard scale in a submerged liquid environment is eight-times of the orifice diameter. Secondly, the fluid velocity and pressure drop across the orifice are another important parameter to consider. Since long and trapped orifice seems to produce higher fluid velocity (higher velocity of more than 200ft/sec requirement for hard scales removal). Thirdly, the jet stream profile referring to the dispersion of the jet stream after it leaves the orifice which is found to have negative impact towards the efficiency of the jet stream. Though, can be corrected through good nozzle shape and addition of frictional reducers. Lastly the issue of well and target coverage as rotational nozzle type take advantage of pulsation effect to provide better coverage than stationary jet (360° coverage). However, suffering jamming problems during long operation in corrosive or open hole (Aslam et al., 2000) is among many challenges it faces .

Luckily multiple nozzle approach can compensate the poor coverage limitation attached to stationary jetting technique as suggested by (Abbas, 2015). While adopting detailed and proper design of internal fluid path, orifice geometry, jet standoff, high pump rate and using computer simulation for job design. Together with selections of appropriate size for both coiled tubing and clean out pumping equipment are the identified solutions to the limitations. Additional solutions include elimination of high energy loss attributed with two-phase fluid in low hydrostatic well (Campbell et al., 2000). Since the emergence of

three distinct categories of tool: Non-rotating high-pressure nozzle, convention drilled nozzle and high-pressure rotating tool have not yet completely solve the limitations.

The evolution of both jetting tools and approaches in the pursuit of archiving multipurpose and universal applicable, effective mechanical descaling solution. That is fast, simple, economical, safe for both equipment and personnel and environmentally friendly. Which selection is not dependable on tools limitations have been on ongoing since the 1940S. Starting with high pressure pure water jetting with limitation of only surface testing available (under atmospheric condition or shallow well). Were newly build equipment will prove excellence and other wise in down-hole condition due to back pressure impact.

An experimental jetting simulation chamber with realistic down-hole condition was built to test different tubing scaling of various scale type including sulphide. The results demonstrated poor performance for pure jetting without dissolvers due to considerable amount of scale left in pipe after descaling the tube with single water jet at traverse rate of 2.4 in/rein (1 mm/s). It's considered non-commercial viability as the jet breaks the scale in large chunk scale size presenting transportation, trapping and surface handling problems (Pittman 1961). Couple with tubing damage of 0.004in (0.1 mm) steel removal after impacting jet in a spot for 3 min.

An abrasive trial by adding small sand concentration (1% by volume) improved performance with consequence of jeopardizing the integrity of completion steel. I.e. focusing the jet for 3 min will lead to 0.19in (0.8mm) steel damage. As choosing round shape particle instead of sharp shape will reduce damage to completion but reduce performance. While reducing particle hardness will reduce damage and reduce performance, lead to the replacement of sand particle with special design sterling bead. The sterling beads performance was exceptional with good well integrity after prolonged jetting on a spot (Ashley et al 1998). Even though the tubing itself was not damage the plastic coating that line the production tubing is damage. Surface equipment like choke and valves are at risk due to high density suspension (liquid and solid) from the beads (Abbas 2014). While (Morkved et al., 2014) added the requirement of complicated delivery pump to deliver the bead slurry and the slurry may end up been deposited on the tubing or other hole completion equipment.

As cavitation negative effects toward reduction in performance of high-water jet down-hole lead the multinationals companies to the introduction of sterling bead (liquid and solid). Environmental and well integrity negative effect of using sterling bead motivated a solid free jetting descaling technique research that will not be affected by cavitation effect. Combining both erosion and stress cycling mechanism by utilizing aerated chambers with incorporated single high-pressure flat fan nozzles. This is to reduce the amount of water getting into the well (Abbas A 2014). Contrary to multiple nozzle recommendations by

(El Kamki 2012) that expect the overlap of the flat fans from multiple nozzles to provides better energy impact for effective descaling.

The single nozzle solid free jetting tubing descaling trials performance was excellence. Its answer questions like cavitation suppression distance (stand of distance), relationship between inlet pressure and cavitation bubble formation mechanism in spray fans, the relationship between aeration and suppression of cavitation. However, surface testing condition limitations still exist even though aeration by pressurizing the system could simulate down-hole condition (Abbas 2014). Configuration of multiple nozzle by incorporating sides, back, forward, down and even angular jet will break the shackle or stationary jet limitation toward hard scale removal, well and target coverage (Gholinezhad, 2006). Rotational nozzle type was selected during effective descaling comparison between rotating and stationary jetting nozzle. The choice basis been due to pulsation effect benefit that allow it to provide 360° degree (Aslam et al., 2000), which can be compensated by multiple jet approach. In case of SO<sub>2</sub> removal in a spray tower were the efficiency archived was attributed to simultaneously use of five nozzles. Which allow full volume coverage of the tower and smaller orifice allows small droplet size over single nozzle. (Codolo & Bizzo, 2013). Overlap from multiple nozzle provides better energy impact and scale coverage for effective descaling (El Kamki 2012). Considering the few among many mention scholars' recommendation on the adaption of multiple nozzle approach. Couple with both the single spray limitation, identified research gaps from the single spray approach and quest for improvement. Motivated the extension of the single nozzle research into multiple nozzle research four years later. The detailing on the mechanism and types of jetting techniques will be done in the forthcoming chapter.

## **2.6.2 Successful mechanical descaling operation.**

Few to mention among many successful mechanical descaling operations around the globe include *statjord* field in North Sea operated by Statoil company. That have a history of drastic production decline with 60% of its STOOIP been recovered via secondary recovery techniques for over 23 years leaving complex distribution of by-passed oil reserve, gas and water due to hard scale deposit. Cost of differing production and long delivery time lead to the replacement of the conventional CT with the combination of wire line brushes (WL) together with stiff wire line brushes, wire-line tractor (WLT) milling and string shots. Immediately after two successful runs of the combination, the scale falls out of the tubing wall. While the multi run of multi finger clipper (MFC) carried to evaluate the level of descaling showed a maximum of 1inc variable scale layer thickness, which was completely cleared (Sr/BaSO<sub>4</sub> hard scale) at the end of the 15.5 days operations (Børeng et al., 2002). After firing several shot using string shots, scale solvers, WLT with torque adapter and mill, brushes and broaches a 630 bbl/d post descaling production result was recorded.

The second successful mechanical descaling scenario will be carbonate producing gas zone of *Ghawar* field suffering from chronic FeS scale deposition. The deposit is responsible for dropped in production rate and making well intervention riskier. Couple with operational challenges like low reservoir pressure, increased reservoir temperature, horizontal open-hole completion, and scale with high specific gravity. Challenges that makes mechanical descaling approach economical and safely preferable over work over. Also, chemical techniques were ruled out due to the poor solubility of FeS in HCl and amount of H<sub>2</sub>S generated in addition to already existing H<sub>2</sub>S in the reservoir. The successful mechanical descaling programme is as follows

- i. Reservoir isolation includes the combination of LCM particle-based pills together with fully cross-linked polysaccharide polymer. To act as chemical packer for proper reservoir isolation of the two laterals open holes (approximately 3,401 ft. length and 57/8-in) instead of the two batches of CaCO<sub>3</sub> earlier tried.
- ii. A motor and mill were successfully run together with slow rotating blasting tools to clean the linear and tubing section which usefully recover finer scale at the surface. The fluid oscillator and hydra jet tools with ball isolation activation sleeves in tandem was effectively and safely used to clean and simulate the open hole section in one trip. While for the horizontal long lateral open hole a combination of acid hydra jetting and matrix acidizing technologies in this naturally fractured carbonate formation was used to achieve simulation.

Comparing the post scaling nodal analysis result from reservoir department, a considerable skin decreases of -3.8, a production increase of 5 MMSCFD to 26 MMSCFD and 27 MMSCFD at a WHP of 2,100 psi at 2008 results. The 2008 pre-treatment well performance analysis result shows -0.45 well skin with a  $k \cdot h$  of 126 md-ft ( $k = 1.9$  md and  $h = 65$  ft.) and production rate of 17 MMSCF/D and 19 MMSCF/D and buttonhole shut-in pressure (BHSIP) of 1, 215 psi. (Buali et al., 2014) reported that the comparison confirms the level of achievement of the descaling program.

Saudi Aramco's past descaling approach in the *Kuff* Gas well by deploying a high-pressure jet (with or without abrasion) through CTU in an under balance well conditions lead to many challenges. The challenges include: Choke erosion by large-scale debris resulting to sour gas leak at surface and CT stuck pipe lead to emergency shutdown of the well. Also embarking on integrated innovated job design with the aim of removing the scale with the rig on side and perforating and removing formation damage in a rig-less approach is our third successful mechanical descaling scenario.

- i. Temporary reservoir isolations using calcium carbonate plugs to ensure controlled, safe and closed system environment with a non-nitrogen gelled fluid for scale removal. Since down-hole motor tubing with mill is expected to cut scale into smaller particles for safe and easy transport.

- ii. The well was clean with high pressure jetting tool, and turbine through combination of 2-3/8 inches FOECT strings and special high temperature gelled (stable up to 325°F) for high pumping rate/annular gel velocity and better suspension/transport
- iii. Abrasive slot cutting tool and CT matrix stimulation monitored and optimized with FOECT real-time down-hole measurements. Including DTS were used to for perforation and formation damage removal.

The implementation of the above programme re-claimed the wellbore accessibility and increase it gas production without final acid simulation for the five tested wells (Bolarinwa et al., 2012).The achievements are described in the Table 2.4 even though scale inhibition have been recommended for inclusion in future descaling operations for both sandstone and carbonate reservoir.

**Table 2.4:** Pre and Post Descaling Results for five Kuff Gas wells (Bolarinwa et al., 2012)

well	Pre-treatment Gas Rate	Flowing WHP	Post treatment Gas Rate	Flowing WHP
A	5 MMSCFD	1,380 psi	7.5 MMSCFD	1,620 psi
B	35 MMSCFD	1,300 psi	31 MMSCFD	1,650 psi
C	20 MMSCFD	2,150 psi	35 MMSCFD	2,170 psi
D	5 MMSCFD	1,450 psi	15 MMSCFD	1,450 psi
E	30 MMSCFD	1,500 psi	37 MMSCFD	2,330 psi

The fourth scenario is field (*EW 873*) in an offshore, a mature field of the Gulf of Mexico that had been producing from an unconsolidated sandstone reservoir of Middle- Upper Pliocene age. With some of the wells like Well A-04 suffering from near wellbore impairment and BaSO<sub>4</sub> scale build up in the tubular throughout their production cycle due to biocide inhibition and water breakthrough related problems.

The implementation of the following five steps descaling programmes with the aim of providing enough well access through the removal of the BaSO<sub>4</sub> scale deposit. In order to create opportunity to conduct a chelate-based HF acid treatment for the impaired NWB was successful. Achieved by removing 3,150 ft. MD of BaSO<sub>4</sub> tubular scale with no environmental or OSHA recordable incidents (Sopngwi et al., 2014). Through a well design coiled tubing- conveyed hydro blasting intervention and the post chelating HF acid treatment increase the well production by almost 305%.

Step one started by selecting the best approach for BaSO<sub>4</sub> scale removal from tubular and a coiled tubing-conveyed hydro blasting technique was selected. Since its performance was tied to the nature and magnitude of the BaSO<sub>4</sub>, as well as effective operational planning.

Step two is using INSITE a well intervention (IWI) software for selection of optimal jet-nozzle configuration and resulting nozzle pressure drop that would optimize both cleaning coverage of BaSO<sub>4</sub> in the tabular and jetting penetration rate.

Step three was the main intervention that include running through the hole with intervention BHA in CT down to 9,000 ft. MD at 60 fpm, while using nitrified brine to break circulation. Then hydro blasting from 12,150 ft. MD at 5fpm while sustaining circulation with nitrifies brine subsequently reciprocating from 9,000 to 12,150 ft. MD at 5 fpm. Finally pulling out both CT and intervention BHA at 60 fpm still maintaining circulation with nitrifies fluid.

Fourth and fifth steps were to conduct an integrated peer review to develop a mitigation plan that will reduce operation, technical, HSE and financial risk associated to the design. While the fifth step (execution) as reported by (Sopngwi et al., 2014) was proven successful after effective design implementation with no environmental or OSHA recordable incidents.

Fifth Scenario will be a Petro Brass operated field in the Brazilian offshore diagnosed with barium or strontium sulphate scale. Which were both not soluble in conventional acid and EDTA even though its reaction to barium sulphate dissolver only attest the scale composition.

A careful jetting technology job design that includes a jet nozzle header with Swivel; drift ring and high-pressure in order to keep scale cuttings in stream until circulated out. A high-pressure filter to serve as a screen mesh that will block large particles and allow only the abrasive particles to pass through. The Schlumberger' special design abrasive material of rounded geometry and small in size to enhances scale erosive performance with little or no damage to the string or jewellery completion is used. In addition to software package for performance optimization and tool selection. Finally maintaining continues gas lift injection, pumping cleaning gel batches (10 bbl.) after every 20 meters sections. Coupled with a nitrogen unit back up for circulation drop during the whole treatment duration for better solid and wellbore clean out due to the low reservoir pressure and fluids production rates.

The 7 days planned operation was successfully completely executed at the eleventh day whit a 1025% production increase by removing depositing around 66,000 lbs of solid debris at the surface. A 19 days' whole intervention pay out time with no records of incidence on both environment and equipment from the QHSE performance result as presented in Table 2.5. Declaring the abrasive jetting an environmentally friendly chemicals or green substitute for conventional environmental unfriendly dissolvers.

**Table 2.5:** Pre-and post-descaling result of field (EW 873) Golf of Mexico (Clameto et al. 2003)

RODUCTION HISTORY	Total Fluid Rate (bpd)	Water Cut (%)	total Oil Rate (bopd)
Before Job	250	23	192
Expected	3,780	50	1,890
After Job	4,390	50	2,195

Sixth scenario will be an iron sulphide inflicted Saudi Arabian carbonate reservoir characterise as high angle non-mono-bore or horizontal open-hole completion with multifaceted challenges due to reservoir depletion. Both descaling approaches attempt in the past have suffers operational setbacks due operational complexities like H<sub>2</sub>S generation and severe induce damage. As a result of souring during chemical dissolution and reservoir isolation processes respectively together with stuck pipe problems.

Starting the job execution with reservoir isolation as supposes for standard gas reservoir descaling approach with a viscoelastic isolation pill and degradable fibre without CaCO<sub>3</sub> chips. For efficient and less invasive alternative to temporarily isolation of the open hole section in the well. Also, serve as base for the CaCO<sub>3</sub> chips plug to achieve safe and efficient underbalance mechanical operations.

For accessibility, a rotary high-pressure jetting tool with a 3-1/2-in OD drift ring was run once and the first 500-ft to 14,736-ft of the open hole was access. Followed by a mechanical clean out using straight fluid down to the end of tubing at 12,940-ft and nitrified to the liner shoe at 14,236-ft. Then a special design beads that is better than sand blasting in performance, 20 times less damaging to the steel was pump through the rotary high-pressure jetting tool to remove hard FeS scale was introduce. While keeping the WHP positive throughout the entire clean out of the tubing and linear at 200-psi and 400-psi all plot respectively. Also, small rocks were observed with the returns in the choke manifold that was expected to be formation rock.

The 15,080 to 17,450-ft section of interest was simulated using the same jetting tool immediately after confirming access to the heel of the open hole. A depth of 16,236-ft or 2,000-ft into the open hole was confirmed to be the maximum depth reach by the CT. Even thou, two separate over-pull incidents were recorded at 13,000-lb and 17,000-lb at 15,878-ft and 14,319-ft respectively. Finally, the CT was pull-out to allow access for bull heading simulation by pumping 967-bbl of emulsified acid and 240-bbl of viscoelastic diverter. Together with added degradable fibres, which lead to a fabulous post descaling nodal result analysis. The result shows improvement from 6-MMSCFD at a bottom-hole pressure of 3,715-psi well flowed back to 10.2 MMSCFD on 32/64-in choke setting at 3,825-psi of flowing bottom-hole pressure (Mukhliss et al., 2014). A post-stimulation flow back data of 0.27 md improved

permeability almost 80% and a better AOF. While the matched skin number was (-5) signifies an effective damage removal and a better reservoir response.

The seventh successful mechanical descaling scenario is still *Ghwar* field sitting on a landmass of more than 250 km [155miles] long by almost 30 km [18.5 miles] wide producing 30 to 31°API oil from the Arab-D carbonate reservoir. Considered to be the world largest most prolific field. It had been suffering from accumulation of hard scale in the production tubing that lead to decrease in production and locking the allocated production. This candidate well is inflicted with Iron Sulphide (FeS) and Siderite (FeCO<sub>3</sub>) as indicated by the XRD analysis. It's a deviated vertical well with 6-in open hole to 7,290-ft completion with 4-1/2-in to 6,564.7-ft, 3-1/2-in to 6,727-ft and 7-in to 6,915-ft production tubing and liner respectively and 2.635-in minimum restriction. Recorded unsuccessful descaling history of gauge cutter and lead impression block (L.I.B.) Interventions in the year 2013. In addition to combine, bull heading descaling treatment and gauge cutter interventions in the same 2013 followed by Lead impression block and sand bailer interventions in the year 2014.

Until the recent introduction of the newly innovated approach that optimise the real time monitoring technique during the under balance coiled tubing deployed technique reduces the job steps. By finishing the program in not more than 4 CT run compared to the 5 CT run earlier design. This is achieved by only drilling of pilot hole using motor and mill from the top of scale down the way below the perforation to ensure communication between the reservoir. While utilizing the enhance form fluid to maintain overbalance and carry the scale debris back to surface. Couple with maintaining constant rate of penetration to generate small cuttings to reduce the risk of auto choke plugging, stuck pipes in the wellbore due to pump failure. Subsequently after the completion of the first stage (drilling pilot hole to desired depth) a 2-7/8 high pressure rotary jetting tools was introduced for clean-up. The jet was operated until it reaches the top of the scale down below the perforation interval at 1.5 bmp pump rate of liner gel and 1,000-scfm achieved due to the utilization of the high rate rugged version of CT with real-time down-hole measurement. The success of operation was not only limited to serving the quantity of pumping fluid but enhance the scale cutting carrying capability back to surface successfully. This leads to work over prevention and full regaining of well accessibility. Furthermore 31% increase in production and \$1MM overall cost saving was archived (Alabdulmohsin et al., 2016). Table 2.6 shows the Production rates after descaling and stimulation operation of the candidate well.

**Table 2.6:** Post descaling and stimulation result of Ghwar field (Alabdulmohsin et al., 2016)

	Gross Rate MBD	Oil Rate %	WC%	Choke Setting
Gain (MBD)	4.3	31%	10	Fully Open

## 2.7 Summary

- The chapter reflects on petroleum production and the challenges involved like concept, mechanism and implication of scale formation problems. Couple with proffer solution including prevention, cure and its economy with cited examples around the world:
- Minerals and heavy hydrocarbon scale deposit remain the most frightening problems among all flow assurance problems.
- Mixture of incompatible water is key among other scale formation influencing factors like temperature, pressure, pH and the rest.
- Scale categorization and classification are based on many factors but scale chemical and compositional analysis by (combination of SEM, EDS, XRD & XRF) is more precise for hard scale and NMR/FTIR for soft scale.
- Barium, strontium and iron sulphide scale are found to be the most troublesome deposit in petroleum production.
- It's paramount to incorporate scale management in the life cycle of a field by proper plan strategy at CAPEX phase of a field. Through predicting and preventing scale formation since is far economically better than remedial/removing the scale deposit at OPEX phase of the field.
- In case of failed scale prevention strategy, the removal of existing deposit remains the only option and must be in a fast and non-damaging manner. (i.e. faster, easier, cheaper and safe for both personnel, well completion and the well environs).
- Chemical descaling approaches are good only on acid soluble scale type with a lot of operational and environmental challenges. Though chelating agent are better in dissolution power but still not yet HSE certified.
- Mechanical descaling approach proved efficient in removing the non-soluble scale types and the rest. Nevertheless, most of the approaches were found far from successful descaling compliance (i.e. explosives jeopardizing the integrity of well completions).
- Jetting techniques are the most effective mechanical approach. Pure water high pressure spray jetting keeps gaining wider acceptance due to its ability to safely clean production tubing in comparison to other approaches (i.e. abrasion by sterling beads and the rest).
- Despite the tremendous achievement of single spray high pressure pure water jetting. Multiple nozzle has been suggested to compensate single nozzle and stationary spray research gaps like poor coverage, archiving more than one jetting mechanism (cycling stress, abrasion, cavitation and erosion) and the rest.

# Chapter 3

## Jet Spray Dynamics and Mechanism

### 3.1 Overview

This chapter provide the fundamental and advantage of solid free high-pressure water jet over others. Starting with explanation on the performance of a nozzle or spraying system in terms of parameters and factors that affect the performance of a spray system. Followed by discussion on atomization process in respect of types and classification of atomisers, patternation and liquid break up process. Then analysis of flow behaviour, spray characterization of multiple nozzle spray focusing investigations on essential parameters like: Droplet velocity, droplet size, distribution and pressure drop. Highlighted advantage and benefit of adopting multiple nozzles over single nozzle and ability of solid free jet to effectively perform down-hole without the use of starling bead. Precise emphasis was provided on flat fan high pressure nozzles, considering its suitability in descaling petroleum production tubing as selected in this research. Subsequently introduces mechanical descaling techniques by concentrating on the aspect of jetting mechanism (erosion, abrasion, cycling stress and cavitation). Closing with their description, influencing factors, uses, operative mechanism, and relationship to fundamental parameters when utilizing multiple spray system including effect of pressure drop, and spray overlap region toward multiple nozzles spray performance. So also, benefit toward effective descaling operations, together with examples of successful jetting descaling operation around the globe.

### 3.2 Nozzle performance

The basic functions of spray nozzles are to distribute liquid, break up liquid into droplet and as meter flow. Spray nozzle performance depend on the level of operating efficiency of the entire spray system. Therefore, it is vital to understand the relationship of spray performance to factors like: The operation conditions i.e. temperature, pressure and variable line speed, type of the liquid been sprayed and the position and placement of nozzle in respect to the target.

#### 3.2.1 Spray system

As earlier mentioned, that the performances of a nozzle are tied to the operational effectiveness of the entire spray systems consisting the atomizer/ headers manifold, system design, fittings/connections, pump etc.

### 3.2.1.1 Pump

All nozzle spray operation is completely dependent to the techniques that provide them with fluid flow either through gravity, air pressure or mechanical pump. However, the pumping system provides flow not pressure to the system. The pressure is more related to the atomizers (flow restriction) that why the output of an un-restricted pump is always 0 psi. Pump selection is always guided by the system pressure and flow rate requirements.

### 3.2.1.2 System design

This includes piping system, connection and fitting that supplies the nozzles with fluid from the pump. It must be designed to deliver the correct pressure at the nozzle inlet with minimal pressure losses. The pumping requirement of a nozzle system can be estimated using equation 3.1.

$$P_{PUMP} = P_{Nozzle} + P_{Pipe Losses} + \frac{pgh}{100000} \quad (3.1)$$

### 3.2.1.3 Nozzle/Headers

The basic principle atomization process is the braking up of volume of liquid into multiplicity of small droplet. With the aid of the kinetic energy of the liquid itself, or exposure to high velocity air or gas the liquid jet sheet is disintegrated into a wide spectrum of droplet sizes. While header requirement in spray system become necessary when target coverage area may need more than one nozzle.

## 3.2.2 Nozzle characterization

The understanding of the relationship of spray operational conditions like pressure, temperature, specific gravity, viscosity and surface tension. Toward some essential spray dynamics like droplet size, velocity, spray angle, capacity, spray pattern and the rest will help toward designing an effective spraying system. Even though most of the essential spray dynamics will later be detail in the chapter.

### 3.2.2.1 Flow rate & capacity

The volume of liquid following through a nozzle primary depend on the difference between the fluid pressure upstream of the orifice and the pressure discharged by the nozzle (usually atmospheric pressure). While the fluid capacities of hydraulic nozzle depend on the spraying pressure and the relationship between pressure and flow within a giving orifice which can be express as in the equation bellow. The flow exponent table below can be utilised to approximate the ratio of pressure to flow based on the type of spray pattern.

$$\frac{Q_1}{Q_2} \sim \frac{(P_1)^n}{(P_2)^n} \quad (3.2)$$

Were Q being the flow rate (usually in lpm or gpm), n is the flow exponent and P is the liquid pressure (in psi or bar).

### 3.2.2.2 Fluid properties

The performance of nozzle flow is significantly affected by the properties of the injected fluid, i.e nozzle flow is principally affected by specific gravity of the fluid. Therefore, flow rate of fluid denser than water are lower than flow rate of water at same pressure since higher energy is required in accelerating denser fluid than lighter fluid. The accompanying relationship exists between flow rates (Q) of liquids with various specific gravity gravities.

$$\frac{Q_2}{Q_1} = \sqrt{\frac{SG_1}{SG_2}} \quad (3.3)$$

#### 3.2.2.2.1 Specific gravity

Specific gravity is one of the main components of injection fluid properties that tremendously influence both nozzle flow and pumping requirement of the system. Thereby specific gravity calculation formula in Eq 3.4 is required when spraying fluid other than water.

$$Q_2 = Q_{2(Water)} \times \sqrt{SG} \quad (3.4)$$

The conversation factor graph captured in Figure 3.1, though limited to effect of specific gravity on capacity not capacity influencing factors. Multiplication of the conversion factor by the capacity of a nozzle when spraying a liquid with specific gravity corresponding to the conversion factor

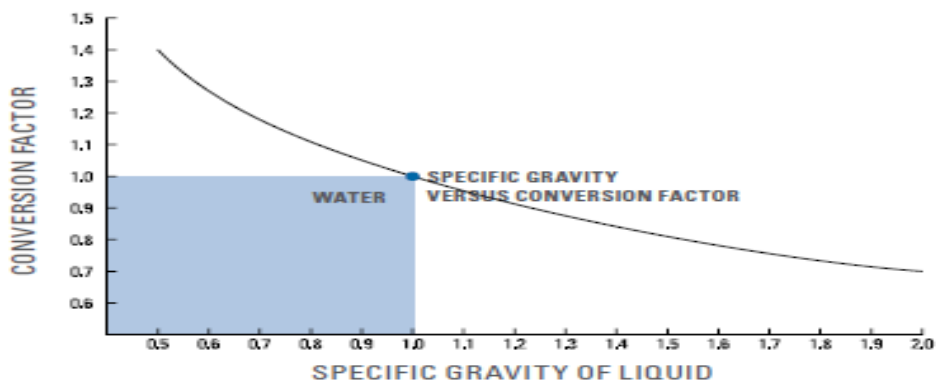


**Figure 3.1** Specific gravity versus conversion factor graph (Spraying system 2015)

#### 3.2.2.2.2 Viscosity

Absolute (dynamic) viscosity of a liquid is a primary influencing factor effecting spray pattern formation that can be explained as the property of fluid that resist change in shape or arrangement of element during flow.

### 3.2.2.2.3 Temperature

Liquid temperature changes do not directly affect nozzle spray performance, but affect other spray fluid properties like viscosity, surface tension and specific gravity. Which on the other hand directly influence the performance of a spray nozzle.

### 3.2.2.2.4 Surface tension

Surface tension affects spray angle, coverage area and operational pressure because higher surface tension tends to reduce the spray angles of especially flat fan and hollow cone nozzles. However, low surface tension can allow a nozzle to be operated at a lower pressure. Even though the properties of surface tension are more apparent at low operating pressure.

### 3.2.2.2.5 Spray angle and coverage

The coverage requirement is the requisite for selecting spray angles for an application. Spray angles estimate the spray coverage base on spray or distribution of water. In an ideal spraying condition, effectiveness spraying angles varies with spray distance. Liquid with higher viscosity than water produce smaller spray angle or some time solid stream depending on its viscosity level, spraying pressure and nozzle capacity. Increase in pressure result in decrease in spray angle of whirl nozzle, while spiral nozzle seems stable over wide range of pressures. In the case of surface tension, wider angles are produced from liquid with surface tension lower than water compared with those that have surface tension higher than water. Figure 3.1 illustrate spray angle relation to coverage area.

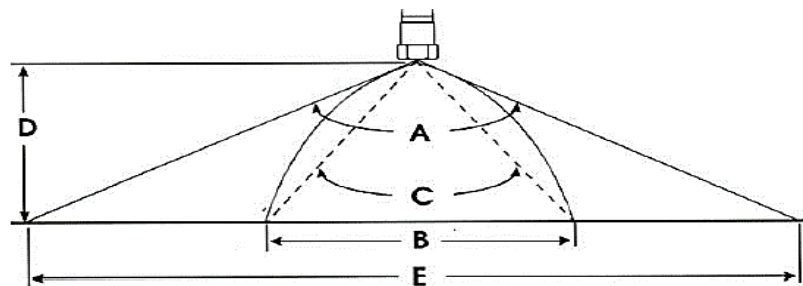


**Figure 3.2:** Spray angle Vs spray coverage (BETE 2018)

Where A is the spray angle measured close to the nozzle orifice, B is the actual coverage at a specific distance D from the nozzle, C is the calculated spray angle from actual coverage B at distance D. while D is the standoff distance from nozzle orifice to target and E is the (theoretical spray coverage) coverage at distance D if the spray moves in a straight line.

### 3.2.2.3 Atomization

Atomization has a direct effect to droplet sizes, droplet distribution and spray pattern. A droplet size refers to individual spray droplet sizes that encompass a nozzle spray pattern. Spray pattern is use in describing the location and density of the liquid released from a nozzle. While the range of spray drop sizes provided by individual spray is term the drop size distribution, which depend on the type of spray pattern, and varies from one type to another. Smallest drop size is obtained through air nozzle atomization while the largest drop sizes are obtained through full cone hydraulic spray nozzle. Droplet size requirement is relative to spray application like gas scrubbing strongly depending on exposing the maximum possible volume of liquid surface to gas stream. Droplet size is affected by liquid property, spraying pressure, nozzle capacity and spray angle. The higher the pressure, the lower the droplet sizes, the higher the nozzle flow, the larger the droplet sizes and the higher the surface tension the larger the drop size. Droplet velocity is dependent on droplet size that why small drop sizes have higher initial velocity but quickly diminish, while larger drop sizes have the ability to maintain velocity for long and travel further. Types of droplet sizes produce from different types of automiser is shown in Figure 3.3. and summary of spray performance is presented in Table 3.1.

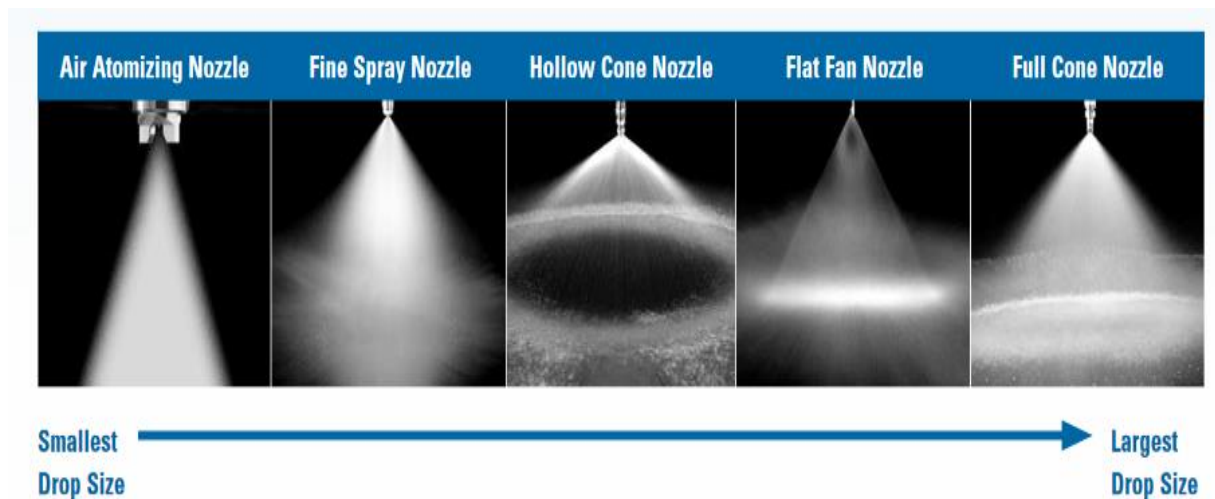


**Figure 3.3:** Atomization (droplet size and distribution) (Spraying system 2015)

### 3.2.3 Spray performance summary

**Table 3.1 : Spray Performance Summary**

Spraying Operational Conditions	SPRAY CHARACTERIZATION					
	Spray Pattern	Drop Size	Spray Angle	Capacity	Impact	Velocity
Increase in operation pressure	Improves	Decrease	Increase then Decrease	Increase	Increase	Increase
Increase in specific gravity	Insignificant	Insignificant	Insignificant	Decrease	Insignificant	Decrease
Increase in viscosity	Deteriorate	Increase	Decrease	Increase in full/hollow cone and decrease in flat	Decrease	Decrease
Increase in fluid temperature	Improve	Decrease	Increase	Subject to type of nozzle and sprayed fluid	Increase	Increase
Increase in surface tension	Insignificant	Increase	Decrease	No effect	Insignificant	Insignificant

### 3.3 Atomization

The main prime purpose of atomization is to produce small droplet. Dombrowski and Munda (Dombrowski et al. 1968) define good atomization “most effective way of utilizing the energy imparted to liquid has a large specific surface before it commences to break down into drops”. A coherent jet of water with enough force and small adequate footprint to guarantee high impact pressure at the surface of the tank of a wall can be produce through careful atomiser design.

#### 3.3.1 Spray jet break up

The idea of spray as a process of dispersing a high momentum liquid to droplet has for long been intriguing research area with wide industrial applications like mechanical, chemical, and medicine. In addition to metallurgy, agriculture and aerospace (Knorsch et al. 3013), (Storch et al. 2013), (Tamhankar et al. 2014) and many others. Although, the complex dynamic nature of spray system emerges from changeability with operational conditions, ambient condition and type of atomizers (Guler et al. 2012). Making the understanding of how types of spray are produced very vital. Improvement in spray research have been on since the 19<sup>th</sup> century, when Lord Rayleigh explored an infinite liquid column while exhibit break up. He likewise proves that the size of the droplet is twice the diameter of the jet for a liquid column break up at low velocity emerging from destructive symmetric turbulence.

Among many-conducted experimental research, emphasis was given to planer liquid jet due to their simplistic behaviour (Dombrowski et al 1962) shown in Figure 3.4. These sheets are utilized generally for purposes connected to impact of the impinging sheet on the solid surface. A typical practice has been the utilization of fan nozzle such an extent that the spray properties are dictated mounted orifice (Dombrowski et al 1960). While examining a fan spray nozzle a network of detached stream formed, this was caused by the aperture (perforation) in the sheet.

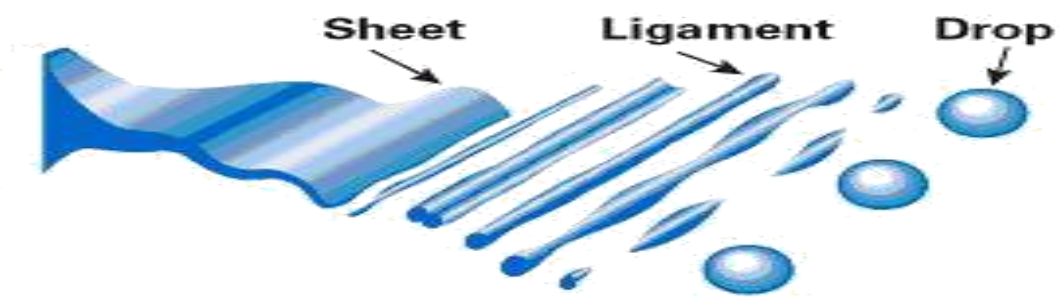


**Figure 3.4:** Sheet disintegration breaks up proposed by (Dombrowski et al. 1962)

While a various spray property does exist, the underlying concern has been the breakup length, characterized as the distance from the nozzle exit to the disintegration point of the continuous part of the liquid jet (Yule et al. 1994). This region implies the primary break up. Although, the produced droplet experiences break up as it goes through an encompassing air, because of relative velocity impact between the fluid and the encompassing (surrounding) air. A non-uniform pressure gradient turns out to be more experienced by the droplets and subsequent deformation is built up which prompts additionally break-up. Dimensionless numbers like Weber number are utilized to portray the momentum of the jet as it exits the nozzle appeared in Eq. 3.5. Lower weber numbers portray low flow rate, which the developing jet has inadequate momentum to form continuous jet while it passes through the ambient surrounding air. Prompting the formation structure dripping shape (Rajendran et al. 2012) which increase in flow rate beyond a definite value empower the formation of the continuous jet.

$$We_a = \frac{\rho_a U_2 d}{\sigma} \quad (3.5)$$

The breakup as shown in Figure 3.2 is related to the disturbance generated by the interaction between gravitational, aerodynamics, capillary and inertial force. Nevertheless, further ahead movement of spray result to secondary break up, due to substantial interaction between the earlier mention forces. Each of the breaks up region is known to control certain spray characterization. Primary break up defines the standoff distance (length of liquid jet) approaching or impinging the target, or amount of fluid impacting on a piston consequently effecting combustion efficiency in the case of combustion process. While droplet sizes and populations are defined by secondary breakup and vital in determining the quality of atomization's as well as evaporation in fuel engine.

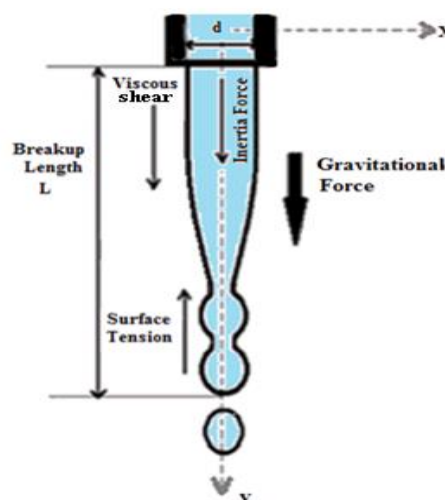


**Figure 3.5:** Forces acting along spray jet (Rajendran et al. 2012).

Various research works confirm decrease in break-up length with increased in injection velocities until a constant value is attained. Different results showed a scope of 20-30m diesel spray break up at inlet pressure of 20 MPa (Arai et al., 1995). Although, the author affirms that the breakup length depends inversely on the ambient pressure, nevertheless have a notion that its more complicatedly depending on injection pressure breakup procedure. Also, momentum changes contribute non-linearly to the breakup length as appeared in Figure 3.6.

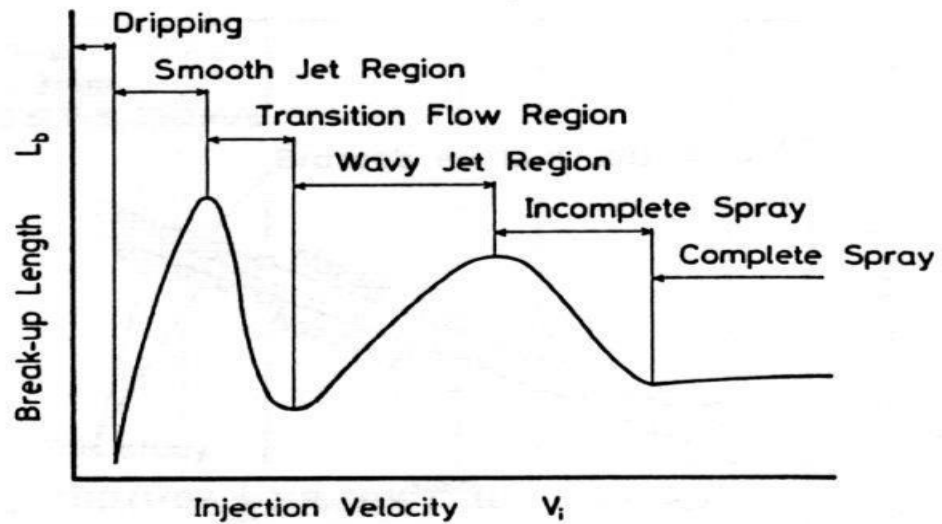


**Figure 3.6:** Break-up length behaviour of liquid jet (Arai et al., 1995)

Figure 3.7 below express the two phases of atomization, and each of the region characterized by varying aerodynamic forces interactions.

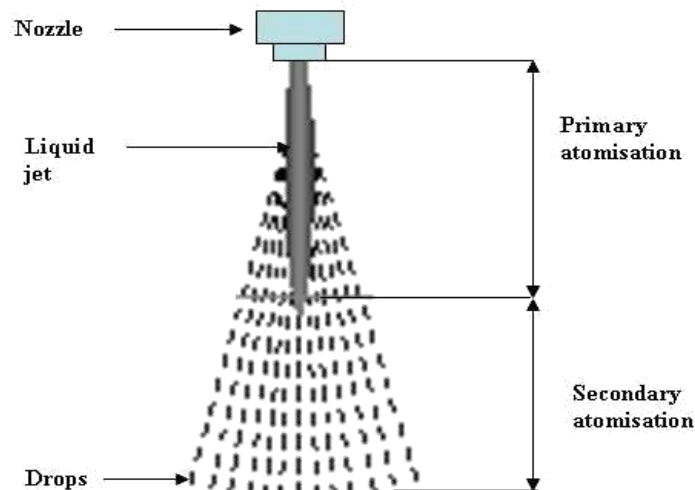


**Figure 3.7:** Liquid atomisation mechanisms (Liu H 2000)

### **3.3.1.1 Primary spray break-up**

At whatever time the fluid leaves the nozzle exit, a swift appearance of smooth jet is noticed, subsequently gradual disturbance in the jet is observed as the fluid moves further away. Which increases downstream until the amplitude of the observed disturbance is equal to the radius of the jet, a position where the droplet starts pinching off from the liquid jet (Rajendran et al., 2012). Consequently, the instability experienced by the jet surface that leads to the pinch of the droplet is attributed to primary break up (Reitz et al. 1987). Certainly, hydrodynamic cavitation within the nozzle and turbulence oscillation of the liquid have been recognised as the controlling mechanism (Arai et al. 1995). Though at higher velocity, the mechanism of break up remains unknown. Conical spray with wide range of droplet sizes and average droplet diameters far smaller than the jet diameter is a result of the chaotic behaviour of jet break up at a short distance from orifice exit (discharge).

### **3.3.1.2 Secondary spray break-up**

Consistent movement of the liquid sheet through the encompasses air experiences additional break up to smaller droplets, a process termed as droplet break up or secondary break up. The droplet created from the essential atomization might be unstable and further break into smaller droplets. This is subject to the competitions at the surface between internal forces due to surface tension, viscosity and aerodynamic forces. The force distribution over the droplet varies with time as the droplet shape changes. Therefore, the droplet remains stable, if either there is an equilibrium between internal and external forces or the external force can be compensated by droplet shape change. Though the larger the external forces the more it deforms up to break into smaller droplets. If the size of the droplets that are stable is referred to as the critical droplet size. In the case of any droplet size larger than the critical size, it breaks up. Time increases with decrease in droplet size. Aerodynamic interaction is the most influencing factor among all the earlier mentioned factors.

In spite of the rich literature and the executed theoretical validations, its detailed mechanism is still unclear. Consequently, comprehensive explanations on the behaviour of break up process remain uncertain, vulnerable and disconnected. The non-uniform shear stress and pressure on the surface of droplet instigated by relative motion of droplet over encompasses-air causing deformation, when overwhelm the surface tension leads to disintegration of the droplets. The newly produced droplet occasionally experiences further break up pending the droplet diameter formed has attained the minimum surface tension required to conquer the external forces. Despite the fact that the conduct of break up is known to be intricate and rely

on injection velocities, cavitation effect and turbulence. Notwithstanding, it's believed that aerodynamics stripping of smaller droplet from heavier droplet as suggested by *Kelvin-Helmholtz* or the effect of stresses causing the disintegration of heavier droplets to finer ones as proposed by *Rayleigh-Taylor* instability. Different dimensionless numbers produce can be utilized to relate the numerous forces of interplay as discussed. The findings make it clear that break up regions experience transition based on the dimensionless group for encompasses air *Ohnesorge number Oh*, which can be mathematical express as follows.

$$Oh = \frac{\mu l}{\sqrt{\rho_a d \sigma}} \quad (3.6)$$

$U_{rel}$  is the relative velocity between the liquid droplets and the surrounding air,  $\rho_a$  is the density of the air surrounding the spray,  $\sigma$  surface tension,  $d$  the droplet diameter and  $\mu$  the liquid molecular viscosity.

### 3.3.2 Spray characterisations /atomizers

There are numerous approaches for producing spray. To minimize drop sizes, the greater part of these requires a high relative velocity between the liquid and encompasses air as possible (Lefebvre, et al., 1989). Key factors like liquid property, type of atomizer, spray angle and capacity must be taken into consideration in order to correctly assess and understand drop size data. The broad categorization of atomizers can be tied to their geometry and application. Types and industrial application of atomiser is shown in Figure 3.8 demonstrating general atomizer classifications base on the technique for using input energy for atomization (Yule & Dunkley, 1994; Abuhesa, 2010).

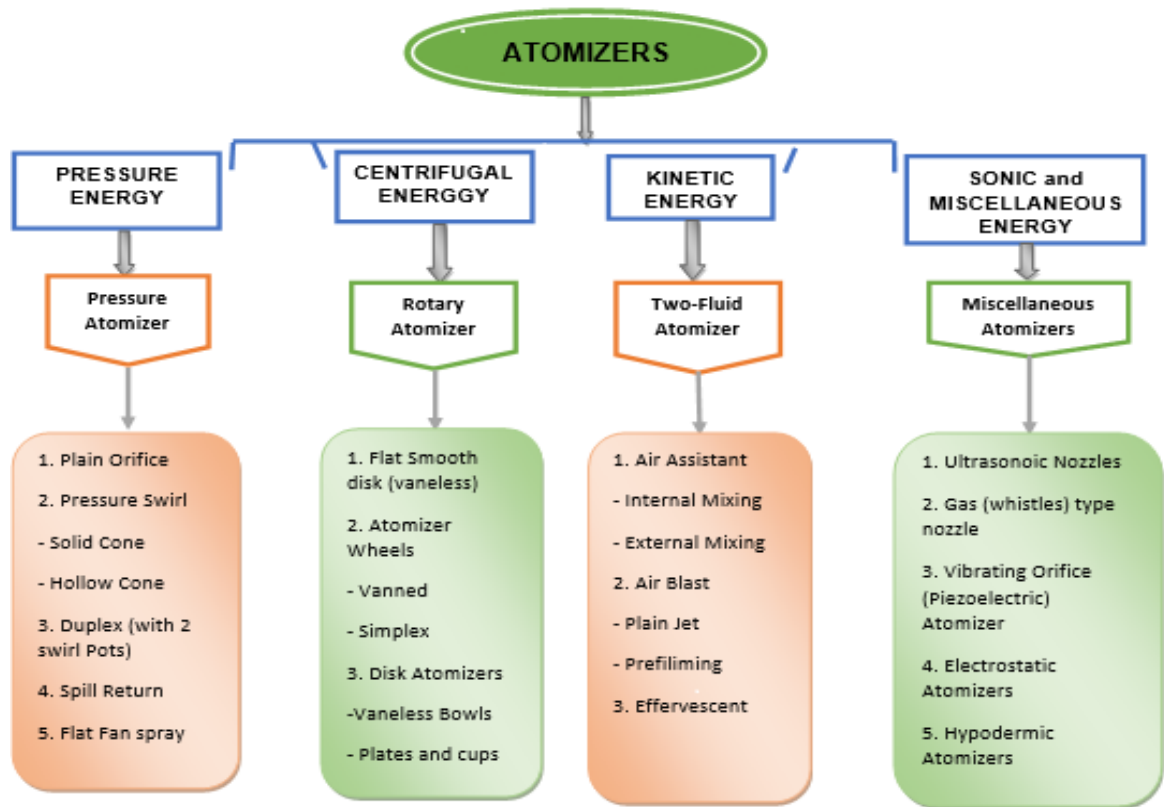


**Figure 3.8:** Classification of atomisers (Yule & Dunkley 1994 ; Abuhesa M . 2010).

### 3.3.2.1 Pressure jet atomiser

Pressure Jet atomizers are mainly utilized in fuel jet injection application, diesel engine in peculiar by utilizing a simple orifice. A small orifice (mostly less than 0.3 mm) and high pressure of (normally higher than 100 MPa) are the requirement for producing a fine spray ( $D_{32} < 200 \mu m$ )

### 3.3.2.2 Pressure swirl atomiser

Pressure swirl atomizers has been for long utilized in the gas turbine engine, furnace, agriculture related spray and petroleum direct automotive engines. The drop size might be correlated with the wavelength that grows on the surface of the sheet as speculated by (Dombrowski et al., 1968) and others. (Rivas et al 2014) reported that the combinations of theoretical and empirical information are the main requirement for analysing this kind of atomisers in terms of estimating their discharge coefficient and spray angle

### 3.3.2.3 Rotary atomiser

The rotary atomizer utilises centrifugal force applied to the liquid with end goal of fling a thing film from a rotating cup, disk or bell. The essentials of the technique are well known (Nasr et

al., 2002) and have two distinct prospective benefits': The likelihood of creating exceptional narrow droplet distribution and the extra adaptability of the utilization of mechanical force to pre film the fluid instead of depending on small orifice. The earlier listed advantage occurs for moderately low flow rate since it requires the atomiser to work in the direct droplet or ligament regimes of break up at the rim of the cup or disk. At higher flow rate continues sheet form at the rim and the size distribution width is like that for the pressure jet atomiser. In any case, this high through put method of operation can be joined with an annular air jet at right angle to the sheet to give a pre-filming atomizer called air blast rotary cup. Mostly, a decrease in liquid flow rate with corresponding increase in rotational speed improve the quality of the atomization. Recent advancement has made it possible to handle flow rate up to 40 kg/s at high wheel periphery speed that produce very fine spray (SMD below 20 microns).

#### **3.3.2.4 Impact-type pressure atomiser**

This is another category of pressure atomiser, with ability to exhibit different types of patterns. Usually the fluid is impacted upon shaped surface as it is developed from an orifice and a flat spray pattern is generated. Normally utilizes when spray pattern is required. Even though, the orifice must be large enough, to reduce the possibilities of blockage. They are usually utilised in safety system where spray must unfailingly function well (Tamhankar et al 2014), i.e. for cooling and gases removal.

#### **3.3.2.5 Ultrasonic atomiser**

Ultrasonic atomizers are less common in comparison to the previously mentioned techniques, yet especially suitable for generating low flow rate (<0.2l/min) spray with relatively narrow size distribution and very low kinetic energy. Its size distribution width can be categorized in an intermediary position between that pressure will atomizer and rotary atomisers in direct droplet regime.

#### **3.3.2.6 Electrostatic atomiser**

This is another niche market technique. Genuine electrostatic atomiser injects charge into the liquid sheet with end goal that the charge at the surface sheet of the fluid act against surface tension thereby causing break up. It is hardly utilised in practical device but utilize actively in numerous areas of application including liquid atomization. Among the advantages are applications to what are regularly refers as electrostatic atomiser, through a release of direct injection of charge.

### 3.3.2.7 Spill return atomiser

These atomisers use a special shaped vane placed at the atomiser inlet, it imparts a rotational action to liquid through the atomiser by virtue of a rotational movement, water exiting the atomiser orifice appears in the shape of full cone. The cone angle is dependent of both the exit speed and the internal design of the atomiser. This varies from  $15^\circ$  to  $120^\circ$ , as shown in Fig. 3.9 for a spill return (BETE 2018). Standard Full Cone atomisers can also be produced as square full cone atomisers, where the square shape of the spray with a pyramidal form is designed by a special outlet orifice.

These atomizers utilize a unique shaped vane positioned at the atomizer's inlet that impart a rotational action to fluid through the atomiser. By temperance of this rotational movement, water leaving the atomiser orifice appeared in shape of full cone. The cone angle is subject to both the exit speed and the atomiser's internal design. Spill return as shown in Figure 3.9 varies from  $15^\circ$  to  $120^\circ$  (BETE 2018). Standard full cone atomisers can also be produced as square full cone atomisers, where the square shape of the spray with pyramidal form is design by exceptional outlet orifice.

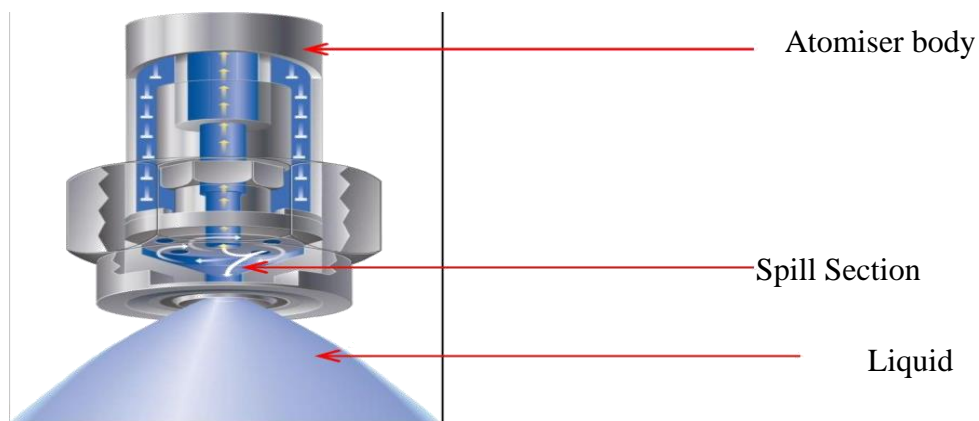


**Figure 3.9:** spill returns atomiser (BETE 2018)

### 3.3.2.8 Hollow cone and solid pressure atomiser

These kinds of atomisers are less utilized than the others, however it is utilized when a wide spray with high impact and uniform coverage (normally between of  $30^\circ$  and  $100^\circ$  total angle). Generally, as reported by (Nasr et al. 2002) a thin exit sheet at the swirl atomiser exit does not happen; the drop sizes are constantly more than that of a hallow cone whirl atomiser of a similar capacity.

### 3.3.2.9 Hollow cone (atomiser)

This atomizer produces liquid fluid flow, with a ring-shaped characterize spray patterns, the impact region where fluid is occupied on the outer edge of the spray patternation. Axial and tangential designs are major available types of hollow cone atomisers.

This type of atomiser is categorised in to three design patterns of whirl chamber hollow, deflected type hollow cone spray and spiral type hollow cone. The whirl chamber rotates the fluid to generate a circular spray pattern characterise with small droplet and high capacity. Mostly used in dust control, water aeration, air gas & water cooling, flue gas desulfurization (FGD) and cooling product on conveyors, it has a spray angle of  $40^{\circ}$ - $165^{\circ}$ .

The deflected type hollow spray utilises a deflector cup to produce an umbrella hollow cone pattern with spray angle of  $100^{\circ}$ - $180^{\circ}$ . It is usually utilised in decorative spray, dust separation, water curtain, and fire protection and flush cleaning of interior of pipes & tubes. Finally, the spiral hollow cone with spray angle of  $50^{\circ}$ - $180^{\circ}$ , produces a circular shape pattern when leaves the void in the spiral with bit coarser drops than the other hollow cone spray types. It delivers a high flow rate in compact nozzle size and have for long been utilise in the areas of dust separation, fire protection, and flue gas desulfurization. Typical hollow cone peatternation is shown in Figure 3.10

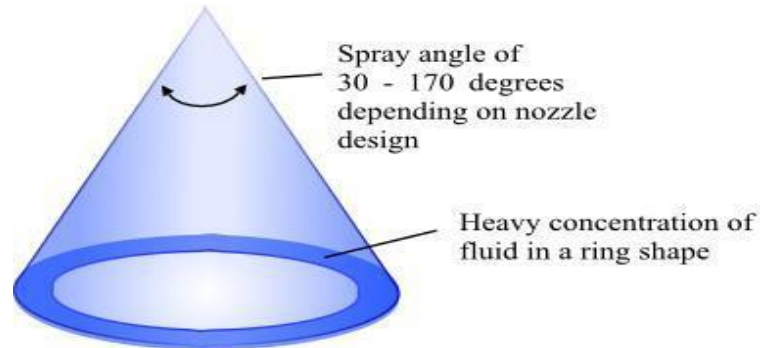


**Figure 3.10:** Hollow Cone Atomiser spray (BETE, 2014)

### 3.3.2.10 Full cone atomizers

Full cone atomiser usually comes in five designs of full cone spray, spiral full cone, oval full cone, square full cone spray and solid stream spray. The earlier listed called the full cone spray has a spray angle of  $15^{\circ}$ - $125^{\circ}$  and utilizes an exceptional internal vane design to create a solid cone shaped spray pattern that comprises of medium to large sized drops. Secondly, the spiral type with  $50^{\circ}$ - $170^{\circ}$  that generate a solid cone shaped spray pattern when the liquid exists the void in the spiral. Containing relatively course drops and it pattern after exiting the internal vane is not as uniform as full cone. Third is the oval full cone spray with  $60^{\circ}$ - $105^{\circ}$  spray angle

that utilises a special internal vane to generate a solid cone shape spray pattern with oval impact area. Characterised with its width almost one half-its length and consist of spray pattern of medium to large size drops. Fourth is the square full cone spray that utilises a unique internal vane to create a solid –shaped spray with square impact with spray angle of (52°-105°). Attributed with uniform spray pattern across the entire spray area. Finally, the solid stream spray with 0° spray angle characterised with the highest per unit area and mainly used in marking and lamina flow application.

The full cone is mostly utilised in application like chemical injection, dust separation, fire protection, metal cooling and washing/rinsing operations. While the spiral type is used in fire protection, dust separation, quenching and flue gas desulfurization. Oval full cone spray is found suitable in applications like cooling/quenching, dust control and air/gas washing. Whereas the square sprays are used in cooling and quenching, fire separation, dust control and air/gas washing operations. Solid stream sprays are more peculiar in making and lamina flow applications respectively. A typical full cone patternation can be shown in Figure 3.11

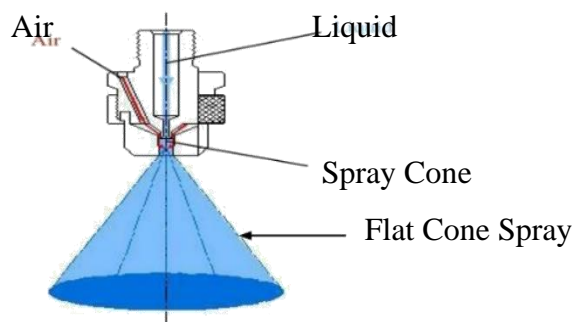


**Figure 3.11:** Full cone Atomiser spray (BETE 2018)

### 3.3.2.11 Flat fan (atomiser)

Flat fan atomisers generate a thin, flat sheet of liquid that expand as it moves away from the atomiser exit. A thin contact line of liquid is produced as the spray hits the target surface. Flat fan nozzles are considered greater than full cone and hollow cone in terms of impact because its liquid is concentrated in a very small area. This type of atomisers produces a flat edge spray pattern, utilised on spray headers to deliver uniform coverage as a result of overlapping distribution. According (Guller et al. 2012) it produces uniform spray in addition to uniform impact distribution across the entire pattern width. A spray overlaps of around 1/3 or 1/4 of the width of spray is recommended for consistent and uniform coverage. Flat fan nozzles are categorised into: Flat fan even nozzles with 25°-65° spray angle, it generates even distribution of medium sized drops across the thin, rectangular spray pattern, utilised in coating,

moisturising cooling and washing operation. Then the tapered nozzle with  $15^{\circ}$ - $110^{\circ}$  that produce a tapered-edge flat fan nozzle, used on spray headers to generate uniform coverage due to overlapping disturbing, utilised in high impact cleaning, label removal and particularly decaling operations. Finally, the deflected flat fan nozzle type categorises with spray angle of  $15^{\circ}$ - $150^{\circ}$ , utilises a deflector surface to produce an even flat spray pattern containing medium sizes drops that are suitably applied in washing and shower in papermaking operations.

Flat fan nozzle atomiser especially the tapered atomiser type is a well-chosen atomiser for descaling proposes and an indispensable spray system. That make it possible to apply liquid in well-define shape with corresponding high velocity on the targeted scale deposited in petroleum tubing. (Bendig et al. 2001). For the purpose of this thesis, these chosen flat fans produced by Lecher coupled into a header from Spray System Company are being considered. The atomisers have been characterised with features like sharp define and linear spray pattern. The optimization of the descaling process in order to achieve an improve scale removal at low energy cost was attain through the proper selection of spray parameters. Thus, this has revolved concept of hydraulic scale removal from a question of high pressure to developing science. Flat fan spray patternation can be seen in in Figure 3.12

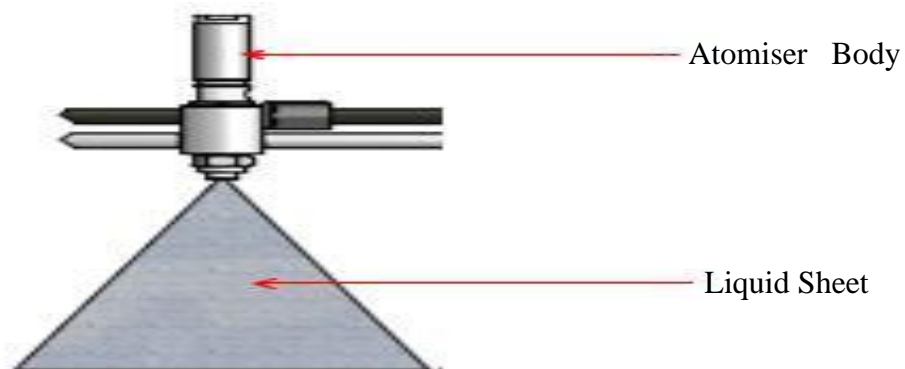


**Figure 3.12:** Flat Spray Pattern atomiser (BET 2014)

The Flat fan spray atomiser produced by Lecher with the ability of delivering high impact even at low flow rate was is utilised in this examination and shown in Figure 3.13

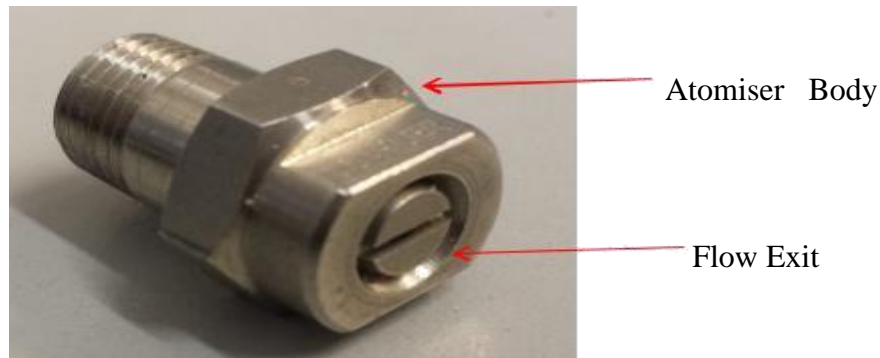


**Figure 3.13:** Flat Spray Atomiser

### **3.3.2.12 Air atomization and air assisted nozzle**

These types of atomizers generate various types of cone and flat spray pattern via the utilization of compressed air to atomise liquid spray, with spray angles of  $18^{\circ}$ - $360^{\circ}$ . Very fine sprays are form from internal mix impingement atomization. Utilise in areas of evaporative cooling, moisturizing, coating and humidification applications.

### **3.3.2.13 Hydraulic fine mist atomisers**

Has range of spray angle of  $35^{\circ}$ - $165^{\circ}$ , generate finely atomised spray, low capacity spray in hallow cone pattern without the use of compress air. Utilise in evaporation cooling, dust suppression, spray drying and moisturizing applications.

## **3.4 Spray analysis**

Understanding the characteristic of a spray can tremendously improves the viability and efficiency of the nozzle and the material to be sprayed. Lot of parameters are considered fundamentally significance when it comes to proper optimisation of a spray solution. Depending on applications, as each parameter may benefit from decrease, increase, or ideally tune setting which can be achieved through detail testing and analysis. Listed below are some of the parameters that can/should be utilised in analysing or characterizing spray. Even though only the most important will be detailed this chapter.

- Droplet sizes
- Droplet velocity
- Volume distribution
- Volume influx
- Spray angle

- Solid Particle
- Droplet shape
- Spray impact
- Rheological testing
- Operation pressure
- Flow rate
- Droplet impact force
- Spray concentration
- Material solid content and the rest

### **3.4.1 Drop size**

Drop size refers to the genuine size of the specific drop that comprises an atomiser spray pattern. The significance of drop size and its application in spray system have considerably increase over the years. Each spray pattern delivers a scope of drop sizes and this range is called the droplet size distribution. The criticalities of drop size depend on the application in question. Processes like gas scrubbing rely upon exposing the maximum amount of liquid surface to gas stream. While other applications like a case were the spray must project into fast moving gas stream requires the droplet size to be as large as possible. Exposing the maximum surface area requires atomizing the liquid in smaller droplet sizes as possible. Drop sizes are influence by factors like atomiser capacity, liquid property, spray angle and spray pressure. Higher spraying pressure provides smaller drop sizes, while lower spraying pressure yield larger droplet sizes.

### **3.4.2 Drop size distribution (DSD)**

Drop size is an essential component for the choosing an atomiser for a specific application. So as drop size distribution is a critical and significant parameter of atomization process in addition to drop mean diameter. Simply refers to as the scope of drop sizes and ranges delivered by a spray pattern. It might have a specific shape for instance (narrow, wide few large drops, etc) for most ideal operations. Figure. 3.14, in which  $\Delta D = 5\mu\text{m}$

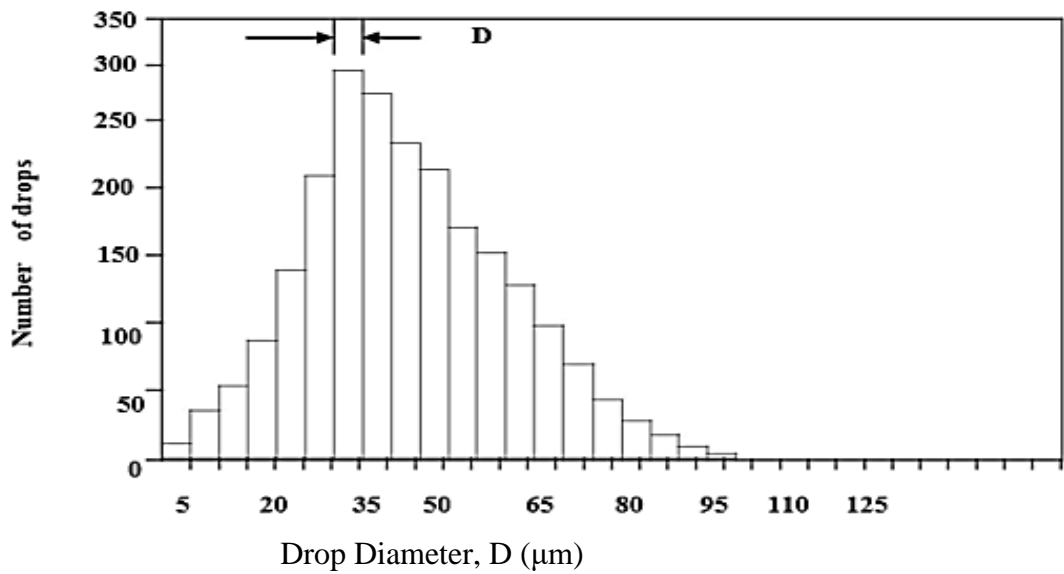


**Figure 3.14:** Typical drop size distribution (Nasr et al. 2002)

Where the spray volume equivalent to a given range of drop size typically, between  $(D-\Delta D)/2$  and  $(D+\Delta D)/2$ , is plotted as a function of drop size as appeared in Figure 3.15. The consequential distribution is skewed to the right as a result of the larger drop weighting effect.

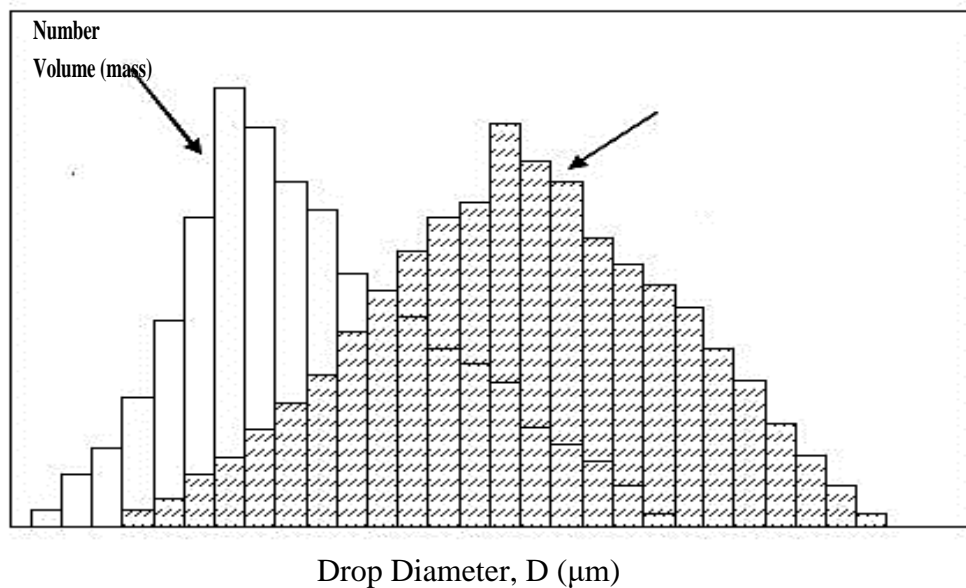


**Figure 3.15:** Drop size bars based on number and volume (Lefbvre 1989)

Frequency distribution curve for the spray can be obtained by making  $(\Delta D)$ , a continue size distribution (numbers as well as volume) curve. Typical frequency distribution curve and shape of cumulative drop sizes are illustrated in Figure 3.13 and 3.14

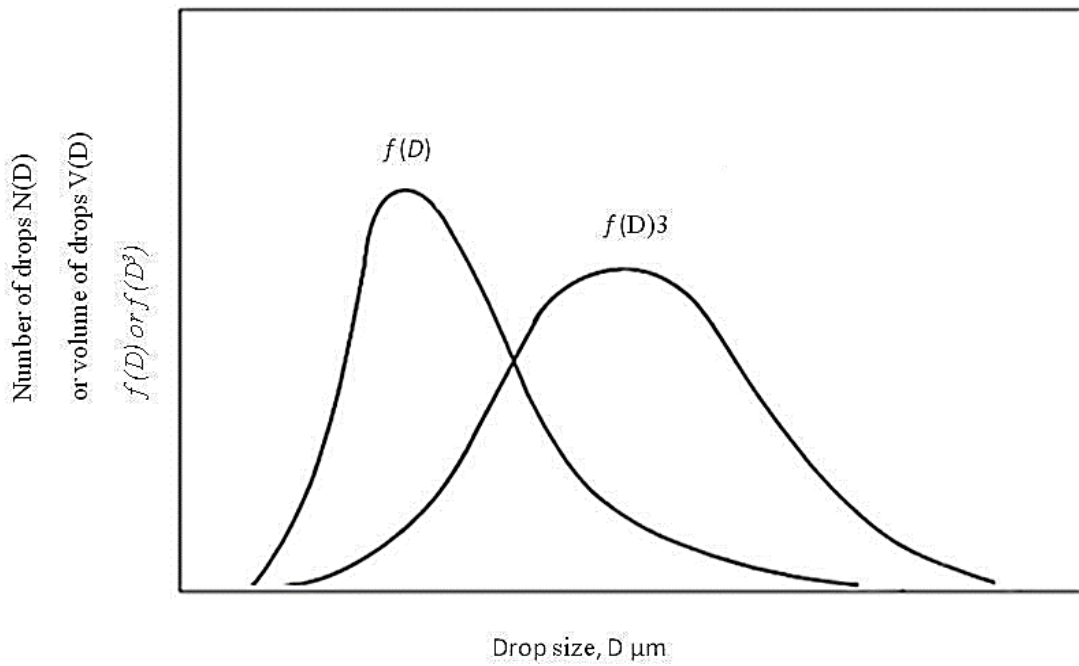


**Figure 3.16:** Usual drop size frequency distribution curves (number and volume)

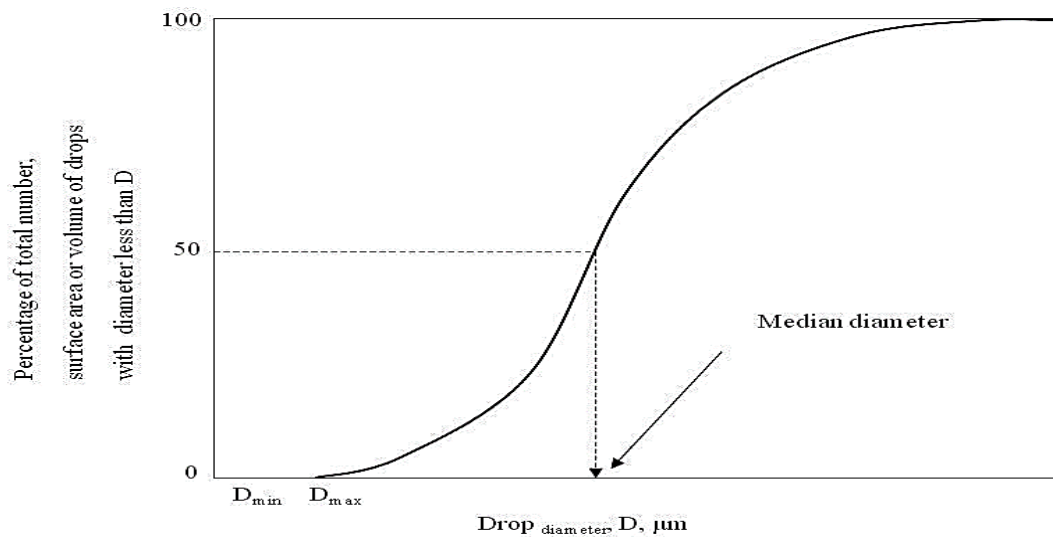


**Figure 3.17:** Usual shape of cumulative drop size

Terminology is frequently the main sources of difference and confusion in understanding drop size. Drop sizes are usually express in microns (micrometre) and to precisely compare drop sizes from one nozzle to another, the same diameter must be utilised. Therefore, in order to choose the appropriate statistical parameter for any given sample, how the data is going to be utilise and what will be compared with most be considered and most common parameters are:

- Mean: - Referring to the average size of a population
- Median: -Refers to size where 50% of the population are above/below.
- Mode: -Refers to sizes with highest frequency

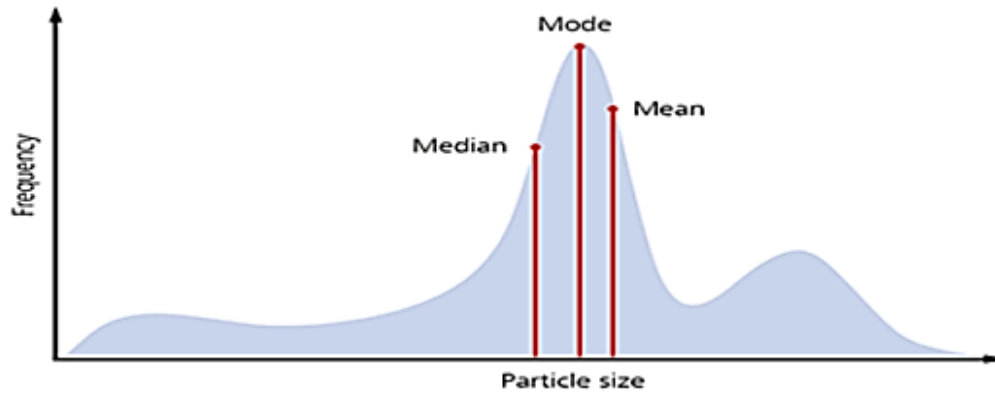


**Figure 3.18:** Particle distribution median, mode and mean (Malvern instrument limited 2015)

A mean diameter can be utilised to depict the quality of spray representing the original set with uniform drops. Means droplet size calculation rely on the application which the data is been utilised for. The way in which the mean diameters are characterise from the measured droplet sizes is showed in table 3.3. Where (N) is number of drops in size class (i) and (Di) is the middle diameter of size class parameters like the Sauter mean diameter ( $D_{32}$ ). Note that the Sauter mean diameter ( $D_{32}$ ) should only be utilised where a genuine motive for utilizing it like the case of were theirs interest in vaporisation rate of the spray (Dombrowski et al 1968). This particular study considers utilising the Sauter mean diameter and details of droplets distributions across various spray applications is shown in Table 3.2

**Table 3.2:** Mean diameters across and their applications (Nasr et al. 2002)

a	b	Name of mean diameter	Symbol	Expression	Application
1	0	Length or arithmetic diameter (AMD)	$d_{10}$	$\frac{\sum N_i d_i}{\sum N_i}$	Comparisons
2	0	Surface area	$d_{20}^2$	$\left(\frac{\sum N_i d_i^2}{\sum N_i}\right)^{\frac{1}{2}}$	Surface area controlling
3	0	Volume	$d_{30}^3$	$\left(\frac{\sum N_i d_i^3}{\sum N_i}\right)^{\frac{1}{3}}$	Volume controlling
2	1	Surface area-length	$d_{21}$	$\frac{\sum N_i d_i^2}{\sum N_i d_i}$	Absorption
3	1	Volume-length	$d_{31}^2$	$\left(\frac{\sum N_i d_i^3}{\sum N_i d_i}\right)^{\frac{1}{2}}$	Evaporation
3	2	Sauter Mean Diameter (SMD)	$d_{32}$	$\frac{\sum N_i d_i^3}{\sum N_i d_i^2}$	Vaporisation
4	3	De Brouckere	$d_{43}$	$\frac{\sum N_i d_i^4}{\sum N_i d_i^3}$	Combustion equilibrium

### 3.4.2.1 Arithmetic mean diameter ( $D_{10}$ )

The arithmetical mean diameter (AMD) refers to the average of the diameters of all the droplets in the spray sample.

### 3.4.2.2 Volume mean diameter ( $D_{30}$ )

The volume means diameter (VMD) is defined as the diameter of a droplet whose volume, if multiplied by the total number of droplets, will equal the total volume of the sample.

### 3.4.2.3 Sauter mean diameter ( $D_{32}$ )

Sauter means diameter (SMD) is one of the most valuable ways of characterizing spray. A way of expressing the fineness of spray in respect of the surface area produces by the spray. Diameters of that droplet whose ratio of volume surface area is exact as that of complete spray sample or the ratio of volume to surface area for the SMD is equal to the ratio of entire spray volume. Air atomise nozzle like XA or spiral atomize series produce the smallest droplet of all and normally whirl nozzle generate larger droplet than the spiral nozzle. For this reason, Sauter means is prefer for calculations.

$$\frac{D_2}{D_1} = \left(\frac{P_2}{P_1}\right)^{-0.3} \quad (3.7)$$

### 3.4.2.4 Mas (volume) median diameter ( $D_{v0.5}$ )

The VMD is a way of expressing drop size in respect of the volume of liquid sprayed. A value where 50% of the entire volume of liquid sprayed comprises of drops with diameter larger than the median value and 50% with smaller diameters when measured in terms of volume. Diameters that divides mas or volume of spray into two equal parts, half of the entire mas comprises of droplet with diameter smaller than the number and the other half with diameters that are larger.

### 3.4.2.5 Volume median diameter ( $D_{v0.9}$ )

The (VMD-  $D_{v.09}$ ) is most suitable utilised where a complete evaporation of the spray is required. A value was 90% of the entire volume of the liquid sprayed comprises of drop with diameters of smaller or exactly as this value and Figure 3.19 demonstrates the relatives drop sizes of different types nozzles.

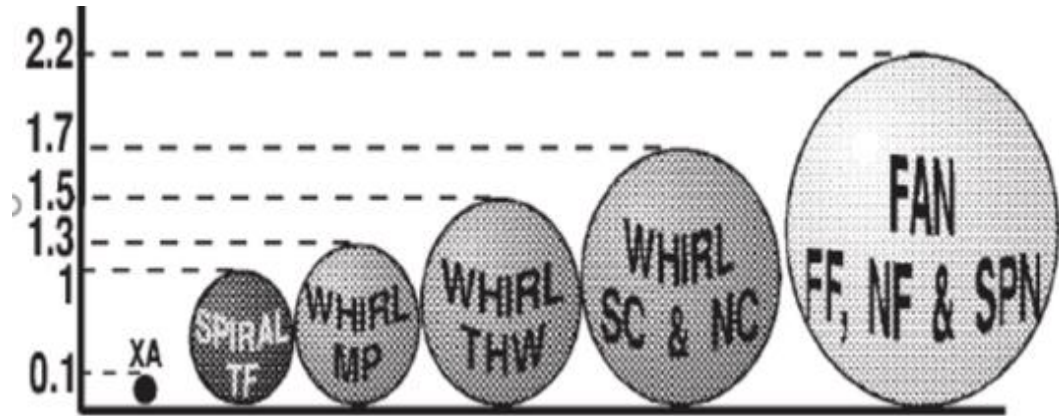


**Figure 3.19:** Relative drop sizes by nozzle series (Spraying System 2017)

### 3.4.3 Spray angle

The choice of spray angle for a specific application rely upon the coverage requirement and its effectiveness varies with spray distance (standoff distance) in ideal spraying condition. Spray angle can be referred to as the angle formed between two straight lines initiated from the tip of the atomiser to the outer periphery of the spray (Lefbvre 1989). Spraying angle is highly influenced by spraying fluid properties, nozzle capacity and spraying pressure. Spiral nozzle has a relatively stable spray angle over wide ranges of pressure, while in the case of spray angle of whirl nozzle decreases with increase with pressure.

Liquid with viscosity more than water forms smaller spray angles or even a solid stream ( $0^\circ$  spray angle) and so fluid with lower surface tension than water produce wider spray angle than those with water equivalent do. Any increase in spray angle will reduce spray drop distribution and vice vasa as illustrated in Figure 3.20. Although most of the capacity chart utilised by manufactures are based on theoretical spray width. Spray angle of less than  $30^\circ$  is referred to as narrow,  $30^\circ$ - $70^\circ$  are called the medium angle, while greater than  $70^\circ$  are the wide angles.

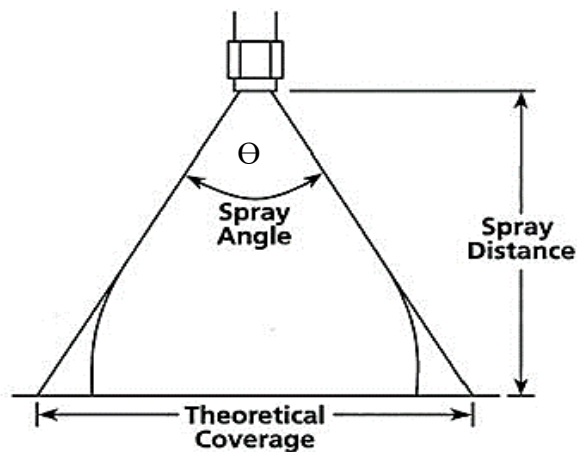


**Figure 3.20:** Spray angle (Naber et al 1996)

### 3.4.4 Droplet velocity

Droplet velocity is considered one of the most vitals of spray analysis and most important parameter for determining the impact of spray of a jet. Keeping in mind that the main aim of this investigation is to utilise impact of high-pressure water for decaling petroleum production tubing's. However, more details of droplet velocity in respect to pressure impact and momentum analysis will be provided in chapter five. As will be further utilise in justifying the suitable standoff distance from nozzle exit for effective descaling. (Opferet al.2013) believed that the velocity of droplet increases with increase in injection pressure and decreases with increase in standoff distance due to effect of aerodynamic forces.

### 3.4.5 Spray impact pressure

Spray impact pressure (SIP) measurement have been considered a critical parameter particularly in high pressure cleaning applications (Bendig et al 2001) with lower angle characterise nozzle proven more efficient. Newton second 2<sup>nd</sup> law of motion can be utilised in generating a model that will be useful in determining the expected impact at the target surface.

Considering a spray jet placed on a distance  $h$ , far away from the surface and spray angle  $\theta$ , as appeared in Figure 3.21. Along the target surface area, the momentum of the water spray is transformed into impact force to generate pressure and hence

$$F = ma \quad (3.8)$$

Where  $F$ , is the force (N),  $m$ , mass (kg), and acceleration is due to gravity, while the vertical component of the flow is the resultant force.

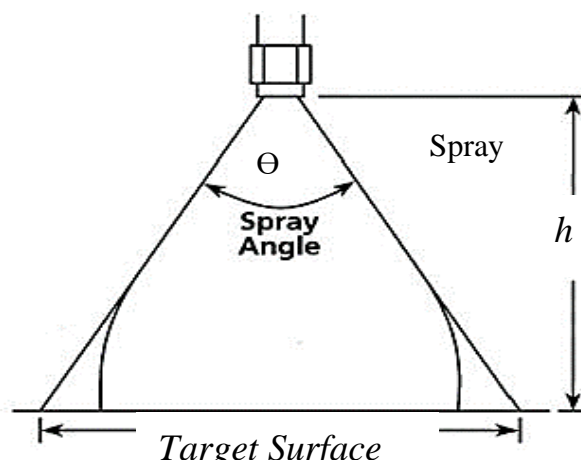


**Figure 3.21:** Spray impact pressure (Naber et al 1996)

Re-writing the component of force  $F$ , in the form of momentum by interchanging the acceleration as velocity gradient by utilising the Bernoulli equation, it has been transformed into pressure and density (Bendig et al., 2001) as driven in equation 3.4. and 3.5 respectively

$$F = \frac{d}{dt}(mxv) = mvxm v = mv$$

Where  $m$  is the mass flow rate and,  $v$  is the velocity gradient considering  $\frac{dm}{dt}=0$  at constant flow rate. Replacing, density and  $m$  in terms of

$$\rho = \frac{m}{v} \text{ and } \Delta p = \frac{1}{2} \rho v^2$$

$$F = V \sqrt{2p\rho} \quad (3.9)$$

Therefore, the Impact pressure is,

$$P_{impact} = \frac{F}{A} = \frac{v \sqrt{2p\rho}}{2dh(\tan \frac{\theta}{2})} \quad (3.10)$$

Since the impacted area by the spray,  $A = 2dh(\tan \frac{\theta}{2})$

Where,  $h$  is the distance from the atomisers exit to the cleaning target distance (standoff distance) and  $d$ , is the spray thickness. The forthcoming section will detail more on utilising impact pressure for jet cleaning.

### 3.4.6 Spray pattern

Spray pattern is used in describing the location and spray density of a liquid that is discharged from a nozzle. Alternatively refers as patternation, describe as the amount of volume per unit area covered by the liquid circumferentially and radially to determine the liquid distribution within spray. For easy definition, shape of the spray boundary and the droplet distribution it comprises within the boundary. Ideally, around 0.07 MPa minimum pressure is needed to create a well develop spray and require a pressure increase to pass through in a case of restrictive atomiser (Nasr et al., 2001). The main class of spray pattern are full cone, flat jet spray and hollow cone.

#### 3.4.6.1 Full cone spray pattern

The application full cone spray pattern varies across numerous cleaning operations that desired a relatively even coverage of fluid over a target area. Also, can only be maintain for a certain

standoff distance, after which the spray forms a fog or mist. Full cone spray patterns are classified into five major designs: Full cone spray, spiral full cone, oval full cone pattern, and square full cone spray and solid stream spray obtain via different atomization techniques.

Full cone spray pattern is generated through the utilization of a unique internal vane design to generate a solid cone spray pattern that is characterise with spray angles ranging from 15°-125° and contains medium to large drop sizes. Usually utilise in chemical injection, dust separation, fire protection, metal cooling and washing/rinsing operations.

The spiral full spray pattern is produced from spiral full cone nozzles that generate a solid cone shaped spray pattern when the liquid exists the void in the spiral. This type of spray pattern is not as uniform as the full cone produce from full cone nozzle that utilises an internal vane instead. It's characterised with spray angle ranging from 50°-170° and comprises relatively course drops. Utilised in fire protection, dust separation, quenching and flue gas desulfurization operations.

The oval full cone spray pattern is product of the oval type of full cone nozzle that utilises a special internal vane to generate a solid cone shape spray pattern. That has an oval impact area characterise with its width almost one half-its length. This spray pattern consists of medium to large sizes drops and have a spray angle ranging from 60°-105° and it found suitable for cooling/quenching, dust control and air/gas washing applications.

The square full cone spray pattern is produced from square full cone atomisers that utilise a unique internal vane to create a solid –shaped spray with square impact. It's attributed with uniform spray with square impact, spray angle range of (52°-105°) and consist of medium to large size drops. Cooling and quenching, fire separation, dust control and air/gas washing operations are most peculiar application of the oval full cone spray patterns.

The solid stream spray pattern is produced from solid stream nozzles with 0° spray angle characterise with the highest per unit area and mainly used in making and lamina flow application

### **3.4.6.2 Flat fan spray pattern**

Flat fan spray patterns are generated through flat fan atomisers that produce thing flat sheet of liquid that expands as it discharges away from the nozzle exit. This flat edge spray pattern is used on spray headers to deliver uniform coverage because of overlap distribution.

These spray patterns are considered to have more impact than hollow and full cone pattern due to liquid concentration into a small area. Normally classified into:

Even spray pattern generated by flat fan even nozzle. This thin rectangular spray pattern consists of an even distribution of medium drop size and have a spray angle ranging from 25°-65°. An edge-edge pattern contact positioning is required when used on header and are utilised in coating, moisturising cooling and washing applications.

The tapered edge flat spray pattern produced from flat fan (tapered) nozzle that used on spray headers to generate uniform coverage due to overlapping distribution. It has a spray angle ranging from 15°-110° and are utilised in high impact cleaning, label removal and particularly decaling operations.

An even flat spray pattern containing medium size drop at spray angle of 15°-150° that is considered suitable for washing and shower in paper making application generated with the aid of deflected flat fan nozzle. This even flat fan spray pattern is produced through the utilization of deflector surface technique that has a large passage design to reduce clogging via the round orifice.

### **3.4.6.3 Hollow cone spray pattern**

Hollow cone spray patterns are characterised as liquid flow with a ring –shaped spray pattern, with impact region around where the fluid is occupied on the outer edge of the spray patternation. Mainly produce from axial and tangential design hollow cone atomisers. Whirl chamber hollow, deflected type hollow cone spray, and spiral type hollow cone spray pattern are part of the main types of hallow spray patterns.

The circular spray pattern that contains small drop size and high capacity is produce when a whirl chamber nozzle rotates the fluid. It has a spray angle of 40°-165° and its mostly needed in in dust control, water aeration, air gas & water cooling, flue gas desulfurization (FGD) and cooling product on conveyors applications.

Umbrella-shaped hollow one pattern with spray angle of 100°-180, is produce from the deflected hollow cone spray nozzle by utilising the deflector cup to generate the spray pattern. Usually utilise in decorative spray, dust separation, water curtain, and fire protection and flush cleaning of interior of pipes & tubes.

Circulars shaped spray pattern with drops slightly courser than those in the other hollow cone sprays and high flow rate in compact nozzle. This spray pattern is produced from the fluid spiral hollow cone nozzle when the fluid leaves the void in the spiral. It has a spray angle of 50°-180° and utilised in dust separation, fire protection, and flue gas desulfurization applications.

### 3.5 Spray jet cleaning

The technique of utilizing high-pressure abrasive water in cleaning by many multinational companies like Schlumberger (Jonson et al., 1996). As well as Philips Petroleum Company in North Sea, Norway (Enerstvedt et al. 2001) has recorded huge success. The rates of mineral growth in hydrocarbons producing well remain the greatest challenge face by the petroleum industries today. Since many wells now days have scale deposition problems. However, the scale blockage issue is getting more rampant as injected water breakthrough is becoming more common and the scale itself becoming more stubborn. Figure 3.22. Illustrate a sample of scale deposit in petroleum production tubing.

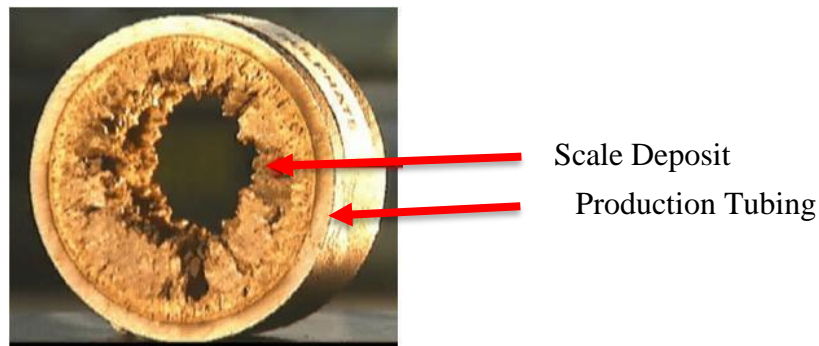


**Figure 3.22:** Scale deposit in a production tubing

Decrease in production because of increase in roughness of the production tubing that leads to decrease or restriction in flowing area has been considered as primary effect of mineral scale growth in production tubing. This leads to increase in pressure drop that consequently result in decrease in production. Accessibility to the lower section of the well become difficult with increase in the mineral growth, and eventually the growth in the tubing itself will block them completely. Continue depletion of reservoir will results to the occurrence of water break through consequently, water with high dissolved mineral will enters the well, and flow upward through the pipe. As it continues to raise a combination of cooling and drop in pressure saturates the liquid. The already dissolved salt comes out of solution and deposit on the tubing, starts to develop along the flow through a production alteration.

A more severe situation is the deposition of insoluble scale like Barium or Strontium sulphide as a result injected seawater breakthrough. This is usually high in sulphate salt mixing with other formation water that have high amount of other salts like barium, strontium and the rest.

The research team of the Schlumberger research centre in Cambridge, UK, were able to develop rough jetting techniques for cleaning both tubing and wellbore hardware without jeopardizing their integrity. A full-scale testing facility was built in the Cambridge centre to be able to test the technique on a realistic condition. This in-depth study on jetting performance utilises jet-cutting rig (JCR), powered by a 750KW capacity pump was able to simulate jetting with backpressure of up to 5000 psi. Also, practical pressure drops achievable in coil tubing operations. The Schematics of schlumberger jetting techniques is shown in Figure 3.23

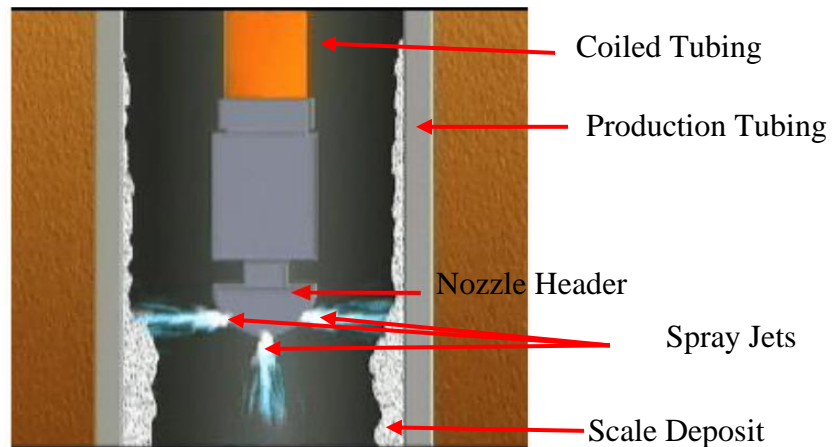


Figure 3.23: Schlumberger Jetting Technique (Schlumberger 2013)

The significant differences in performance of the jet at surface condition and down-hole condition were the most important findings in the research. At surface condition in absence of backpressure, small bubbles were form on the jet. It has a high erosive effect when it collapses on the target, a phenomenon refers to as cavitation. While at down-hole condition, both the bubble formation and its erosive clasping behaviour were suppressed. Ideally, the jet was found to be four times more erosive around the surface than in the down-hole condition. Indicating that the descaling technique is efficient in shallow wells. However, under realistic down-hole conditions, its performance substantially reduce. Investigation on scale tubing removed from a production well proves the absolute inefficiency of using pure water jet without dissolvers.

Additions of small amount of sand into the system alter both characteristic and performance of the system. The abrasive jetting was an improvement in terms of scale removal but with side effects of damaging both the production tubing and integrity of the well completion. The quest for developing efficient jetting techniques that will effectively removes scale without harming the integrity of the well. Leads to a comprehensive study of the interaction between abrasive particle target scale and the integrity of the well. Considering the criticality of the behaviour of individual particles, a particle impact tester was integrated into the testing system

to study the collision and high-speed particle impact. The shape of the particle was found critical in respect to the erosion of ductile materials like steel tubing. Examples is the way a sharp sand particle will plunge the steel surface and cut away the steel leading to high level of damage. Nevertheless, the impact of hard spherical particle on the surface will deform the surface leaving a spherical hole. However, much less damaging compared to the sharp sand particles. In the case of other brittle materials like scale, the shape of the abrasive particle is not important, because the impact process not the powering action of the abrasives removes the surface. The impact process causes nucleate networks of fractures through the material and hence the choice of spherical particles could completely solve the problem. Another abrasive property tested was the hardness of the particle considered as a key parameter in fracture toughness. If the abrasive is very week or the target surface is very strong, the impacting particles end up shattering into fine dust without making any damage to the scale surface.

The scientific study to design the effective abrasive material that will not harm the integrity of the well resulted to the invention of stealing bead materials (stony beads). The performance of sterling beads was exceptional by effectively descaling the production tubing with no damage to the tubing. The invention of this technology has open door for the development of new generation tubing cleaning tools. A realistic post decaling testimony can be deriving from one of Stumberger clients. Who's after exhausting many techniques to remove calcium carbonate scale without success and 2000 tons of carbide mills were destroyed in a day before given the strong beads system a trial. The strong beads trials were able to clean a 25ft of tubing at between 30 to 90 ft/lb, but the mechanical integrity of the tubing was at risk (Mirza et al 1999), (Leal et al 2009). Together with high environmental concern, even though the treated section of the deposited scale has been completely cleaned.

The Research by the Schlumberger recorded some interesting result, though could not establish nether the opportunity for enhancing cavitation as a jetting mechanism for enhancing erosion nor developed an environmentally friendly option. Contrariwise, the proposed abrasive jetting technique was attributed to negative consequences like environmental concerns and the destruction of the production tubing when used for several years. The forthcoming section discusses the main jetting mechanism techniques and detailed more on cavitation as a jetting erosion enhancement, which was the genesis of the introduction abrasive particles.

### **3.5.1 Mechanism for jetting technique**

Water jetting techniques break down scale deposit through the utilization of any or combination of erosion, abrasion, stress cycling and cavitation mechanism. History of series of laboratory and field experimental programs to find the effects of varying jet velocity and fluid viscosity, jetting head rotation. As well as jet stand-off distance toward the rate of scale removal. In addition to the effects of abrasives, effects of using a gas shroud to increase the jet's effective distance as a reason for effective jet cleaning. The result from this series of test prove instead of the above mention parameters but rather more attach to the principle jetting mechanism utilize during cleaning. Achieved either in combination or in isolation of: Stress cycling because of continues application, removal and relaxing of pressure and abrasion through scraping of material by the friction of two moving fluid. Erosion due to high rate jet striking deposit, and the less utilize mechanism called cavitation when localised liquid vaporises to create a pocket, the pocket collapses and high pressure liquid rushes in (Campbell & Brunskill, 2013). The respective jetting mechanisms are detailed in the forthcoming sub heads

#### **3.5.1.1 Erosion mechanism**

Erosion is an effective cleaning mechanism that significantly weathered through and across the scale deposit or target which power relies on the jetting efficiency or the rate at which the accelerated fluid strikes the deposit. Achieved by focusing the kinetic energy of the high velocity of a fluid on the target surface to attain the desired results depending on the type of scale deposit. It has for long been utilized in the petroleum industries for numerous operations like produce sand removal, drilling solid and the rest. Tools utilizing high-powered rotating jetting have been chosen due to effective erosion linked to complete well bore coverage advantage but were found relatively expensive. Leaving gap between simple, inexpensive swirl nozzles and new generation rotating tools like the non-rotating high-pressures vortex nozzle. This nozzle harnesses the action of high-speed fluid swirl to remove deposit through four tangential offset nozzles. Producing high-powered vortex (swirling mass) of fluid inside the tubing, casing or open hole. The combination of the created vortex in the wellbore and the resulted descaling debris will introduce abrasion mechanism. There by satisfying the economic, simple and effective operation requirement even though limited to effective removal of weaker scale (Campbell & Brunskill, 2013), i.e. calcium sulphate scales deposits.

### **3.5.1.2 Abrasion mechanism**

Abrasion mechanism is an unsafe but effective jet cleaning technique that relies on the ability of the friction between two moving particles (sand and water slurry, sterling beads etc.) to mechanically scrap the targeted surface (scale deposit). It has for long been documented in cutting of hard metal/rocks, blast cleaning and paint preparation. Also peculiar in oil field operations like slots and hole cutting or tubing complete cut under down-hole condition. This is depending on the exploited forces of either ductile or brittle erosion. The earlier mention weathering through the material by cutting or gauging the target material surface in respect of angle of attack which is optimum around  $25^\circ$  and reduces towards  $90^\circ$  (Caffey 1992). Hardness to fracture strength ratio like the abrasive to target material hardness ratio should be two for ductile cutting. For the shape of the abrasive particles angular shaped were found with enhance cutting and gauging mechanism than the round shape which are less effective both less damaging to steel. While for the size factor larger particles demonstrated more cutting wear due to less momentum contract of smaller particles that made them bounce back with little impact on target (Campbell & Brunskill, 2013).

Even with the discuss abrasive selection guide challenges like abrasive cost, scale removal ability, safety and integrity of the tubular still exists. This is making it difficult to balance between the economy of effective removal ability and the post descaling conditions of the tubular. Pure water jet seems safe and only effective on soft scale, but leading large particle cut sizes which are not good for hole cleaning and surface equipment. The addition of sand to the jet will increase cleaning efficiency by removing hard scale with consequences of jeopardising the integrity of both the tubing and down-hole equipment. While the sterling bead introduction that proves to clean scale without causing damage to the tubular and (Gholinezhad, 2006) believed it's still not completely environmentally friendly certified couple with CT pumping limitations

### **3.5.1.3 Cycling stress mechanism**

Cycling Stress is another more surface-active scale destructive mechanism by continues quick stressing and relieving a localize area. It can wear or destroy hard material like steel cutting in the manufacturing industries using pulsating water jet technique. In addition to hard scale removal abilities in the oil industries through the optimization and control of the stress cycling mechanism has since been put to record. Hard scale removal can be achieved through continues down-hole inducement of cycling stress by rotating jetting nozzles localizing stress (Campbell & Brunskill, 2013). As result of the jet impact on the local area and pressurizing

the structure of the material to be removed through fissures and micro cracks already existing on the surface and the matrix of the deposit

Another way can be the utilization of combine CT and fluid oscillator tools to develop alternating bursts of fluid. That create pulsating pressure waves within both wellbore and formation fluid to break up near wellbore damages and enhance the permeability of both perforation and near wellbore. The oscillator generates compressive waves that hit and cause vibration to the target material. Seizing the advantage of differences in materials (different vibrating resistance) of scale or formation damage causing disintegration and fall apart as vibration continues

#### **3.5.1.4 Cavitation mechanism**

Cavitation mechanism is the process of making transient vapour-filled cavities in a fluid at ambient fluid pressures exceeding the vapour pressure in the cavities. This can cause wear on material or metal by the imploding of the collapsing void near the metal surface producing cyclic stress through repeated impulsion. It is attributed to issues like damage to both ship and pump propeller. Instances like pump impeller wear that bends toward were the sudden change in the direction of liquid occurs.

Cavitation can be categorized into behavioural classes like initial (transient) cavitation or non-initial cavitation. Furthermore, when it occurs in low-pressure area during the fluid flow through an obstruction or surface of an oscillating body is referred as passive cavitation. The terms activate cavitation mostly employed to enhance hole making, cleaning of reservoir rock, completion equipment from scale deposit and other down-hole tasks (since new cavitation tools can reach 300m and more down-hole).

Cavitation can be achieved through the use of liquid hammer enhancement to produce vapour bubbles at very high ambient pressure (Bakker, Ivannikov, & International, 2002). Cavitation in general has since been utilized in biomedical field for the destruction of kidney stones through wave lithotripsy shock. As well as chemical engineering for homogenize, or mix and break down, suspended particles in a colloidal liquid compound such as paint mixtures or milk and vegetable oil refining. Still utilized in the petroleum industries for cleaning due to its sufficient power to overcome the particle-to-substrate adhesion forces by cleaning tube, plugged screen in water, oil and gas wells. Further utilization including the cleaning of non-acid soluble scale type, environmental/energy engineering for improved sludge conversion into biogas (Bakker et al., 2002). Also (Restivo, Brune, & International, 2016) reported its utilization in marine industries for marine removal through ROV and cavitation

An alternative cavitation explanation will be the concept of turbulent water jet. With artificial induce vapour and gas cavities simulated to grow so that when it is imping against a surface. The cavities collapse on or near the surface in the high-pressure stagnation where the jet impacted the solid material. Additionally, due to the concentration of collapse energy over many very small areas during collapse producing an extremely very high localize stress. Even though, the impact pressure outside the bubble toward increase in collapse violence have since been proven both theoretically and experimentally. Making ambient pressure environment favourable for cavitation erosion in drilling (Bardin et al. 1998). Cavitation number is very important parameter as express in equation 3.11 and 3.12 bellow.

Other factors affecting cavitation efficiency apart of cavitation number is the standoff distance between the orifice and the target material and this control the rate of growth and collapse of cavity burbles in the jet. Coupling with more surface jetting performance compared to virtually none or little existence down-hole because of high ambient pressure (disappear with increase in depth and above 300psi) (Campbell & Brunskill, 2013) .Credence for the possibility of extending cavities for improved bottom-hole cleaning even at maximum depth can be drawn from the improvement.

$$Eu = \frac{\text{Pressure Force}}{\text{Initia Force}} = \frac{(p_u - p_d)L^2}{(\rho L^2)(V^2/L)} = \frac{p_u - p_d}{\rho v^2} \quad (3.11)$$

Were  $\rho$  is the density of the fluid,  $p_u$  is the upstream pressure,  $p_d$  is the downstream pressure and  $V$  is the vertical velocity of the flow. The above dimensionless number equation used in calculating fluid flow calculation known as Euler number or can be referred to Runark Number (Ru) if inversed. This expresses the relationship between a local pressure drops caused by a restriction and the kinetic energy per volume of the flow. Also, use to characterize energy losses in the flow, where a perfect frictionless flow corresponds to a Euler number of zero (0).

While cavitation number (Ca) is identified as dimensionless number use in flow calculations. Although, this time expressing the relationship between differences of local absolute pressure from the vapour pressure and the kinetic energy per volume. It's used to characterize the potential of the flow to cavitate. Where  $\rho$ , is density of the fluid,  $p$  as the local pressure,  $p_v$  as the vapour pressure of the fluid and  $V$  characteristic velocity of the fluid.

$$Ca = \frac{p - p_v}{\frac{1}{2}\rho v^2} \quad (3.12)$$

### 3.5.1.5 Classes of cavitation

The concept of cavitation has for long been attributed to the pressure variation along liquid system. However, the pressure variation can be as a resulted of different types of forces, which further used as basis for cavitation categorization. The broad classes of cavitation are hydrodynamic, acoustic, optical and particles as appeared in fig. 3.24

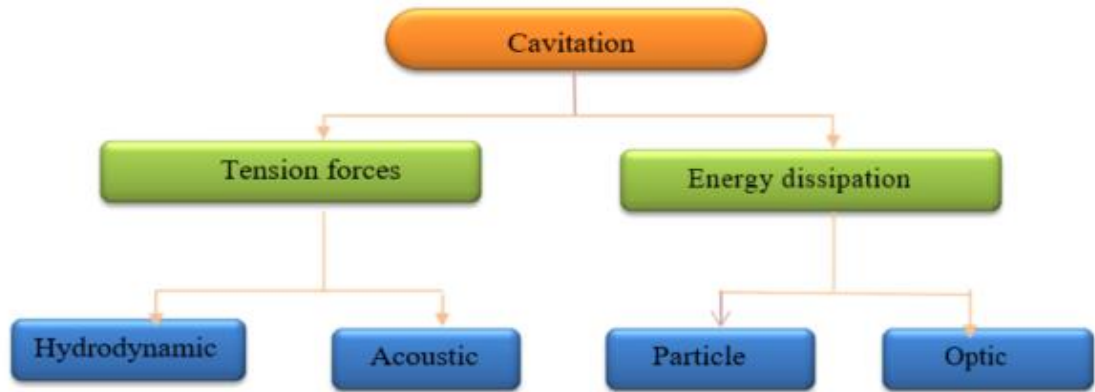


**Figure 3.24:** Classification of cavitation (Lauterborn 1980)

#### 3.5.1.5.1 Hydrodynamic cavitation

The hydrodynamic cavitation is attributed to pressure drop along a flowing fluid to the saturated vapour pressure of water. Mostly experienced in hydraulic machineries like impellers, turbine, nozzle, hydrofoil and the rest as appeared in Figure 3.24. This class of cavitation remain a major concern in the industries up to date due rate of material degradation it causes on material surface.

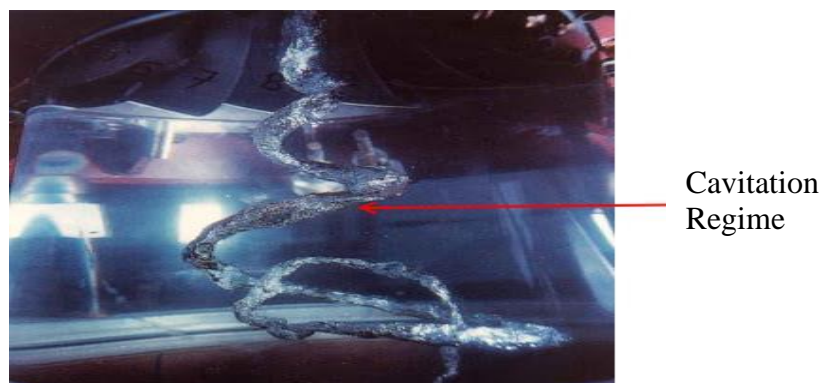


**Figure 3.25:** Cavitation regimes along Francis turbine (Brennen., 1995)

### 3.5.1.5.2 Acoustic cavitation

The occurrence of acoustic cavitation is as a result pressure shocks related to the acoustic waves, which turn continues along nucleation, growth and later collapse of the bubble. Application fields like sonochemistry, sonoluminescence and sonoporation have for long recorded the utilization of acoustic cavitation. Other fields of successful application include the medical field, in terms of genes transfer, cancer treatment and the nobble at of crushing kidney stone known as lithotripsy (Zhang A 20013). Figure 3.26 illustrated a typical light emission by a trapped cavitation bubble.

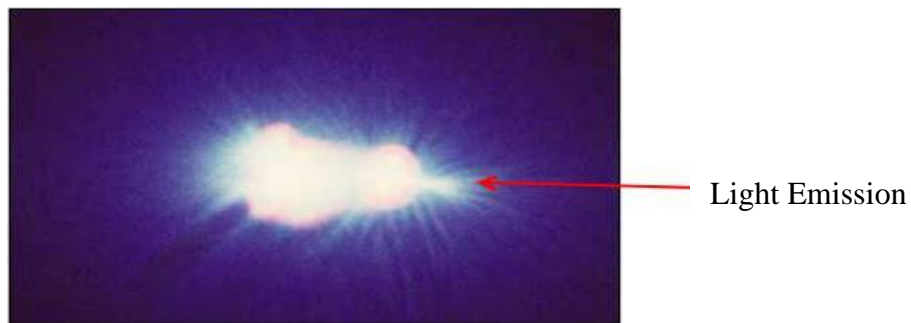


**Figure 3.26:** Light emitted by a trapped cavitation bubble (Zhang Y 2013)

### 3.5.1.5.3 Optic cavitation

Optic cavitation is created through a medium radiated by high intensity beam of laser and have been on record since 1950, been utilised in bubble chamber. Normally, extreme condition result to the breakdown of the medium liquid that cause the cavitation bubble. In some case the liquid breakdown due to the local deposit of energy that result to a " hot spot" and a type of micro explosion. In optic cavitation the liquid is being raptured by the cavitation photons even though, any type of high-energy particle may be used (W.Lauterborn 1997). Figure 3.27 illustrate the creation of electro optics shocks from laser plasma.

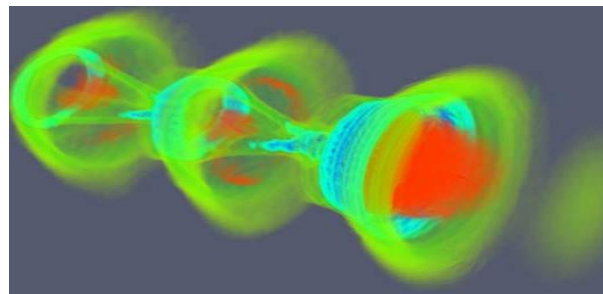


**Figure 3.27:** Electro optic shock created by laser plasma (D.F Gardon 2008)

#### 3.5.1.5.4 Particle cavitation

Particle cavitation is caused by the passage proton or neutron particles within the medium that result to the ionisation of some part of the medium. Also due to subsequent energy transfer resulting to rapid heating and formation of tiny bubbles called particle cavitation. So, it's now clear that cavitation bubble can be generated by other elemental particles like neutron and photon aside of the photons in optics cavitation. For long (Raza B.1996) have reported it utilization in the aspect of rubber toughening epoxies application and the rest. Figure 3.28 show how cavitation bubble was caused by a 50-Volt spark at  $t=0$  ms.

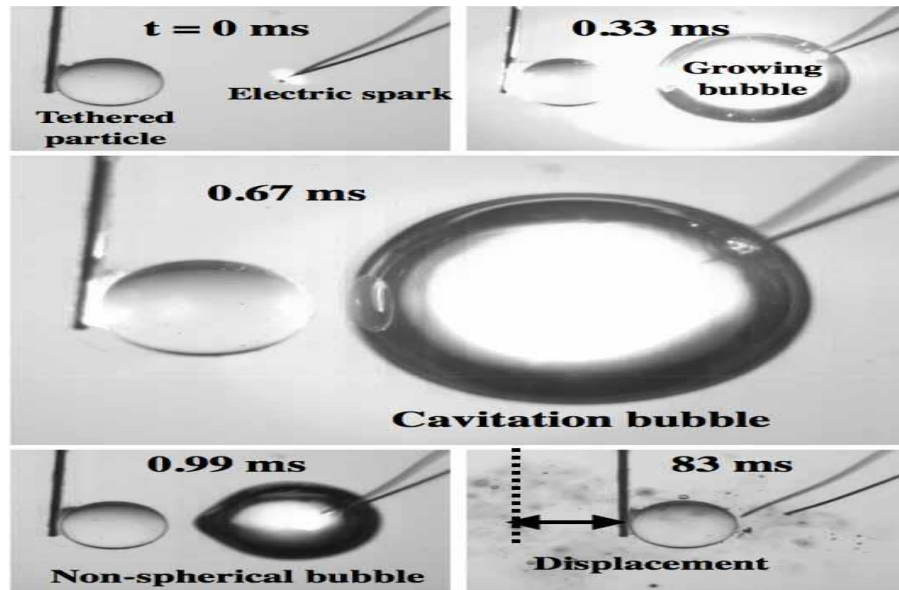
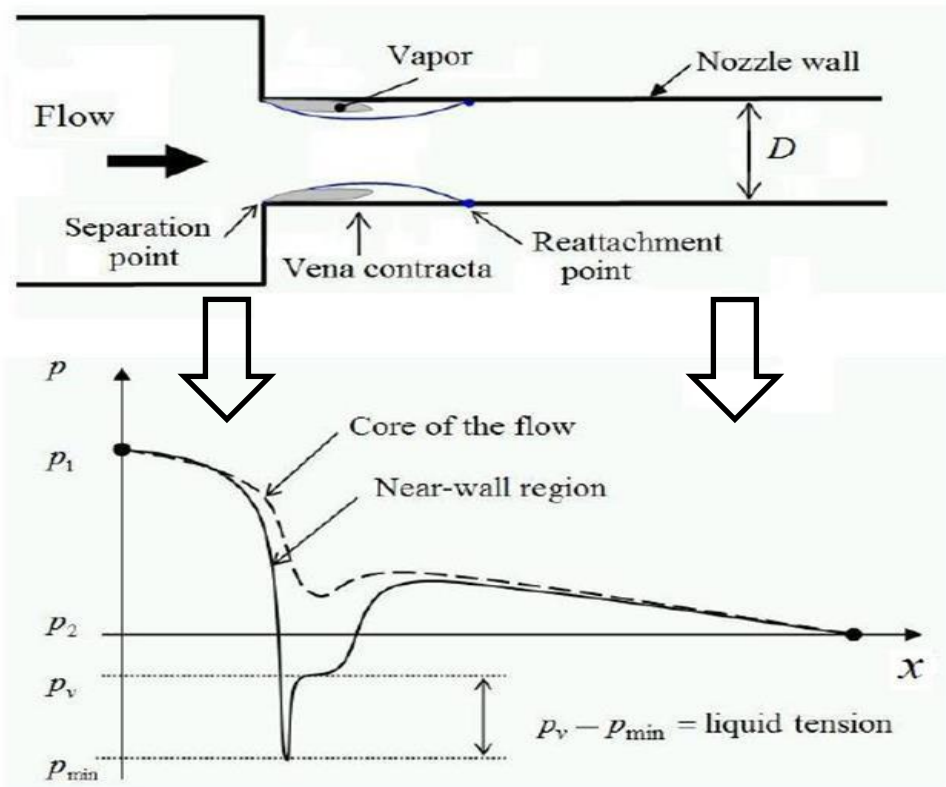


Figure 3.28: particle cavitation (DFD 2015)

#### 3.5.1.6 Cavitation in spray nozzles

Fluid flow through nozzle can be characterise based on the rate of fluid flow obtained in respect of nozzle geometry, pressure difference, size and the properties of the flowing fluids like surface tension, viscosities and the rest. The occurrence of cavitation at the exit flow can be related to the sufficient increase in pressure difference through the orifice. Instigating the boundary layer to try to separate from the wall of the orifice wall due to some sudden changes in both the cross-sectional area of the flow and direction (Desantes et al., 2003). Therefore, cavitation will occur each time the sharp edge of the orifice, results to flow separating from the wall of the orifice (Koivula T 2000) which create a hole named as *vena contracta*. Subsequently leading to a circulation region between the *vena contracta* and the wall of the hole. A flow behaviour where the inlet flow passing through an orifice, increase flow across the *vena contracta* results to higher velocity at downstream sector is illustrated in fig 3.32.



**Figure 3.29:** Typical flows through a nozzle (Martynov et al. 2006)

Thus, causing a decrease in the static pressure head and increase in dynamic pressure leading the pressure decrease reaching saturated vapour pressure  $P_v$ , mostly occurring in the core of the flow as appeared in fig 3.32. Consequently, leading to the emergence of cavitation. Cavitation bubbles flow downstream alongside the water flow, but later on collapse due to increase in pressure, consequently decreasing the downstream pressure increase the cavitation bubble length (Koivula T 2000). Increasing the water acceleration result in pressure depression, which consequently result to cavitation so far, the static pressure attains the saturated vapour pressure of water. Now it is clearly established on how important downstream pressure is toward cavitation bubble length.

The extension of cavitation bubble growth downstream is achievable by lowering downstream pressure. While the implosion of cavity and violent behaviour of cavitation shock wave is attributed to sudden pressure recovery in the downstream (Koivula T., 2000). Hence, beyond the mention studies, other scholars have the notion that higher injection in respect of flow rate result to low pressure bellow critical value particularly at vena contracta generates vapour cavities (Arai et al. 1985). This is known as hydrodynamic cavitation whit capacity of improving spray jet breakup (Martynov et al. 2006). Further established that at the zenith of

cavitation, decrease in downstream pressure does not necessary increase flow rate due existence of a phenomenon known as chocking.

Researchers on their pursuit for experimentally examining the cavitation flow along nozzle came up with two dimensionless numbers (Reynold number and Cavitation number). As the most important dimensionless group that can express cavitation,  $\sigma$  shown in Eq. 3.13

$$\sigma = \frac{P_{\infty} - P_V}{0.5 \rho v_{\infty}^2} \quad (3.13)$$

Where  $\sigma$  is the cavitation number,  $P_{\infty}$  is the pressure of the fluid,  $\rho_w$  is density, the saturated vapour pressure and velocity of the fluid is  $P_V$  and  $R_e$  is the Reynold number as express in Eq.3.14

$$R_e = \frac{\rho_w u d}{\mu_w} \quad (3.14)$$

Where  $\rho_w$  is the density of water, velocity of water,  $U$ , diameter,  $d$ , and viscosity of water as  $\mu_w$ .

### 3.6 Descaling Operations

The process of applying high pressure jet water to remove scale (oxide deposit) from metal surface in hot rolling application is the most renowned descaling process (Nasr et al., 2002). Moreover, it's recently more attributed to hydraulic scale removal in the petroleum industries. Optimization of descaling process has always been tied to proper selection of spray parameters. Archiving low energy cost and better scale removal is done through improving nozzle designs. Thereby, turning hydraulic scale removal from simple question of high pressure to developing science (Anon 1995) such as the development of special nozzles with knife like (cut) impact stream for optimal descaling (Brown et al., 1993). Another important requirement for archiving optimal descaling is the complete coverage of the target surface. This is achieved through proper nozzle arrangement that includes some spray overlap for better coverage and safety factors. Therefore, perquisite to optimizing descaling systems is nozzle configurations in terms of size, type and arrangement on the header in order to achieve both the highest impact force & target coverage at lower water requirement and energy cost. Experience from the past emphasise on impact force apart of other parameters like droplet sizes and injection pressure in removing hard surface scale, especially in steel making (Nasr et al., 2002). Since it has a tremendous impact on the spray pattered, though the surface

condition differs. Spray overlap from multiple nozzle descaling header is shown in Figure 3.30.

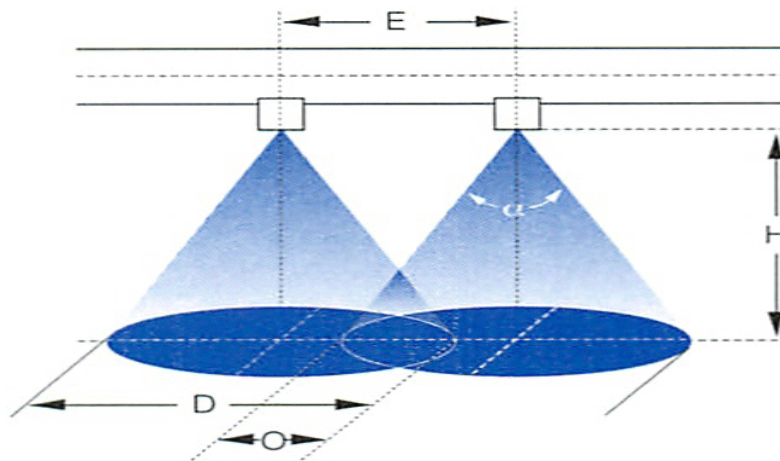


**Figure 3.30** : Arrangement of nozzles on descaling header (spray overlap) (Nasr et al 2002)

For complete descaling special nozzle arrangement are necessary on the descaling header. A- jet jet length, B, C-width, D-overlap,  $h_2$ -vertical spray distance  $\beta$  angle of inclination and  $\alpha$  nozzle jet angle.

### 3.6.1 Spray overlap

This is another very important spraying parameter that has direct effect on almost all the above fore listed parameters like droplet sizes, droplet velocity perttenation and liquid volume influx of the droplets. Spray overlap is essential for descaling purpose due to coverage and impact spraying requirement, even though nozzle orientation and tubing diameter constraint will not allow the multiple jet selected for the project to overlap well. A novel research on effect of spray overlaps toward essential spraying parameters like the droplet diameter, droplet velocity and influx within the spray overlapping region of two and three atomiser at different downstream position and injection pressure has been conducted by spray research group of the University of Salford. The result of the PDA experiment obtained at the 25, 50 and 75mm downstream overlap region of two and three nozzles at 3.7, 4.8 and 6 MPa injection pressure established a relationship that suggest the increase of droplet diameter with increase in downstream position. At the same time with a homogenous SMD distribution across the spray and the smaller droplet focussed near the centre of the spray (Nourian, 2016). While the highest droplet velocity was found to be close to the centre line too and decreases with increase in downstream region.

### 3.6.2 Pressure drop (multiple nozzle)

Despite the advantage of good scale or target circumferential coverage seized from the utilization of multiple nozzles. The relationship of pressure drops to number of nozzles utilised needs to be carefully considered. Since pressure drop is directly connected to flowrate meaning the larger the flow rates the larger the pressure drops. Also, nozzle with higher pressure drops will generate higher jet velocity. While on the other hand the more the number of nozzles, the low the expected pressure drops (Huang et al., 2018) as illustrated in Figure 3.22. Where the pressure drops of combination of 3,4,5 and 6 nozzles increases with flow rates and the nozzle impact reduces with increase in number of nozzles due to increase in the areas of their orifice.

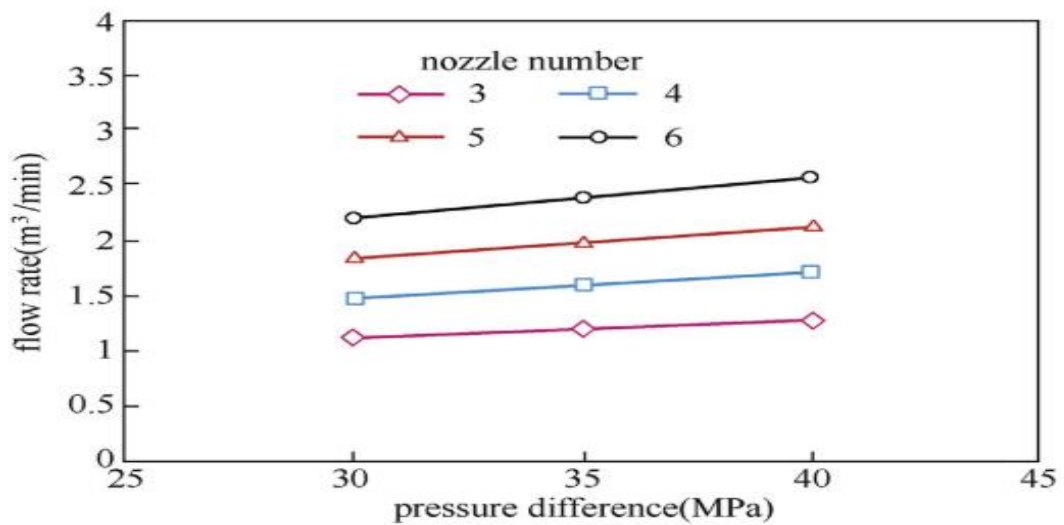


**Figure 3.31:** Nozzle pressure difference Vs flow rates of different numbers of nozzles (Tian, Li, Huang, Niu, & Xia, 2009)

### 3.7 Summary

After reviewing various behaviours of water flow in this chapter, the following outline can be drawn:

- The solid free jetting approach in down-hole cleaning is getting wider acceptance as replacement for sterling beads (solid particles) by the multinational's companies. Because of the negative promising end of the sterling bead technology.
- The performances of a nozzle sprays are mostly tied to the operational effectiveness of the entire spray systems consisting the atomizer/ headers manifold, system design, fittings/connections, pump etc.

- Multiple nozzle overlaps increase the spray target coverage during descaling but produces low pressure drop or low spray impact.
- Descaling through water jetting was found to be completely relying on any and/or combination of erosion, abrasion, cyclin stress, cavitation mechanisms.
- Cavitation erosion has been of great concern in many industries due to it consequential effect that are attributed to cost of repair/replacement of machinery part and the eroding of concrete surface water dam spillway.
- Cavitation create micro bubbles which when hit a surface will collapse in a violence behaviour that generate a pressure shocks that leads to a severe mechanical degradation of materials called cavitation erosion.
- The substantial pressure drop experience at nozzle *vena contracta* when using high velocity water flow in nozzle generate cavitation within and beyond the downstream of the nozzle
- The material weakening effect and enhance pressure wave front due to aeration (compression) have been sought to be applied as an abrasion compensation or replacement of sterling beads on down-hole cleaning due to it high erosion effect.

# Chapter 4

## Experimental Set-up and Procedure

### 4.1 Overview

This chapter presents the experimental design and set up including, procedures and description of detail steps required to guarantee the achievement of the precise research objectives. The Chapter covers the two phases including:

**Phase 1:** The pre-descaling experiment that are conducted outside the descaling chamber, in preparation of descaling experiments, as further classified into three sections:

**Section 1:** Design, construction and assembling of the upgraded descaling rig including the descaling chamber (ambient, compressed and vacuumed condition) in simulation of ideal descaling conditions.

**Section 2:** Design/ fabrication of wax scale moulder and its further utilization to produce soft scale samples candidate of different sizes and shape that can simulate different stages of scale growth in production tubing.

**Section 3:** Chemical characterization of both the available hard samples and constructed soft scale sample by compositionally analysing the hard scale samples via (EDs, SEM & XRD technique) and the soft scale samples through (NMR & FTIR).

**Phase 2:** The main experimental descaling trials will be conducted by utilizing the special constructed descaling chamber and is divided into three sections:

**Section 1:** Studying the effect of descaling parameters like injection pressure, numbers of nozzles, stand-off distance and header configurations toward the rate of scale removal.

**Section 2:** Studying the effect chamber water/air concentration i.e. ambient, compressed and vacuum air condition toward the rate of scale removal.

**Section 3:** Determining the optimum descaling requirement for the effective scale removal of different types scale deposit in petroleum production tubing

Particulars of the experimental plan and steps are given in the flow chart shown in Fig.4.0. Also, the experimental setups, methodology, procedure in addition precautionary measures and source of errors are itemized in each individual section.

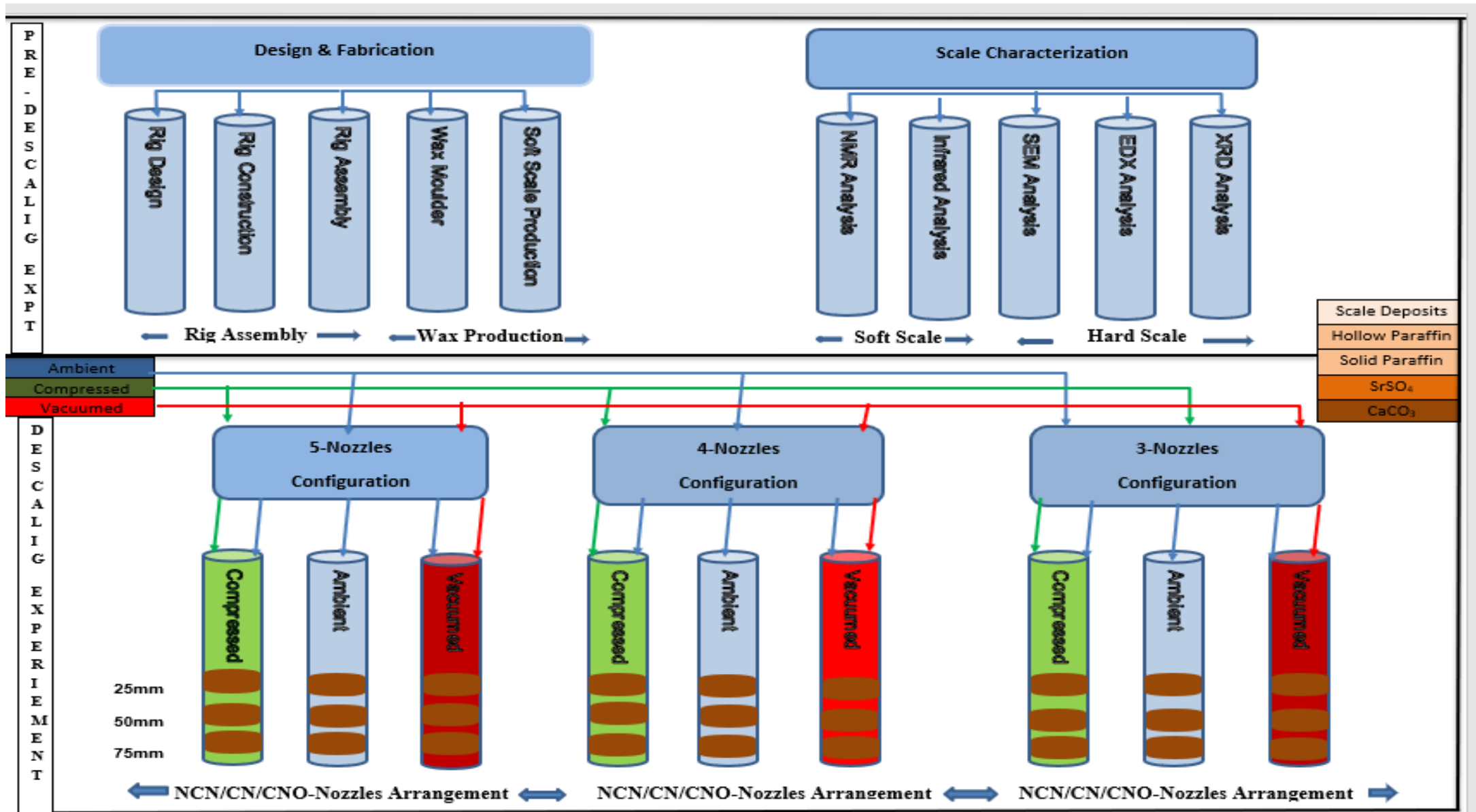


Figure:4.0 Experimental Setup

# Phase One

## 4.2 Descaling rig design and assembly

### 4.2.1 Descaling rig assembly

The complete descaling rig assembly consist of specials constructed descaling chamber made up of different component and other important descaling rig componet like water tank, compressed air system, vacuum pump, high-pressure water pump and the rest.

#### 4.2.1.1 Descaling rig component

Most vital component of the rig assembly beside the descaling chamber includes a 286 jet std DTB 402 with working pressure of 4000psi (600 bar), 1250 rev/min speed and 12gpm pumping capacity. This diesel driven ultra-high-pressure water pump with 2000 litter water capacity was rented from SLD Pumps and powers Ltd as shown in Figure 4.1C. In addition to a high capacity (6 bar) in-built air compression system of the SPGR lab that was utilised for the compressed operation (desired air concentration) in Figure 4.1A. While Figure 4.1B is a picture of the direct derive rotary vane vacuum pump (DD 300) with dual 2.3 cfm, 11/220 vac of -1bar vacuum pressure capacity was rented from GVE pump Manchester for the suction related experiments.

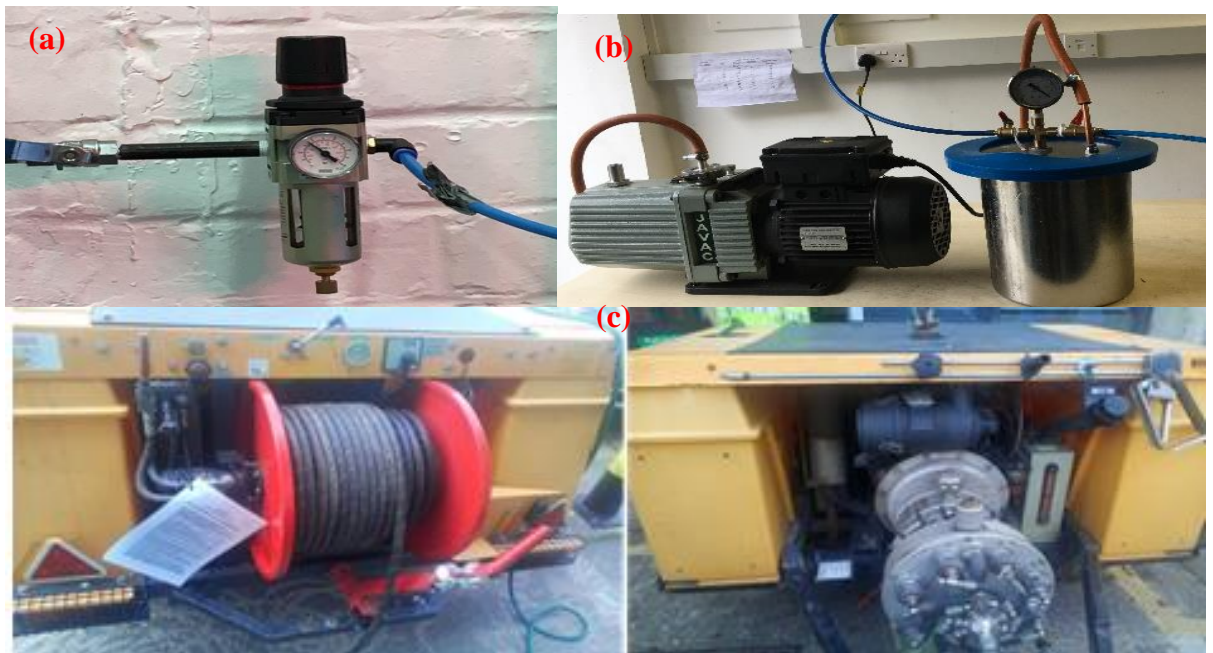


**Figure 4.1:** Descaling rig components, (a) Compressed air system, (b) Vacuum pump & (c) high pressure water pump

### 4.2.1.2 Chamber Control Board

A control board was design with Visio software and the equipment were selected and purchase from Swagelok Ltd base on the experimental desires and constraints. The components were later assembled on the board and incorporated into the rig as per design by the researcher. This special design and constructed control panel comprising of air and water line was utilised for easy and precise monitoring and controlling of the experimental parameters during operation. The water line consists of high capacity pressure gauge (0-160 bar range) and 80 l/min capacity flow meter connected through a high-pressure regulator valve (0-200 bar capacity) to measure/regulate water flow from the high-pressure pump into the chamber. While the airline encompasses of a combine pressure/vacuum gauge (-1 to 9 bar capacity), 80l/min capacity flow metre connected via high pressure regulator valve of (-6.8 to 6.8 bar capacity) to alter the air concentration of the chamber through compressor or vacuum pump. Schematic design of the board is shown in Appendix A1 and picture of the assembled control board is illustrated in Figure 419

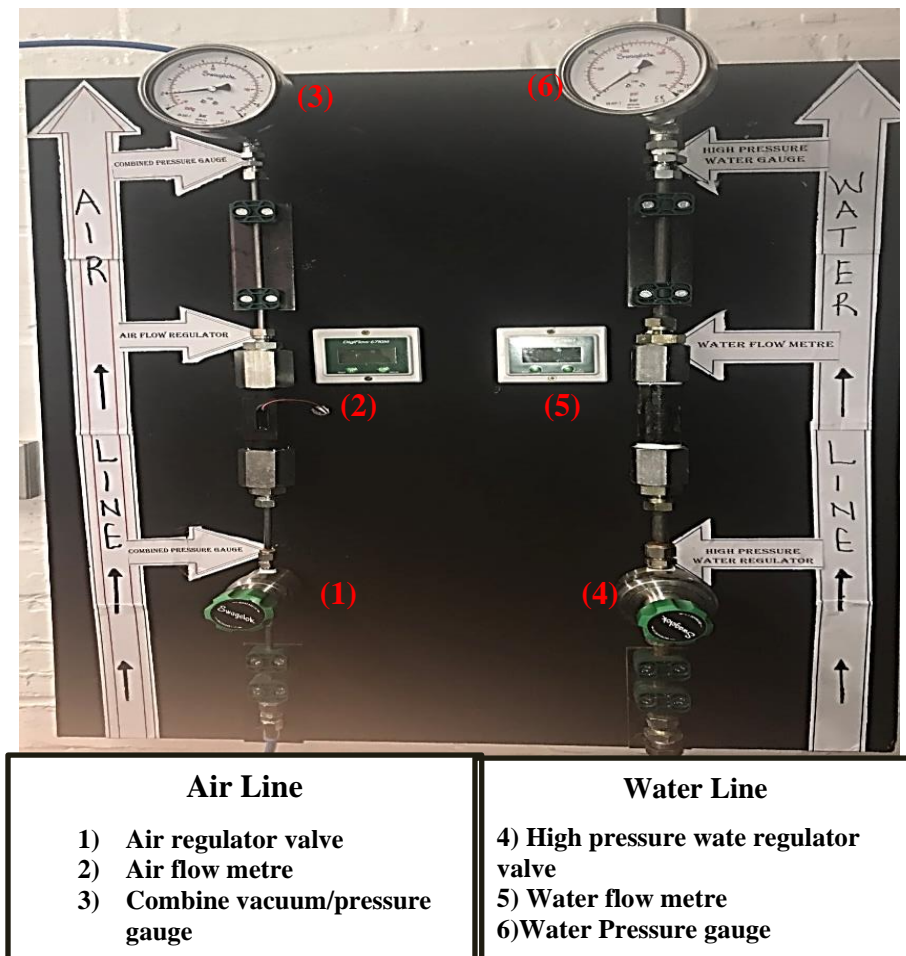


Figure 4.2: Picture of the assembled control board

### 4.2.1.3 Descaling rig set up

The scale removal experiment was led with the same special design descaling chamber set up notwithstanding including the scale sample clamped into the fixed position as appeared in Fig.4.3. The experimental descaling set up was designed with the intention of simulating realistic onshore oil and gas production tubing to appropriately execute the test. The scale cleaning trial was set up as appeared in Figure 4.13. Compressed air from the central air compression system or suction air from the vacuum pump passes through the selection valve, further into the airline of the control board and through the high-pressure air valve. The flow rate and the compression or suctioning of the air will be measured via the air flow meter and a combined vacuum/pressure gauge respectively to determine the air concentration of the chamber through the chamber plate. coupled with pressure relieve valve attached to the top of the chamber for evacuating or normalising the air concentration of the tube. High-pressure water pump feed by the water tank will be utilised to supply high-pressure water spray that is regulated into the water line of the control board via the high-pressure water regulator valve and into the multiple nozzle's header. The waterline flow meter and pressure gauge were utilised in measuring the pressure and flow rate of the spray through the multiple nozzle header in the chamber. The descaling chamber housing the scale samples, holder/support component and the multiple nozzle header. Its connected to the waterline/airline from the control board and pressure relieve valve through the top chamber plate and the discharge valves through the bottom plates as shown in Figure 4.3.

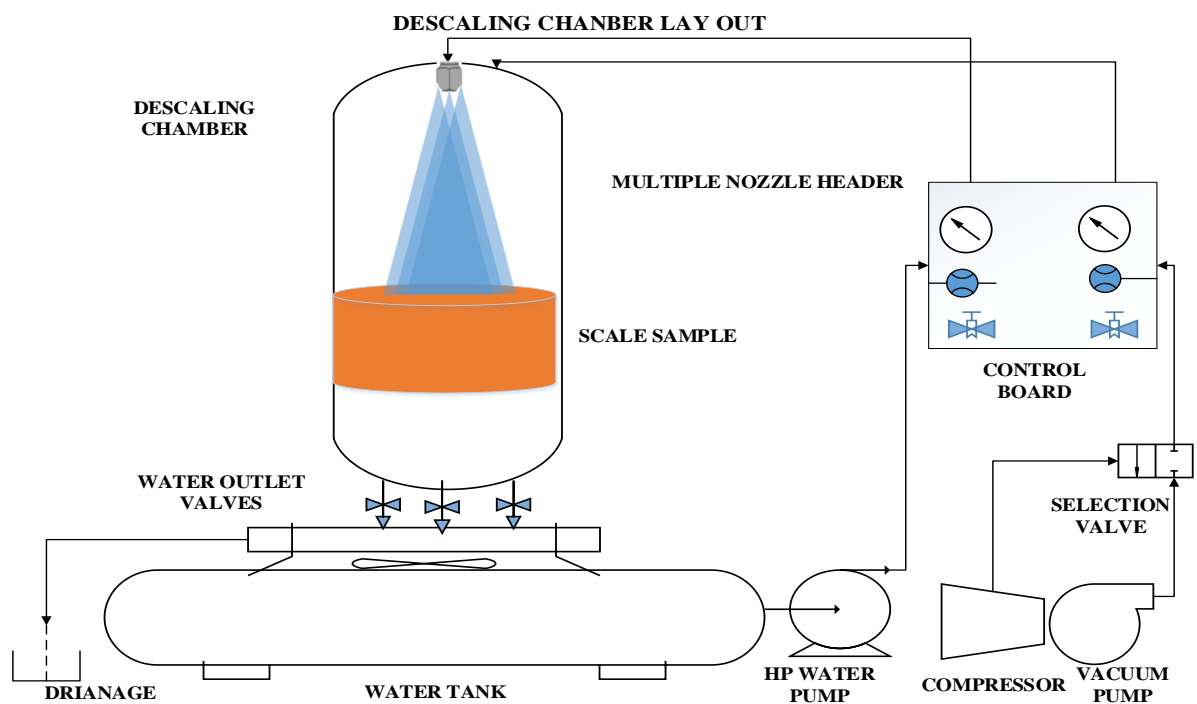


Figure 4.3: Descaling rig set-up

## 4.2.2 Descaling chamber design, construction and set up

### 4.2.2.1 Design principle

Scale deposit are mostly located at base or bottom hole along the production tubing's thousands of meters far down from the Christmas tree, since pressure increments is a function of depth. Therefore, a reasonably high-pressure chamber is important to comprehend the performance of jetting techniques regarding scale removal and other jet properties like cavitation, impact force and erosion potentials. The chamber display configuration is appeared in Figure 4.4

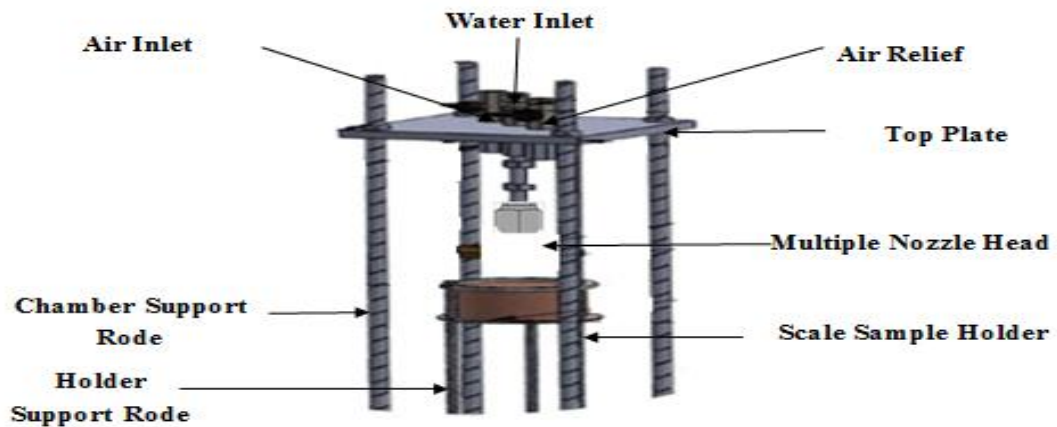


Figure 4.4: Design of the chamber

### 4.2.2.2 Design of descaling chamber

The material of construction determination depended on the encompassing working states of the chamber. Since the pressure chamber requires holding higher pressure than the ambient. It was important to evaluate the pressure rating of the chamber first, before choosing the sort of material reasonable. The numerous inner and outer constituents of the chamber are shown in Figure 4.5

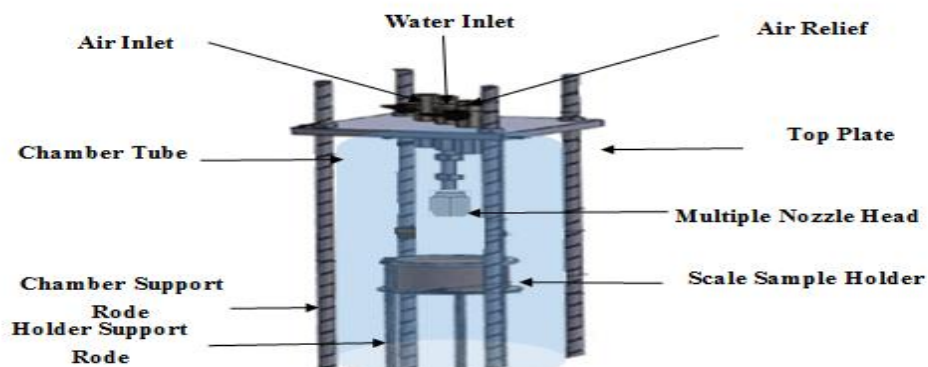
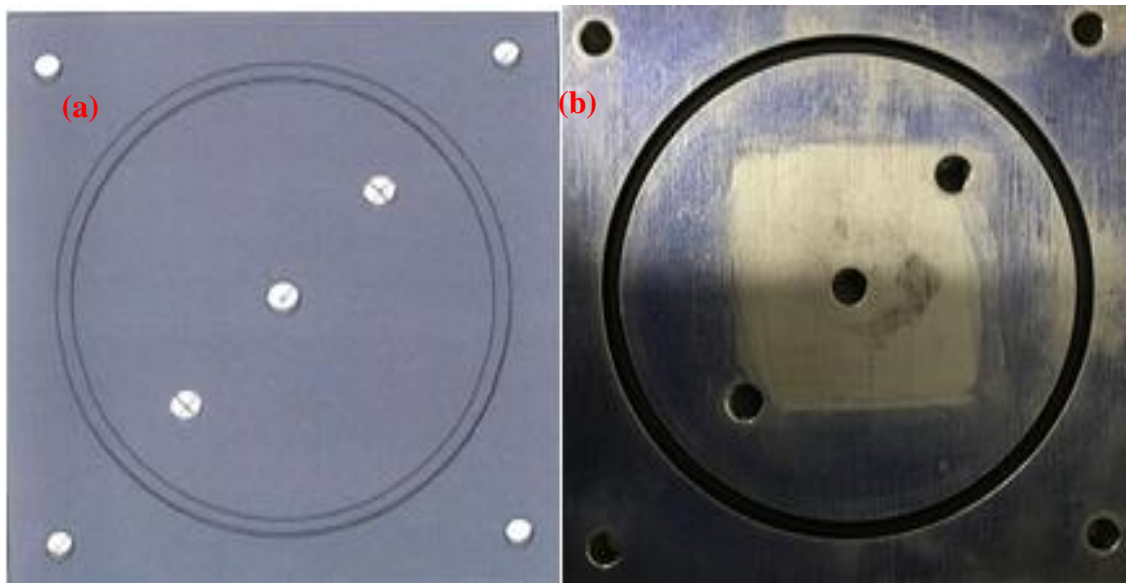


Figure 4.5: Interior section

## 4.2.3 Descaling Chamber component

### 4.2.3.1 Metal Plate

A special two symmetrical 200mm by 200mm square stainless metal plate was design using solid works and fabricated by Hartwell manufacturing company UK. While some pieces of O Ring FKM rubber seal gasket of BS 164 X 5mm thickness were purchased from E.A.P international seal company for the assembly. The two symmetric 15mm thickness special design metal plate serves as support / housing for both the 2M by 160mm acrylic tube, Scale holder and multiple nozzle header. In addition, as main connection into the chamber from compressor, vacuum pump, and water pump via the control board and from the descaling chamber to the drainage via the evacuation valves. Four length of 10mm diameter rode's of 2.5m length each were used to support the bottom and top plate amid housing of the tube. Subsequently details of 2D Solid work design is shown in Appendix A2, A3, A4 & A5. While the 3D and constructed camber plates are shown in Fig. 4.6, and the assembly of top & bottom plates are illustrated in 4.7 and 4.18.



**Figure 4.6:** metal plate (a) 3D image and (b) picture with O ring seal

Both details of design, construction of the camber plates and the assembly of top & bottom plates are illustrated in Figure 4.7 (a), (b) and (c) respectively.

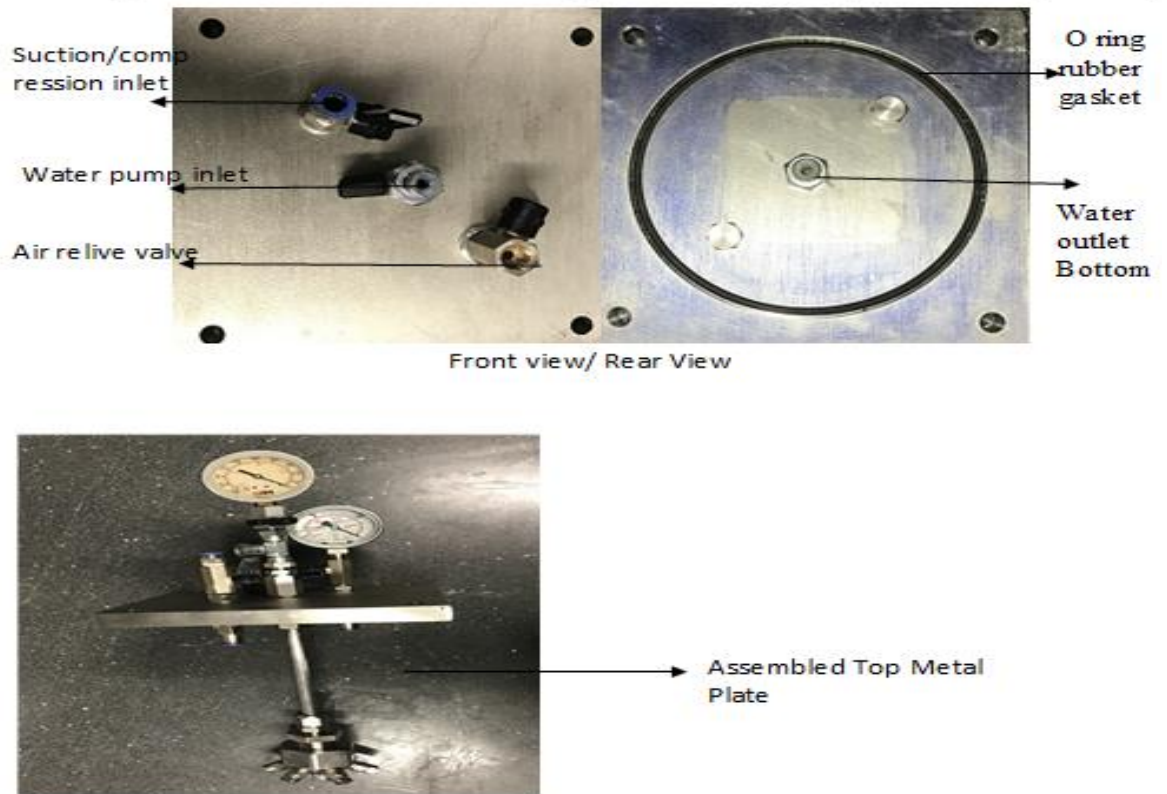


**Figure 4.7:** (a) Top plate (outside view) (b) Bottom plate (inside view) and (c) Assembled views of metallic top cover

The metallic plate, water inlet, air (compressed/vacuum) horse, relieve valve, atomizer header and the scale sample together with-it holder made up the chamber assembly. The assembly situated appropriate for positioning straightforwardly into the chamber as appeared in Figure 4.8. Both the airline and high-pressure water line connection horses from the control board made to be simply and easily fitted into assembly amid the experimental session.

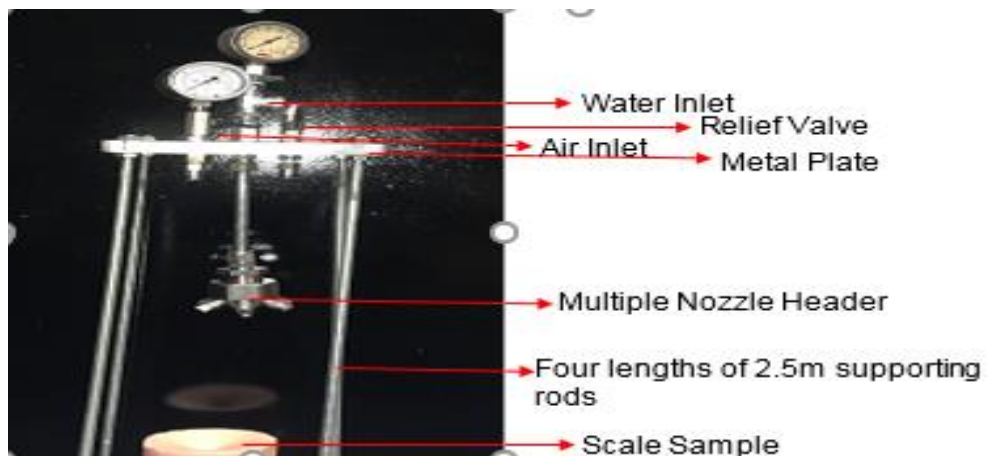


**Figure 4.8:** Scale sample assembly (without chamber tube)

#### 4.2.3.2 Clear acrylic tube

The result from volume/residence time calculation, size constraint of the multiple nozzle header, need for experimental visualization. Together with chamber design philosophy of simulating real production scenario by pressurizing the chamber lead to the selection and purchased of a 160 mm OD by 150mm ID ( 10mm thickness) of 2 M length from the Plastic shop Company UK.

The pressure calculation was performed in light of the ambient air pressure along the production tubing. Evaluated to primarily increment with increase in depth as the major contributory elements, consequently utilizing the pressure equation as in Eq. 4.1:

$$P = \rho gh \quad (4.1)$$

Where P, is the bottom pressure,  $\rho$  the density of air along the void column of production tubing amid maintenance, g, is the gravity, and h, the height to the scale formation. Taking the density of air as 1.224 kg/m<sup>3</sup>, g as 9.8 m/s<sup>2</sup> and an inexact height of 2000 m, at that point

$$P = 1.224 \times 9.81 \times 2000 = 23,990.4 \text{ Pa} = 0.24 \text{ bar}_{\text{ gauge}}$$

$$P = 0.24 + 1.013 = 1.25 \text{ bar}_{\text{ absolute}}$$

Having figured the anticipated pressure along the tubing, in spite of the much accessibility of numerous materials capable of handling this pressure. A clear, transparent acrylic tube was then picked. In view of its pressure rating of 6 bar (most extreme) and transparency to aid imaging the investigation and recording the perceptions.

#### Volume and residence time calculations

The diameter of the chamber supposed to be based on the size of typical oil and gas Saudi Aramco production tubing size. Nevertheless, due to some operational and experimental constraints like size of the multiple nozzle headers, shape and size of the scale sample and high spray impact from multiple high-pressure nozzles, high volume of utilize spray fluid and the rest. A lager diameter tube was considered for the experiment, with 160 mm outside diameter and 150mm inside diameter (10mm thickness) of 2m length. Thereby the basis of selecting the convenient tube length, a residence time calculation was conducted which corresponds to sufficient 2m length as available with manufacturer. While Appendix A6 show case the clear acrylic tube (a) vendors specifications and (b) 2-meter length clear acrylic tube with a 2.25m measuring ruler.

$$V = \frac{\pi d^2 l}{4} \quad (4.2)$$

$$V = \frac{\pi(0.15)^2 \times 2}{4} = 35.4 \times 10^{-3} m^3 = 35.4 \text{ litre}$$

Taking the flow rate of the flat-fan nozzle at 10 MPa as 11.3 litre/min

$$\text{Residence Time of Water} = \frac{\text{Volume}}{\text{Volumetric Flow rate}} \quad (4.3)$$

$$\text{Residence Time of Water} = \frac{35.4}{11.3} = 3.133 \text{ min} = 188 \text{ sec}$$

#### 4.2.3.3 Multiple nozzle header assembly

A 1-inch diameter Fog Jet 7N-SS-10 fine spray female connection optional TWD hydraulic atomiser header, housing seven set of small angle air mist nozzles was purchase from Spraying Company System. This hydraulic atomiser was purchased to be amended for descaling purpose by replacing the seven in-fitted air mist atomizers with high-pressure flat fan nozzles from same vendor.

Seven numbers of ¼ MEG 2550 Wash jet high pressure flat fan nozzle of 25° standard spray angle, 3000 psi and 5.2 gallon per minute flow rate capacity. This was earlier selected from the wash jet standard angle performance chart to replace the fine mist atomizers inbuilt in the 7N Fog jet header. Unfortunately, the above-mentioned replacement nozzles were found unsuitable for the test due to their high flow rate in comparison to the size of the chamber and descaling time requirement (Residence time of 188sec). Leading to the identification and replacement with another seven set of ¼ inch NPT male thread, 25° standard spray angle with 11.3 l/min capacity at 10 MPa (602.481.A3.07.00.0) from Lechler Ltd. Similar to the flat fan atomiser specifications used for the single nozzle research. Additional numbers of CP2812-SS (blank plugs) were procured from spray header manufacturers to block and vary atomizing numbers in other to archive the desired header configuration. Figure 4.9, 4.10 ,4.11 and Appendix A7 & A8 illustrate individual header component before and after assembly/amendment.

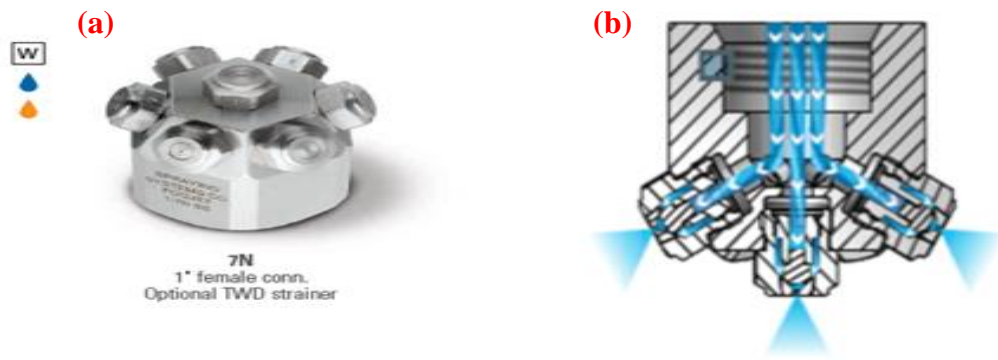


**Figure 4.9:** Multiple nozzle header, (a) picture, (b) operational cross-section



**Figure 4.10:** High-pressure nozzle, (a) picture, (b) operational cross-section

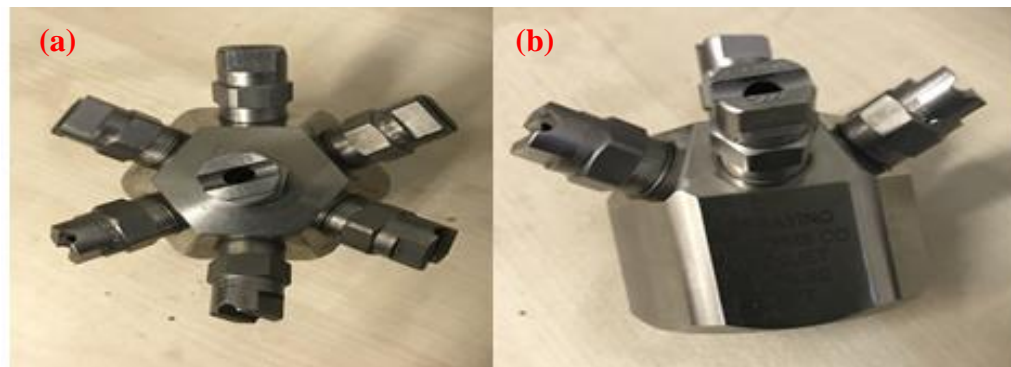


**Figure 4.11:** Assemble nozzle header, (a) Arial & (b)side view

#### 4.2.3.4 Tube fittings

Hand full of tubing fittings of reducers, gasket copers, unions and connectors were obtain from Swagelok company limeted. In order to connect the nozzle header to metal plate, water supply and the rest through a 1/2 inch stainles steel tubes in order to adjust the header to target scale distance based on the desired stand off distance. Table A.9 in Apendix A shows type, list, discription and purpose of fitting selected for use from the sawagelok company catalogue.

#### 4.2.4 Scale holder

Scale holders with other scale experimental support component were design and fabricated on solid works and 3D printer respectively. The 3D fabricated components were later assembled based on experimental desires as shown in Figure 4.12. The complete scale holder support comprises of: Firstly, an asymmetric top and bottom hollow ring of 20mm thickness, 130 mm ID by 20 mm height connected to ¼ inch by 800 mm length rode (A, B & K) for supporting hollow scale type. Secondly, four set of star shape support of 20mm length by 75mm pitch diameter connected to the rode were used for supporting solid shape scale (G & H) and bracing the iron rods against buckling (C&D). Thirdly, two set 20 mm thickness by 20 mm height asymmetric hollow rings embedded with a fine and coarse sieve respectively (E&F) for sieving the eroded scale sample particles against blocking the chamber discharge. Finally, a two set of 20 mm thickness by 25 mm and 50 mm packers respectively (I & J) for adjusting the stand of distance between the scale sample and multiple nozzle header based on the experimental desires. Figure 4.12 elaborates the entire scale holder (a) & (b) component and (c) assembly, While Figure 4.13 showcase the complete assembled descaling rig and Appendix A:12 shows respective holders components 2D solid work design.



**Figure 4.12:** Scale holder (a) & (b) component and (c) assembly

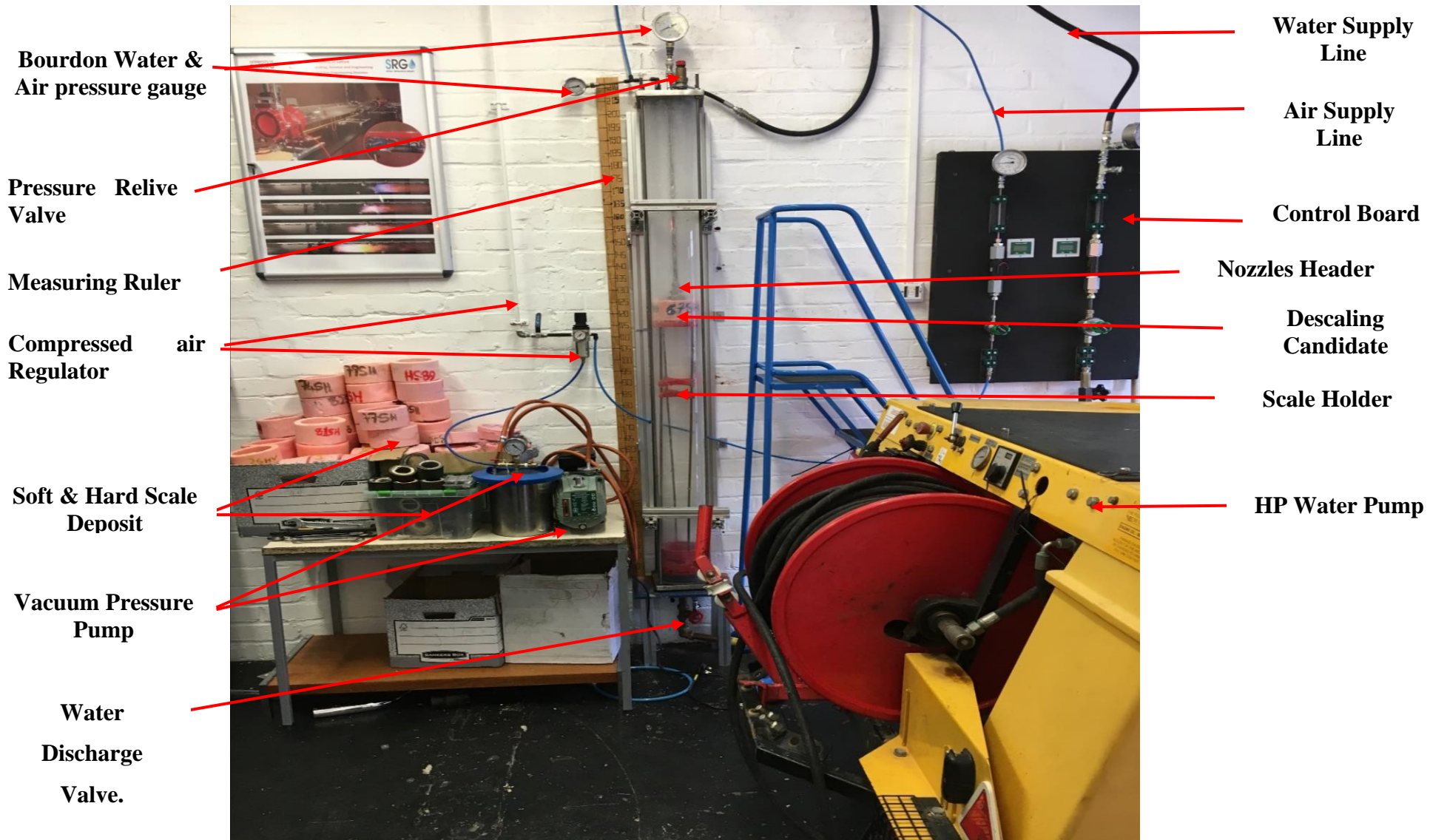


**Figure 4.13:** Complete assembled descaling rig.

## 4.3 Soft scale production

### 4.3.1 Wax moulder design

Solid works software was used to design a hollow shape and round solid shape convertible holder for preparing the wax scale sample. The separate and letter assemble design was exported to 3D printer to construct the moulder. Keeping in mind the selection of suitable material that can withstand the wax melting temperature as demonstrated in Appendix A:15 and A:16 for the 2D and 3D solid works moulder design drawings respectively. In addition to the picture of both (a) individual moulder component consisting of the side, centre and base component and (b) complete assembled moulder for solid and hollow shape production in 4.14 respectively.

(a): Wax Moulder Components



(b): Assembled Wax Moulders



**Figure 4.14:** 3D Pictures of wax moulder (a) component and (b) assembled

### 4.3.2 Wax scale preparation

The sample of the wax scale was prepared by utilizing a wax material (household candles which has similar low API gravity to that of paraffin). These were cut to pieces, melted and afterward embedded through a reasonably composed holder to give the desired fitting shapes of the moulder. The complete assembled moulder will produce a 150mm outside diameter and 110 inner diameters (20 mm thickness) hollow wax sample. Simulating early stage growth of scale in production tubing (before it blocks the entire tubing). While if the centre component of the holder is removed, it produces a 150mm diameter solid sample with 40mm thickness. Simulating complete tubing blockage by the deposit. Figure 4.15 demonstrate the graphical sequence of both hollow and solid shaped soft scale sample production while the production procedures are as follows.

- (a) The household candles were cut to smaller pieces and put in metal baking pan
- (b) The pan was put in an oven and set for (120 C)
- (c) The melted wax was carefully removed from the oven and allowed to cool down and become a bit denser to reduce the risk of slippage when poured into the moulder
- (d) The settled melted wax was then poured from the metal baking pan into the desired scale moulder
- (e) The melted wax was allowed to cool and solidified to desired shape before removing from the mould.
- (f) Reference number was written on both sides of the sample with permanent marker and measured with weighing balance.
- (g) Their individual details were recorded into the scale identification register.

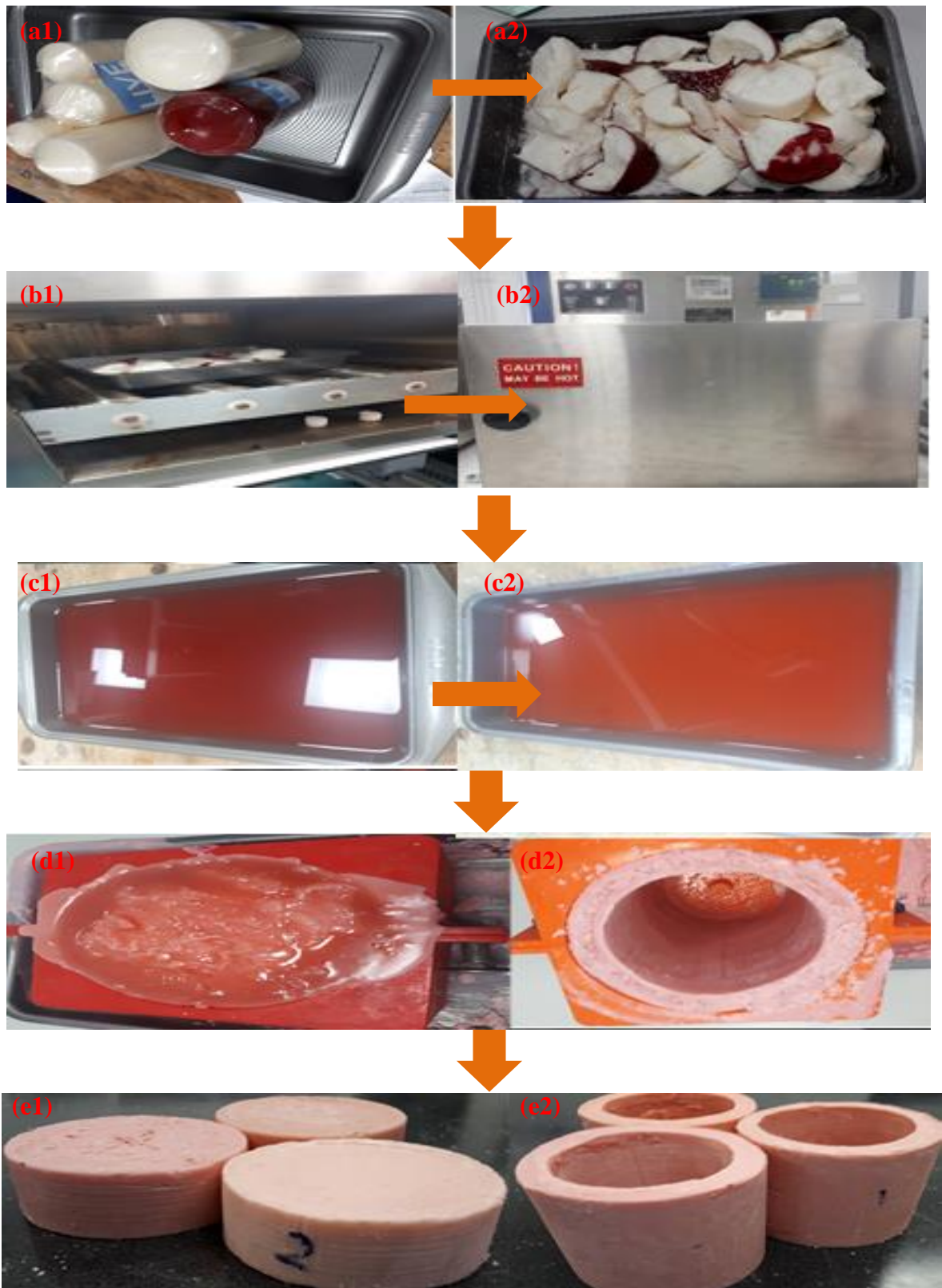


**Figure 4.15:** Prepared wax scale samples preparation and after cooling

## 4.4 Scale characterization

### 4.4.1 Soft Scale compositional & chemical analysis

The constructed soft scale samples of different sizes and shapes from Section 4.3.2 were subjected to NMR and FTIR analysis. In order to determine if they truly have the same chemical properties with the paraffin scale deposit usually found in petroleum production tubing. Figure 4.16 showcase constructed soft scale samples of (a) hollow and (b) solid shapes respectively.

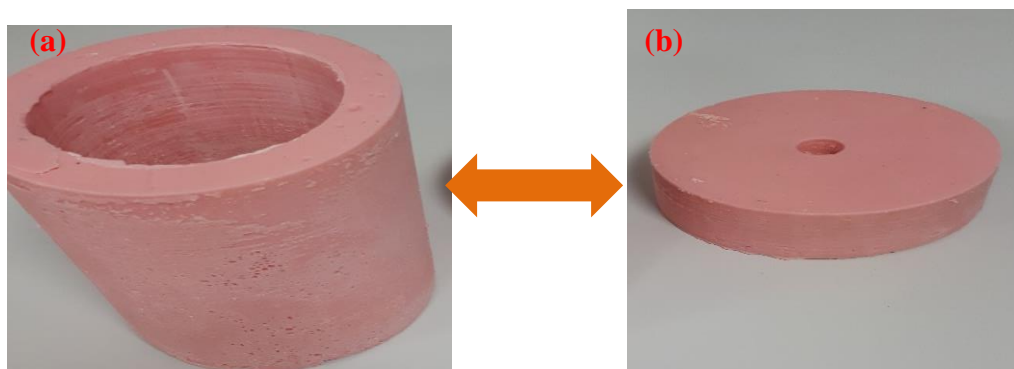


**Figure 4.16:** Constructed soft scale (a) hollow shape, (b) solid shaped samples

#### 4.4.1.1 Soft scale NMR analysis procedure

Nuclear Magnetic resonance spectroscopy is a very useful technique employed in characterising organic samples (both aliphatic and aromatic). Like other spectroscopy techniques, NMR works on the principle that molecules interact with electromagnetic radiations thus increasing their energy level (quantization). This energy difference will determine the molecular environment of each nucleus present in an organic sample. However, only the atoms with spin (odd mass number) are detected by NMR. Nuclei observed with NMR include  $^1\text{H}$ ,  $^{13}\text{C}$ ,  $^{15}\text{N}$  etc. The most common nuclei used analysing organic compounds is the  $^1\text{H}$  and  $^{13}\text{C}$  and this makes it a versatile tool for investigating varieties of petroleum products. In order to probe a sample by NMR method, the sample must be completely dissolved in a deuterated solvent. The most common deuterated solvents used include chloroform ( $\text{CDCl}_3$ ), water ( $\text{D}_2\text{O}$ ) and acetone- $\text{d}_6$ . Not necessarily, however, some solvents are calibrated with a standard reference. Tetramethylsilane (also abbreviated TMS), is one of the commonly used reference compounds used in solvents because it is used to indicate the starting point of all signal peaks (in ppm) that appear on the spectra. About 10-50mg of soft scale sample is required for NMR analysis and was solubilised in deuterated  $\text{CDCl}_3$  on a Bruker Advance 400 MHz NMR.

1. 10mg of starting material was used to clean the tube
2. The crushed wax sample was dissolved in 0.7ml of deuterated solvent ( $\text{CDCl}_3$  in this case) as 4.5-5 cm is recommended as a suitable height of solvent for good spectra
3. The NMR tube is carefully capped and the sample name is written on it.
4. The sample was gently shaken to ensure effective dissolving of the sample and precautions were taken to avoid contaminating the sample due to solvent cap contact.
5. The spinner and the NMR tube were cleaned with 2-propanol and lab tissue to wipe out all dirt and fingerprints
6. The NMR tube was gently inserted into the spinner and the spinner automatically rotated into the magnet to ensure the whole sample experiences a homogeneous magnetic field. The spinner is placed in a sample gauge to prevent the bottom of the NMR tube from sitting far into the NMR probe to reduce the risk of damaging the spectrometer as each probe has its own sample depth.
7. The sample was placed into the NMR spectrometer and a Varian 400 MHz spectrometer equipped with an autosampler was utilised
8. The spectra were processed, and peaks were assigned in the spectrum.

#### **4.4.1.2 Soft Scale FTIR analysis procedure**

A Thermo Scientific Nicolet iS10 Fourier-transform infrared spectroscopy (FTIR) situated in Analytical Laboratory Service in Crowcroft building of University of Salford was utilised in analysing the constructed wax samples as per the set up in Figure 4.17. The concept of infrared spectroscopy lies around the interaction of infrared light and molecules either by measuring its emission, absorption or deflection for analysing and identification of chemical substance, functional group in a compound and other applications. In other words, molecules absorb some exact frequency of light that are characterised by the corresponding structures of molecules. The shape of the molecular surface, the accompanying vibrational coupling, and the mass corresponding to the atoms determines its energies. Normally, light atoms and stronger bonds will vibrate at a high stretching frequency (wavenumber). The following procedures were followed to effectively analyse the samples with the experimental set up in Figure 4.17.

- i. 1-Started by logging in to the OMNIC software windows in the FTIR analyser dedicated computer system and select the smart FITR Diamond ATR accessory
- ii. 2- The system drop window was properly cleaned with propanol and a lab tissue paper.
- iii. 3-Then the ATR was screwed against the sample holder until a click sound is heard.

- iv. 4-The 'Col BKg' was clicked on the software menu for sample background 'run' and generate background spectrum at the completion of 36 scans while monitoring the status bar
- v. 5- A small piece of the wax deposit (as in Figure 4.27A) was placed on the sample holder and the ATR is screwed against the sample until a click sound is heard.
- vi. 6- The sample spectra were then obtained by clicking the 'Col Smp' button with 36 scan background collection as required.
- vii. 7- The Selection of the peak of interest was done by putting ON the 'Analyze' menu and changing the axis absorbance to transmittance and the general spectra were replaced with the new specific spectra.
- viii. 8- The paraffin spectra were selected from the national institute of standard and technology (NIST) through the FTIR data base and superimposed against the wax scale spectra for comparison.
- ix. 8 -Step 6 to 7 were repeated for liquid paraffin analysis after pouring small quantity on the sample drop and properly screwing the ATR screw.
- x. 9- The liquid paraffin spectra generated results were superimposed with the generated wax sample spectra for comparison.

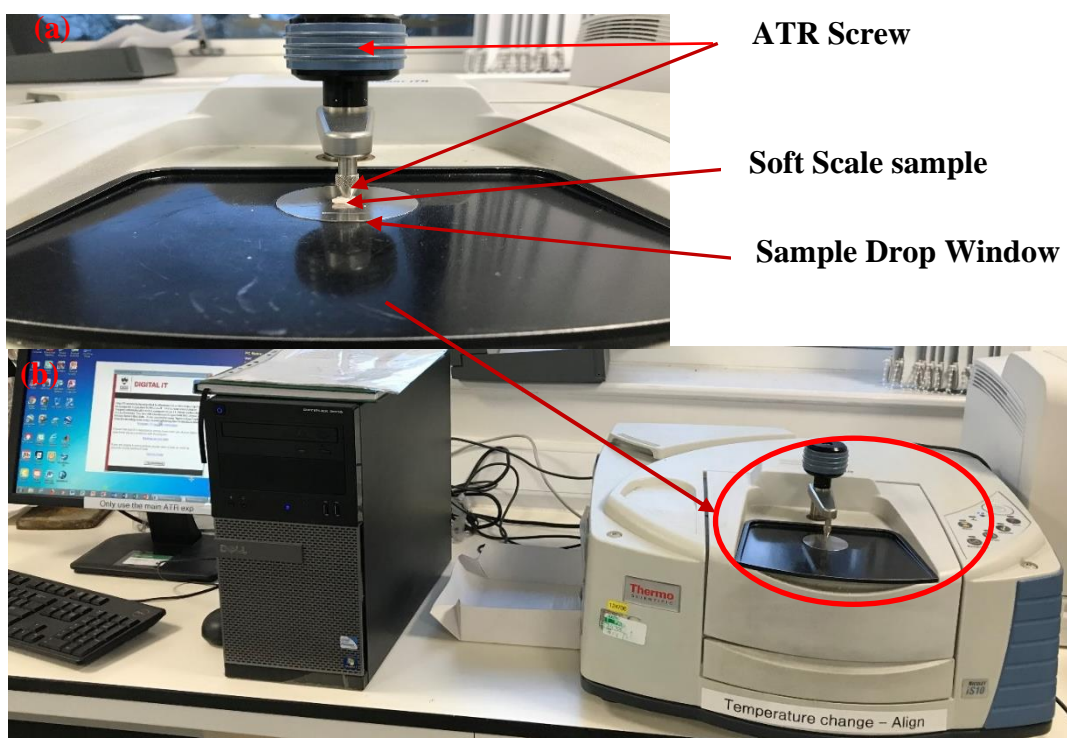


**Figure 4.17:** Thermo Scientific Nicolet iS10 Fourier-transform infrared spectroscopy (a) ATR sample drop window (b) complete FTIR system

#### 4.4.2 Hard scale compositional & chemical analysis

The most available Libyan oilfield acquired hard scale sample left from the single nozzle research was selected for this research. Also, send for comprehensive chemical/composition analysis at the Analytical laboratory service of the University of Salford as recommended in the single nozzle research. The main aim of subjecting the samples to combine SEM, EDs and XRD analysis was to have idea of the exact type of scale we are dealing with and understand the descaling requirement of each sample in question. The two samples tagged sample A and B and shown in Figure 4.18 were cut to small pieces and grinded in to powder form and label as unknown white powder A and B. Both Unknown white powder A and B were subjected to three sequential combination of comprehensive analysis (SEM, EDs & XRD) in order to precisely classify and identify them prior to the descaling operations.

#### 4.4.3 Hard scale compositional analysis

The harder genuine scale samples utilized as a part of the examination are the unused samples from the single nozzle campaign, acquired from Libyan wells appeared in Figure 4.18. So, as to practically explore with the harder scales sorts regularly experienced in petroleum production.

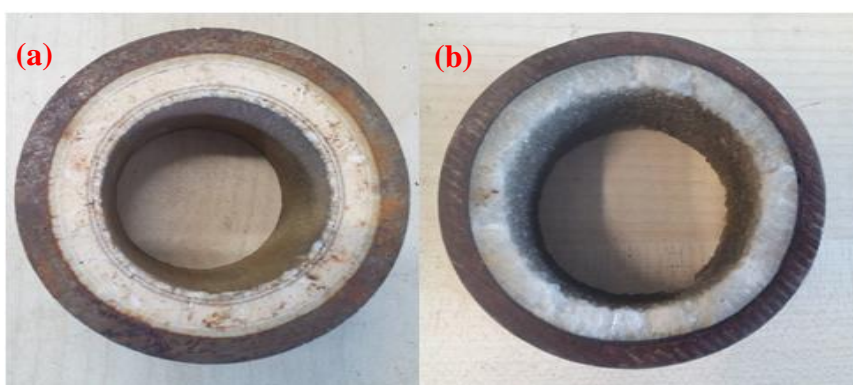


**Figure 4.18:** Hard Scale samples (a)  $\text{CaCO}_3$ , (b)  $\text{SrSO}_4$

Two of the Libyan oilfield available left hard scale samples utilised in the single nozzle research, were subjected to combine chemical/compositional analysis (SEM, EDs and XRD) as recommended in the single nozzle research. Beside the scale analysis recommendation from the single research, a need to understand the descaling requirement for descaling the scale in question is vital. In addition to know the exact scale type we are working on, also, to establish what it takes to descale each type of scale. The analysis was done by the researcher in conjunction with technical staffs of the Analytical service laboratory, Crowcroft building of the University of Salford as follows.

- i. The scale samples in question were cut and grinded into small pieces powder foam (tag as unknown powder)
- ii. The unknown powders were first off, all send for SEM analysis using the scanning electron microscope to identify the surface topography and composition of the powder
- iii. The Unknown white powders results were further sent for EDs analysis using the energy dispersive X ray spectroscopy to examine the elemental and quantitative chemical composition of the compound in the unknown white powder.
- iv. For final and confirmatory analysis to determine the crystalline material (mineralogy) of the compound. The grinded white unknown powders were subjected to X ray powder diffraction analysis.
- v. Step 1 to 4 was followed for both samples.

#### **4.4.3.1 Scanning electron microscope (SEM)**

The two unknown white powder labelled sample A & B were first off, all, send for scanning electron microscopy analysis in order to identify their surface topography and compound composition through the magnifying lances of the microscope. The SEM works by detecting secondary or backscattered electron signal from the focus electron bean that was restrain across the sample surface by the SEM. Since both SEM and energy dispersive X-ray Spectroscopy (EDS) worked in conjunction for the characteristic x-ray separation of different element into energy diagram, which can be utilised in determining the presence and quantity of a particular element down to a region the size of microns. In addition to having similar or connected procedure, only the EDs operating protocol will be detailed in the report.

#### **4.4.3.2 Energy dispersive X-ray analysis (EDX)**

For the purpose of elemental identification and quantitative compositional information, the samples were further subjected to EDX analysis after the SEM analysis. It depends on the interaction between the sample and some source of X-ray excitations, resulting in the EDx detector measuring the relative abundance of emitted X-rays against their energy. The focus electrons pass through the sample on an atomic level that leads to the occurrence of different electron displacement, with each displacement emitting electrons or X-rays. Subject to the return, displacement is separated and analyse to generate elemental maps and images, just like the results of sample A and B as appeared in Figure 5.6 and 5.7 at different spectrums. After the successful execution of the SEM analysis of the two hard scale samples by magnifying them in different resolution, the following procedures were performed for generating their respective elemental maps with EDx spectroscopy.

- i. The sample was mounted, and the holder was placed into the chamber in line with the orientation to the arrow on the bottom of the holder.
- ii. The picture of the sample was taken to check how it will appear on the monitor
- iii. The chamber was closed with its clip, 'EVAC' was pressed for 2 seconds until its light is solid and the left side Robinson chamber view was turned on.
- iv. 'VLC' app was selected to show the camera on the monitor and the sample was pushed to the SEM
- v. The 'Click Spectrum' was pressed 'EV/Chan' for spectrum collections
- vi. The 'point analysis' was clicked to transfer the to TEAM Eds system from SEM
- vii. 'Collect spectrum' button was clicked, while an area of interest was chosen to allow spectrum collection and report was initiated
- viii. 'Mapping' and 'collect mapping' were sequentially clicked and 'finished' and 'reporting' tabs were afterward clicked to generate summary of the data
- ix. The 'line scan' and 'collect line' buttons were clicked for better resolution configurations.
- x. Finally, procedure 1 to 9 was repeated for the second sample analysis.

#### **4.4.3.3 X-ray diffraction analysis**

For final confirmatory analysis, the samples were subjected to x-ray powder diffraction analysis for the characterization of their crystalline material. This rapid analytical technique uses Bragg's law to principally identify the crystalline material and in addition provide information on unit cell dimensions. Bragg's law works on the concept that the observed peaks of scattering intensity when x-ray is scattered from crystal lattice will correspond to the following conditions: The angle of incidence will be equal to angle of scattering while the difference in path length is equal to an integer number of wavelengths. After samples are finely ground, homogenised and average bulk composition is determined. The following procedure was adopted for XRD analysis of the two hard scale samples.

- i. A small piece of both samples was cut and separately ground to a fine powder form.
- ii. A fine mesh sieve was placed above the Si Crystal
- iii. About 20 mg of sample A was poured on to the sieve and cautiously directed above the Si crystal on the mount
- iv. The sieve was lifted from the bench to make sure the monolayer of sample covers the Si crystal surface
- v. The XRD powder pattern was collected
- vi. The instrument door was opened, and the sample holder was mounted into the instrument

- vii. The Commander software suite (An XRD powder pattern collecting program) and the standard data collected scan was loaded by pressing the 'Wizard' tab.
- viii. A 20-minute scan running time was selected for better powder XRD pattern resolution.
- ix. A wavelength range comprising of angle range ( $2\theta$ ) that was scanned at (5-70 °) that was more suitable for inorganic materials was selected.
- x. The 'start' bottom was pressed for data collection initiation.

# Phase Two

## Descaling Experiment

### 4.5 Scale removal experimental design procedure

The experimental descaling parameters selection for removing both the constructed hard wax scale and Libyan field oil scale were done based on experimental desires and limitations through carefully considering optimum descaling requirement needed for effectively removing each type of scale deposit. Since each deposit response to unique descaling mechanism that require special approach due to their differences in physical and chemical properties being produce by different deposition mechanism and reservoir formations (Zongyi 2014). Also, considering the need of replicating an ideal oil well descaling condition for easy experimental upscaling and real field applications. Details on basis for selection of sole and combination of scale parameters is shown in Section 5.4.2.1 and the scale removal experimental design process in Figure 4.19

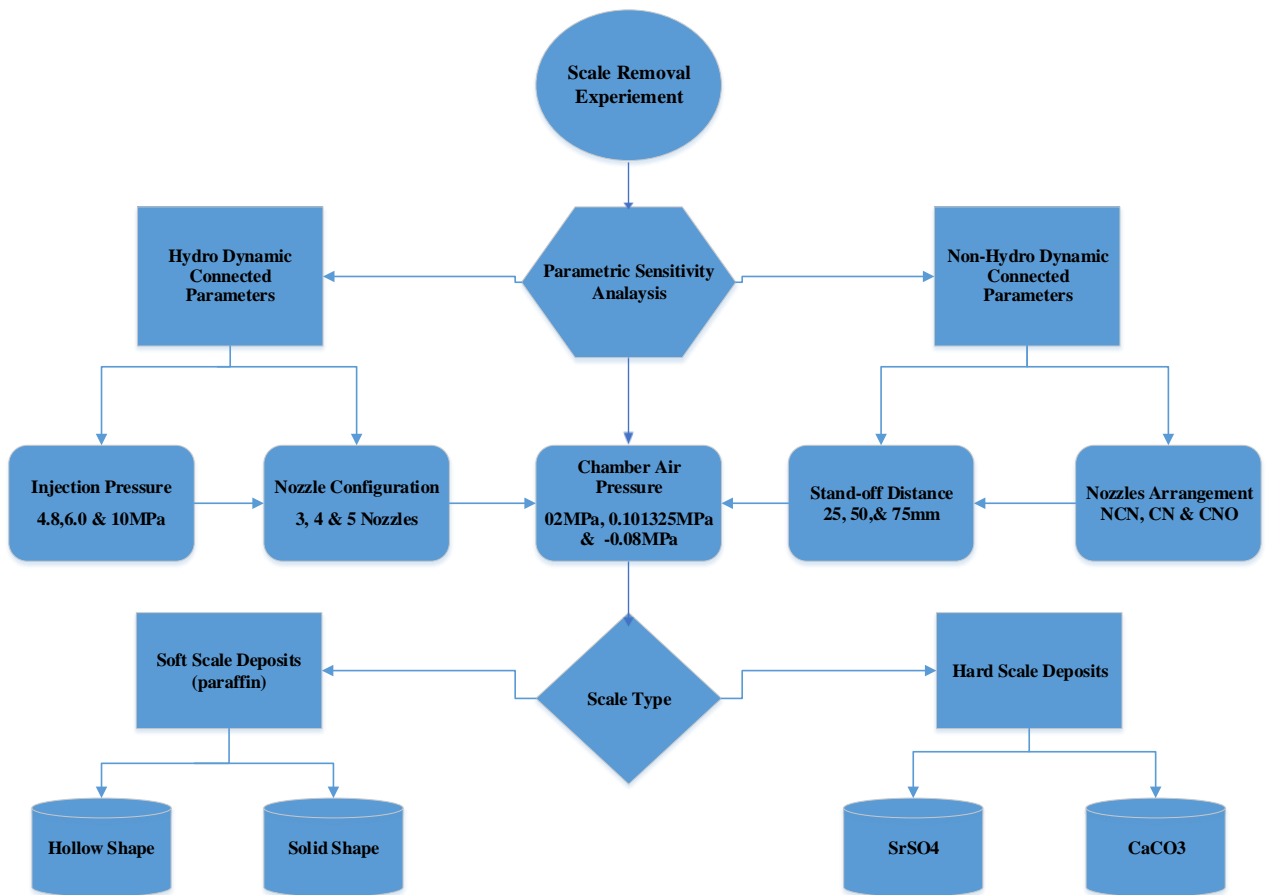


**Figure 4.19:** Experimental design process

## **4.5.1 Descaling experiment preparations**

The samples utilized as a part of this examination comprise of two segments that are typically like the scale deposit experienced during oil and gas production. They incorporate the wax scale experienced while producing highly paraffinic hydrocarbons characterize with low API gravity. In spite of the fact that this scale sample is normally found on topside of production facility. It might be experienced along production tubing particularly around the Christmas tree because of build-up and condensation of heavier hydrocarbons. Other scale sample includes the genuine specimen of oil field scale acquired from Libyan wells for the single nozzle research. These samples had been chemically analysis using combination of XRD, EDS and SEM by the researcher.

### **4.5.1.1 Pump calibrations**

For the purpose of familiarization of the pump and the rig system and maintaining pressure at constant rate. The mass flow rate of the desired combination of nozzles at different injection pressure was measured in preparation of the main descaling trials of both soft and hard scale candidates. This was also carried out to monitor the consistency on the pressure gauges at the pump, the water line of the control board and pressure drop on the gauges on top of the top plate. So as, individual desired pressure, build up time and operational synergy between the pump, control board, descaling chamber and the discharge evacuation system. The bucket weighing method was utilised and the following procedures were followed to properly measure mass flow rate of different combinations of nozzles at different injection pressures.

- i. The desired numbers of nozzles were properly fitted in to the header and the un-desired properly blocked with the blank plugs.
- ii. The hydraulic connections from the pump to the control board to the top plate of the chamber to the header are properly secured
- iii. The header in properly inserted into 35liter measuring tank and sealed away from leakage. With the tank properly seated on a table for easy evacuation through the tank discharge valve to the measuring bucket.
- iv. The HP pump was switched on and the timer was set to determine the pressure build-up time for the desired pressure.
- v. The HP pump was switched off once the desired pressure was reached, the time taken to build pressure was recorded and the mass of the water build up (dead water) was measured with the weighing balance

- vi. Step 5 was repeated at least 3 time for all combination of nozzles at different injection pressures
- vii. The pump was operated for a period of 3 minute after achieving stabilise desired pressure.
- viii. The pump was switched off immediately after achieving 3 minutes stabilise pumping, and drained, while the mass of water collected (Live Water) was measured.
- ix. Step 8 was repeated at least 3 times for all combination of nozzles at different injection pressures for the purpose of repeatability and precision.
  
- x. All the above-mentioned steps were repeated for the remaining numbers of nozzle combinations (3,4 and 5) and different injection pressures (4.8, 6.0 and 10MPa)

The Eq.4.4 was used for the calculation of mas flow rate at different nozzle combination and injection pressures:

$$Mass\ flow\ rate_{after\ build-up} = \frac{Mass\ of\ water_{after\ build-up}}{3\ minutes} \quad (4.4)$$

#### 4.5.1.2 Descaling parameters

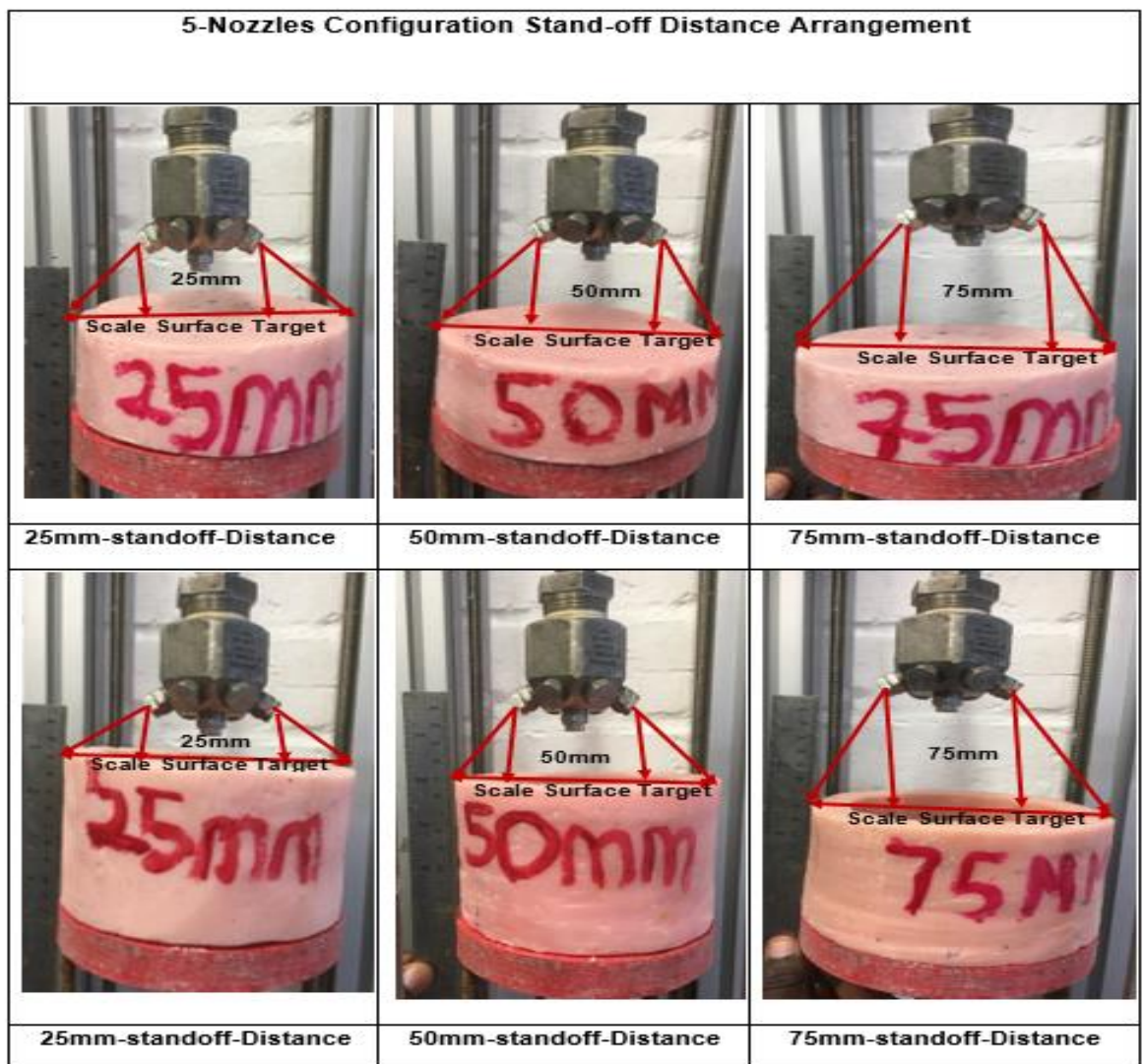
The trials vary and considered all the below mentioned decaling parameters hand in hand with each other, under separate chamber condition for better and detailed result presentation.

- i. **Scale samples:** The (4) four scale samples consisting of two types of constructed soft scale of hollow and solid shapes signifying different stages of paraffin growth in production tubing. In addition to the analysed scale sample ( $SrSO_4$  and  $CaCO_3$ ) were descaled under different decaling condition and parameters. As presented in Figure 4.20



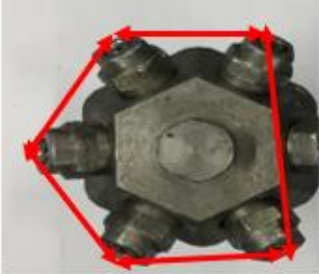
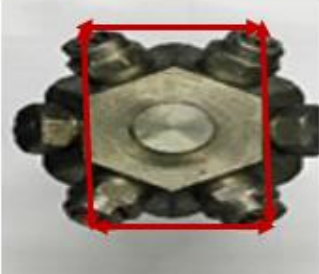
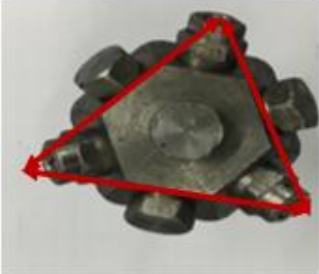
**Figure 4.20:** Scale deposits

- ii. **Injection Pressure:** Different injection pressure of 4.8 6.0 and 10 MPa were generated by the pump and utilised for the removal of all the scale samples at separate standoff-distance, nozzle arrangement, number of nozzles and chamber pressure.
- iii. **Chamber pressure condition:** Chamber air concentration had been varied from ambient to compressed and vacuumed condition in conjunction with the remaining descaling parameters when descaling each sample. Therefore, chamber air concentration is going to be the basis for the result presentation.
- iv. **Stand-off distance:** The entire descaling experiment was conducted at different stand-off distance (25, 50 and 75mm) between the tip of side atomisers and the surface face of the scale target. Figure 4.21 elaborate different stand-off distance when using 5 nozzles configurations for example.



**Figure 4.21:** Stand-off distance arrangement

**Header & Nozzle configurations:** Different numbers of nozzles at different nozzle arrangements have been fitted in to the nozzle header for each individual experiment. The numbers of nozzle on the header were purposely varied to find the required numbers of nozzle needed for efficient descaling of each scale deposit. The desired numbers of nozzles (3, 4, or 5 nozzles) were fitted in to the header and the remaining un-desired nozzles socket were blocked with blank plugs. Subsequently nozzle configuration (nozzles arrangement on the header) was done hand in hand with header configuration (number of nozzles) by arranging in order of any of the three (3) nozzles configurations styles elaborated in Figure 4.22.

No of Nozzles	Header/Nozzle Configuration		
	Non-Centre Nozzle Configurations (NCN)	Centre Nozzles Configurations (CN)	Centre Nozzle Overlap Configurations (CNO)
5			
	Pentagon	Envelope	Trapezium
4			
	Rectangle	Pyramid	Kite
3			
	Triangle	Diagonal	Right-angled

**Figure 4.22:** Header and nozzles configurations

## **4.5.2 Experimental procedures for scale removal**

Preceding the beginning of the analysis, there was the requirement for guaranteeing the safety, reliability of all equipment and devices utilized, amid each trial. The same procedure and precautions were utilised for both soft scale and hard scale sample removal trials. Even though may differ when working at different chamber air concentrations

### **4.5.2.1 Ambient descaling procedure**

The general trial strategies for scale removal at ambient condition for both soft and hard scale samples at different injection pressure, standoff distance and header/nozzle configuration are as per the following:

- i. The mass of scale sample was re-measured and noted according to their reference number as in the scale identification register.
- ii. The picture of each scale sample was taken, utilizing a still standard camera, before, and after each trial from different perspective.
- iii. The required numbers of nozzles were properly fitted in to the header and the un-desired properly blocked with the blank plugs.
- iv. The desired nozzle arrangement was generated from the required numbers of nozzles (NCN, CN or NCO)
- v. The scale sample were properly placed on the scale sample holder and secured in position.
- vi. The right size and combinations of packers were ensured in order to achieve the desired stand-off distance from the sample to nozzle header.
- vii. The scale sample with the base assembly were ensured to be effectively put to coincide with the vertical axis of the atomiser, fitted to multiple nozzle head.
- viii. All the chamber and rig connection were ensured to be properly and sequentially done, like top and bottom plate to the chamber. Also, the hydraulic connections from the pump to the control board to the top plate of the chamber to the header and chamber bottom plate were used and pump starting procedures were followed
- ix. The pump was switched on and throttle to the desired pressure to begin with, at an underlying low pressure to 4.8 MPa pressure, and after then adjusted to acquire the desired flow rate and pressure
- x. The water line pressure gauge, flow meter on the board and the pressure gauge on the top plate were confirmed to have corresponded to the desired pumping pressure requirement through board regulator valve

- xi. The timer was set to count for three (3) minute descaling time immediately after achieving the desired pumping pressure.
- xii. The pump was completely throttle off and switched off after achieving the 3-minute descaling time from the stopwatch timer.
- xiii. The descaled sample was removed and dried for 12 hours. Later, measured and it picture re-taken with same still camera
- xiv. The broken samples were collected from the two sieves below the packers, dried and later weighed with a measuring scale (range  $\pm$  (0.1g) for confirmation.
- xv. Step 1 to 14 above were repeated for desired pressure of 4.8 and 6 and 10 MPa at the desired flow rate flat fan spray atomisers respectively for 3 minutes each.
- xvi. Step 1 to 15 above were repeated for desired standoff distance of 25mm, 50mm and 75mm respectively and operated for 3 minutes each.
- xvii. Step 1 to 16 above were repeated for desired numbers nozzles (3, 4 and 5 nozzles) respectively
- xviii. Step 1 to 17 above were repeated for desired nozzles arrangement (NCN, CN & CNO) respectively
- xix. All the above technique or sequence were applied and repeated for various scale samples (soft hollow & solid and SrSO<sub>4</sub> & CaCO<sub>3</sub>) deposits.
- xx. All readings from each trial were recorded for further analysis.

#### **4.5.2.2 Compressed descaling procedure (compression)**

Almost similar experimental strategies with the scale removal at ambient condition, though carried out in a compressed chamber condition. The operation incorporates a 0.2 MPa compressed air into the chamber through the control board airline to the top plate of the chamber. Both soft and hard scale samples were descaled at different injection pressure, standoff distance, and header/nozzle configurations using the following steps.

- i. The mass of scale sample was re-measured and noted according to their reference number as in the scale identification register.
- ii. The picture of each scale sample was taken, utilizing a still standard camera, before, and after each trial from different perspective.
- iii. The required numbers of nozzles were properly fitted in to the header and the un-desired properly blocked with the blank plugs.

- iv. The desired nozzle arrangement was generated from the required numbers of nozzles (NCN, CN or NCO)
- v. The scale sample were properly placed on the scale sample holder and secured in position.
- vi. The right size and combinations of packers were ensured in order to achieve the desired stand-off distance from the sample to nozzle header.
- vii. The scale sample with the base assembly were ensured to be effectively put to coincide with the vertical axis of the atomiser, fitted to multiple nozzle head.
- viii. All the chamber and rig connection were ensured to be properly and sequentially done like top and bottom plate to the chamber. Also, the hydraulic connections from the pump to the control board to the top plate of the chamber to the header and chamber bottom plate were used and pump starting procedures were followed
- ix. The isolation/selection valve was used to select the desired chamber air condition (compression) and vary the air concentration according to experimental desire. Also, the proper connection of compressed air from the compressor system to the control board airline and up to top plate air gauge inlet was ensured.
- x. The HP water pump was switched on and throttle to the desired pressure to begin with, at an underlying low pressure of to 4.8 MPa pressure, and after then adjusted to acquire the desired flow rate and pressure
- xi. The water line pressure gauge, flow meter on the board and the pressure gauge on the top plate were confirmed to have corresponded to the desired pumping pressure requirement through board regulator valve
- xii. The compressed air system was opened to the required air compression and the regulator on the airline system of the control board and the discharge regulator at the bottom plate were operated to maintain the required chamber air concentration (0.2 MPa) at both combine pressure gauge, flow meter and top plate pressure gauge throughout the 3-minute operations.
- xiii. The timer was set to count for three (3) minute descaling time immediately after achieving the desired pumping pressure and air concentration.
- xiv. The compress air system was closed and the HPW pump was completely throttles-off and switched off immediately after achieving the 3-minute descaling time from the stopwatch timer.
- xv. The descaled sample was removed and dried for 12 hours. Later, measured and it picture re-taken with same still camera
- xvi. The broken samples collected from the two sieves bellow the packers were dried and weighed with a measuring scale (range  $\pm$  (0.1g) for confirmation

- xvii. Step 1 to 16 above were repeated for desired pressure of 4.8 and 6 and 10 MPa at the desired flow rate flat fan spray atomisers respectively for 3 minutes each.
- xviii. Step 1 to 17 above were repeated for desired standoff distance of 25mm, 50mm and 75mm respectively and operated for 3 minutes each.
- xix. Step 1 to 18 were repeated for desired numbers nozzles (3,4 and 5 nozzles) respectively
- xx. Step 1 to 19 above were repeated for desired nozzles arrangement (NCN, CN & CNO) respectively
- xxi. All the above technique or sequence were applied and repeated for various scale samples (soft and hard scale sample)
- xxii. All readings from each trial were recorded for further analysis.

#### **4.5.2.3 Vacuum descaling procedure (Suction)**

The vacuum operations share similar decaling strategies with compressed experiment as in above, but the compressed air system was replaced with a vacuum pump. The vacuum pump was incorporated into to the chamber through the control board airline into the top or bottom plate of the chamber to generate suction air concentration (-0.08 MPa). Both soft and hard scale samples were descaled at different injection pressure, standoff distance and header/nozzle configuration using the following steps.

- i. The mass of scale sample was re-measured and noted according to their reference number as in the scale identification register.
- ii. The picture of each scale sample was taken, utilizing a still standard camera, before, and after each trial from different perspective.
- iii. The required numbers of nozzles were properly fitted in to the header and the un-desired properly blocked with the blank plugs.
- iv. The desired nozzle arrangement was generated from the required numbers of nozzles (NCN, CN or NCO)
- v. The scale sample were properly placed on the scale sample holder and secured in position.
- vi. The right size and combinations of packers were ensured in order to achieve the desired stand-off distance from the sample to nozzle header.
- vii. The scale sample with the base assembly were ensured to be effectively put to coincide with the vertical axis of the atomiser, fitted to multiple nozzle head.
- viii. All the chamber and rig connection were ensured to be properly and sequentially done like top and bottom plate to the chamber. Also, the hydraulic connections from the pump to the

control board to the top plate of the chamber to the header and chamber bottom plate were used and pump starting procedures were followed

- ix. The isolation/selection valve was used to select the desired chamber air condition (Suction) and vary the air concentration according to experimental desire. Also, the proper connection of the vacuum pumps to the control board airline and up to top or bottom plate air gauge inlet were ensured.
- x. The HP water pump was switched on and throttle to the desired pressure by beginning with, at an underlying low flow rate 8 l/min corresponding to 4.8 MPa pressure, and after then adjusted to acquire the desired flow rate and pressure
- xi. The water line pressure gauge, flow meter on the board and the pressure gauge on the top plate were confirmed to have corresponded to the desired pumping pressure requirement through board regulator valve
- xii. the vacuum pump was switched on, while the regulator on the airline system of the control board and the discharge regulator at the bottom plate were operated to maintain the required suctioned chamber air concentration (-0.08MPa) at both combine pressure gauge, flow meter and top plate pressure gauge throughout the 3-minute operations.
- xiii. The timer was set to count for three (3) minute descaling time immediately after achieving the desired pumping pressure and air concentration.
- xiv. The HP water pump was stopped once the vacuum pressure of the chamber drops to -0.06MPa to suctioned back the chamber back to -0.08MPa
- xv. The HP water pump and vacuum pump were turned off and the completely throttle off immediately after achieving the 3-minute descaling time from the stopwatch timer.
- xvi. The descaled sample was removed and dried for 12 hours. Later on, measured and it picture re-taken with same still camera.
- xvii. The broken samples collected from the two sieves bellow the packers were dried and weighed with a measuring scale (range  $\pm$  (0.1g) for confirmation
- xviii. Step 1 to 16 above were repeated for desired pressure of 4.8 and 6 and 10 MPa at the desired flow rate flat fan spray atomisers respectively for 3 minutes each.
- xix. Step 1 to 17 above were repeated for desired standoff distance of 25mm, 50mm and 75mm respectively and operated for 3 minutes each.
- xx. Step 1 to 18 were repeated for desired numbers nozzles (3,4 and 5 nozzles) respectively
- xxi. Step 1 to 19 above were repeated for desired nozzles arrangement (NCN, CN & CNO) respectively

- xxii. All the above technique or sequence were applied and repeated for various scale samples (soft and hard scale sample)
- xxiii. All readings from each trial were recorded for further analysis.

### **4.5.3 Safety precaution measure**

Health safety and environment (HSE) are the fundamental worry now, they are the most significant dangers that require serious consideration and change in our reality today. Safety measures are activities and precaution engage to improve safety, i.e. diminish hazard related with human wellbeing or health. The safety measures taken in during this trial are as follows.

- a. All fittings and installations were appropriately confirmed and fixed well to keep away from pressure loss due to leakages.
- b. Circuit's breakers were introduced to keep away from appliance damage, which could emerge from surplus voltage.
- c. The distinct units of the equipment's were kept in their appropriate position keeping in mind the end goal to work accurately to their most efficient productivity.
- d. The water tank was loaded with water to the required most maximum water level.
- e. The power supply was switch off to the water pump after utilization.
- f. The water tank was completely drained at the end of the day to avoid Legionnaires' disease.
- g. Appropriate personal protective equipment's were worn and additionally safety gloves and ear to protect the operator from harm and injuries.
- h. The vacuum pump was switched off immediately it's about to overheat or suction in water.
- i. A Fire extinguisher was accessible if there should be an occurrence of fire incidence.

### **4.5.4 Source of errors in the scale removal test**

- a. Difference in amount of scale removed when descaling similar samples under the same descaling conditions
- b. Difference in hardness of the produce wax due to lone production and different setting time.
- c. Pressure variation due to pressure drop effect when operating the high-pressure water pump
- d. The chamber pressure differential effect as a result of back pressure when compression/suctioning the chamber
- e. Error in measuring the mass of descale samples in wet conditions due to difficulties of getting it 100% dried.

- f. Poor contact of the water jets on the hard scales sample due to reduced ID of the sample compared to the size of header.
- g. Sporadically, when operating at high pressure of 10 MPa the nozzle header would move laterally before stabilizing, therefore changing the impact position of the water jets.

#### **4.5.5 Scale removal error mitigation measures**

- a. Repeatability was maintained throughout the experiment by repeating each experiment by three (3) runs and their average were recorded.
- b. The wax scale samples were produced in batches and Colling curve test was conducted to make sure they have the same setting or hardening time.
- c. The high-pressure pump (600 bars most extreme) was operated within a tolerance of  $\pm 1$  bar
- d. The pressure differential was kept consistent by including the chamber pressure during the compression/cavitation test because of variation in back pressure in the pressurized or suctioned chamber
- e. The quantitative estimation for the mass of the scale recovered during each test was kept within  $\pm 0.1$  g to justify the mass of water soaked by the scale amid the analysis, which could not be gotten dry because of time constraint.
- f. The high-pressure water pump was operated by gradually building up to the desired high pressure from lower injection pressures to avoid the multiple nozzle header from vibrating due to sudden high-pressure drop effect.

#### **4.5.6 Experimental error analysis**

To ensure precise and accurate result were obtained during the entire experiment, every set of experiment was run three times and the average results were recorded. Also, Table 4.1, 4.2 and 4.3 shows the closeness of the merging of error (0.8 maximum standard deviation) for 3 nozzle descaling experiment at different injection pressure, nozzle arrangements and chamber air concentrations.

**Table 4.1:** Error analysis of 3 nozzles ambient descaling results

Scale Type	Ambient descaling results											
	NCN Arrangement											
	4.8MPa				6.0MPa				10MPa			
	Run1 (g)	Run2 (g)	Run3 (g)	S/D (g)	Run1 (g)	Run2 (g)	Run3 (g)	S/D (g)	Run1 (g)	Run2 (g)	Run3 (g)	S/D (g)
Hollow	42	41.9	42.1	0.082	94	93.9	93.8	0.082	254	253	254	0.471
Solid	5.2	5.26	5.18	0.034	7.3	7.2	7.5	0.125	103	102	102	0.471
SrSO <sub>4</sub>	2.3	2.4	2.35	0.041	2.9	3	3.1	0.082	6.5	6.7	6.9	0.163
CaCO <sub>3</sub>	1.5	1.6	1.53	0.042	2	1.9	2.1	0.082	4.4	4.6	4.8	0.163
Scale Type	CN Arrangement											
	4.8MPa				6.0MPa				10MPa			
	Run1 (g)	Run2 (g)	Run3 (g)	S/D (g)	Run1 (g)	Run2 (g)	Run3 (g)	S/D (g)	Run1 (g)	Run2 (g)	Run3 (g)	S/D (g)
	Hollow	32.6	32.7	32.6	0.047	89.4	89.6	89.5	0.082	236.8	237	238
Solid	5.2	5.2	5.3	0.047	7.2	7.3	7.1	0.082	104	103.7	103.9	0.125
SrSO <sub>4</sub>	2.1	2	2	0.047	2.9	2.9	2.8	0.047	4.6	4.4	4.5	0.082
CaCO <sub>3</sub>	1.6	1.5	1.6	0.047	1.8	1.9	1.93	0.056	6.4	6.6	6.7	0.125
Scale Type	CNO Arrangement											
	4.8MPa				6.0MPa				10MPa			
	Run1 (g)	Run2 (g)	Run3 (g)	S/D (g)	Run1 (g)	Run2 (g)	Run3 (g)	S/D (g)	Run1 (g)	Run2 (g)	Run3 (g)	S/D (g)
	Hollow	24.5	24.7	24.6	0.082	6.9	6.8	7	0.082	205.1	204.9	205.3
Solid	4.8	4.7	4.5	0.125	6.8	6.8	6.9	0.047	81	81.1	79.8	0.591
SrSO <sub>4</sub>	1.4	1.6	1.6	0.094	2.6	2.8	2.7	0.082	5.8	6.1	5.9	0.125
CaCO <sub>3</sub>	1.3	1.2	1.1	0.082	1.9	1.8	2.1	0.125	4.3	4.1	4.4	0.125

**Table 4.2:** Error analysis of 3 nozzles compressed descaling results

Scale Type	Compressed descaling results											
	NCN Arrangement											
	4.8MPa				6.0MPa				10MPa			
	Run1 (g)	Run2 (g)	Run3 (g)	S/D (g)	Run1 (g)	Run2 (g)	Run3 (g)	S/D (g)	Run1 (g)	Run2 (g)	Run3 (g)	S/D (g)
Hollow	88.6	89.1	90.2	0.668	206.9	208.2	207.7	0.535	290.3	291.5	289.8	0.713
Solid	8.4	8.2	7.8	0.249	14.3	14.9	15.2	0.374	199.8	200	201.4	0.712
SrSO <sub>4</sub>	2.1	2.2	1.9	0.125	2.7	2.8	3.3	0.262	7.6	7.3	7.1	0.205
CaCO <sub>3</sub>	1.5	1.7	1.8	0.125	2.1	2.3	2.5	0.163	5.9	6.2	5.8	0.170
Scale Type	CN Arrangement											
	4.8MPa				6.0MPa				10MPa			
	Run1 (g)	Run2 (g)	Run3 (g)	S/D (g)	Run1 (g)	Run2 (g)	Run3 (g)	S/D (g)	Run1 (g)	Run2 (g)	Run3 (g)	S/D (g)
	Hollow	89	88.8	89.1	0.125	208	207	209	0.816	291	292	293
Solid	12.6	12.9	12.7	0.125	20	20.1	20.3	0.125	203	204	202	0.816
SrSO <sub>4</sub>	2.7	2.8	2.9	0.082	3.4	3.5	3.6	0.082	8.4	8.3	8.2	0.082
CaCO <sub>3</sub>	2.1	2.4	2.3	0.125	2.8	2.9	2.7	0.082	7.1	7.4	7.5	0.17
Scale Type	CNO Arrangement											
	4.8MPa				6.0MPa				10MPa			
	Run1 (g)	Run2 (g)	Run3 (g)	S/D (g)	Run1 (g)	Run2 (g)	Run3 (g)	S/D (g)	Run1 (g)	Run2 (g)	Run3 (g)	S/D (g)
	Hollow	46.7	46.5	45.9	0.340	168.9	169.5	169.2	0.245	246.8	247.2	247.5
Solid	11.8	12	12.4	0.249	18.3	18.7	18.9	0.249	216.6	217	216.8	0.163
SrSO <sub>4</sub>	2.1	2.4	1.9	0.205	2.9	3.1	3.4	0.205	7.5	7.8	8.1	0.245
CaCO <sub>3</sub>	1.8	1.9	1.6	0.125	2.3	2.5	2.2	0.125	6.3	6.5	6.6	0.125

**Table 4.3:** Error analysis of 3 nozzles vacuumed descaling results

Vacuumed descaling results												
NCN Arrangement												
Scale Type	4.8MPa				6.0MPa				10MPa			
	Run1 (g)	Run2 (g)	Run3 (g)	S/D (g)	Run1 (g)	Run2 (g)	Run3 (g)	S/D (g)	Run1 (g)	Run2 (g)	Run3 (g)	S/D (g)
Hollow	54.2	54.4	53.8	0.249	197	198	198.2	0.525	264	265	263	0.816
Solid	12.8	13.4	13.6	0.340	7.1	7.4	6.9	0.205	233	232	234	0.816
SrSO <sub>4</sub>	2.3	2.5	2.6	0.125	2.9	3.3	3.2	0.170	7.9	8.1	8.3	0.163
CaCO <sub>3</sub>	1.7	1.9	1.6	0.125	2.5	2.7	2.3	0.163	6.3	6.7	6.9	0.249
CN Arrangement												
Scale Type	4.8MPa				6.0MPa				10MPa			
	Run1 (g)	Run2 (g)	Run3 (g)	S/D (g)	Run1 (g)	Run2 (g)	Run3 (g)	S/D (g)	Run1 (g)	Run2 (g)	Run3 (g)	S/D (g)
Hollow	90	90.3	90.4	0.17	209	208.6	209	0.189	294	295	294	0.471
Solid	9.2	9.3	9.5	0.125	16	16.2	15.9	0.125	202	203	202	0.471
SrSO <sub>4</sub>	2.5	2.7	2.9	0.163	3.3	3.2	3.5	0.125	8.1	8.5	8.7	0.249
CaCO <sub>3</sub>	1.9	2.1	2	0.082	2.7	2.8	2.9	0.082	6.7	6.8	6.9	0.082
CNO Arrangement												
Scale Type	4.8MPa				6.0MPa				10MPa			
	Run1 (g)	Run2 (g)	Run3 (g)	S/D (g)	Run1 (g)	Run2 (g)	Run3 (g)	S/D (g)	Run1 (g)	Run2 (g)	Run3 (g)	S/D (g)
Hollow												
Solid	4.9	4.7	4.5	0.163	170.2	171	169.8	0.499	251.2	250	250.6	0.490
SrSO <sub>4</sub>	12.3	12.8	12.9	0.262	19.2	19.8	19.4	0.249	219.7	219	218.9	0.356
CaCO <sub>3</sub>	2.5	2.2	2.3	0.125	2.9	3	3.2	0.125	7.1	7.5	7.8	0.287

## 4.6 Summary

The technique of this experiment took after a successive way to deal with scale removal utilizing the accompanying plan:

- The upgraded descaling rig was designed, constructed and assembled for the experiment.
- A convertible moulder was fabricated and utilised to construct soft scale samples of various shapes and sizes.
- Both the constructed soft scale samples and the accrued hared scale samples were chemically and physically characterised.
- Mass flow rate of different combination of nozzles at different injection pressure was measured in preparation of the scale removal trials.
- Due to environmental and economic advantages, high pressure water spray was utilized in the descaling medium. Also was exclusively adopted to substitute the utilization of solid particles in blend with the water as of now used for industrial scale removal.

- Scale removal trials were executed with different header/nozzle configurations at different chamber air concentration, injection pressure and standoff distance for both constructed soft scale sample and the analyse hard scale sample.

The forth coming chapter will provide the outcomes from the different tests in this chapter, and the investigation and analysis. The outcomes will be introduced in a similar way in which the experimental description followed as appeared in Fig 4.0.

# Chapter 5

## Results and Discussion

### 5.1 Overview

This chapter presents the outcomes (results) acquired from the experimental examination led by the plan set out in Fig. 4.0. As per the original target of this examination, of utilizing multiple high-pressure circular nozzles in a special descaling chamber (ambient, compressed and vacuum condition) to clean mineral and organic scale deposit in petroleum production tubing. Some descaling experimental preparation have been conducted by designing and constructing scale mould through exporting the solid work design to a 3D printer. Subsequently used to prepare the wax scale sample candidate of different shapes and sizes. In addition, the oil field scale obtain from Libyan oilfield and the constructed soft scale candidate were chemically/compositionally analyse using the combination of (SEM, EDs, XRD, Infrared and NMR).

The outcomes are categorized into sections under phases in which the experimental succession follows:

**Phase 1:** The pre-descaling experiments which were conducted outside the descaling chamber ahead of the descaling trials as further classified into two sections:

**Section 1:** chemical and compositional characterization of constructed soft scale sample through NMR and FTIR techniques.

**Section 2:** Chemical and compositional characterization the available hard samples through the combination of EDs, SEM & XRD technique

**Phase 2:** The main experimental descaling trials was conducted by utilizing the special constructed descaling chamber and dived in to three sections:

**Section 1:** Studying the effect of descaling parameters like injection pressure, numbers of nozzles, stand-off distance and nozzle arrangement toward the rate of scale removal at different chamber pressure

**Section 2:** Studying the effect chamber water/air concentration i.e. ambient, compressed and vacuum air condition toward the rate of scale removal.

**Section 3:** Determining the optimum descaling requirement for the effective scale removal of different types scale deposit in petroleum production tubing

# PHASE 1

## Pre-descaling Experiment

### 5.2 Scale characterization

#### 5.2.1 Chemical/compositional analysis

The outcome of the experiment in Section 4.4 of the methodology chapter on how the appropriate techniques were utilised chemically and compositional analysing both the soft and hard scale samples will be given due consideration in this section.

#### 5.2.2 Soft scale compositional & chemical analysis

Findings from the chemical and compositional analysis of the constructed soft scale samples using NMR and FTIR techniques as elaborated in Section 4.4.1 of the methodology chapter will be detailed in the two coming Sections (5.2.2.1 and 5.2.2.2) respectively

##### 5.2.2.1 NMR analysis of soft scale sample

As detailed in the Section 4.4.1.1 on how the nuclear magnetic resonance spectroscopy technique was utilised in investigating the presence of the chemical properties of typical oil field scale deposits (paraffin) in the constructed soft scale samples. The spectra of the  $^1\text{H}$  NMR in figure 5.1 proofs the presence of olefinic protons between  $\delta = 0.5 \text{ ppm} - \delta = 1.5 \text{ ppm}$  are characteristics of hydrogens on CH, CH<sub>2</sub> and CH<sub>3</sub> groups. This region of the peaks corresponds with spectra reported in the literature (Palou et al., 2014). As mentioned earlier, singlet at  $\delta = 0.0 \text{ ppm}$  is assigned for TMS and mainly used as a calibration peak. The singlet peak at the extreme ( $\delta = 7.278 \text{ ppm}$ ) is assigned to the deuterated chloroform (CDCl<sub>3</sub>) solvent which was used to dissolve the sample. The characteristic signals of the spectra confirm the presence as saturated hydrocarbon (signals in the upfield). No peaks were observed in the aromatic region of the spectra between  $\delta = 7.0 \text{ ppm}$  and  $\delta = 8.0 \text{ ppm}$ .

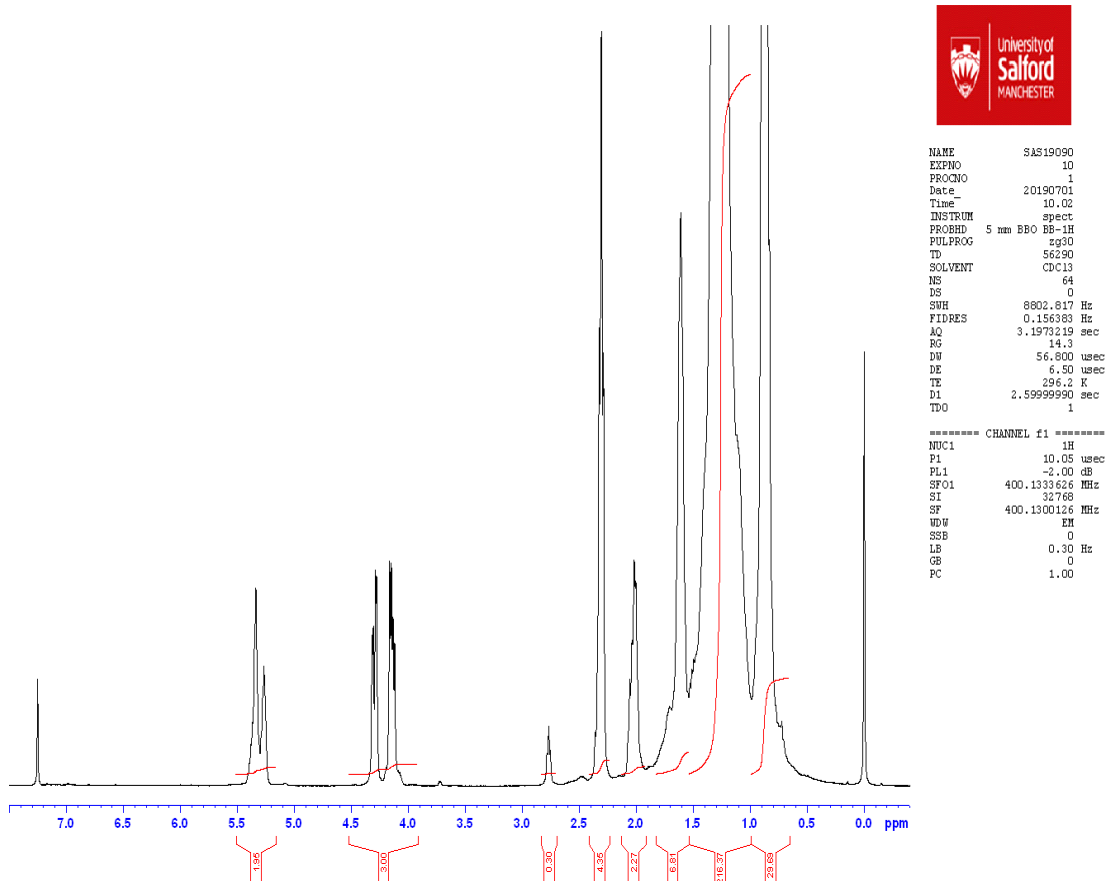
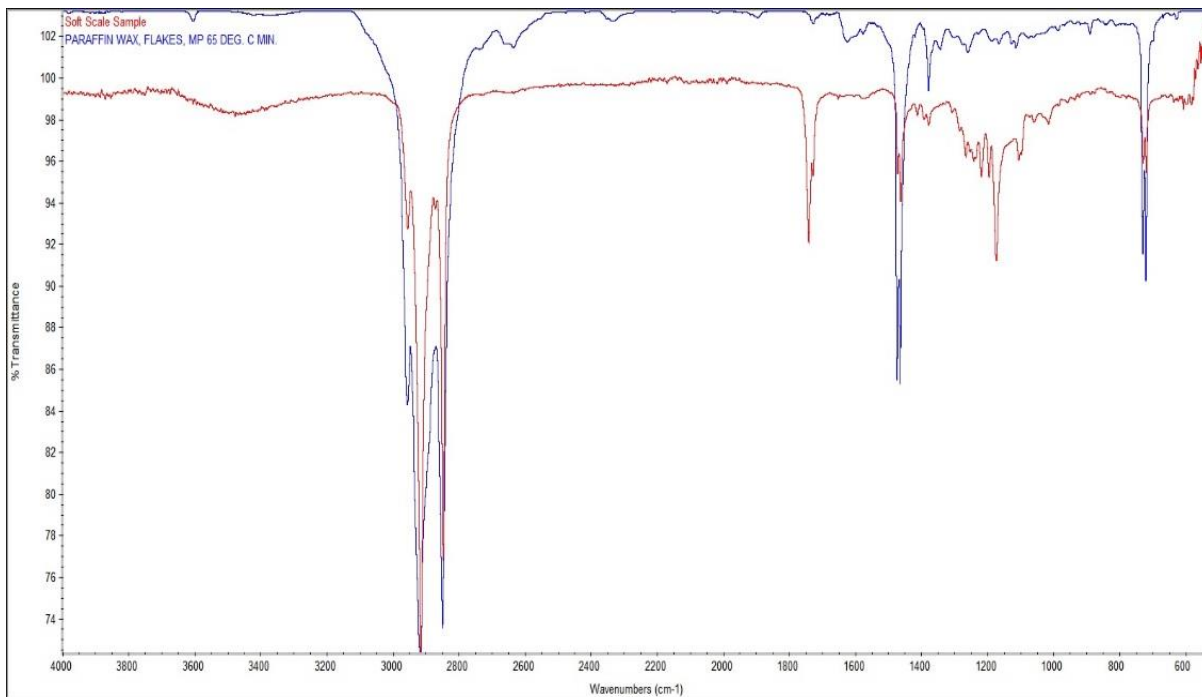


Figure 5.1: NMR result of soft scale sample

### 5.2.2.2 Infrared analysis of soft scale sample

The constructed wax scale deposit was further subjected to Infrared spectroscopy analysis for verification of the NMR result and re-affirmation of its chemical representativeness of the oil field scale deposit (paraffin). As discussed in Section 4.4.2.2 of the methodology chapter, the results generated by Thermo Scientific Nicolet iS10 for the prepared wax sample, were revalidated. Through superimposing the results with the paraffin flakes results from the system in built archived (database) which seems to share same functional groups in Figure 5.2. Both spectrums coincide by revealing similar fingerprint and bands for a functional group of paraffin. Furthermore, FT-IR in Figure 5.2, the absorption peaks between 2900 cm<sup>-1</sup> and 2800 cm<sup>-1</sup> is assigned for stretching and vibrations of CH<sub>2</sub> and CH<sub>3</sub>, which confirms the nature of paraffin present in the sample as aliphatic. (Manoj et al., 2012). The absorption peaks also matched with those retrieved from National Institute of standard and technology (NIST) database of FT-IR spectra



**Figure 5.2:** Infrared analysis compared to paraffin flakes from NIST data base

Likewise, for more validation and confirmation, the soft wax ample spectra were superimposed and compared with the results from the liquid paraffin confirmatory test as explained in Section 4.2.2.2 and presented in Figure 5.3, were both the spectrum soft wax and liquid paraffin share the same peaks and bands of paraffin functional group.

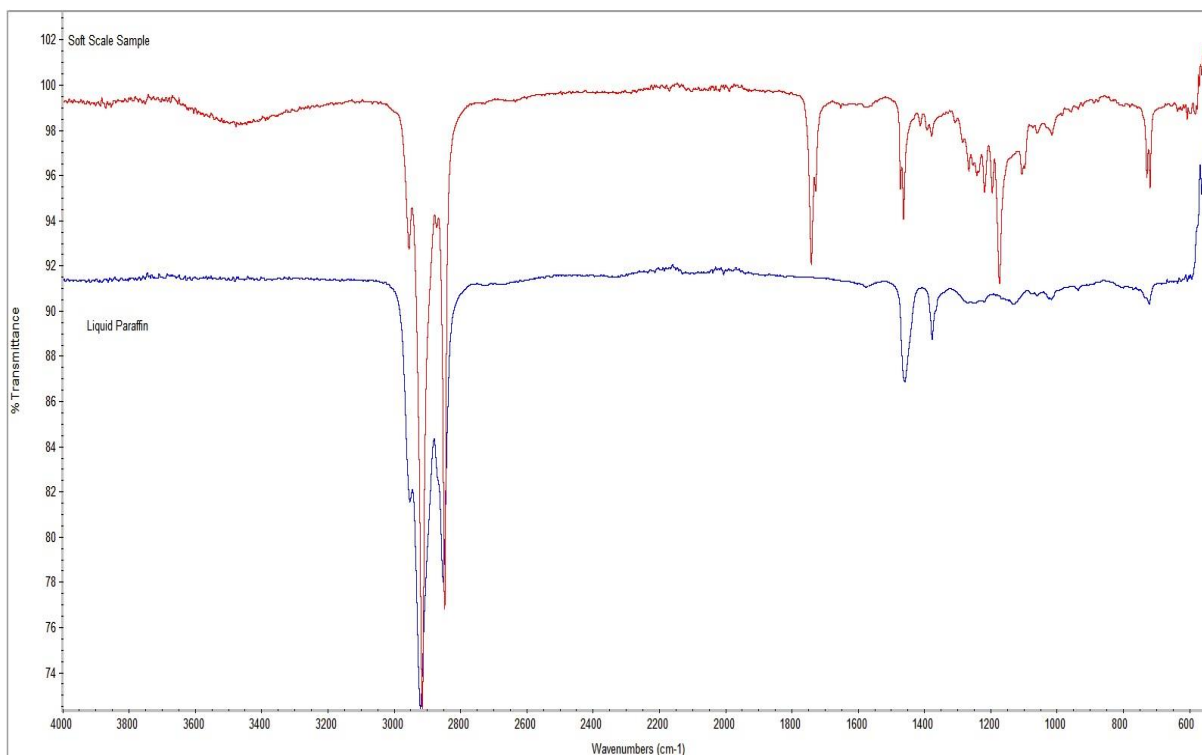


**Figure 5.3:** Infrared analysis compared to liquid paraffin

### 5.2.3 Hard Scale compositional & chemical analysis

The findings from the chemical and compositional analysis of the hard scale samples using the combination of SEM, EDX & XRD as recommended in the single nozzle research and elaborated in Section 4.4.3 of chapter four will be presented and analysis in these section.

#### 5.2.3.1 Scanning electron microscope (SEM)

The results of the two unknown samples labelled sample A & B that were first off, all, send for scanning electron microscopy analysis in order to identify their surface topography and compound composition through the magnifying lances of the microscope are as follows. The high-resolution images in Figure 5.4 and 5.5 revealing the surface topography of the samples at different magnifications of 1 mn, 30  $\mu\text{m}$ , 40  $\mu\text{m}$  and 100  $\mu\text{m}$  respectively were generated from the adopted analysis procedure in Section 4.4.3.1.

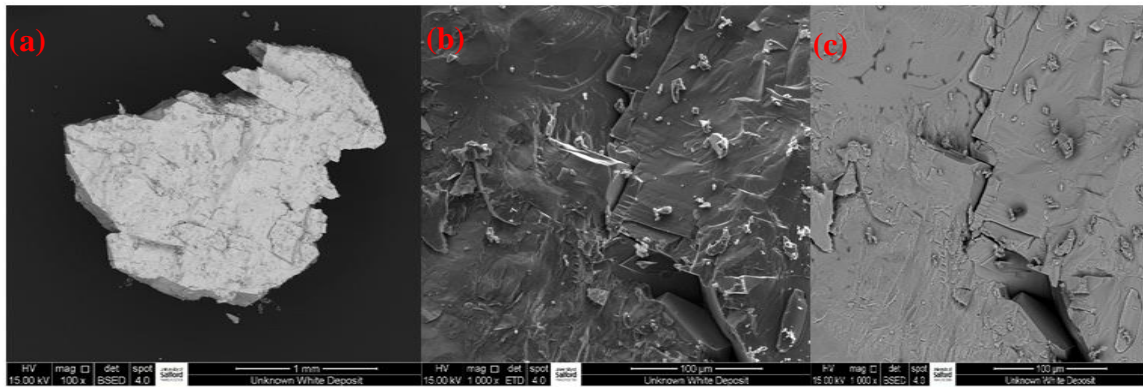


**Figure 5.4:** SEM Results of Sample A at (a) 1 mn, (b) 40  $\mu\text{m}$  and (c) 100  $\mu\text{m}$  magnifications

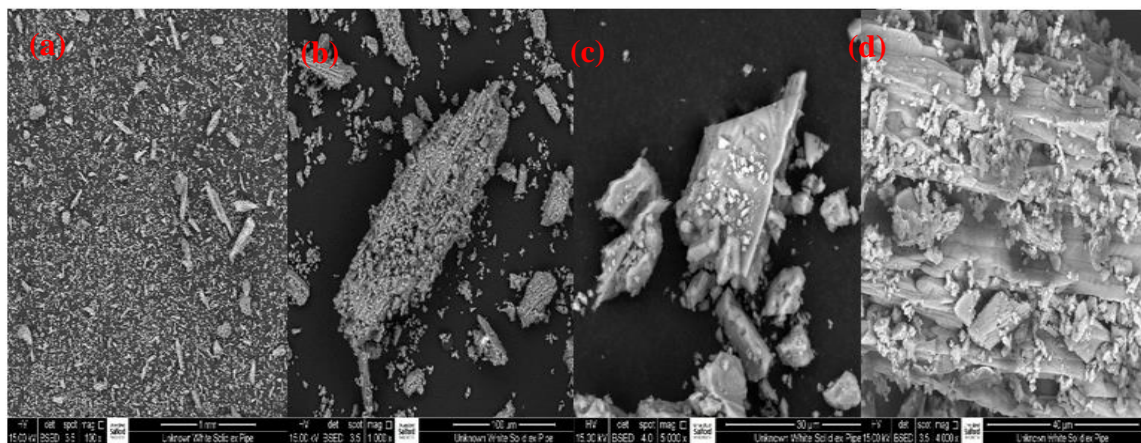


**Figure 5.5:** SEM Results of Sample B at (a) 1 mn, (b) 30  $\mu\text{m}$ , (c) 40  $\mu\text{m}$  and (d) 100  $\mu\text{m}$ , magnifications

### 5.2.3.2 Energy dispersive X-ray analysis (EDX)

The outcomes of further progressing the SEM result to EDX analysis for elemental identification and quantitative compositional information as elaborated in Section 4.4.3.2 are presented in Figure 5.8 and 5.9 at different spectrums for sample A & B respectively.

The EDs results of sample A at different spectrums as shown in Figure 5.6 and Appendix A10 indicated the presence of elements like carbon, oxygen, strontium, calcium and barium in the sample. Combining the two set of EDs results, strontium was found to be the far overweighting element (strontium sulphide likely).

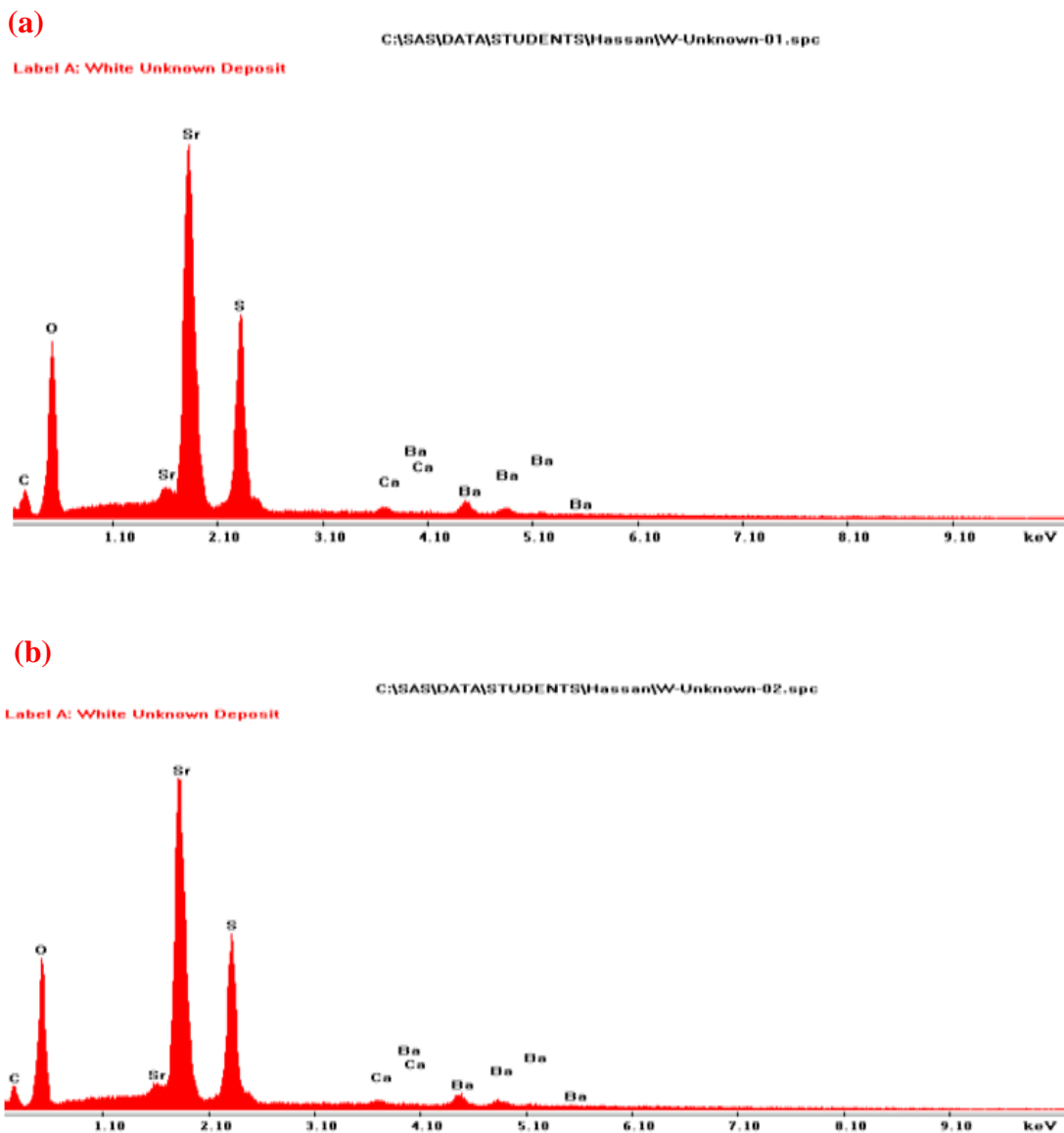
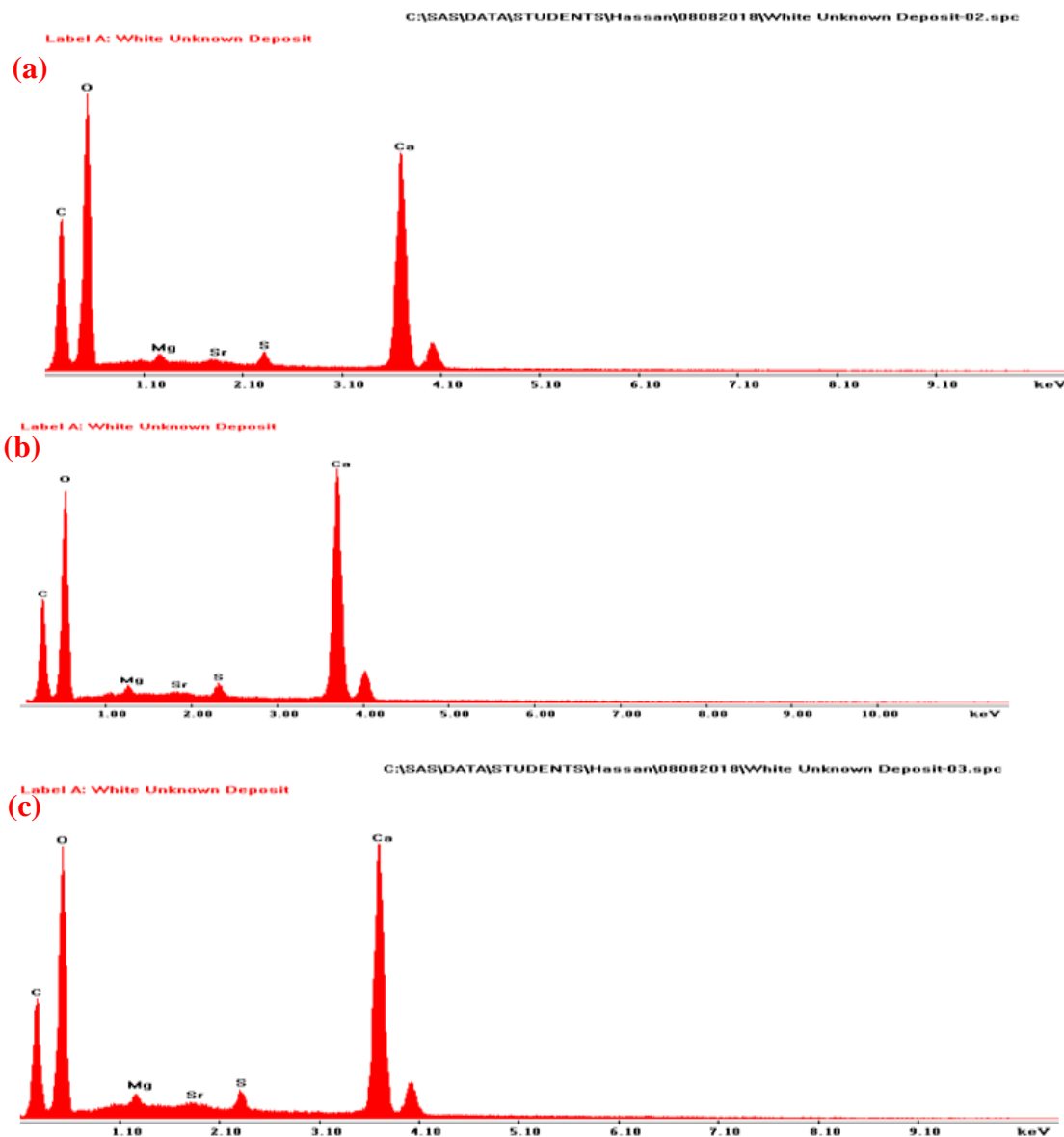


Figure 5.6: EDX Result Sample A at (a) 0.1, (b) 0.2 spectrums

In the case of the second sample (unknown sample B), the EDX analyser detected high presence of elements like carbon calcium and oxygen, together with low strontium, magnesium and sulphur presence in the compound. Even though it looks obvious from the three set of elemental maps presented in Figure 5.7 at different spectrum that calcium, oxygen and carbon have the most presence in the background. Unfortunately, could not generate quant EDX result for sample B due to non-flat constraints of the sample in question, which result even if generated will be meaningless.



**Figure 5.7:** EDX Result for Sample B at (a) 0.1 (b) 0.2, (c) 0.3 spectrums

### 5.2.3.3 X-ray diffraction analysis

As explained in Section 4.4.3.3 how the two grinded powders (A & B) were subjected to x-ray powder diffraction analysis for final confirmatory analysis, characterization of their crystalline material. The analyser reveals the following set of mineralogy results for both samples.

The XRD analysis result confirm the Unknown white powder sample A to be Strontium sulphide compound and Celestine, sync- ( $\text{SrSO}_4$ ) to be precise

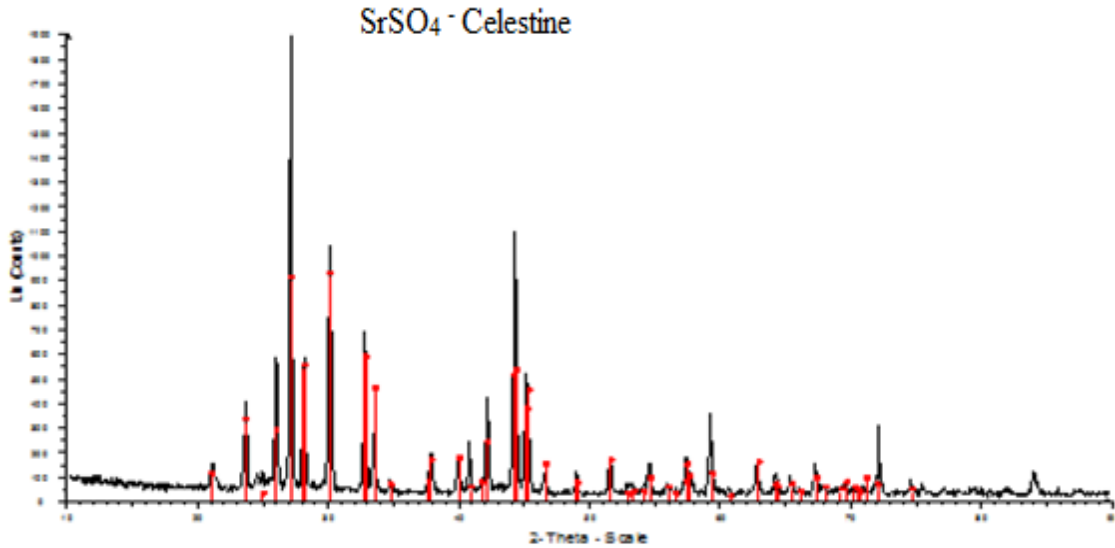


**Figure 5.8:** XRD result Sample A

While for the second sample (unknown white powder B) was confirm by analyser to be calcium carbonate compound and a calcite scale sync- ( $\text{CaCO}_3$ ) to be precise as prove in Figure 5.9.

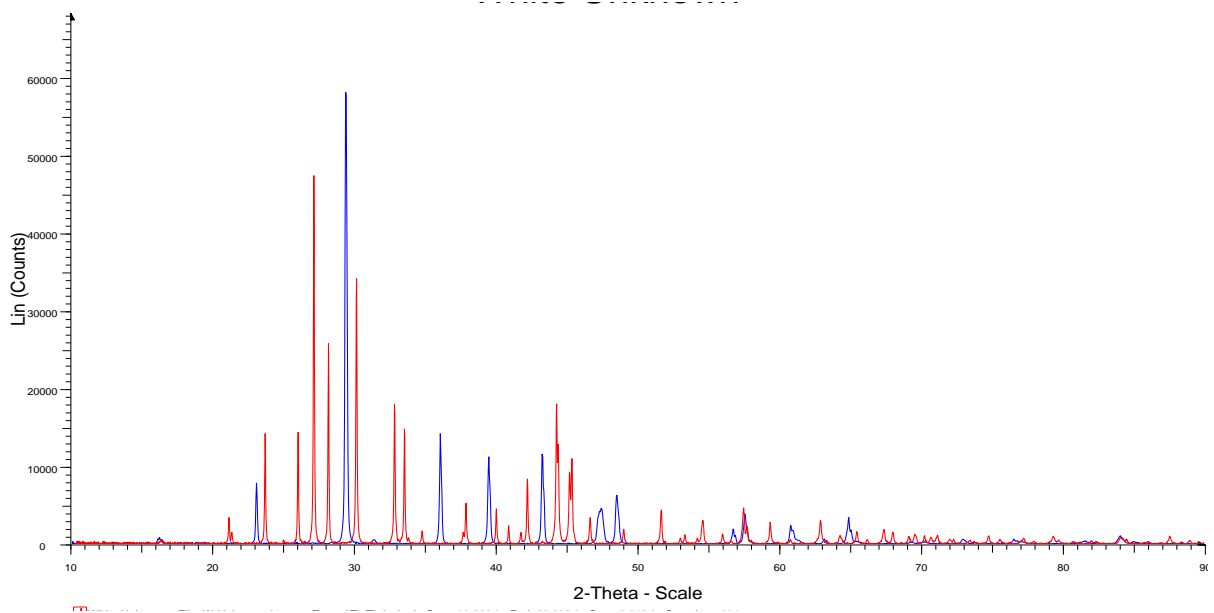


**Figure 5.9:** XRD results sample B

# **PHASE TWO**

## **Descaling Experiment**

### **5.3 Scale removal experiment**

As already discuss in the methodology chapter, the special assembled descaling rig had been utilised in descaling both the constructed soft scale sample of different shapes and sizes simulating different scale growth stages in production tubing. Since constructed wax scale was proved to have similar chemical and physical properties with paraffin (soft scale) as elaborated in Section 5.2.2.1 & 5.2.2.3 (Palou et al., 2014; Manoj et al., 2012). In addition to the analysed hard scale samples which are found to be strontium sulphate and calcium carbonate scale respectively (Yeoun et al., 2014; El hajj et al., 2015). The descaling experiments were conducted under different chamber conditions of ambient, compressed and vacuum air concentration, all in simulation of a real oil well descaling scenario.

#### **5.3.1 Ambient decaling experiment**

This section will cover and present all the quantitative and qualitative results achieved during the decaling experiments under ambient chamber condition for the constructed wax scale (hollow and solid) and analysed hard scale ( $\text{SrSO}_4$  and  $\text{CaCO}_3$ ) samples. The 1344 numbers of scale samples including test and repeatability sample of hollow (8mm length by 10mm thickness), solid (150 mm diameter by 20 mm thickness) and 3cm by 1.5cm diameter of the hard scale samples ( $\text{SrSO}_4$  and  $\text{CaCO}_3$ ) were descaled and analysed. The impact of descaling parameters like numbers of nozzle, injection pressures and standoff distance, header and nozzle configuration towards the amount of scale removed from each scale deposit under ambient chamber condition will be given due consideration in this section. Even thou, emphasis will be more given on the 25mm stand-off distance trials, at its best nozzle's configuration arrangement. See Appendix C 1 for more details on the de-scaling remarks.

##### **5.3.1.1 Hollow soft scale samples**

Appendix C2 summarised mass of scale removed during the entire ambient descaling experiment for the constructed hollow shape scale sample and Figure 5.10 captured the 25mm-distance operations of this experimental phase.

Starting with the investigation of the effect of nozzles arrangement at 4.8, 6 & 10 MPa injection pressure for 5, 4 & 3 nozzle at 25mm distance during the ambient scale removal operation as presented in Figure 5.10. The A part of the result (4.8 MP) has quantitatively demonstrated an average scale removal of 2.9, 2.3 & 1.8% across the NCN, CN & CNO nozzle arrangements, which qualitatively drilled some holes across all descaled samples at the nozzle configurations of the entire 4 & 3 nozzle operations. Also, 5.6, 5.5 & 4.9% of scale removal was achieved for the respective configurations after increasing to 6.0 MPa injection pressure, that pictorially show a complete scale breakage at the NCN arrangement of 3nozzles operation in the part B. Further increasing the injection pressure to 10 MPa, increases the average removal throughout the respective header/nozzle configurations to 24.6, 21.2 & 18.1% with complete scale breakage all through, if not for holes observed for the 5 nozzle operations as shown the C part of Figure 5.10. The investigation ranked the NCN configuration as the most effective for the hollow shaped scale removal because of its ability to even break sample with 5-nozzles configuration. Attributed to absence of centre nozzle which diverted the jet strength to the side nozzles that are in good contact with scale sample and aid the effect of hoop stress. The NC and NCO are less effective due to the jet strength being diverted to centre nozzle, that spray through the hollowness of the scale deposit. An average difference of 0.6, 1.1 & 3.45% was observed between NCN and the other nozzle configuration for respective injection pressures.

Investigating the impact of respective injection pressures in relations to the amount of scale removed with the NCN arrangement of 5, 4 & 3 nozzle configurations demonstrated a linear increase in amount of scale removed to increase in injection pressure across all the nozzle configurations. A significant increase from 1.7 g to 1.2 g and later 56.6 g of mass of paraffin removal was observed after increasing the injection pressure from 4.8 MPa to 6 MPa and subsequently to 10 MPa when descaling with 5nozzles of N-C-N configuration as shown in figure 5.10. While same figure demonstrated how descaling operations with 4 nozzles at 4.8 MPa initially removes 6.2g of scale deposit that increase by 3.8g and further skyrocketed by almost 70.4g after increasing the injection pressure by 1.2 MPa and subsequently by 5.2 MPa. Better result of removal value of 42.8g was initially achieved with 4.8 MPa injection pressure of 3 nozzle configuration that doubled by 50.9g and subsequently almost a fourfold increase (211g) after increasing to 6.0 MPa and later 10MPa respectively. Similarly, the amount of scale removed by 5, 4 & 3 -NCN arrangement as shown in figure 5.10 A & B produce a slight quantitative and qualitative improvement as a result of increasing the injection pressure from 4.8 to 6.0 MPa. Compared to Figure 5.10 C that increase by many folds

and pictorially break all the samples across the 5,4 & 3 nozzle configurations which was due to high pressure variation of 5.2 MPa than 1.2 MPa difference of the earlier injection pressure increase.

Reducing the numbers of nozzle to 3 nozzles at ambient condition show greater impact than 4 and 5 nozzle header configurations due to multiple nozzle pressure drop effect (Tian, et al., 2009). Although, still demonstrated increase in descaling rate with increase of injection pressure. A very small difference of rate of scale removal of 4.5g from 1.7 g was recorded when the nozzle configuration was reduced from five to four nozzles. Contrary to the almost 25 times increase of 41.1g to be precise, when further reducing the numbers of nozzle to three nozzles from four nozzles at same 4.8 MPa injection pressure as shown in Figure 5.10A. The B part of Figure 5.12 shows how reducing the number of nozzles from 5 to 4 when operating at 6.0 MPa doubled the removal from 2.9g by 7.1g and subsequently by 84g after reducing to 3 nozzles which was able to pictorially break the sample. The analysis of the impact of number of nozzles at 10 MPa injection pressure demonstrated a good result that qualitatively broke through all the descaled samples at the NCN arrangement of 5, 4 & 3 nozzles configurations. The value of 58.3g of scale removed with 5 nozzles at 10MPa was slightly increased by 18.3g and consequently by 195g after reducing the header configuration to 4nozzles and later 3nozzles respectively.

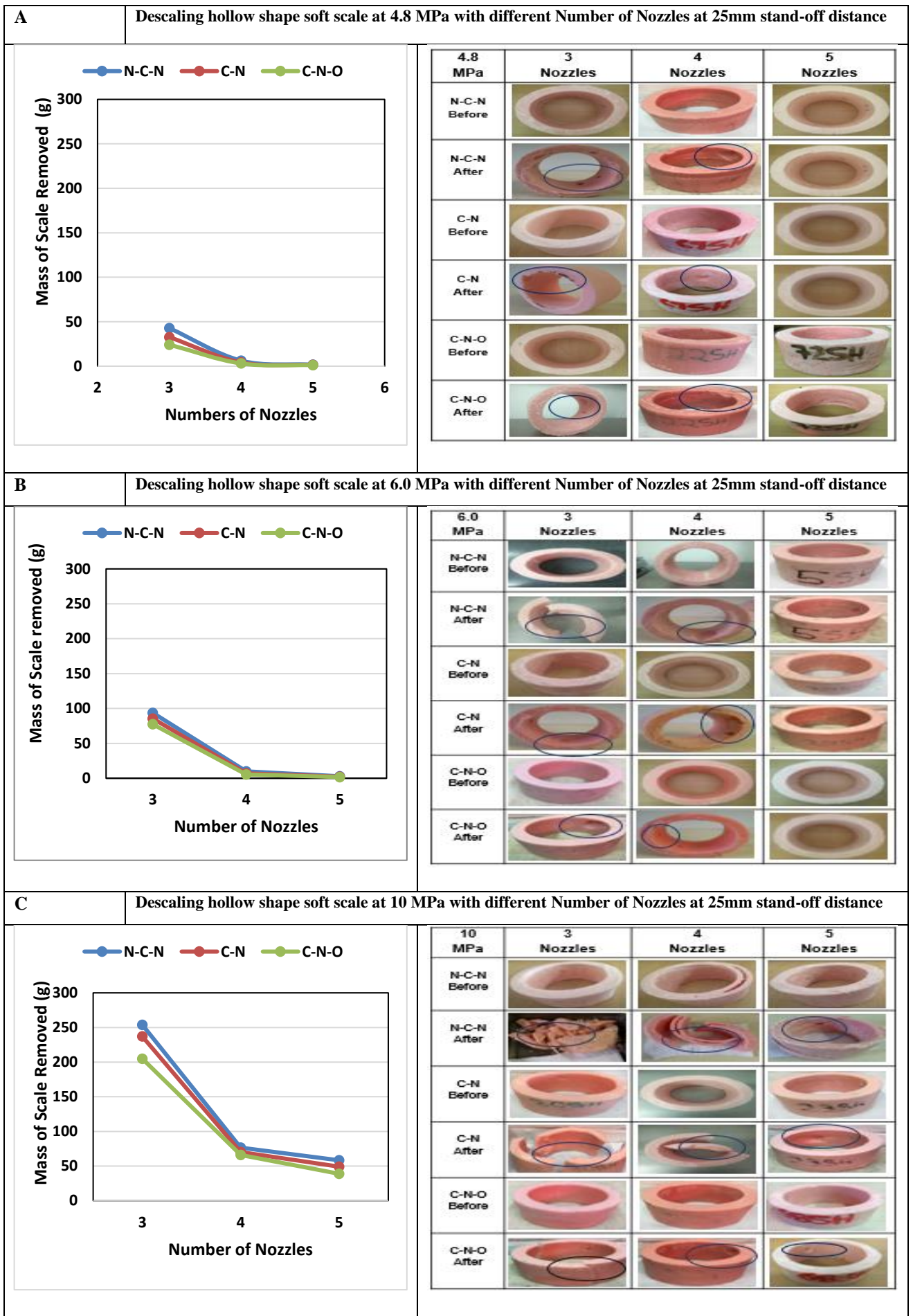


**Figure 5.10:** Ambient descaling results for hollow soft scale at 25mm-distance

### 5.3.1.2 Solid soft scale sample

Figure 5.11 demonstrates both quantitative and qualitative results generated from the ambient descaling investigation of solid shaped scale samples at 25mm stand-off distance, while the entire ambient descaling results for solid soft scale samples can be found in Appendix C3.

The A part of Figure 5.11 quantitatively elaborates how 5, 4 and 3 nozzles were able to averagely remove 0.2, 0.5 & 0.4% of the scale samples at low pressure of 4.8 MPa across the respective nozzle arrangements. Even though, could only qualitatively generate uniform erosion across board. Increasing the injection pressure to 6.0 MPa across the respective header/nozzle configurations as shown in the B part quantitatively removes 0.2, 0.7 & 0.5% of the scale sample. While was pictorially only able to demonstrates mild holes for entire 3nozzles configurations. Further increasing the injection pressure to 10 MPa, increases the average scale removal to 6.6, 10.4 & 8.3% respectively, which qualitatively broke all the 3nozzles configuration descaled samples and drilled hole across the remaining samples as shown in Figure 5.11C. The highest removal impact observed, was in ranking of NC, NCO and NCN in descending order and have value of 0.3, 0.5, 3.8% more than the rest of the nozzle arrangements at respective injection pressures. NC configuration performance is attributed to the good jet -scale surface contact with centre nozzle configurations which aid both cyclin stress and sample particle abrasion jetting mechanism.

Analysing the results achieved from descaling soft solid samples in ambient condition at 25mm, proves to increase with increase in injection pressure and reduction in both of numbers of nozzles and stand-off distance. A mass of 1.2g was initially removed with 5 nozzles at 4.8 MPa injection and increases by 0.6g & 30.5g after increasing the pressure to 6.0 & 10 MPa respectively. While the 4nozzle operation removed 2.6g of solid scale deposit at 4.8 MPa that slightly increases by 1.3g and significantly increase by 48.1g after throttling to 10 MPa. More significant removal can be sighted in Figure 5.11C where the 3nozzle operation originally removes 5.2g of scale at 4.8 MPa injection, that slightly increase by 2.1g and later by many folds of 9.9g as a result of subsequent increase of the injection pressure to 6.0 MPa and 10 MPa respectively.

Operating 5nozzles at 4.8 MPa initially remove 1.2g of scale that increases by 1.5g and 4g after reducing the number of nozzles to 4 and later 3nozzle with no noticeable qualitative impact in Figure 5.11A. Injecting at 6.0 MPa with 5nozzles was able to remove 1.8g of scale that was rise by 2.1 with 4nozzles and better off by 5.5g after reducing to 3nozzles were some holes were drilled all cross in Figure 5.11B. The utilization of 5nozzles at of 10 MPa was able to substantially remove 32g that increased by 19g and later almost 72g after reducing the nozzles numbers to 4 and later 3nozzles that was able to break all the samples in the C part of Figure 5.11.

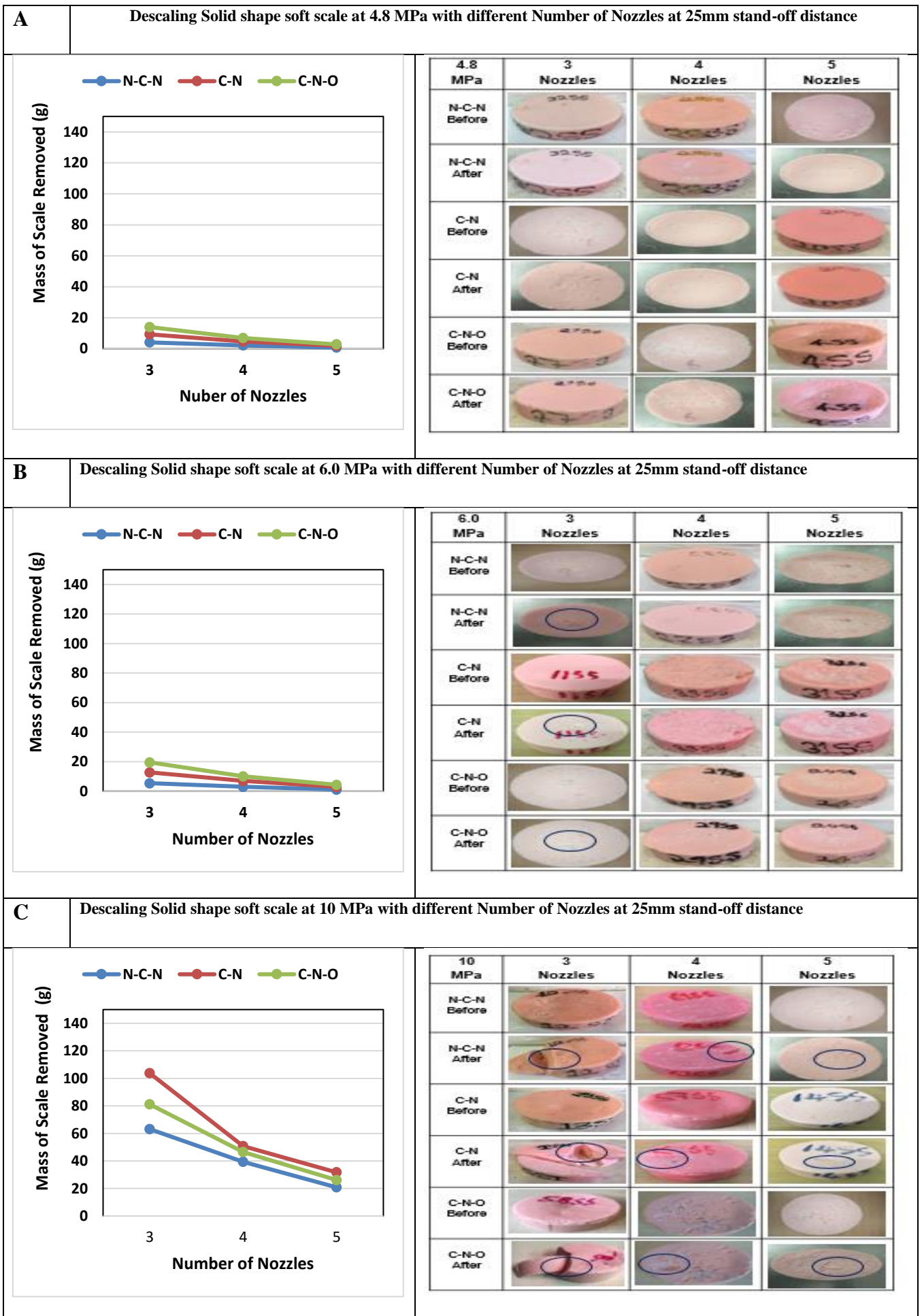


Figure 5.11: Ambient descaling results for solid soft scale at 25mm-distance

### 5.3.1.3 Strontium sulphate scale sample (SrSO<sub>4</sub>)

The descaling rate of the analysed hard scale sample (SrSO<sub>4</sub>) with all the nozzle configurations at ambient chamber condition has similar descaling trend with solid soft scale samples. Even though lower in terms of amount of scale removed when compared to the amount achieved in the soft solid descaling experiment and better than that of the results of CaCO<sub>3</sub>, since erosion mechanism depend on the mechanical properties that are guiding the deposit failure pattern (Zongyi 2014). Refer to Appendix C4 for the ambient strontium sulphite deposit removal results and 25mm standoff distance results are presented in Figure 5.12 bellow.

An average scale removal of 0.19, 0.23, 0.2% were achieved at low pressure of 4.8 MPa for all the respective header & nozzles configuration and was only able to pictorially generate a uniform erosion throughout figure 5.12A. Slight increase of 0.25, 0.32 & 0.39% was observed after adjusting the injection pressure to 6.0 MPa for all respective header/nozzles configuration, which shows no qualitative improvement too, in the Figure 5.12B. Almost a threefold increase in average scale removal of 0.6 ,0.9 & 0.8% across the respective header/nozzle configurations was achieved after further throttling the injection pressure to 10 MPa. As the C part of the Figure 5.17 demonstrate how it break the samples with 4 nozzle-CN arrangement and all the three nozzles arrangements of the 3nozzle experiment. Even though, the impact of nozzle configuration in decaling the entire hard scale sample was very poor due to the reduce size of the scale sample leading to very poor scale surface -jet contact. The centre nozzles configuration (CN) seems to be more effective as it removes 0.04, 0.14 & 0.3% more scale deposit than other nozzles arrangements for both 4.8, 6.0 & 10 MPa respectively.

Like the descaling trend of other deposits, the amount of SrSO<sub>4</sub> remove in this operation increase with injection pressure and reduce with increase in number of nozzles and stand-off distance. The 5nozzle configuration descaling experiment started by removing 0.6g of SrSO<sub>4</sub> that increase by 0.3 and 2.6g due to the increase of injection to 6.0 MPa and 10 MPa respectively. While the 4nozzle removes 1.3g that increase by 0.4g and 3.8g due to the respective pressure increase and value of 2g that increases to 0.9g & 4.5g due to respective pressure increase was recorded with the 3nozzles configuration. The amount of 0.6g of scale was removed with five nozzles at 4.8 MPa that was doubled by 0.7g and tripled by 1.4g after reducing the numbers of nozzles to 4nozzle and later 3 nozzles as presented in Figure5.12A, with no any visual impact. Still with no visual improvement, Figure 5.12B elaborates a moderate removal of 0.9g of SrSO<sub>4</sub> with 5 nozzles at 6.0 MPa that increase by 0.8g and more significantly to 2g after reducing the number of nozzles to 4 and subsequently 3nozzles. An improved qualitative result that shows SrSO<sub>4</sub> breakage across the C-N arrangement of 4nozzle and entire nozzle arrangements of 3nozzle configuration due to the reducing of number of nozzles from 5 to 4 and later 3nozzles with initial removal of 3g to 1.9g and later 3.3g at 10MPa was observed in Figure 5.12C

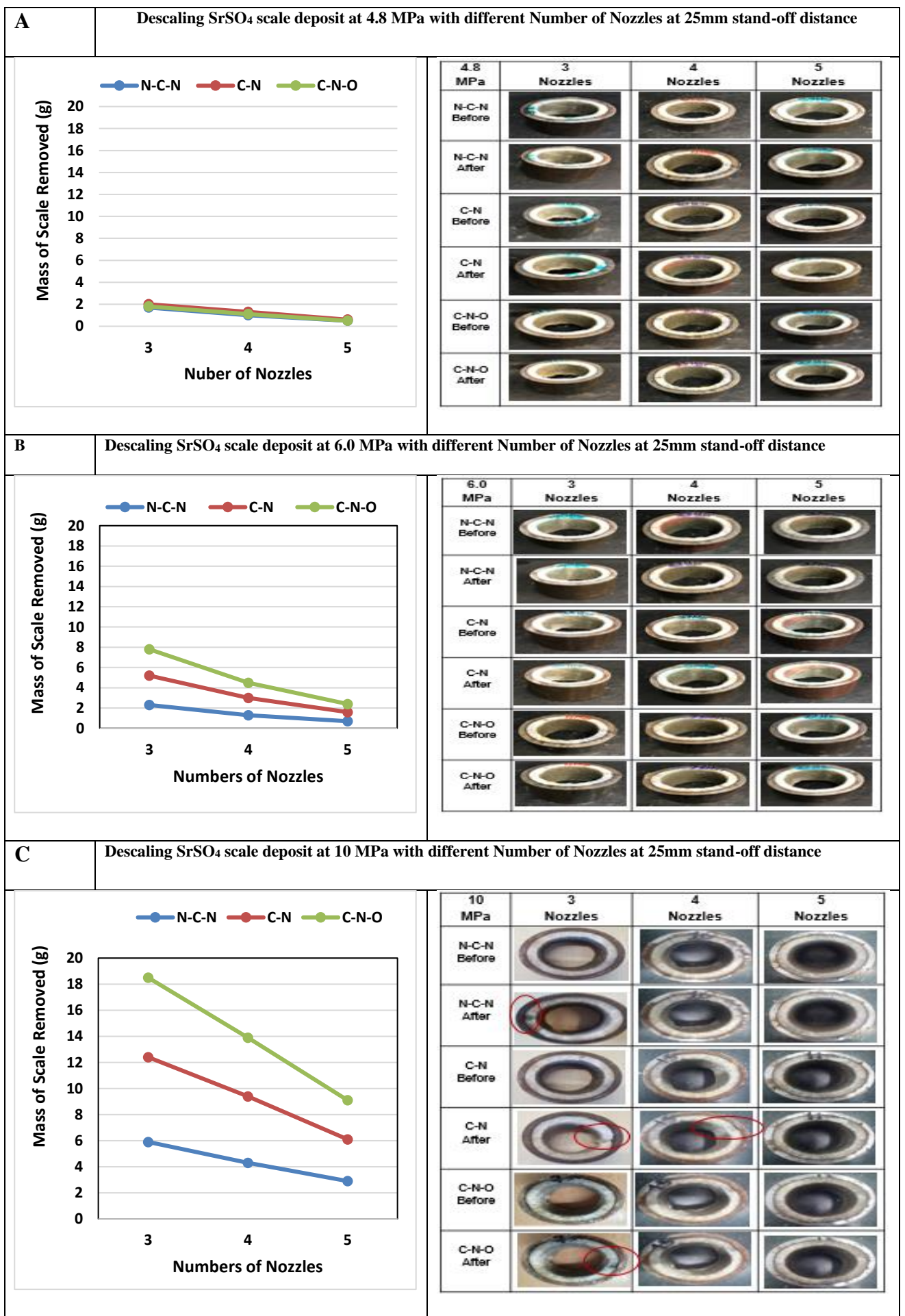


Figure 5.12: Ambient descaling results for SrSO<sub>4</sub> scale deposit at 25mm-distance

#### 5.3.1.4 Calcium carbonate scale sample (CaCO<sub>3</sub>)

The descaling rate of calcium carbonate hard scale sample (CaCO<sub>3</sub>) at ambient chamber condition regardless of all descaling parameters resembled the descaling trend of strontium sulphate scales deposit. Although, amount of CaCO<sub>3</sub> scale removed is less than that attained when removing strontium sulphate under the same descaling conditions. Notwithstanding this can be attached to the difference in mineralogy and hardness of the sample as the SrSO<sub>4</sub> is of crystalline based and the CaCO<sub>3</sub> is aggregate fine grains. Since the earlier expected to originates from sandstone formation and later from limestone or carbonate reservoir. The ambient descaling details for calcium carbonate removal at ambient condition can be found in Appendix C5 and the result of the investigation under 25mm distance is presented in Figure 5.13. An average value of 0.13, 0.17 & 0.14% of CaCO<sub>3</sub> scale deposit was removed with respective header and nozzles configurations when pumping at low pressure of 4.8 MPa as shown in Figure 5.13A. This slightly increases to 0.19, 0.22, & 0.20% respectively after increasing the injection pressure to 6 MPa as presented in Figure 5.13B. More significant increase of 0.46, 0.56 & 0.51% of average scale deposit removal was observed after further increase of the injection pressure to 10 MPa as captured in figure 5.13C. Qualitatively, figure 5.18 could only showcase a uniform erosion across the entire descaled samples and a difference of 0.14, 0.03 & 0.1% of more scale removal by the CN arrangement than the NCN arrangement was recorded.

The C-N configuration of 5nozzle configuration was able remove 0.4g of CaCO<sub>3</sub> at 4.8 MPa that slightly improved the removal by 0.2g and subsequently 1.4g after adjusting the injection pressure to 6.0 MPa and 10 MPa respectively. Similar removal of 0.8g that improves by 0.3g and later 2.1g after altering the injection pressures of the 4nozzles operation from 4.8 to 6.0 and 10 MPa respectively. More improved removal of 1.5g of CaCO<sub>3</sub> that further improved by 0.5g and 2.9g after the subsequent throttling of the injection pressures of the 3nozzles operation from 4.8, to 6.0 and later 10 MPa.

Descaling CaCO<sub>3</sub> in ambient condition with 5nozzles at low pressure of 4.8 MPa removes 0.4g, which later improved by half (0.4g) and tripled (1.1g) due to the reduction of header configurations to 4 and later 3nozzles as shown in Figure 5.13A. Better improve quantitative result is shown in in figure 5.13B, were the initial scale removal of 0.6g that improvement 0.5g and later 1.4g was recorded due to the adjustment of header configuration to 4 and 3nozzles respectively. While figure 5.13C showcase the best removal results of the CaCO<sub>3</sub> in ambient condition, were almost 1.8g of scale was initially remove and later improved by 1.1g and 2.6g due to adjusting the header configuration of 5 nozzles (10 MPa operation) to 4 and later 3nozzles. The entire Figure 5.13 translates a very poor qualitative results from the CaCO<sub>3</sub> ambient descaling campaign that could only uniformly erode all the samples.

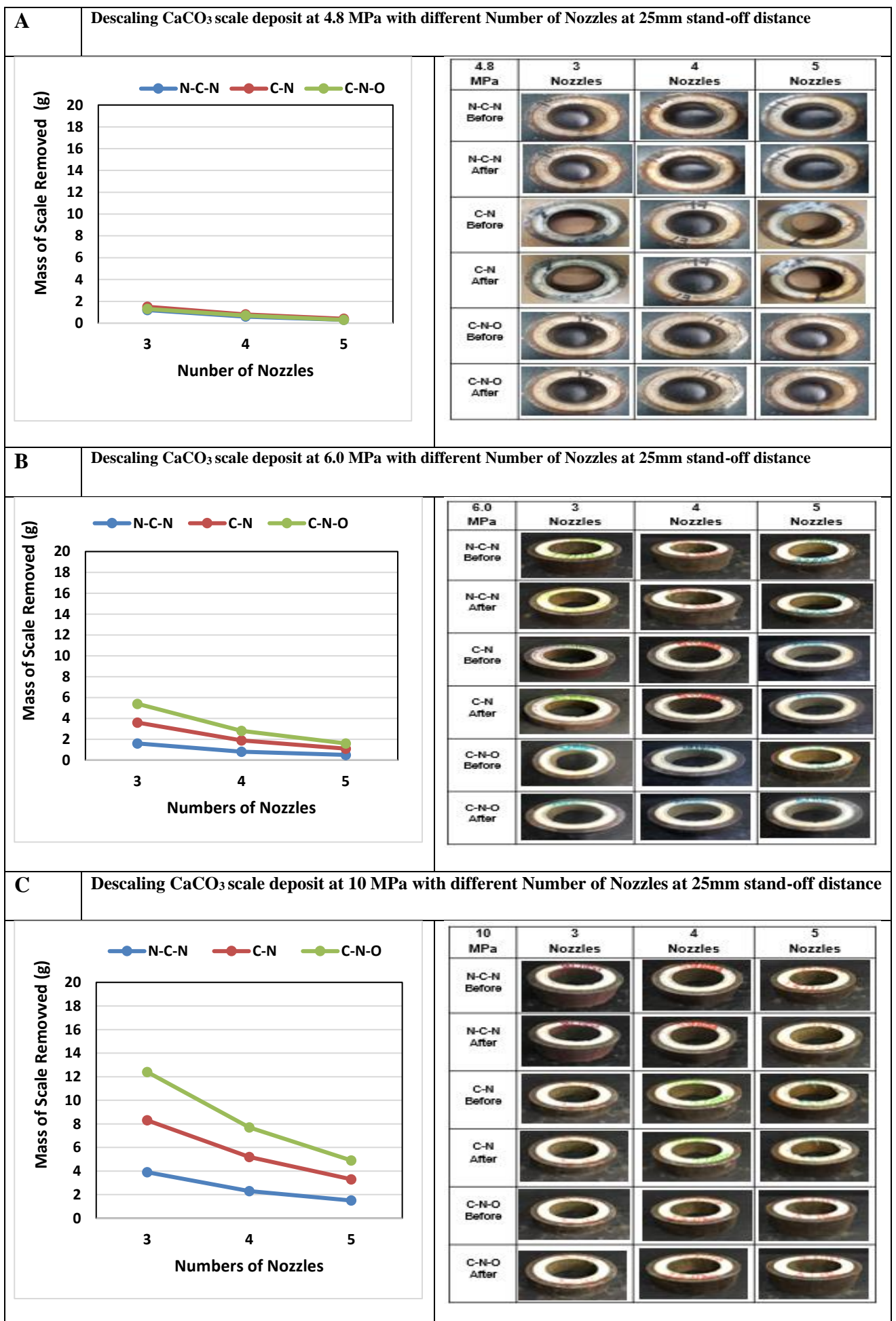


Figure 5.13: Ambient descaling results for  $\text{CaCO}_3$  scale deposit at 25mm-distance

## 5.3.2 Compressed descaling experiments

The compressed descaling experiments were conducted inside the special assembled chamber but in a compressed air chamber condition for the removal of all the four scale samples. As explained in the descaling methodology section that a compressed air of 0.2 MPa was introduced and maintained while simultaneously pumping water at different injection pressure to remove different scale candidate at different jetting position with different header and nozzle configuration. This is done with the aim of utilising the additional compressive stress generated from the compression operation to enhance rate of scale removal.

### 5.3.2.1 Hollow soft scale samples

The hollow shape soft scale descaled under compressed chamber air conditions as summarised in Appendix C6 proves to have attained better scale removal than the ambient trials but with similar descaling trend. The trend that attached the increase in amount of scale remove to increase in injection pressure and decrease in both number of nozzle & stand-off distance and better off with (NCN) non-centre nozzle arrangement. The additional compression on samples from the compressed air during the compression sessions is a key reason for the additional scale removal over the ambient experimental results. Additionally, the introduced compress stress enhances both erosion, cyclin stress and sample particle abrasion mechanism

The investigation of effect of nozzle configuration when removing hollow shape scale deposit in a compressed chamber air condition at 25mm stand-off distance for different injection pressures and number of nozzles as presented in Figure 5.14. Proves NCN arrangement to be most effective among others. As average values of 5.9, 3.8 & 3.4% deposit removal was initial achieved with 4.8 MPa cross respective header and nozzle configurations, which visually drilled holes through the entire descaled samples with 3 & 4 nozzles configurations in Figure. 5.14A. The average value of scale removed was tripled to 14.4, 12.8 & 11.2% across respective header and nozzle configurations after increasing the injection pressure to 6 MPa, with scale deposit breakage across the entire 3nozzle configurations and holes for the remaining descaled samples as shown in Figure 5.14B. Increasing the injection pressure to 10MPa, skyrocketed the average scale removal value to 30.1, 27.4 & 25.4%, which completely break all the scale samples across all the header and nozzle configuration as shown in Figure 5.14C. Still obvious, that NCN configuration is 1.6, 16 & 3.3% more effective than CN & CNO respectively in removing soft hollow shape scale deposits. Although, the improvement is more attributed to the additional compressive stress that aid cyclin stress, and other jetting mechanism.

The descaling of soft hollow scale samples in compressed conditions with 5nozzles using the NC-arrangement shows a better improvement in terms of mass of scale removed than that removed with 5 nozzles at ambient condition even at high injection pressure. Five nozzles at low

pressure of 4.8 MPa initially removed 2.8g of scale that was slightly improved by 2.5 g and subsequently 65.6g with corresponding increase of injection pressure to 6.0 MPa and later 10 MPa. This was almost fifty times increased attributed to the wide pressure variation between 10 MPa injection pressure and that of 4.8 & 6.0 MPa. The 4nozzle configuration started by removing substantial amount of scale (9.3g) at 4.8 MPa injection pressures that was a bite raised by 5.6g after increasing to 6.0 MPa and increasing the injection pressure to 10 MPa resulted to a massive growth of descaling rate by 141.g. Whereas, the 3nozzle configuration was able to highly increase the initial removal at low pressure of 4.8 MPa to 89.1g that was increased by 119.1g and doubled by 201.4g due to the increase of injection pressure to 6.0 MPa and subsequently 10 MPa. Analysis of the impact of altering header configurations for corresponding injection pressure shows improvement in the amount of scale removed with reduction of number of nozzles in compressed descaling trials due to multiple nozzle pressure drop effect (Huang et al., 2018). Pumping water at low pressure of 4.8 MPa with five nozzles removed 2.8g of scale that substantially increase by 6.5g and skyrocketed by 86.3g after reducing the numbers of nozzles to 4 and later 3 configurations. Pictorially figure 5.14A displayed some holes across all the descaled samples at 4 & 3nozzle configurations experiments. While increasing the injection pressure to 6.0MPa with 5nozzles configuration initially removed 5.3g of scale that was improved by 9.6g and substantially more removed by 203g after adjusting the header configuration to 4nozzles and later 3nozzles. The pictures in Figure 5.14B demonstrated how most of the descaled samples are either holed drilled 5-4 header configuration and broken in the 3nozzle configuration. The results of the investigations of impact of altering the nozzles configurations at high pressure of 10 MPa yielded the highest and best scale removal result with the highest variation observed between three and four nozzles. Pumping at high pressure of 10 MPa with five nozzles resulted to the substantial removal of 68.4g of scale that was increased by 82g after reducing to four nozzles. This was further highly increased by 223.1g after subsequently reducing to three nozzles. Figure 5.14C pictorially marked all the header configuration trial with broken descaled samples.

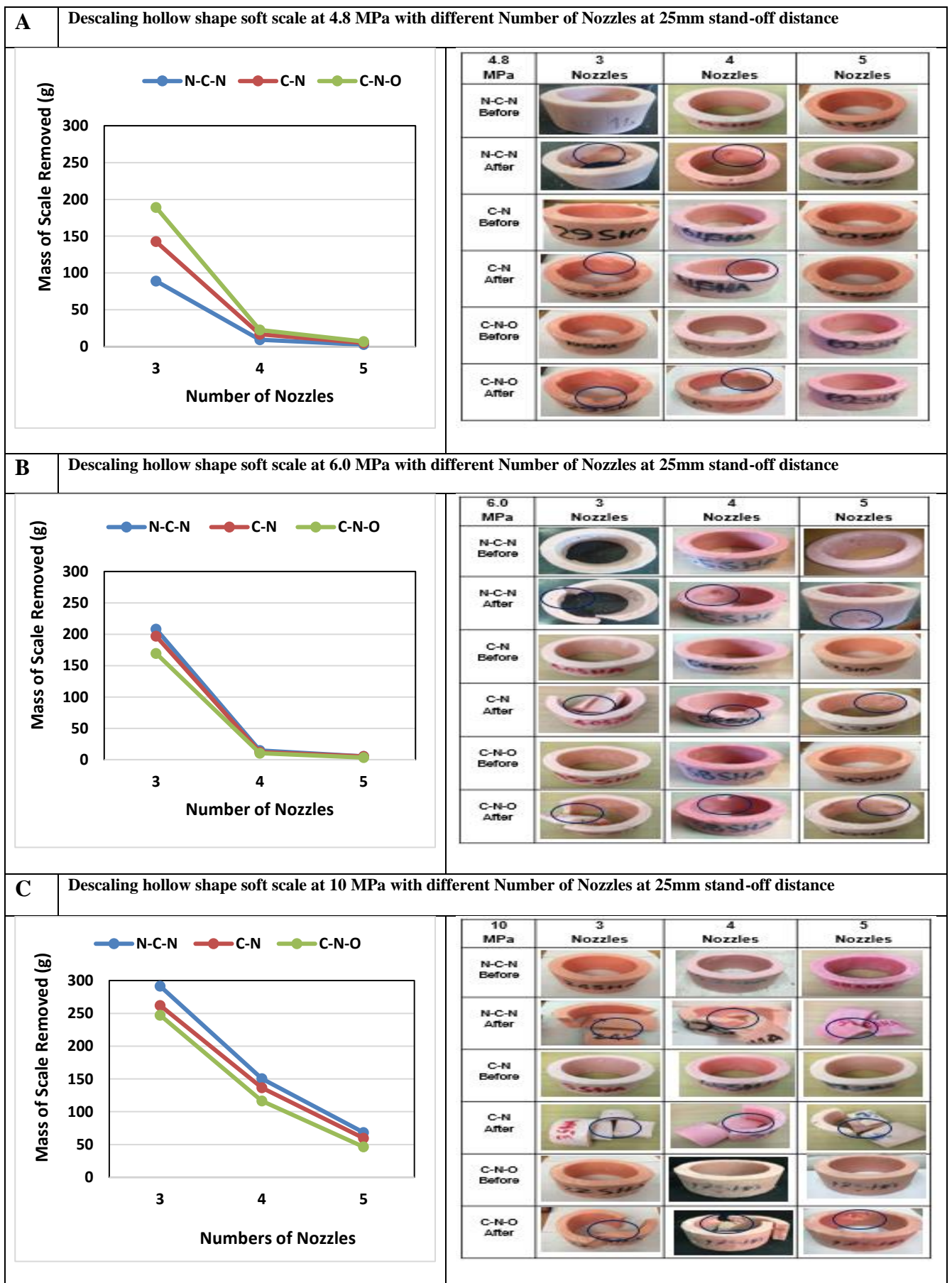


Figure 5.14: Compressed descaling results for hollow soft scale at 25mm-distance

### 5.3.2.2 Solid soft scale sample

The results from the simultaneous introduction of compressed air of 0.2 MPa and high-pressure water spray with other descales parameters during this experiment is summarised in Appendix C7 and it 25mm distance results in Figure 5.15. The experiment proves to achieve higher descaling rate than the ambient trials but with similar descaling trend. The additional compression on samples from the compressed air is a key reason for the additional scale removal over the ambient trial results. In addition to the erosion jetting mechanism during ambient condition, the extra compressive stress provided by the compression introduces cyclin stress and sample particle abrasion mechanism that further enhance the scale removal.

An average scale removal value of 0.8, 1.13 & 1.01% was achieved, that slightly increase to 1.4, 2.2 & 17% and further improved to 20, 25 & 21% across respective header and nozzles configuration after increasing the injection pressure from 4.8 MPa to 6.0Mpa and subsequently 10 MPa. Pictorially, holes were drilled across the entire CN arrangement and 4 & 3 nozzle configurations of 4.8 MPa operation as shown in Figure 5.15A which improved to scale breakage across the CN configurations and entire 4 & 3 nozzle configurations in Figure 5.15B of the 6 MPa operations. While figure 5.15C shows a complete scale deposit breakage across board for 10 MPa injection. The CN configuration was able to remove 0.33, 0.8 & 5% more scale deposit than the NCN configuration, and even drilled a hole with low pressure of 5nozzle CN configuration.

Descaling soft solid scale in compressed condition lead to the breakthrough of breaking solid scale samples at even lower injection pressures. Utilising 4.8 MPa with 5nozzles removed 2g that increase to 0.7g and much better by 57.7g, while with 4nozzles removed 4.8g and increase by 6.8 that skyrocketed by 128g due to subsequent adjustment of injection pressure to 6.0 and later 10 MPa. Varying the nozzle configuration to 3nozzle at 4.8 MPa increase the removal to 12.6g that was increased by 7.5g and highly improved by 217g as a result of trothing up the injection pressure by 1.2 MPa and subsequently 5.2 MPa.

Varying the header configurations from 5 to 4 & 3 nozzles configuration at 4.8 MPa removed 2g of scale that consequently increases by 2.8g and later 10.6g respectively with holes all crossed except for breakage at CN configuration of the 3nozzles trials in Figure. 5.15A. The 6.0 MPa injection operation visually drilled holes across 5nozzles configuration and broke all the sample of the 4 & 3 nozzles configuration as shown in Figure 5.15B started by removing 2.7g that increase to 8.9g and later 17.4g after adjusting the header nozzles from 5 to 4 and later 3nozzles configuration. High scale removal of 60g that increase by 73g and by 170g was achieved after reducing the number of nozzles of the 10 MPa 5nozzles operation to 4 and later 3-nozlls that visually break all the samples in the entire campaign as capture in Figure 5.15C.

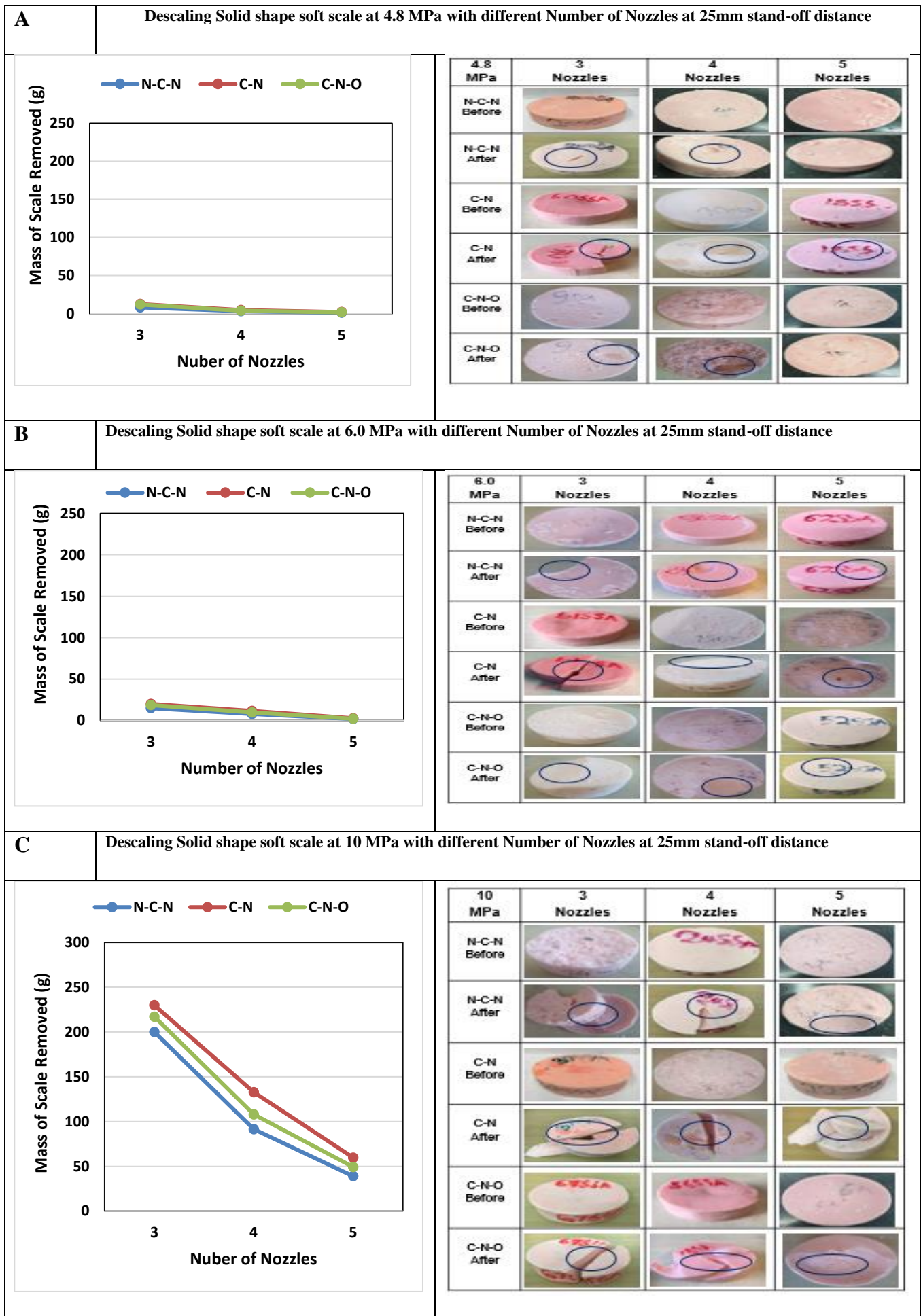


Figure 5.15: Compressed descaling results for hollow soft scale at 25mm-distance

### 5.3.2.3 Strontium sulphate scale sample (SrSO<sub>4</sub>)

As earlier mentioned, the subjection of SrSO<sub>4</sub> scale samples to 0.2 MPa compressed descaling conditions and parameters makes a remarkable improvement in terms of amount of scale removed compared to the ambient trials result. The amount of SrSO<sub>4</sub> removed under compressed condition increase with increase in injection pressure and reduction in stand-off distance & numbers of nozzles and better with CN nozzle arrangement. Details of the entire strontium sulphite compressed descaling results can be found in Appendix C8 and 25mm stand-off distance results are graphically presented in Figure 5.16

Pumping at low pressure of 4.8 MPa while compressing the chamber with 0.2 MPa averagely removed 0.29, 0.36 & 0.32% of SrSO<sub>4</sub> deposit across the NCN, CN & CNO arrangements of 5,4 & 3 nozzles configurations respectively as shown in Figure 5.16A. While increasing the injection pressure to 6 MPa under the same descaling condition removes 0.37, 0.46 & 0.41% of scale deposit respectively as shown in Figure 5.16B. Subsequent increase of the injection pressure to 10 MPa tripled the values to 1.01, 1.14 & 1.08% respectively, which was only able to break the samples at CN & CNO configuration of the 4 nozzles and the entire 3 nozzle configurations as presented in Figure 5.16C. Making the CN configuration better by 0.09, 0.09 & 0.13% than the other nozzle arrangements.

The compressed descaling of SrSO<sub>4</sub> deposit with 5 nozzles at low pressure of 4.8 MPa started by removing 1.2kg of scale that was increased by 0.4g and 2.9g after increasing to 6.0 MPa and 10 MP respectively. While 4nozzle removes 2g of scale that increasing the injection pressure to 6.0 and 10 MPa improved by 0.5g and 3.9g respectively. The case of 5 nozzles at 10 MPa injection removed better (2.7g of scale) that increase by 0.7 and by three times (5.7g) due to the injection pressure increment to 6.0 and 10 MPa respectively.

The 5nozzle compressed approach started by removing 1.3 g of SrSO<sub>4</sub> at low pressure of 4.8 MPa that increase by 0.8g and 1.5g due to the subsequent adjustment of header configuration to 4 & 3nozzles respectively that pictorial uniformly erode across the Figure 5.16A. Figure 5.16B still suggested uniform erosion all across after initially removing 1.6g of scale that improved by 0.9g and 1.8g due to the consequential adjustment of 5nozzle header configurations to 4 and later 3nozzles at 6 MPa injection pressure. Finally, Figure 5.16C captured how the 10 MPa operation with 5nozzles that was only able to uniformly erode the samples, while 4 & 5 nozzles configuration were able to break the samples. Were an initial removal 2.7g of SrSO<sub>4</sub> deposit was recorded and later improved by 0.7g and 5.7g due to altering the header configurations to 4nozzles and 3nozzles respectively.

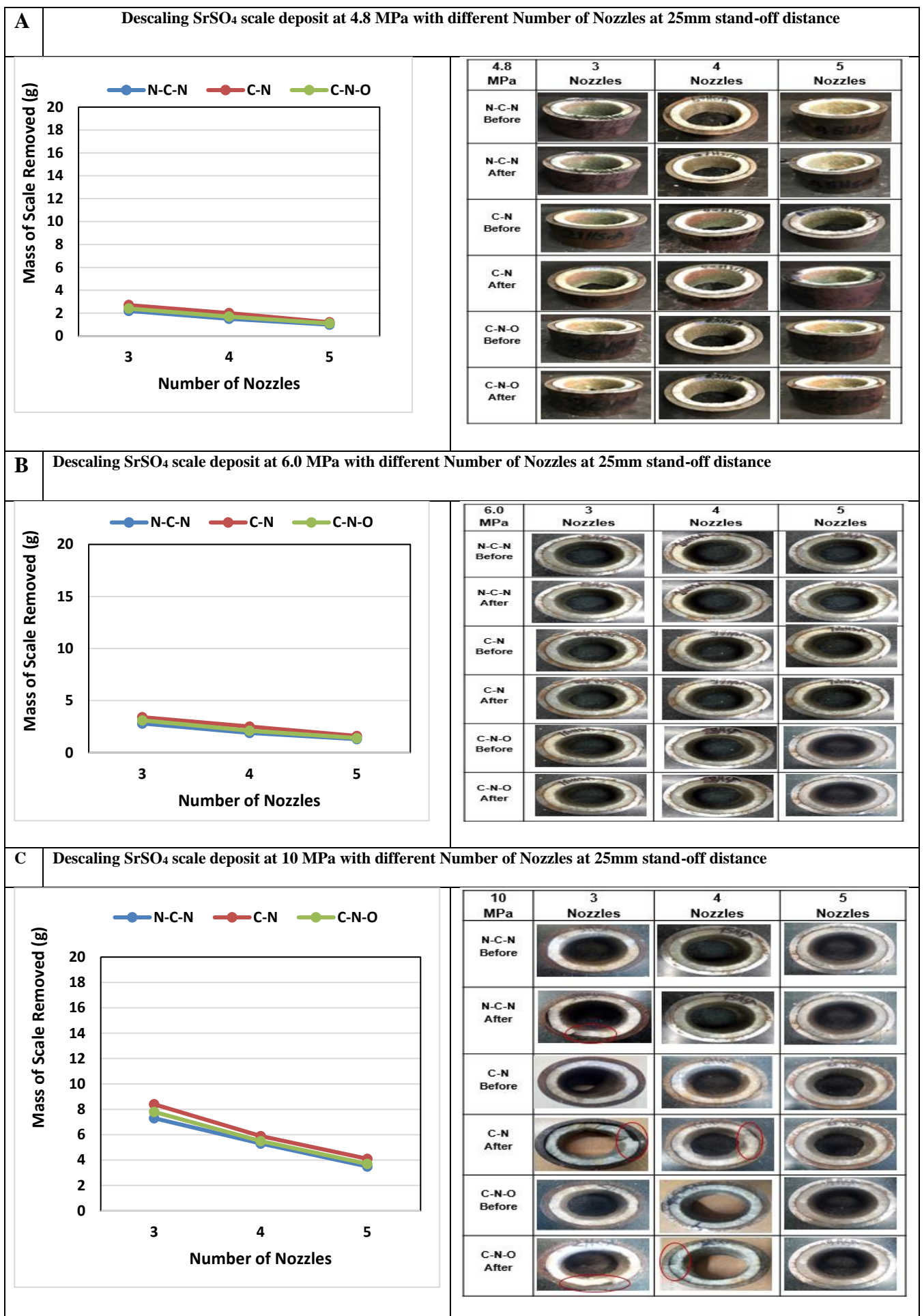


**Figure 5.16:** Compressed descaling results for SrSO<sub>4</sub> scale deposit at 25mm-distance

#### 5.3.2.4 Calcium carbonate scale sample (CaCO<sub>3</sub>)

The result from the calcium carbonate compressed descaling campaign was not as impressive as that of strontium sulphate due to their difference in hardness and materials composition. In addition to the poor spray jet and target contact constraint experience in the entire hard scale removal trials. Although its removal rate was less compared to that of strontium sulphate under compressed condition but it's better than removing CaCO<sub>3</sub> in ambient condition. Appendix C9 have presented the detailed results of removing calcium carbonate in compressed conditions and Figure 5.17 present the 25mm-distance results of the experiments. An average value of 0.22, 0.31 & 0.25% of CaCO<sub>3</sub> was removed with 4.8 MPa injection pressure across the respective header & nozzle configurations, that slightly increases to 0.32, 0.39 & 0.35% after increasing the injection pressure to 6.0 MPa, as shown in Figure 5.17A&B respectively. The value significantly increased to 0.86, 1.0 & 0.92% respectively due to further increasing the injection pressure to 10 MPa as graphically elaborates its ability to break the sample with the centre nozzle configuration (CN) of 3nozzles as shown in figure 5.17C. In this case CN configuration is 0.09, 0.07 & 0.14% more effective than the rest and is the only configuration that break the deposit even at 10 MPa with 3nozzle as shown in Figure 5.22C

Descaling CaCO<sub>3</sub> in compressed condition with 5nozzles at 4.8 MPa injection pressure considerably removed 0.9g that was increased by 0.5g and by 2.7g after increasing the injection pressure to 6.0 MPa and 10 MP respectively. A reasonable removal of 1.6g was observed with 4nozzles at 4.8 MPa injection that after increasing to 6.0 & 10 MPa improved by 0.6g and by 4.1g respectively. While the low-pressure (4.8 MPa) trials of 3nozzles configuration removed a substantial amount of 2.1g of CaCO<sub>3</sub> that improved by 0.7g and subsequently by 5g due to pressure increment to 6.0 and 10 MPa respectively.

Analysing the impact of adjusting header configuration at low pressure of 4.8 MPa removes 0.9g of CaCO<sub>3</sub> that as a result of subsequent adjustment of the header configuration to 4 and 3nozzles improved by 0.7g and by 1.2g respectively. This could picture wise in Figure 5.17A only prove uniform erosion across the entire trials. Increasing the injection pressure to 6.0 MPa with 5nozzle removes 1.6g of scale that improved by 0.6g and later 4.1g due to subsequent reduction of number of nozzles to 4 and the 3nozzles. Even though with increase in quantitative results compared to A part of the figure, the B part (qualitative) could not demonstrate better than uniform erosion too. While the high-pressure trial (10 MP) with 5 nozzles result was impressive compared to the rest by removing 2.1g that increase by 0.7 and 5g after respective nozzle adjustment, which qualitative concurs by breaking one samples at the C-N configuration of 3 nozzle header arrangement as shown in Figure 5.17C.

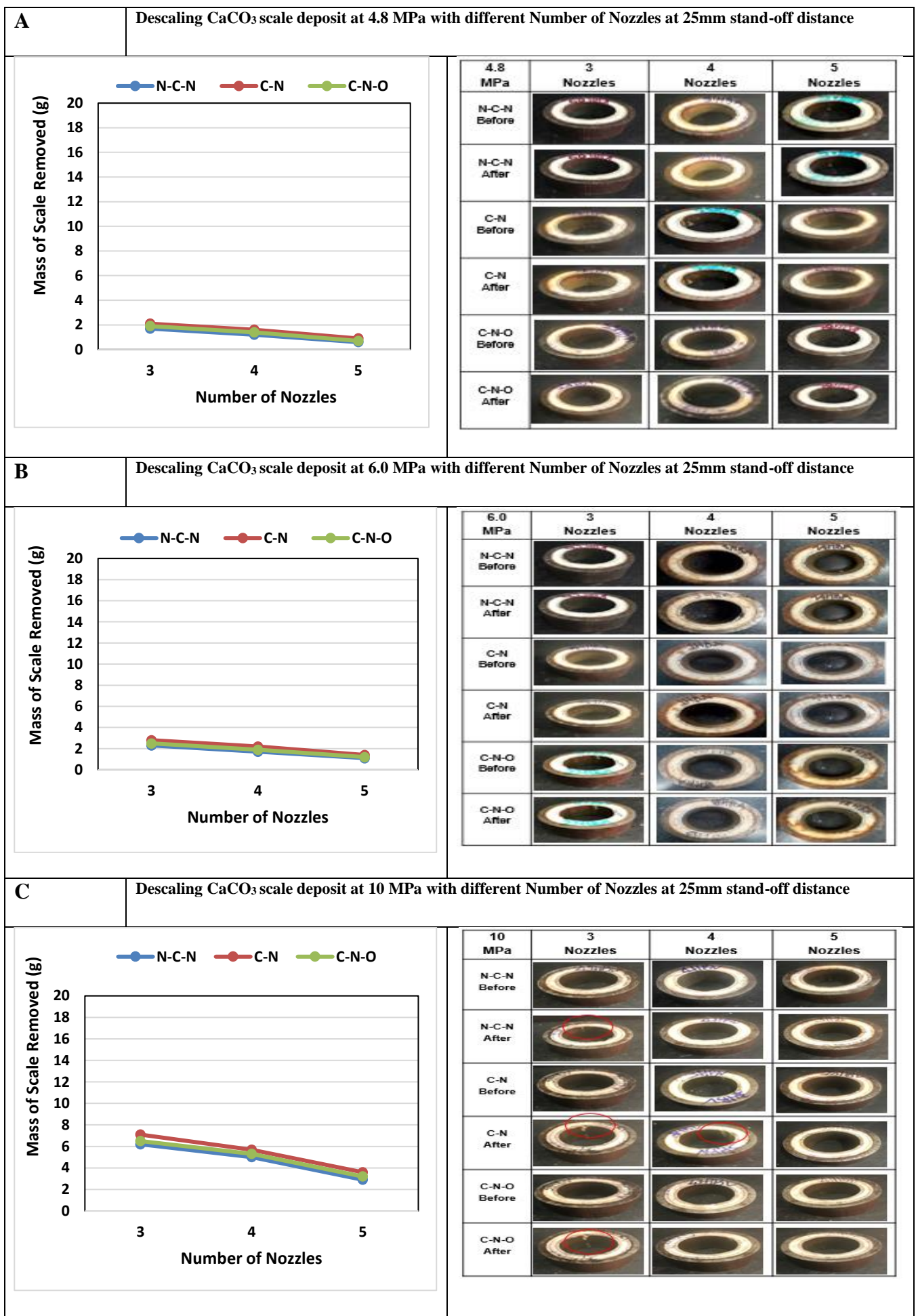


Figure 5.17: Compressed descaling results for  $\text{CaCO}_3$  scale at deposit 25mm-distance

### 5.3.3 Vacuum descaling trials

The vacuumed air descaling experiments are conducted inside the special assembled chamber but in a suctioned air chamber condition (-0.08MPa) for the removal of all the four scale samples. As explained in the descaling methodology section that suctioned air of -0.08MPa was introduced and maintained while simultaneously pumping water at different injection pressure and other descaling parameters to remove different scale sample. With the aim of utilising the introduce negative air chamber pressure to enhance rate of scale removal via aiding some of the jetting mechanisms.

#### 5.3.3.1 Hollow soft scale samples

The hollow shape soft scale descaled in a suctioned chamber air conditions as summarised in Appendix C10 and its 25mm-distance result in Figure 5.23 proves to have attained better scale removal than both ambient and compressed trials but with similar descaling trend. The trend that attached the increase in amount of scale remove to increase in injection pressure and decrease in both number of nozzle & stand-off distance and better off with non-centre nozzle (NCN) arrangement. The introduced suction air into the chamber using the vacuum pump to remove the samples is a key reason for the additional scale removal over both ambient and compressed trial results. Additionally, the introduced vacuum pressure enhances both erosion, cyclin stress, sample particle abrasion mechanism and hoop stress.

A significant amount of 6.34, 4.11 & 3.33% of the samples were averagely removed with 4.8 MPa injection pressure at respective header and nozzles configuration that was able to drill holes across the entire 4nozzles configuration and breaks all the 3nozzles configurations samples as captured in Figure 5.23A. A better value of 13.9, 12.4 & 10.9% was attained after increasing the injection pressure to 6 MPa and pictorially improved the removal by drilling throughout the entire 5nozzle configuration and breaks the entire samples for the 4 & 3nozzle configurations as captured in Figure 5.23B. While Figure 5.23C demonstrate the highest removal value of 31.7, 28.1 & 25.11% of paraffin deposit after increasing the injection pressure to 10 MPa that breaks all samples during the 10 MPa vacuumed descaling campaign. The NCN configuration removes 2.23, 1.5, & 3% more scale deposit than the rest across all descaling permutation and combination coupled with the hoop stress been aided by the introduced vacuum pressure.

The set of result obtained from the descaling experiment of soft hollow scale samples in vacuumed conditions with all the header configurations, particularly NCN-configuration's remove the highest amount of scale even at lower injection pressure compared the other two chamber condition experiments. The five-nozzle configuration vacuumed descaling experiment was able remove 3.4g of paraffin at low injection pressure that improves by 2.6g and much more by 66.6g at medium and high injection pressure respectively. Reducing the number of nozzles to 4 nozzles at lower pressure (4.8 MPa) improve the removal to 10g that was later improved by 5.7g and by fifteen time (142.5g)

due to subsequent increase of the injection pressures to 6.0 and 10 MPa respectively. Further reduction of the header configuration to 3 nozzles at 4.8 MPa injection produces the highest initial paraffin removal of 90g that was later improved by 11.9g and by fivefold (204.3g) after rising the injection pressure to 6.0 and later 10 MPa respectively.

Also, the best set of quantitative and qualitative result of hollow paraffin removal regarding the impact of altering header configurations for corresponding injection pressure was attained in the vacuumed descaling trials that is presented in the Figure 5.23 bellow. Starting by injecting water at low pressure of 4.8 MPa with five nozzles initially removed 3.4g of paraffin that significantly increase by 6.6g and shoot up by 86.3g after altering the header configuration to 4 and subsequently 3 nozzles configurations. Figure 5.23A exhibited holes being drilled across all the descaled samples at 4nozzle and subsequent scale breakage for the entire 3nozzle configurations trials. Subsequent increase of the injection pressure to 6.0 MPa with 5 nozzles configuration increase the initial paraffin removal to 6g that was boosted by 9.6g and skyrocketed by 203.3g as a result of altering the header configuration to 4 nozzles and subsequently 3 nozzles. Better qualitative descaled result that drilled holes across 5 nozzles configurations and complete scale breakage across both 4 & 3 nozzles configuration is exhibited in Figure 5.23B. The further increment of injection pressure to 10 MPa with five nozzles configuration that generated a high removal of 70g of paraffin and later substantially improved by 83g and much more by 225g was the consequences of varying the header configuration to 4 & 3 nozzles respectively. Figure 5.23C showcase the best and breakthrough qualitative results of removing paraffin that breaks all the samples across all header and nozzle configurations.

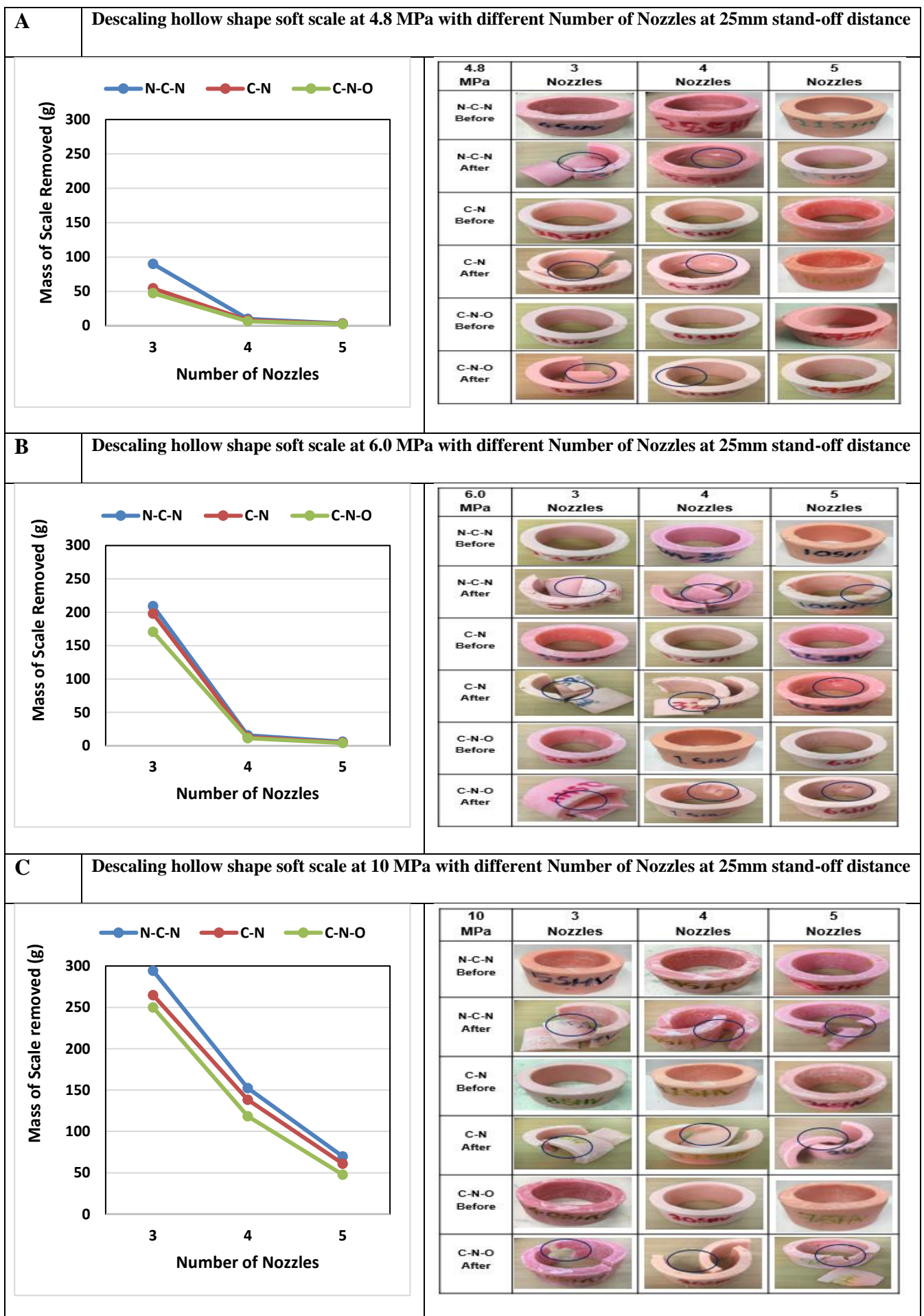


**Figure 5.18:** Vacuumed descaling results for hollow soft scale at 25mm-distance

### 5.3.3.2 Solid soft scale sample

The simultaneous introduction of suctioned air of -0.08MPa and high-pressure water together with other descales parameters during the entire (3) three-minute descaling session of solid shape soft scale samples is summarised in Appendix C11 and its 25mm distance results in Figure 5.19. The introduction of suctioned air into the chamber while utilising the remaining descaling parameter is a vital reason for the additional scale removal compared to ambient experiment even though less than the compressed experimental results. Also, the increase in scale removal that increase in injection pressure and decrease of stand-off distance & number of nozzles was due to the better contact between the introduce centre nozzle orientation and the solid scale sample, making the CN & CNO to be more effective than NCN arrangement.

An average scale removal of 0.44, 0.70 & 0.62% were initially realised with 4.8 MPa injection pressure across the respective header and nozzle configurations that was able to drill hole across the entire 4 nozzle configuration and break the 3nozzles configurations as in Figure 5.19A. The 6.0 MPa descaled pictures drilled holes across the 5nozzle configuration and scale breakage for both 4 & 5 nozzles configurations that double the average removal to 1.48, 1.91 & 1.71% as shown in figure 5.19B. While Figure 5.19C showcase how the entire descaled sample were broken across the entire nozzle/header configuration during the 10 MPa injection, even thou still more effective with CN-configurations, it increases the average scale removal to many folds of 17.7, 21.7 & 20.3% respectively. Also, an average scale removal difference of 0.26, 0.43 & 4% was observed between the CN and the other configurations for the respective pressures.

The descaling results attained from the removal of solid scale samples in vacuumed conditions with all the header configurations, especially NC-configurations descaled more paraffin deposit than the other two chamber condition experiments. Thou still lower than the hollow vacuumed results at all injection pressure due to difference in thickness of the samples. The investigatory results from 5 nozzle configuration vacuumed descaling experiment initially removes 2.3g of paraffin that improves by 0.8g and much more by 58.4g at both 6.0 and 10 MPa injection pressure respectively. Adjusting the header configuration to four-nozzles at lower pressure (4.8 MPa) improve the initial removal amount to 5.4g that was boosted by 7g and better off by 129g as a result of the subsequently increasing the injection pressures to 6.0 and 10 MPa respectively. Further adjusting the header configuration to 3 nozzles at low pressure of 4.8 MPa removed substantial amount of paraffin (13.4g) that was improved by 7.8g and skyrocketed by 218g due to the effect of rising the injection pressure to 6.0 and subsequently 10 MPa respectively.

In terms of investigating the effect of injection pressure and header configuration when removing hollow shape paraffin samples, vacuumed descaling result was a breakthrough of the campaign with impressive qualitative and quantitative result presented in the Figure 5.19. The experimental results of utilising low pumping pressure of 4.8 MPa with five nozzles started by removing 2.3g of paraffin

that improved by 3.1 and more significantly by 11.2g due to the subsequent alteration of the header configurations to 4 and 3 nozzles configurations respectively. Figure 5.19A unveiled how holes were drilled across all the descaled samples at 4 nozzle and all the scale entire 3 nozzle configurations samples were shattered. Throttling the injection pressure to 6.0MPa with 5 nozzles configuration rise the initial paraffin removal amounts to 3.1g that was furthered by 9.3g and by 18.1g because of the header configuration alteration to 4 nozzles and 3 nozzles respectively. Improved qualitative descaled result that drilled holes across 5-nozzles configurations and complete scale breakage across both 4 & 3 nozzles configuration is displayed in Figure 5.19B. Finally, trothing the injection pressure further to 10 MPa with five nozzles configuration produced an impressive paraffin removal result of 61g that doubled by 74g and boosted by 171g from the consequences of header configuration alteration to 4 and subsequently 3 nozzles. Figure 2.19C displayed a breakthrough qualitative results of removing solid shape paraffin that breaks all the samples across all header and nozzle configurations.

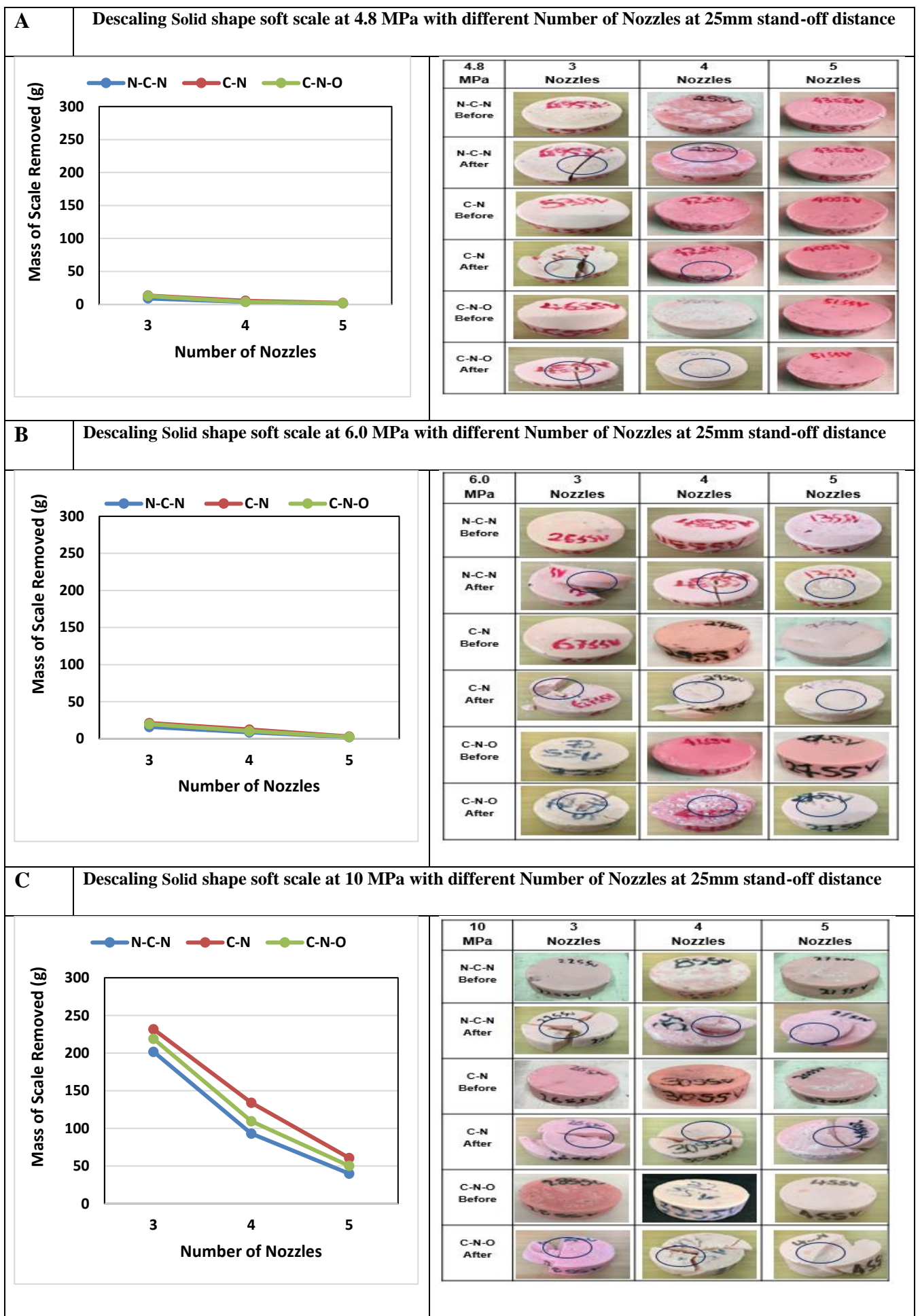


Figure 5.19: Vacuumed descaling results for solid soft scale at 25mm-distance

### 5.3.3.3 Strontium sulphate scale sample (SrSO<sub>4</sub>)

The result from the strontium sulphide vacuumed descaling experiment as presented in Appendix C12 and it 25mm distance results in figure 5.20 was not as impressive as that of solid shape soft scale. This is due to their difference in hardness and materials composition in addition to the poor spray jet and target contact constraint experience in the entire hard scale removal trials. Although its removal was still better compared to that calcium carbonate and Strontium sulphide under ambient condition but less than the result achieved from it compressed operations.

An average removal of 0.25, 0.31, & 0.28% of scale was initially observed when pumping at 4.8 MPa across the respective header and nozzles configuration that couldn't break any sample during the operation as shown in Figure 5.20A. A better value of 0.31, 0.41, & 0.36% were attained after increasing the injection pressure to 6.0 MPa, which was only able to break the deposit with CN arrangement of the 3nozzle configuration. Also, a better removal of 2.69, 3.1 & 2.85% was attained after increasing the injection pressure to 10 MPa that improve by breaking some samples with CN arrangement of 4 nozzle configuration and the entire 3 Nozzles configuration as shown in Figure 5.20C. The CN configuration was 0.06, 0.16 & 0.41% better than NCN at respective pressures.

Descaling SrSO<sub>4</sub> at low pressure of 4.8 MPa with 5 nozzles in a vacuumed condition reasonable removed 1g of SrSO<sub>4</sub> deposit that improved by 0.4g and by 2.8g after adjusting the injection pressure to 6.0 and later 10 MPa respectively. Reducing the number of nozzles to 4nozzles and descaling at same 4.8 MPa improved the removal to 1.8g that further improved by 0.5g and 3.9g due to the subsequent increase in injection pressure to 6.0 and 10 MPa. Further reduction of the header configuration to 3 nozzles and descaling at 4.8 MPa that was subsequently increased to 6.0 and 10 MPa removed 2.5g of SrSO<sub>4</sub> that subsequently improved by 0.8g and 5.6g respectively.

Analysing the impact of adjusting header configuration from 5 nozzles to 4 nozzles and subsequently 3 nozzles at low pressure of 4.8 MPa removed 1g of SrSO<sub>4</sub> that improved by 0.8g and almost doubled by 1.5g respectively. This was only able to graphically uniformly erode all the samples in Figure 5.20A. While utilising the medium pressure of 6.0 MPa and adjusting the header configuration to respective configuration was only able to break the sample at CN configuration of the 3 nozzle trials as in Figure 5.20B. Leading to the initial removal 1.4g of scale that was subsequently improved by 0.9 and by 1.9g respectively. Finally, the result of adjusting the header configuration at 10 MPa initially removed 3.8g that improves by 1.9g and 4.3g due to respective header adjustment that could break the samples at CN configuration of 4 nozzles and the entire 3 nozzles trials as in Figure 5.20C.

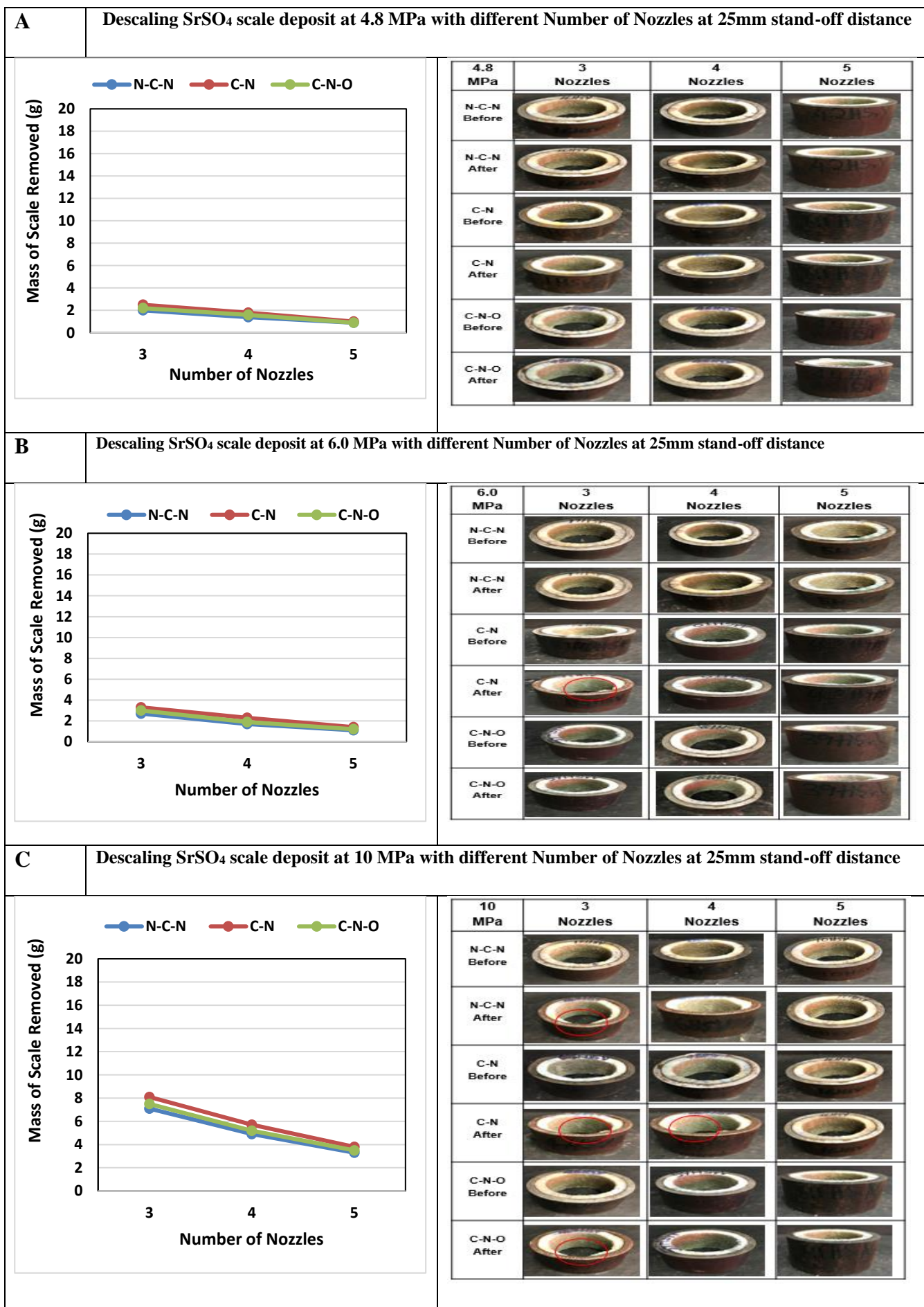


Figure 5.20: Vacuumed descaling results SrSO<sub>4</sub> scale deposit at 25mm-distance

### 5.3.3.4 Calcium carbonate scale sample (CaCO<sub>3</sub>)

Subjection of CaCO<sub>3</sub> scale samples to -0.08 MPa vacuumed descaling conditions and parameters makes a remarkable improvement in terms of amount of scale removed compared to the ambient result but less than the compressed results. The amount of CaCO<sub>3</sub> removed under this condition increase with increase in injection pressure and reduction in stand-off distance & numbers of nozzles and better with CN nozzle arrangement. Details of the entire calcium carbonate vacuumed descaling results can be found in Appendix C13 and the 25mm stand-off distance results are graphically presented in Figure 5.21.

An average removal values of 0.18, 0.24 & 0.21% was initially achieved when injecting at 4.8 MPa for the respective header and nozzle configuration that increase to 0.27, 0.34 & 0.3% after injecting further to 6.0 MPa that was not able to break any sample as shown in Figure 5.21 A&B respectively. The average removal value increases to 0.73, 0.89 & 0.8% after rising the injection to 10 MPa, which was able to mildly break the samples at the CN nozzle arrangement of the 4 nozzles and the entire 3 nozzles configuration as shown in Figure 5.21C. An average difference in removal of 0.06, 0.07 & 0.16% across the respective injection pressure was observed between CN and NCN configurations.

Analyses of the impact of low pressure of 4.8 MPa with 5nozzle configurations during the vacuumed descaling of CaCO<sub>3</sub> initially removed 0.7g that improved by 0.4g and 2.5 g after adjusting the injection to 6.0 MP and 10MPa respectively. Subsequently, the utilization of 4 nozzle configuration at low pressure increase the initial removal to 1.4g that improved by 0.5g and by 3.4g after rising the injection pressure to 6.0 and 10 MPa. Meanwhile, the 3nozzle configuration did better by substantially removing 3.2g of scale that improved by 1.6g and later 3.5g as a result of increasing the injection pressure to 6.0 and 10 MPa respectively.

The vacuumed descaling results of 5nozzles at low pressure of 4.8 MPa removed 0.7g that doubled by 7.0g and furthered by 1.2g as result of reducing the nozzles configuration to 4 nozzles and subsequently 3-nozzles. Figure 5.21A was only able to graphically show better erosion across all trials. While increasing the injection pressure to 6.0 MPa with 5 nozzles boost the removal amount to 1.1g and improved it by 0.8g and later 1.6g because of header nozzles reduction to 4 and 3 nozzles respectively. Like the A part of the Figure 5.21, Figure 2.21B could only exhibit uniform weathering all along. Further increment of injection pressure to 10MPa was able to further increase the scale removal to 3.2g that improved by 1.6g and later 3.5g as a result of adjusting the header configuration to 4 nozzle and 3 nozzles respectively. Figure 2.21C was only able to break the samples with CN arrangement of the 4nozzle configuration and the entire configuration of the 3nozzle operation.

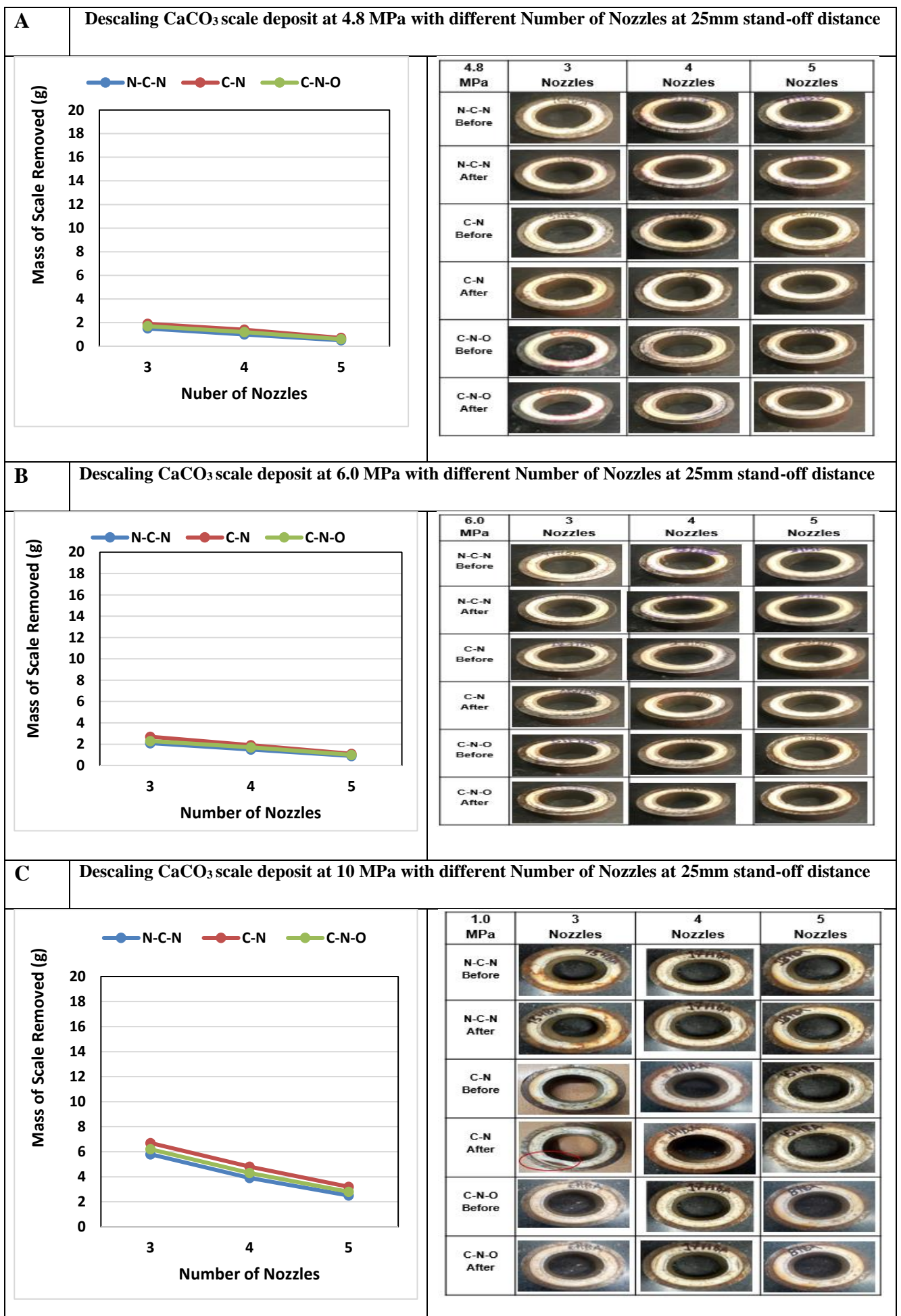


**Figure 5.21:** Vacuumed descaling results for  $\text{CaCO}_3$  scale deposits at 25mm-distance

### **5.3.4 Chamber pressure comparison**

Perhaps the descaling results of respective scale samples in all the chamber pressure were generally impressive, though attached to relationship of the shape of the scale in question to the utilisation of chamber pressure as analysed in Section 5.3. Although, the experimental results from the entire ambient experiment were constantly found to generate the least result in respect of the shape of the scale, compared to the performance of the other two chamber condition results that were relatively dependent on the shape of the descaled samples. The removal of soft hollow shape scale that concurs to the thin-walled hoops stress conditions was slightly more impressive under the (-0.08MPa) vacuum pressure than compressed and far better than ambient condition as shown in equation 5.4. The introduction of 0.2MPa of compressed air into the chamber aided the cyclic stress removal mechanism of the soft solid shape deposit and the entire hard scale samples due to additional fatigue from the compression (Qin et al., 2006), descaling better than the other chamber condition. While the removal of entire hard scale samples, despite being hollow in shape, was better with compressed condition than vacuum due to their ability to only satisfy the thick-walled conditions of the hoops stress mechanism as shown in equation 5.3. Even though, the utilisation of chamber air concentrations was having more direct impact on the scale sample, it affects the performance of the spray jet too. Since, in respect of scale type, the impact of varying chamber concentration against amount of scale removed during the entire descaling experiment tends to be more noticeable at medium and high pressure (6.0 & 10 MPa) operations and lower header configuration (3nozzle). Notwithstanding, choice of nozzle configuration plays a big role in the amount of scale removed when varying the chamber air concentration. At ambient chamber air concentration, both the jet strength and all the jetting mechanisms are not altered, while the introduction of the 0.2MPa compressed air suppressed the kinetic energy of the jet but aided both the cyclic stress and particle abrasion on the samples. Whereas, suctioning the chamber pressure by -0.008MPa increases the kinetic energy of the jet and enhances the hoops stress mechanisms on the samples as shown in equation 5.2. The following sections digest the effect of varying chamber air concentration when removing each type of scale samples at their best nozzle arrangement with different injection pressure and header configurations. In addition to given due consideration to effects of the various chamber pressures toward the respective jetting mechanisms that contributed in removing each type of scale.

#### **5.3.4.1 Hollow soft scale samples**

The results from the investigations of impact of varying chamber air concentration to remove soft hollow shape sample (paraffin) at different injection pressure and header configuration for NCN nozzle configuration is presented in figure 5.27. The effect of hoops stress tends to play a vital role in breaking the hollow samples across all the chamber pressures. Importantly, the effect of hoop

stress mechanism aids the ambient hollow scale removal that provide a high removal result that is close to the values of compressed and vacuumed conditions.

$$\frac{Pr}{t} = \tau_{hoops} \quad (5.1)$$

Were P being internal resultant pressure (chamber pressure+ jet pressure), r, is the radius of the hollow sample and t is its thickness. Considering the 10MPa injection pressure, the internal resultant pressure for vacuum is (10+0.0101352+0.008) MPa, ambient is (10+ 0.101325) MPa, while compressed is (10+0.0101352-0.2) MPa. Henceforth, Vacuum=10.021MPa, Ambient=10.101MPa and C<sub>compressed</sub>=9.901MPa. Contrary to eqq.5.2., compressed descaling results slightly lagged vacuum and better than ambient because 0.2 MPa compressed air introduction was able to impressively aid the cyclin stress mechanism that significantly improved removal by propagating the natural fissure and cracks of the sample.

$$\tau_{hOOPS\ Vac} > \tau_{hOOPS\ Amb} > \tau_{hOOPS\ Comp} \quad (5.2)$$

The result of analysing the effect of varying chamber pressure when descaling hollow scale sample at 4.8 MPa with the CN header configurations is presented in Figure 5.22A. Where 5nozzles configuration initially removes 1.7 g of paraffin at ambient pressure, which improved by 1.1 g and by 1.7 g due to altering the chamber pressure to compressed and later suctioned respectively. Similarly, corresponding value increase from 6.2 g and by 3.1 g & 3.8 g was recorded at respective chamber pressure of 4nozzles operations, while the 3nozzles removes 42.8 g at ambient and improved by 46.3 g and 4.7.2 g as a result of altering to compressed and vacuum respectively. The 6.0 MPa ambient operation presented in Figure 5.22D removes 2.9g of paraffin with 5nozzles that improves by 2.4 and 3.1 due to respective chamber alterations, while 4nozzle ambient removes 10g that improves by 4.9g and 5.7g respectively. Significant removal impact due chamber alteration can be seen in the 3nozzle operation that remove 93.7g at ambient and increase by 114.5g and 1.15.6g due to chamber alteration to compressed and later vacuum conditions. Figure 5.22G recorded an impressive initial removal at 10 MPa, 5nozzle ambient operation of 58.3g of paraffin that improved by 10g and 12g due to perspective chamber alterations and more impressive at 4nozzle operation were the ambient removal of 77g of paraffin was doubled (74g and 76g respectively) as a result of respective chamber alteration. While the respective chamber alterations with 3nozzles remove 253.g at ambient that was improved by 38g and 41g of scale removal.

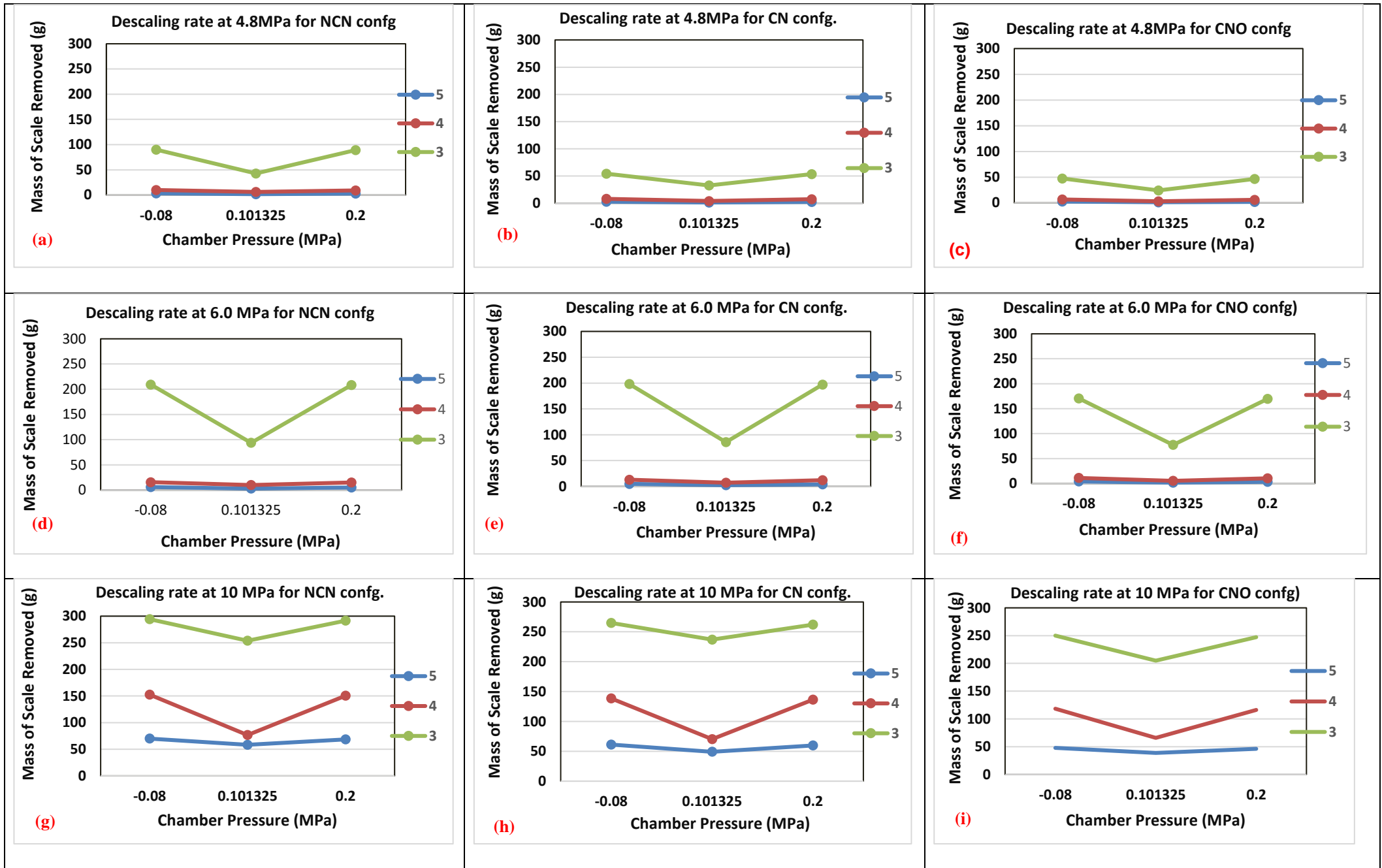


Figure 5.22: Chamber pressure impact comprising for descaling hollow soft scale at 25mm-distance

### 5.3.4.2 Solid soft scale sample

Results of the investigation of impact of varying chamber air concentration when descaling solid shape paraffin scale at different injection pressure and header & nozzles configurations can be found in Figure 5.23. Singling the CN nozzles arrangement result for analyse due to their better performance demonstrated a trend. Contrary to hollow removal, were the compressed condition removed better than all the chamber condition due to the direct impact of the introduced 0.2 MPa compressed air over the entire deposit surface that propagate the natural fissure and cracks of the sample through cyclin stress mechanism. Vacuum condition was fairly lagging the compressed conditions and better than ambient as a result of having more resultant pressure as discussed in Sectioned 5.3.3.2.

Figure 5.23B graphically present the analysis of the investigation of the effect of varying chamber pressure to remove solid scale at 4.8 MPa with different number of nozzles in CN configuration. The 5nozzle operations remove 1.2g mass of paraffin that was qualitatively improved by 1.1g and 0.8g after altering the chamber pressure from ambient to compressed and later vacuumed pressure respectively. For the 4nozzle configuration, the ambient removal was 2.6g and improved by 2.8g and by 2.2g as result of compressing the chamber by 0.2 MPa and later suctioning it by -0.008MPa respectively. While in the case of 3nozzle configuration that recorded a better removal value of 5.2g ambient pressure improved by 8.2g and 7.4g as a result of respective alteration of the chamber conditions. The 6.0 MPa operation of CN configurations of the respective number of nozzles as presented in figure 5.23E shows how 5nozzle was able to remove 1.8g of paraffin at ambient condition that improved by 1.3g and 0.9g after introducing compressed air and suctioned respectively. Likewise, the 4nozzle operation at ambient condition removes 3.9g of paraffin that was improved by 8.5g and 7.7g due to the respective chamber air alterations. While the 3nozzles operations at ambient condition impressively removes 7.3g of scale that almost doubled (14g and 13g respectively) due to respective chamber alterations. The consecutive alteration of chamber pressure from ambient to compression and vacuum respectively, remarkably removes 32g of paraffin and significantly enhanced by 29g and 28g at the 10 MPa of the 5nozzles operations. While the 4nozzles increase the ambient removal to 51g that improved to 83g and 82g across respective chamber conditions. A high removal value of 104g was recorded for ambient removal of 3nozzles with significant improvement by 128g and 126g due to the respective chamber air alterations as in Figure 5.23H.

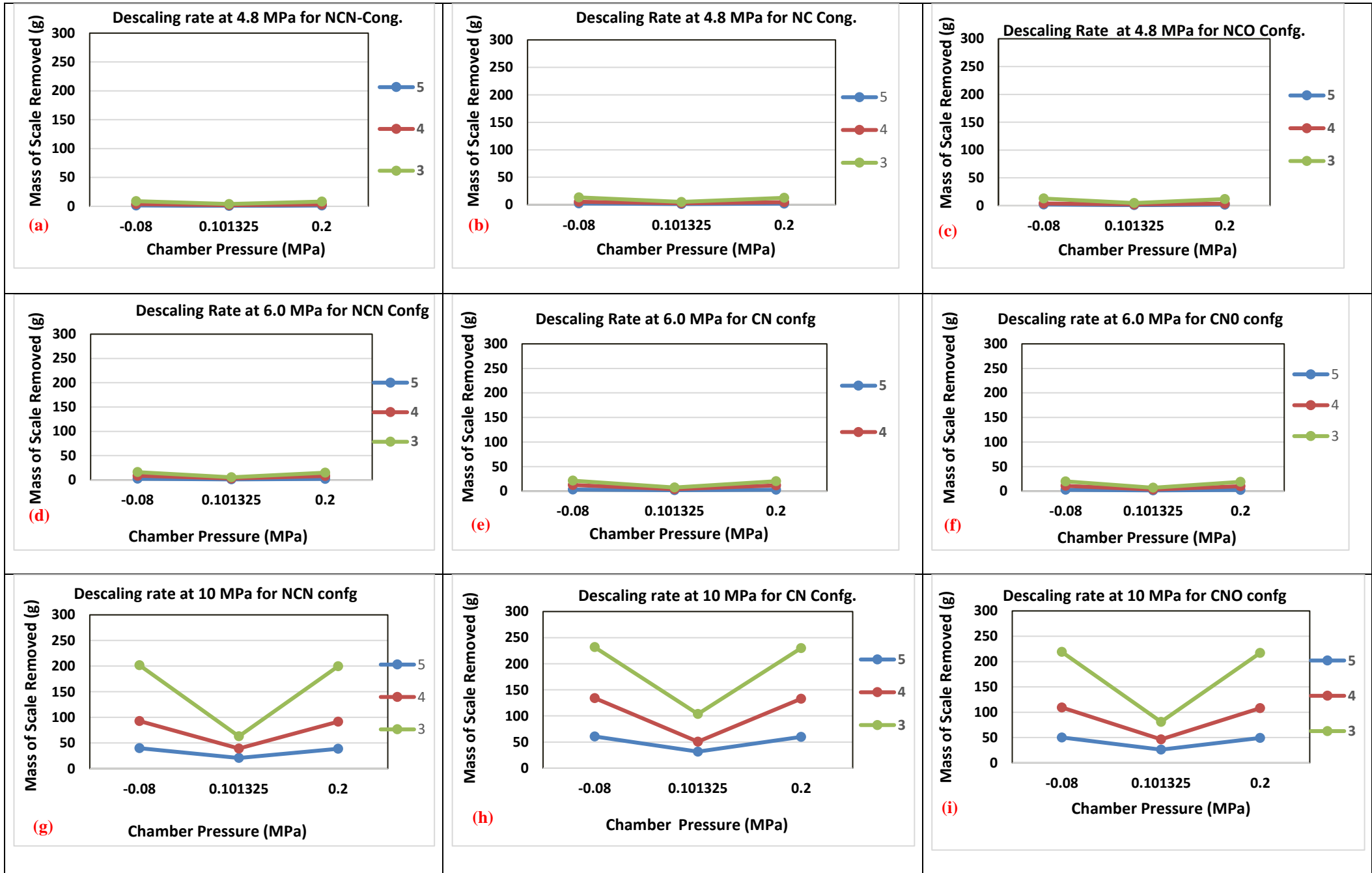


Figure 5.23: Chamber pressure impact comprising for descaling solid soft scale at 25mm-distance

### 5.3.4.3 Strontium sulphate scale sample (SrSO<sub>4</sub>)

The investigatory outcomes of altering chamber air concentration to enhance the removal of SrSO<sub>4</sub> at different injection pressures and header & nozzle configurations can be found in Figure 5.24. The outcomes were found to follow a trend which can be more affiliated to the soft solid scale, despite having a hollow type shape like the hollow soft scale. This can be attributed to the ability of the samples to only comply to thick walled hoops stress condition as shown in equation 5.3 which deny it from benefiting from hoops stress mechanism.

$$\frac{D}{t} > 20 \quad (5.3)$$

Were the diameter of the samples being 30mm and its thickness  $t$  is equal to 10mm; therefore, it has not satisfied the thin walled condition of hoops stress because  $\frac{D}{t} < 20$ . Section B, E & H of Figure 5.24 demonstrate the CN configuration results of varying chamber pressure to remove SrSO<sub>4</sub> with different header configurations at 4.8, 6.0 & 10 MPa injection pressure respectively. A value of 0.6g of SrSO<sub>4</sub> deposit was removed at 4.8 MPa ambient operation of 5nozzles configuration that doubled by 0.6g and 0.4g due to alteration of the chamber pressure to compressed and vacuum pressures respectively. Reducing the nozzle to 4nozzle increase the ambient removal to 1.3g that improved by 0.7g and 0.5g due to respective chamber pressure alterations. Better removal of 2g was achieved with the 3nozzles ambient operation which later improved by 0.7g and 0.5g as a result of respective chamber pressure alterations. The 6.0 MPa operations was impressive and started with removing 0.9g of SrSO<sub>4</sub> with the 5nozzles ambient operation that was improved by 0.7g & 0.5g after altering the chamber pressure to compressed and later vacuum condition. Similar with 4nozzles a 1.7g of SrSO<sub>4</sub> was removed at ambient and improved by 0.8g & 0.6g due to the respective chamber pressure alterations. More impressive ambient removal of 2.9g was achieved with 3nozzles and enhanced by 0.5g & 0.4g due to respective chamber pressure alterations. Finally, the result of altering chamber pressure by 0.2 MPa or -0.08MPa at 10 MPa impressively removes 3.2g for ambient condition that's better by 0.9g & 0.6g with 5nozzles. While with 4nozzles removes 5.1g that improves by 0.8g & 0.6g due to respective chamber alterations. A very impressive ambient removal result of 6.5g of SrSO<sub>4</sub> was achieved with the 3nozzles configurations that improved by 1.9g & 1.6g due to the introduction of 0.2MPa compressed air and suctioning of -0.008MPa pressure from the chamber respectively.

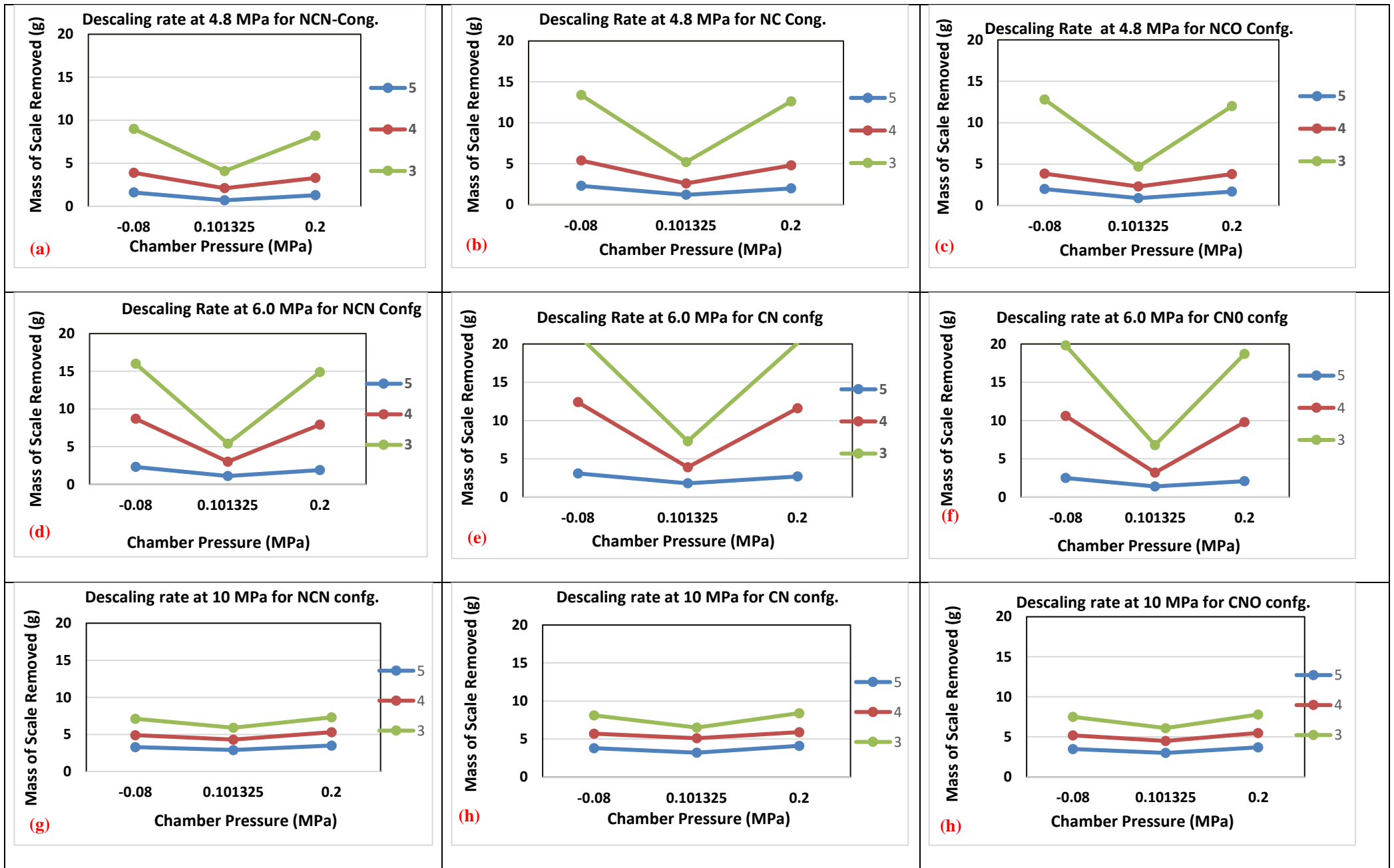


Figure 5.24: Chamber pressure impact comprising for descaling SrSO<sub>4</sub> scale deposit at 25mm-distance

#### 5.3.4.4 Calcium carbonate scale sample ( $\text{CaCO}_3$ )

The results of altering the chamber pressure when removing  $\text{CaCO}_3$  scale deposit at respective injection pressure and header/nozzles configurations was less impressive than the results obtained from the removal  $\text{SrSO}_4$  but shares a very similar removal trend. Although having similar shapes with  $\text{SrSO}_4$  that couldn't comply with the thin walled condition of hoop stress as expressed in equation 5.3 narrowing its removal prospects mechanisms to cyclin stress, erosion and particle abrasion mechanism.

The effect of removing  $\text{CaCO}_3$  deposit in ambient condition, in compressed air condition and vacuumed chamber condition at respective injection pressure and header & nozzles configuration is demonstrated in Figure 5.25.

Figure 5.25B demonstrated how the CN configuration of the 5 nozzles removed 0.4g of  $\text{CaCO}_3$  at 4.8 MPa injection in ambient condition, that was risen by 0.5g & 0.3g after the introduction of compressed air (0.2MPa) and suction the chamber (-0.08MPa). At 4.8 MPa injection with 4nozzle configurations removed 0.8g at ambient condition that as a result of altering the chamber pressure to compressed and subsequently vacuum condition improved by 0.8g and 0.6g respectively. While 3nozzle configuration at 4.8 MPa removed 1.5g at ambient condition and consequently improved by 0.6g and 0.4g after altering the respective chamber pressure. The effect of altering chamber pressure at 6.0 MP was more impressive as shown in Figure 5.25E, where the 5nozzle ambient operation removed 0.6g that better by 0.8g & 0.5g due to respective chamber pressure alteration. Its 4nozzle ambient operation was better to 1.1g that subsequently doubled by 1.1g due to chamber compression and 0.8g due to suctioning of the chamber. More removal was noted at the ambient operation of the 3nozzle configuration that removed 2g and improved it by 0.8g & 0.7g due to respective chamber alterations. The investigatory results of chamber pressure alteration at high pressure of 10 MPa for respective nozzle configurations was more noticeable than others as shown in Figure 5.25H. A case, where the 5nozzle ambient approach removed 1.8g of  $\text{CaCO}_3$  that improved by 1.8g and 1.4 due to respective chamber alteration, while the 2.9g ambient removal result of 4nozzles configuration was improved by 2.8g & 1.9g. Finally, 3nozzle configuration impressively removes 4.4g at ambient condition and the respective chamber pressure alteration improved it by 2.7g & 2.3g respectively.

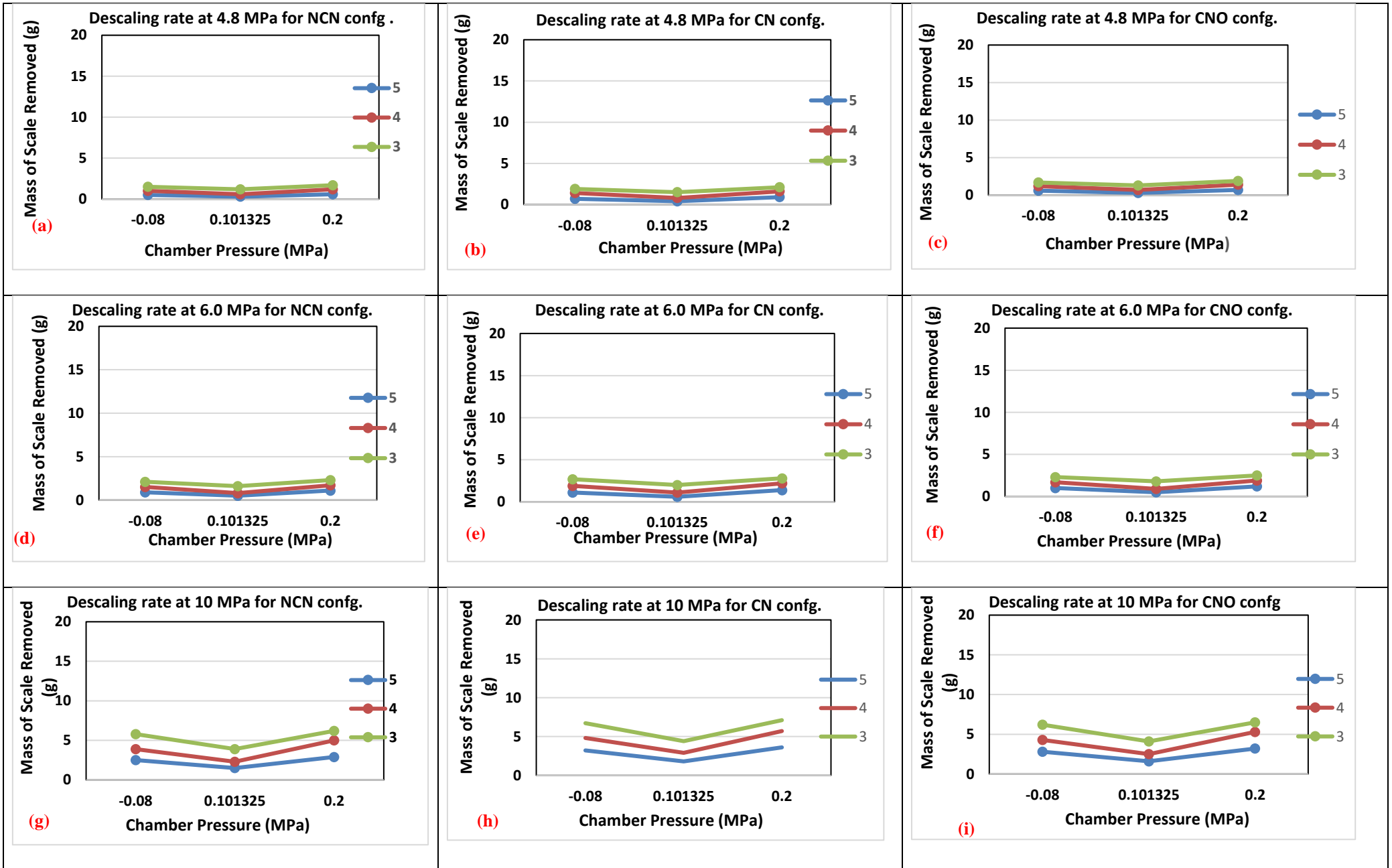


Figure 5.25: Chamber pressure impact comprising for descaling  $\text{CaCO}_3$  scale deposit at 25mm-distance

### **5.3.5 Optimum descaling requirement**

Despite the detailed research results obtained from section 5.3 that elaborates the erosion behaviour of multiple high-pressure flat fan nozzles in descaling petroleum production tubing's embedded with different types and shapes of scale deposits. Through the adoption of both hydrodynamic connected parameters like injection pressure & numbers of nozzles and the non-hydro connected parameters like stand-off distance & nozzles arrangements and chamber pressure. That lead to achieving the main research goal of enhancing the removal capacity via the permutation and combination of the respective descaling parameter. Theirs still need of determining the best combination of descaling parameters required for effectively and efficient descaling of each type of scale deposit. Thereby, developing an operational guide for removing each type of scale type and shape when utilising multiple high-pressure nozzles and other descaling parameters will be very valuable for the petroleum production technologist handling the flow assurance of a scale inflicted well.

#### **5.3.5.1 Non-hydrodynamics connected parameters**

The selection of the best non-hydrodynamics connected parameters like stand-off distance and nozzles configurations which have no direct effect to the pumping requirement, mass flow rate but interact with each other during the operations seems to play a vital role in enhancing the removal of all the types of scale deposits

#### **5.3.5.2 Stand-off distance**

During the entire removal of all the types of scale deposits, a linear trend that increase the deposit removal amount with decrease in stand-off distance when in combination with all the hydrodynamic connected parameters and chamber pressure was established. Although, despite the effect of adjusting the downstream distance towards all the scale deposit yielded the best result at 25mm, poor result for 50mm and very poor results for the 75mm distance due to poor jet to surface target impact (jet-profile) (Opferet al.2013). The 50mm and 75mm distance were occasionally able to perform wonderfully to the extent of breaking the samples due to selection of a good nozzle-configurations (nozzle arrangements on the header) and other parameters. The introduction of centre nozzles when descaling solid soft or hard scale deposit at high pressure with few nozzles can be a good example like the graphical elaborations of the 3nozzle scenario at various stand-off distance in Figure 5.26A, B & C. We're exploring the effect of adjusting the automiser to deposit distance with 3nozzle configurations at low pressure (4.8 MPa) removes 4.8g of hollow (paraffin) at 25mm

distance that reduces to 9.7g and far less to 1.1g after adjusting the jetting position to 50mm and 75mm respectively. While the case of solid shape that removes 5.2g, 2.1 & 0.6g across the respective stand-off distance. A removal value of 2g & 0.8g, 0.3g and 1.5g, 0.6g & 0.2g was recorded at respective distance for both SrSO<sub>4</sub> and CaCO<sub>3</sub>. A removal difference of 79g & 13.8g, 4.1g & 2.3g, 2g & 0.5g, 1.2g & 0.5g was observed after respectively adjusting the atomiser from 25mm to 50mm and from 50mm to 75mm distance when utilising 6.0 MPa injection to remove hollow & solid paraffin, SrSO<sub>4</sub> and CaCO<sub>3</sub> deposit respectively. Wider removal difference of 224g & 83g, 84g & 19g, 5.2g & 0.7g, 3.4g & 0.6g was also recorded at high injection pressure operations (10 MPa) when removing hollow, solid, SrSO<sub>4</sub> and CaCO<sub>3</sub> deposit respectively at sequential stand-off distance increase. The high removal differences as a result sequential stand-off distance increase when removing hollow shape scale was due to poor performance of the NCN configuration with increase in stand-off distance. While the CN configurations was averagely performing at deeper downhole due to good centre jet contact with the surface at wider distance when removing both solid and the hard scale samples.

### **5.3.5.3 Nozzle configurations (arrangement)**

Probably if not the most important descaling parameter, the nozzles configurations (header arrangement) which selection is govern by the shape of the scale deposit in question is the first determining factor before the selection of other descaling parameters. Section 5.31 demonstrated how each nozzles arrangement (NCN, CN & CNO) configurations was able to suite or perform in a distinct manner when removing each type of scale deposit. As discussed in section 5.3 and further elaborated in Figure 5.26D, E & F by singling the removal behaviour of respective types of scale and header configurations at 10 MPa injection pressure under different nozzle configurations suggest: That in general NCN was better, followed by CN and CNO in decreasing order for the removal of hollow shape samples and CN followed by CNO and NCN configuration in descending order for both solid soft scale and the two hard scale samples. With 5nozzles, a mass of 58g of scale was removed by NCN configurations at 10 MPa that decrease 49g and 39g after altering the configurations to CN and CNO respectively. While the CN configurations removes 32g, 3.2g & 1.8g of Solid, SrSO<sub>4</sub> & CaCO<sub>3</sub> deposits respectively, that reduce to 26g, 3g & 1.6g when altered to CNO configuration that further reduces to 21g 2.9g & 1.6g due to further alteration to the NCN configurations. The NCN 4nozzle configurations recoded a removal of 77g, 39g, 4.3g & 2.3g across the hollow, solid, SrSO<sub>4</sub> and CaCO<sub>3</sub> deposit respectively, while a value of 70g, 51g, 5.1g & 2.9g was recoded for CN removal across the respective scale deposit and mass of 66g, 46g, 4.5g & 2.5g for CNO removal across the respective scale deposits. Finally, the most impressive results

achieved from the 10 MPa-3nozzles descaling operations as shown in figure 5.26F demonstrate a removal difference of 16.8g & 48.9g due consecutive alteration of NCN configurations to CN and later CNO respectively when descaling hollow samples. A value of 23g & 41g was the removal difference due to altering CN configuration to CNO and later NCN when removing solid shape wax sample. While for  $\text{SrSO}_4$  and  $\text{CaCO}_3$  deposit, removal difference of 0.4g & 0.6g, 0.3 & 0.5g was recorded after the consecutive alteration of the nozzle configurations from CN to CNO and NCN respectively.

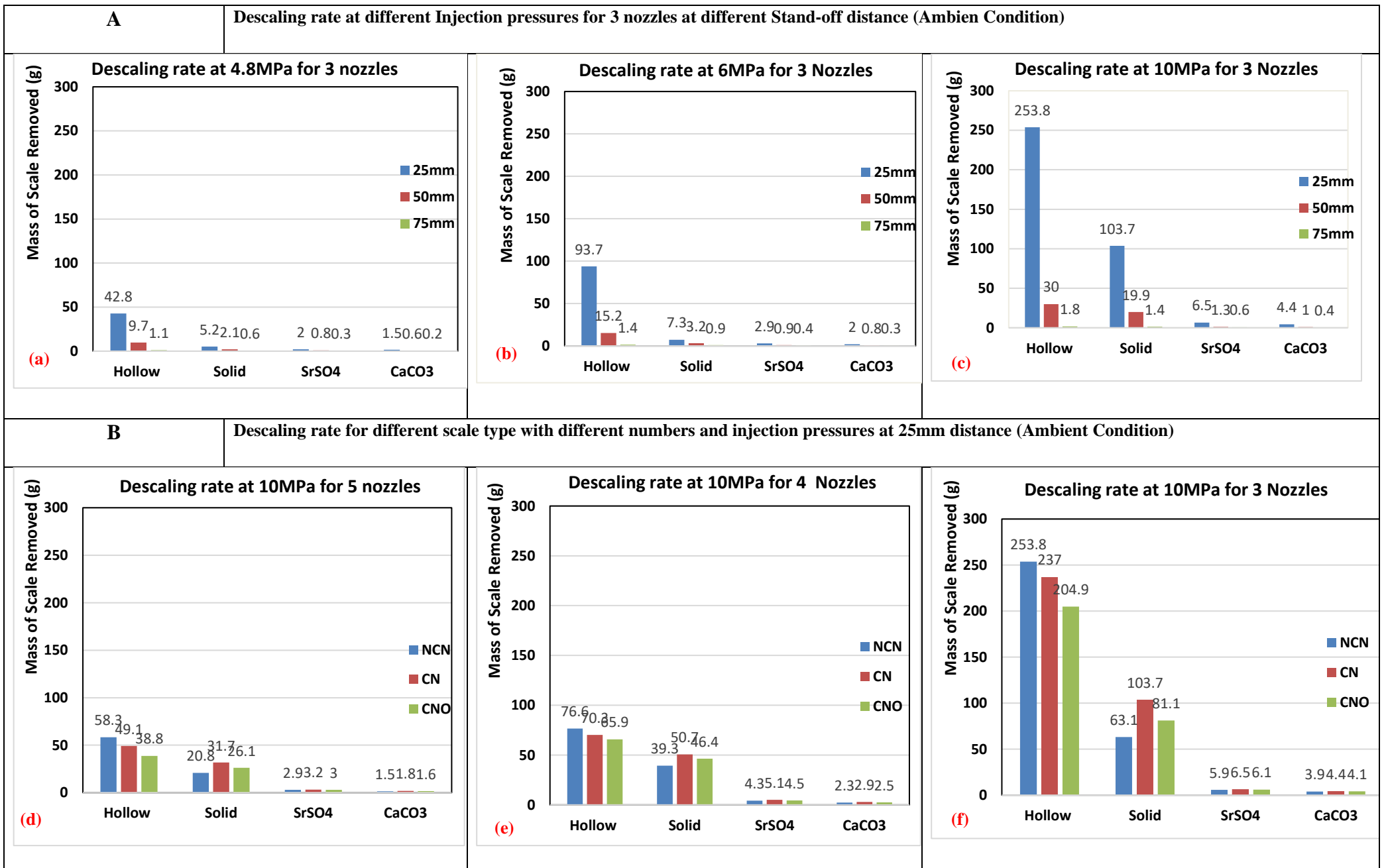


**Figure 5.26:** Descaling impact of non-hydro-connected parameters for respective deposits

### 5.3.5.4 Hydro dynamic connected parameters

The most vital set, of all descaling components that determine the direct scale removal force of the jet (kinetic energy and pressure drop across the nozzles) which performance depend on each other are the injection pressure and header configurations (number of nozzles). The relationship between header configuration and injection pressure is graphically demonstrated in figure 5.32 and mathematically in equation 5.7, as its clear that more injection pressure will be required to produce higher pressure drop with a greater number of nozzles than few nozzles.

#### 5.3.5.1 Injection pressure

The relationship and high dependency of the amount of scale deposit removed in respective of its type against the utilisation of different injected pressures has clearly been established in section 5.3 and Figure 5.27 A, B & C is singled to summarise the finding of the investigations. The effect of injection pressure and its variations on scale removal can be mathematically expressed equation 5.4 and 5.5 also, since injection pressure is directly proportional to velocity of the jet (Jet impact). Were  $P_t$  being the total pressure,  $P_d$  is the dynamic pressure (injection pressure),  $P_s$  is the static pressure that is constant in ambient pressure only, another reason for the vacuum and compressed pressure performing better. Therefore, the difference between static pressure and the stagnation pressure is equals to the dynamic pressure (injection pressure) represented as the kinetic energy per unit volume of a fluid particle.

$$P_t = P_s + P_d \quad (5.4)$$

$$P_d = K_e = \frac{1}{2}mV^2 \quad (5.5)$$

$$v = \sqrt{2p/m} \quad (5.6)$$

The consequences of increasing injection by 1.2 MPa and by 4 MPa when descaling with 5nozzles configuration yielded a removal difference of 1.2g & 56g, 0.6g & 30g, 0.3g & 2.3g and 0.2g & 1.2g for hollow, solid wax, SrSO<sub>4</sub> and CaCO<sub>3</sub> deposit respectively. Likewise, the 4nozzle operations increased the removal difference to 3.8g & 67g, 1.3g & 47g 0.4g & 3.4g and 0.3g & 1.8 of the respective scale deposits. While the 3nozzle operations due to increase in pressure drop across the nozzles improved the removal difference to 51g & 160g, 2.1g & 96g, 0.9g & 3.6g and 0.5g & 2.4g of hollow, solid wax, SrSO<sub>4</sub> and CaCO<sub>3</sub> deposit respectively. Therefore, in respective of scale type only a slim improvement is notice due to increasing the injection pressure by 1.2 MPa, compared to significant removal achieved by the subsequent increase by 4 MPa, was due to wide pressure variation between the two pressure ranges, hardness of the samples, size and pressure drops.

### 5.3.5.2 Number of nozzles

The most important of all the descaling parameters and the determinant of the of the jet impact that account for most of the removal is the header configuration. The pressure drop across the nozzles is proportional to the injection, fluid flowrate and inversely to the nozzle's areas (number of nozzles). Therefore, for same nozzle diameter to generate a large nozzle pressure drop a larger flow rate is required and the fewer the number of nozzles the larger the pressure drop expected. In other words, a higher velocity jet will be yielded from the nozzle that have greater pressure drop (Tian et al., 2009). In our case, the scale sample target will be impacted by a high pressure drop (kinetic energy), thereby resulting to sample breakage. Records from the analysis from Section 5.3 show how much contribution the effect of altering header configuration have made in enhancing the amount of scale removal of the respective scale samples and Figure 5.28D, E & F summarised it effect against respective injection pressures.

$$P_b = \frac{513.559Q^2 p}{A^2 C^2} \quad (5.7)$$

Were  $P_b$  is the pressure drop (MPa),  $Q$  is the flowrate (11.3lt/s),  $p$  is the density of water (0.98),  $C$  is the nozzle discharge coefficient (0.9) and  $A$  is total areas of nozzle (0.5mm x number of nozzles)<sup>2</sup>, therefore, inserting values into the above equations.

$$P_{b-5NOZZLES} < P_{b-4Nozzles} < P_{b-3nozzles} \quad (5.8)$$

Figure 5.28D graphically demonstrates how the alteration of number of nozzles from 5nozzle to 4nozzles generate a slight removal difference 4.5g, 1.4g, 0.7g & 0.4g of paraffin hollow & solid, SrSO<sub>4</sub> and CaCO<sub>3</sub> deposit respectively from the initial removal of the 5-nozzles ambient operations at 4.8 MPa. More improve removal difference of 37g, 2.6g, 0.7g & 0.7g for respective scale deposits was observed after altering further to 3nozzles at the same descaling conditions. Likewise in Figure 5.28E, the 6.0 MPa injection trials demonstrated a set of more improved results in term of difference in amount of scale remove due to reducing the number of nozzles from 5 to 4nozzles by 7.1g, 2.1g, 0.8g & 0.5g of the respective scale deposit and better result of 84g, 3.4g, 1.2g & 0.9g of the respective deposit due to subsequent reduction of the number of nozzles to 3nozzles . Finally, the best set of scale removal amount due to header alteration can be found in 10 MPa operations in Figure 5.28F were doubled amount than the previous result (4.8 & 6MPa) of altering header configuration from 5 to 4nozzles of 18g, 19g, 1.9g & 1.1g was achieved. Also, almost tenfold of the earlier descaling amount of the low and medium pressure, of 177g, 53g, 1.4g & 1.5g was obtained for the respective scale deposit due to pressure drops generated from the further alteration oh header configurations from 4 to 3nozzles.

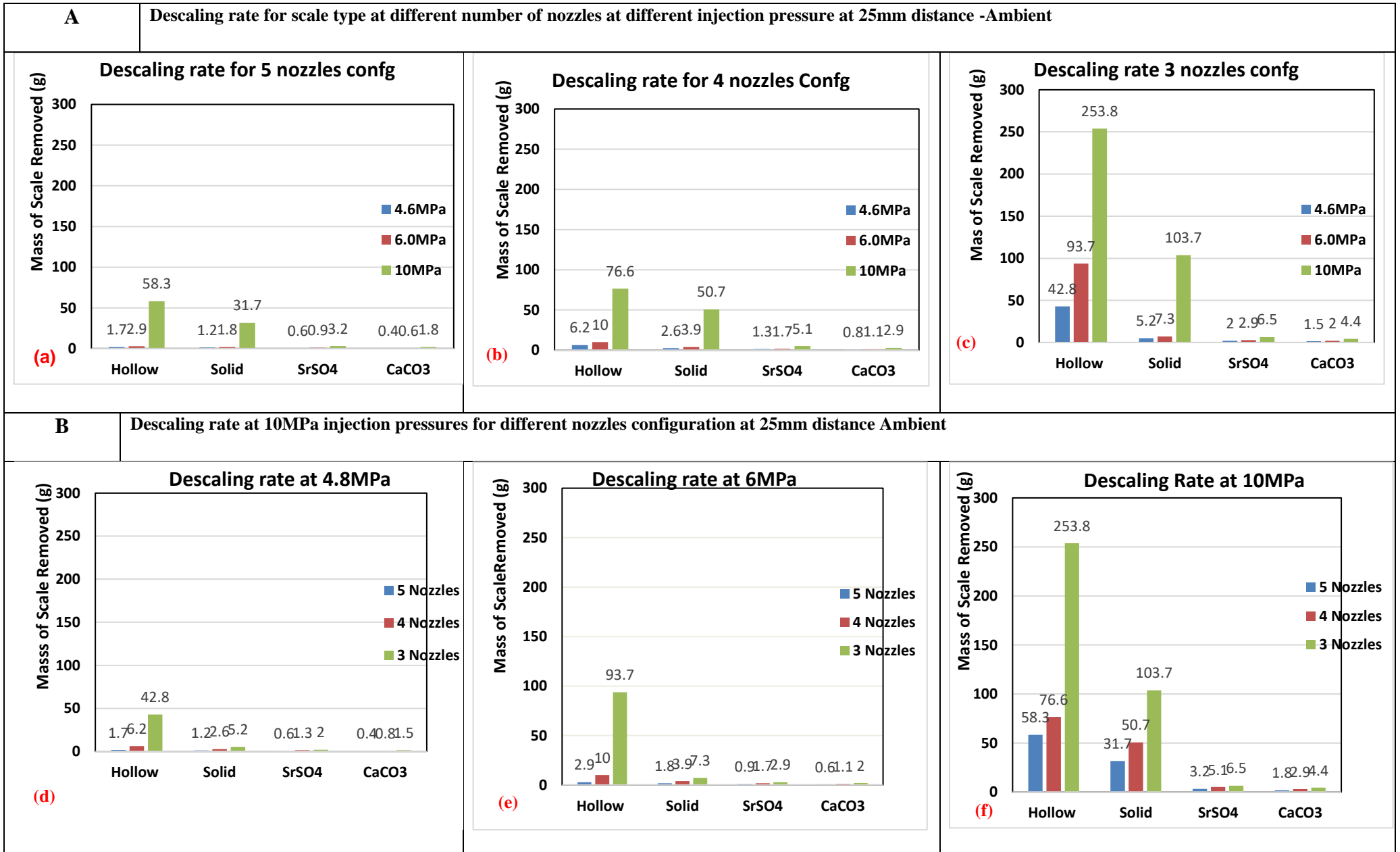


Figure 5.27: Descaling impact of hydro-connected parameters for respective deposits  
201

### 5.3.5.3 Chamber pressure

The effect of varying chamber pressure while removing any type of scale deposit in respect of the utilised descaling parameters can be very noticeable and highly aids in one way or the other almost all the jetting mechanism (Zongyi 2004). Might be a supplementary but important descaling parameter due to its dependency on the performance of the other descaling parameters and shape of the scale sample as detailed in Section 5.3.5 and graphically summarised in Figure 5.33A, B & C for the 3nozzle operations. Generally, the ambient chamber pressure descaling approach that depend on kinetic impact was found to remove less amount of scale deposit across all the scale types compared to compressed approach that enhance kinetic impact, cyclin stress and particle abrasion. So, also to suction chamber approach that enhance both kinetic energy, particle abrasion, cavitation and hoops stress for scale deposits of particular shapes. Although to be precise in term of descaling capacity, the effect of chamber pressure alteration between ambient pressure to the other two chamber pressures is very significant and noticeable, while the results between compressed and vacuum pressure is very insignificant. Descaling hollow samples at low pressure (4.8 MPa) of 3nozzles with respective best configurations produce a removal difference of just 1g from the utilization vacuum and compressed pressure and 47g between vacuum and ambient pressure utilisation. Likewise the removal differential values of 0.8g & 8.2g, 0.2g & 0.7g and 0.2g & 0.6 were recorded due to respective chamber alterations from vacuum to compressed condition and ambient to compressed during the removal of solid wax,  $\text{SrSO}_4$  and  $\text{CaCO}_3$  deposit respectively as presented in Figure 5.33.A. Similar trend with improved removal difference of 1.1g & 116g was observed when removing hollow soft scale at medium pressures (6.0 MPa) with 3nozzles due to respective alteration of chamber pressure from compressed to vacuum and from ambient to vacuumed pressure. Also, an improved difference in mass removed of 1.1g & 14g, 0.1g & 0.5g and 0.1g & 0.8g of solid wax,  $\text{SrSO}_4$  and  $\text{CaCO}_3$  deposit respectively was observed from the consequences of altering chamber pressure this time from vacuum to compressed and ambient to compressed respectively as shown in figure 5.33B. Figure 5.33C present the highest difference in mass remove when descaling the respective scale samples at high pressure (10 MPa) with 3 nozzles with a slight difference of 2.8 and later 40.5g of hollow paraffin due to chamber alterations from compressed to suction and from ambient to suction. Finally, the solid wax,  $\text{SrSO}_4$  and  $\text{CaCO}_3$  deposit respectively produce a removal difference of 1.9g & 139g, 0.2g & 1.4g and 0.4g & 2.3g as a result of altering the chamber pressure from vacuumed to compressed and from ambient to compressed chamber pressure respectively.

### 5.3.5.4 Descaling efficiency

An effective descaling technique is defined as the ability of a scale removal approach to regain the accessibility of a scale inflicted well in economic, fast, easy and safe ways for both the rig equipment's and rig personals. In order words, an operation that is cheaper, faster, easier, safer and greener than other available techniques at the market disposal. Therefore, the reason of calculating and ranking the efficiency of removing the respective types of scale deposit from petroleum production tubing using the analyse descaling parameters results was to assesses and ranked hand in hand the amount of scale removed in consideration of the volume of water utilised during each operation. Moreover, this will cover the energy and cost requirements of the operation through the utilization of the descaling efficiency formula expressed in equation 5.9 and the efficiency calculation of utilising 3nozzle at respective injection pressure and other descaling parameters against different chamber pressure is sectioned in Figure5 5.28D, E & F. The efficiency results demonstrated a trend that is proportional to the amount of scale removed, which increases with increase in injection pressure and reduction of numbers of nozzles, and stand-off distance that depend on the choice of nozzle configuration. Still the results were found to be inversely proportional to the volume of water utilise (the less the amount of water utilise the less the well flooding tendency) which is in line with the hydro-dynamic descaling parameters.

$$\text{Descaling Efficiency } \eta = \frac{\text{Mass of Scale Removed}}{\text{Mass of Water Utilised}} \times 100 \quad (5.9)$$

The descaling operations of 3nozzle at low pressure of 4.8 MPa that utilises 37.5kg of water recorded an ambient efficiency of 7.8%, 0.9%, 0.4% & 0.3% for the respective scale types. The impact of compressed air increases the efficiency by many folds (16.2%) for hollow sample, doubled to 2.4% for solid and increase of 0.1% across the hard scale samples. Slight improvement to 16.3% and a decrease to 2.3% and 0.3% was recorded for solid soft and CaCO<sub>3</sub> deposit during the vacuum operations. Likewise, the 37.8kg volume of water utilised during the 6 MPa operation of 3nozzles was found to have an efficiency value of 17%, 1.3% 0.5% & 0.5% for the respective scale deposit at ambient condition. The introduction of compressed air respectively tripled the hollow and solid soft scale efficiency to 37% & 38% and no improvement was recorded for the hard scale deposits in both including vacuum condition, while the vacuum condition increase the hollow removal slightly efficiency by 0.2% and slightly reduces solid to 0.2%. Finally, a more reasonable removal efficiency of 45%, 16%, 1% & 0.7% was observed due to the utilization 42.4kg of water at 10 MPa with 3-nozzles to remove the respective deposits at ambient condition. The values significantly increase to 51%, 37%, 1.3% & 1.1% due to compression, were as 52.3%, 36%, 1.3% for hollow & solid soft and no improvement for hard scale due to suctioning operations.

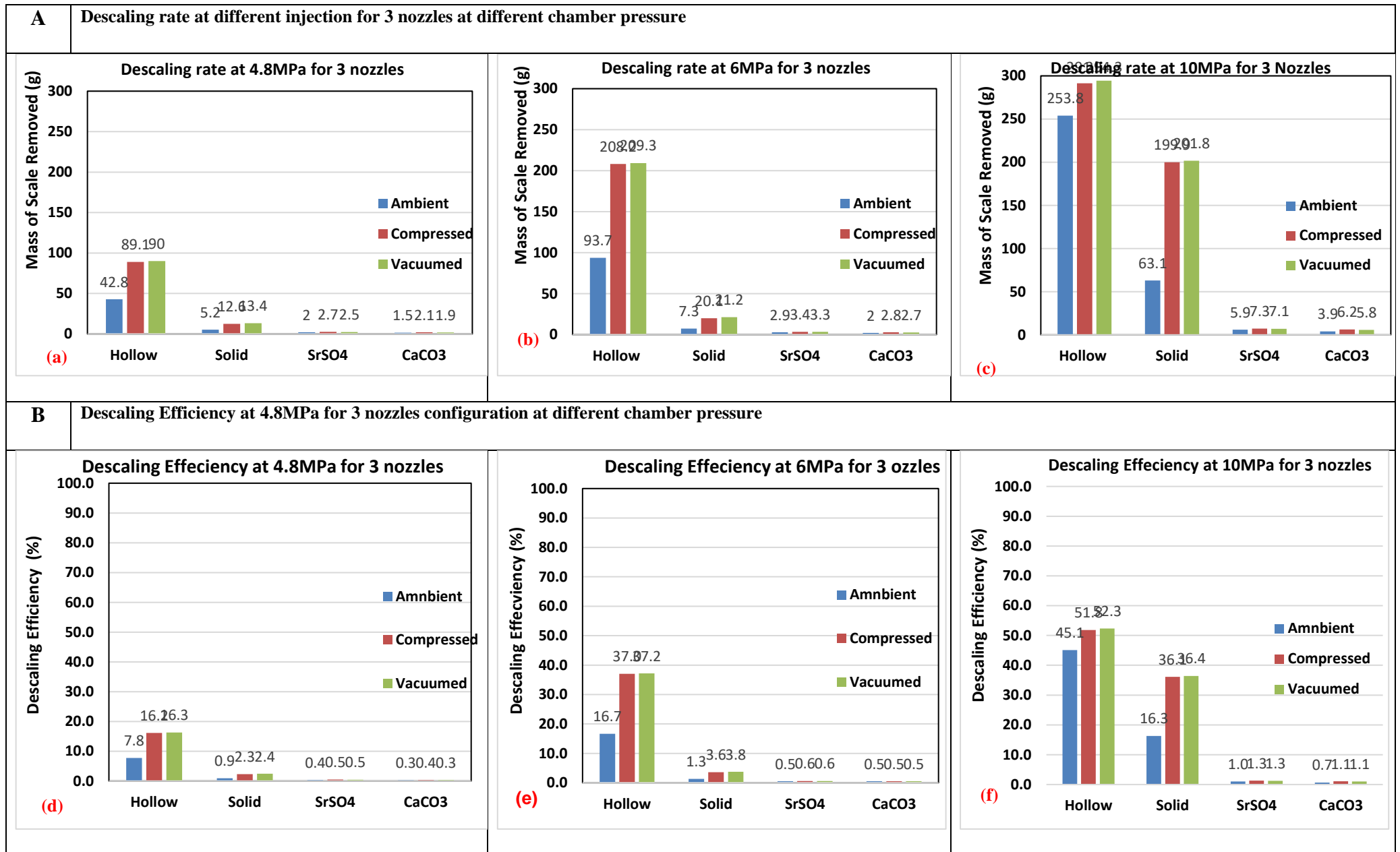


**Figure 5.28:** Descaling impact of chamber pressure and its efficiency for respective deposits

**Table 5.1:** Multiple High-Pressure Circular Nozzle Descaling Operations Guide

<b>DESCALING PARAMETERS SELECTION GUIDE</b>																	
<b>Scale Deposit Name</b>	<b>Scale Deposit Shape</b>	<b>Header Configuration</b>			<b>Injection Pressures (MPa)</b>			<b>Stand-off distance (mm)</b>			<b>Nozzle Configurations</b>			<b>Chamber Pressure (MPa)</b>			<b>Efficiency (%)</b>
		<b>5</b>	<b>4</b>	<b>3</b>	<b>4.8</b>	<b>6.0</b>	<b>10</b>	<b>25</b>	<b>50</b>	<b>75</b>	<b>NCN</b>	<b>CN</b>	<b>CNO</b>	<b>-0.08</b>	<b>0.101</b>	<b>0.2</b>	
<b>Paraffin (C<sub>n</sub>H<sub>2n+2</sub>)</b>	<b>Hollow</b>			<b>V</b>			<b>V</b>	<b>V</b>				<b>V</b>			<b>V</b>		<b>25</b>
	<b>Solid</b>			<b>V</b>			<b>V</b>	<b>V</b>					<b>V</b>			<b>V</b>	<b>19</b>
<b>SrSO<sub>4</sub></b>	<b>Hollow</b>			<b>V</b>			<b>V</b>	<b>V</b>					<b>V</b>			<b>V</b>	<b>6</b>
	<b>Solid</b>																
<b>CaCO<sub>3</sub></b>	<b>Hollow</b>			<b>V</b>			<b>V</b>	<b>V</b>					<b>V</b>			<b>V</b>	<b>4</b>
	<b>Solid</b>																

### 5.3.6 Summary

The following conclusion have been drawn from this chapter.

- The constructed soft scale sample was proven to have the same chemical properties with paraffin wax through FTIR and NMR analysis.
- So also, the Libyan field acquired hard scale samples were found to be  $\text{CaCO}_3$  and  $\text{SrSO}_4$  respectively through the combination of SEM, EDX and XRD techniques.
- The choice of descaling technique is a function of type and shape of the scale deposit in question
- Likewise, the choice of nozzle configuration (arrangement) relies on shape of the deposit. i.e NCN configuration is best for hollow shapes deposit and CN & CNO for solid deposits.
- In respective of type of scale deposit, the removal increases with increase in injection pressure and reduction in numbers of nozzles
- The descaling performance of all the types of scale rely on increase of kinetic energy or spray velocity (injection pressure) which reduces with increase in number of nozzles.
- The jet performance reduces with increase in jetting position even though can be compensated by the right choice of nozzle configuration & chamber pressure for each scale deposit.
- The impact of chamber air pressure on the removal also depend on the shape & type of deposit and optimum selection of other descaling paraments
- Introduction of 0.2MPa compressed air into the chamber at with the best parameters approximately favoured the removal more solid soft and  $\text{SrSO}_4$  &  $\text{CaCO}_3$  than hollow, through enhancing cycling stress and particle abrasion jetting mechanism.
- While suctioning the chamber by -0.008MPa when utilising the best parameters increases the average removal of hollow deposits more than the solid  $\text{SrSO}_4$  &  $\text{CaCO}_3$  through enhancing kinetic energy, hoops stress, particle abrasion and cavitation jetting mechanism.

# Chapter 6

## Conclusion and Recommendations

### 6.1 Conclusions

The results from the investigation of the descaling behaviour of oilfield scale deposits of 1, 2 & 3 Mohs scale hardness index from petroleum production tubing with multiple high-pressure circular nozzle recorded a massive improvement. Also, yielded the following conclusions after adopting the option of altering both the descaling parameters and the chamber air/water concentration.

- The oil field soft scale deposit (paraffin) have effectively being mimic, descaled and characterised to have similar chemical properties with paraffin a through FTIR & NMR analysis respectively.
- Additionally, the Libyan field acquired hard scale samples were effectively descaled and characterised via the combination of SEM, EDX and XRD techniques and were found to be  $\text{CaCO}_3$  and  $\text{SrSO}_4$  respectively.
- The multiple high-pressure nozzle approach at all descaling parameter combination recorded an impressive enhancement in terms of amount of scale removed compared to the single nozzles aerated approach. For instance, the ambient 3nozzles CN configurations technique impressively removed 104g, 9g & 8g of solid soft,  $\text{SrSO}_4$  &  $\text{CaCO}_3$  deposits respectively, compared to the 10g, 6g 5g of the single nozzle ambient approach. While also the compressed approach of 3nozzles removed 200g, 14g & 10g of solid soft,  $\text{SrSO}_4$  &  $\text{CaCO}_3$  deposits respectively more than the single nozzle aerated amount of 67g, 12g & 7g.
- Considering the distinct chemical and physical properties of each scale deposit, will consequently respond to different erosional mechanisms and require unique optimised descaling conditions for its effective descaling.
- Therefore, the selection of the best descaling requirement for each deposit depends on the shape, size, hardness and location of the deposit in question.
- Consequently, a high level of interaction and dependency between all the descaling parameters and the amount of scale removed, especially within the hydro dynamic connected and non-hydro dynamic connected parameters respectively exist.
- The amount of scale removed in respective of type of deposit in related to the hydrodynamic parameter's increases with increase with injection pressure (kinetic energy) and decrease

with increase in number of nozzles (header configuration) due to multiple nozzle pressure drops effect.

- While the amount of scale removed for all the respective deposits in connection with the non-hydrodynamic parameters decreases with increase in jetting position and the poor downhole jet performance can be corrected with the right choice of nozzle configurations
- So also, the selection of nozzle configuration (header arrangement) is govern by the size and shape of the sample, as NCN configuration was able to remove 7% & 13% than CN and CNO configuration when descaling hollow shape scale at the best of other parameters in ambient condition. While CN configuration removed 6%,4% & 0.1%, 0.08% &0.1%,0.02% more deposit of solid,  $\text{SrSO}_4$  and  $\text{CaCO}_3$  than the CNO and NCN nozzles configurations respectively.
- Fifth descaling mechanism (hoop stress) effective in removing early growth stage scale deposit (hollow shape) was discovered and was found to be more active in suction chamber condition together with cavitation mechanism. Even, do the compressive chamber condition was more effective in removing complete tubing blocked deposits (solid) and hollow shape deposit that does not fulfil the hoop stress tin wall condition through erosion, cyclin stress and particle abrasion mechanism
- The introduction of 0.2 MPa compressed air into the chamber with the best parameters approximately increase the removal of hollow by 23%, sloid soft by 27% and  $\text{SrSO}_4$  &  $\text{CaCO}_3$  by 0.4% & 0.5.% through enhancing cycling stress and particle abrasion jetting mechanism.
- While suctioning the chamber by -0.008MPa when utilising the best parameters increases the average ambient removal of hollow by 26% solid by 18% and  $\text{SrSO}_4$  &  $\text{CaCO}_3$  by 0.3% & 0.4% through enhancing kinetic energy, hoops stress, particle abrasion and cavitation jetting mechanism.
- The hollow shape paraffin deposit was the only deposit that was effectively removed in ambient chamber condition due to hope stress effect and was only lagging by 38g and 40g behind the compressed and vacuum chamber condition removal respectively.
- The efficiency of each descaling technique from any permutation of descaling parameters is a function of amount of the amount of scale it removes and the volume of water it utilises during the operation

## 6.2 Recommendations

Despite the high-level of breakthrough and the enhancement in scale removal that was recorded from this investigation, coupled with detailed designed, construction and modification procedures of the utilised facilities, some research question remained un-answered due to time and scope constraint. Therefore, the following recommendation will effectively be filled in the existing research gap and contribute to the knowledge area.

- CFD model could be design for comparison with experimental result and simulations of other non-suitable experimental measurements like cavitation measurement and the impact spray overlap.
- A more compactable nozzle header should be design in order to reduce the size of the descaling chamber into a typical Saudi Aramco production tubing size of 100mm diameter that will generate good spray profile contact with the typical oilfield hard scale deposit of 100mm diameter.
- The future nozzle header should be flexible enough to allow the alteration of the nozzle's header orientation angles to 15°, 25°, 30° & 60° contrary the present one that have fixed 45° for the side nozzles and 90° angle for the centre nozzles.
- Carry out the cavitation bubble length measurement of each nozzle configurations and study of how-to extend cavities flair for scale removal instead of supressing cavitation will improved the jet performance for effective scale removal.
- For safety and effective removal, selection of stronger, transparent and longer experimental chamber that can withstand at least 1 MPa chamber pressure, accommodate high injection pressure of 20 MPa and longer descaling time of at least 5 minutes is recommended. Since the present perplex chamber has maximum design pressure of 0.6 MPa and a water resident time of 188 sec only.
- Mechanical failure pattern and fracture mechanisms of the respective deposit should be investigated in order to corelate the quantitative and qualitative removal of each sample, because in this investigation some sample were highly eroded without breaking while other break with low removal.
- Also, the combination of different type of nozzles on the spray header i.e. flat, fan and solid stream jet might provide a better answer to the problem.
- A means of utilising Knoop or Vickers hardness technique should be devised in order to allocate each scale deposit it real Moh's scale of hardness index

## Reference

- Abbas, A. J. (2014). Descaling of Petroleum Production Tubing utilising Aerated High Pressure Flat Fan Water Sprays.
- Abulhamayel, N., Leal, J., Ayub, M., Driweesh, S., & Aramco, S. (2015). Recent Developments in Mechanical Descaling Operations : A Case Study.
- Al-Matar, H., Al-Ashhab, J. K., Mokhtar, M., & Ridzaudidin, S. (2006). Techniques used to monitor and remove strontium sulfate scale in UZ producing wells. Paper
- Al-Khalidi, M. H., Al-Juhani, a. M., Al-Mutairi, S. H., & Gurmen, M. N. (2011). New insights into the removal of calcium sulfate scale. *Society of Petroleum Engineers - 9th European Formation Damage Conference 2011*, 2, 1052–1070. Retrieved from <http://www.scopus.com/inward/record.url?eid=2-s2.0-80052441716&partnerID=tZOtx3y1>
- Al-Taq, A. A., Muhaish, S. A., Nakhli, M. M., & Alrustum, A. A. (2015). Organic/Inorganic Deposition in Oil Producing Wells from Carbonate Reservoirs: Mechanisms, Removal and Mitigation. SPE 177447. *Abu Dhabi International Petroleum Exhibition and Conference*, 1–15. <https://doi.org/10.2118/177447-MS>
- Alabdulmohsin, Y. A., El-zefzafy, I. M., Al-malki, M. H., Al-mulhim, A. A., & Ali, A. (2016). SPE-181286-MS Underbalanced Coiled Tubing Mechanical De-Scaling Operations : A Case History for an Oil Well in Ghawar Field from Saudi Arabia, 1–14.
- Almubarak, T., Ng, J. H., Nasr-el-din, H., & Texas, A. (2017). SPE-185636-MS Oilfield Scale Removal by Chelating Agents : An Aminopolycarboxylic Acids Review, (Iii).
- Anwar, M., & Abubakr, M. (2017). Innovation Technique and Successful Scale Removal Job With Coiled Tubing in Belayim Oil Field, Egypt: A Case History. Paper presented at the Offshore Mediterranean Conference and Exhibition, Ravenna, Italy. <https://doi.org/>
- Amjad, Z., & Demadis, K. D. (2015). Mineral scales and deposits: Scientific and technological approaches.
- Ayirala, S., & Yousef, A. (2014). Injection water chemistry requirement guidelines for IOR/EOR. Paper presented at the SPE Improved Oil Recovery Symposium.
- Armacanqui, J. S., Eyzaguirre, L. D. F., Flores, M. G., Zavaleta, D. E., & Camacho, F. E. (2016). SPE-181162-MS Testing of Environmental Friendly Paraffin Removal Products Current Practices to Remove Paraffin Deposition.
- Aslam, J., Alsalat, T., & Corporation, P. (2000). SPE 58780 High-Pressure Water Jetting : An Effective Method To Remove Drilling Damage.
- Bakker, T. W., Ivannikov, V. I., & International, W. (2002). SPE 75352 Cavitator for Effective Well Cleaning, 1–4.
- Bakr, M., Hay, A. A., & Hamdy, E. (2012). SPE 154455 A Successful Removal RI Inorganic Hard Scale Deposits in an Offshore Pipeline in Gemsa Oil field , Egypt : Field Study, 1–7.
- Bajammal, F. A., Biyanni, H. M., Riksa, A. P., Poitrenaud, H. M., & Mahardhini, A. (2013, March 26). Scale Management in Mature Gas Field: Case Study of Peciko. International Petroleum Technology Conference. doi:10.2523/IPTC-16675-MS

- BETE, "Full Cone Nozzles - Air Atomising Design," 2014. [Online]. Available: <http://www.bete.co.uk/spray-nozzles/full-cone-nozzles/air-atomising-nozzles>. [Accessed: 29-Jul-2018].
- BET, "Air actuated flat fan nozzles," 2014. [Online]. Available: <http://www.bete.co.uk/spray-nozzles/flat-fan-nozzles/air-actuated>. [Accessed: 29-Jul-2018].
- Birk, N. (2013). SPE 163904 First Field Application of 2-7 / 8 " Scale Removal Tool for Offshore Well Abandonment, (July 2010).
- Bolarinwa, S., Jauregui, J. L., Buali, M., Aramco, S., Kharrat, S. P. E. W., & Kovalenko, K. (2012). SPE 156021 Innovative Integrated Procedure for Scale Removal in Khuff Gas Wells in Saudi Arabia, (1), 1–16.
- Børeng, R., Skinnemoen, O. K., Vigen, A., Vikane, O., Andrews, J., Asa, S., ... Hauptmann, T. (2002). SPE 86479 A Successful Scale Removal Operation by Use of New and Old Technology, (June).
- Bourne, H. M., Heath, S. M., McKay, S., Fraser, J., Stott, L., & Müller, S. (2000). Effective Treatment of Subsea Wells with a Solid Scale Inhibitor System. Paper presented at the International Symposium on Oilfield Scale, Aberdeen, United Kingdom. <https://doi.org/10.2118/60207-MS>
- Buali, M., Ginest, N., Leal, J., Sambo, O., Chacon, A., & Vielma, J. (2014). Extreme Challenges in FeS Scale Cleanout Operation Overcome using Temporary Isolation, High Pressure Coiled Tubing, and Tailored Fluid Systems. *SPE International Oilfield Scale Conference and Exhibition*. <https://doi.org/10.2118/169759-MS>
- Campbell, A., & Brunskill, D. (2013). Advances in Coiled Tubing Jetting Technology. *SPE/ICoTA Coiled Tubing Roundtable*. <https://doi.org/10.2118/60721-MS>
- Civan, F. (2014). Analyses of processes, mechanisms, and preventive measures of shale-gas reservoir fluid, completion, and formation damage. Paper presented at the SPE International Symposium and Exhibition on Formation Damage Control.
- Crabtree, M., Eslinger, D., Fletcher, P., Miller, M., Johnson, A., & King, G. (1999). Fighting scale—removal and prevention. *Oilfield review*, 11(3), 30-45.
- Chakraborty, S., Lehrer, S., Ramachandran, S., & Incorporated, B. H. (2017). SPE-183974-MS Effective Removal of Sour Gases Containing Mercaptans in Oilfield Applications, 1–13.
- Codolo, M. C., & Bizzo, W. A. (2013). Experimental study of the SO<sub>2</sub> removal efficiency and volumetric mass transfer coefficients in a pilot-scale multi-nozzle spray tower. *International Journal of Heat and Mass Transfer*, 66, 80–89. <https://doi.org/10.1016/j.ijheatmasstransfer.2013.07.011>
- Davis, J. P., & Cassel, T. E. (2001). Apparatus for removal of milling debris. In: Google Patents.
- El-Hattab, M. (1985). Scale deposition in surface and subsurface production equipment in the Gulf of Suez. *Journal of Petroleum Technology*, 37(9), 1640–1652. Retrieved from <http://www.onepetro.org/mslib/servlet/onepetropreview?id=00011449>
- El Hajj, H., Pal, O., & Zoghbi, B. (2015). Compositional Analysis and Treatment of Oilfield Scales.

- SPE Saudi Arabia Section Annual Technical Symposium and Exhibition*, (1), 21–23. <https://doi.org/10.2118/178002-MS>
- Elkhatatny, S., & Fahd, K. (2017). SPE-183914-MS New Formulation for Iron Sulfide Scale Removal, (March), 6–9.
- Esbai, R. E., Palanisamy, G., & Petroleum, T. (2016). SPE-184204-MS Eliminating Scale Buildup Challenges and Lessons Learnt from the Fadhili Reservoir Awali Field.
- Espinosa, G., Mauricio, A., Leal, J. A., Driweesh, S. M., Buali, M. F., Khnaifir, W. K., . . . Arifin, M. (2016). First Time Live Descaling Operation in Saudi using Coiled Tubing Fiber Optic Real-Time Telemetry Rugged Tool, Foamed Fluid and Pressure Fluid Management System. Paper presented at the SPE Kingdom of Saudi Arabia Annual Technical Symposium and Exhibition.
- Farrokhrouz, M., & Asef, M. R. (2010). SPE 135854 Production Enhancement via Scale Removal in Nar Formation. *Changes*, (June), 8–10. <https://doi.org/10.2118/135854-MS>
- G, M. A. E., Leal, J. A., Driweesh, S. M., Buali, M. F., Khnaifir, W. K., & Jasim, A. J. (2016). First Time Live Descaling Operation In Saudi Using Coiled Tubing Fiber Optic Real-Time Telemetry Rugged Tool , Foamed Fluid And Pressure Fluid.
- Gholinezhad, J. (2006). Evaluation of latest techniques for remedial treatment of scale depositions in petroleum wells. *SPE Eighth International Symposium on Oilfield Scale 2006, 2006*, 17–23. <https://doi.org/10.2523/99683>
- Guan, H. (2015). Scale Deposition Control and Management in Subsea Fields, (5480), 1–12.
- Guimaraes, Z., Franca, A. B., Duque, L. H., de Souza, R. B., Porto, M., Neves, D., & Peixoto, C. (2007). Case histories of barium sulfate scale removal in offshore wells, Brazil, using a new engineered combination of coiled-tubing tools. Paper presented at the SPE/ICoTA Coiled Tubing and Well Intervention Conference and Exhibition.
- Ghouri, S. A., Ali, I., Shah, N. M., Ejaz, M., & Haider, S. A. (2018, January 1). Downhole Scales Management in Mature Gas Fields. Society of Petroleum Engineers. doi:10.2118/195659-MS
- Haghtalab, A., Kamali, M. J., & Shahrabadi, A. (2014). Prediction mineral scale formation in oil reservoirs during water injection. *Fluid Phase Equilibria*, 373, 43-54.
- Hamid, S., De Jesus, O., Jacinto, C. M., Izetti, R., Pinto, H., Drougett, E., . . . Dagenais, P. (2013). A practical method of predicting chemical scale formation in well completions. Paper presented at the SPE Asia Pacific Oil and Gas Conference and Exhibition.
- Hafiz, T., Hoegerl, M., Alsuwajj, A., Almathami, A., & Hughes, B. (2017). SPE-183954-MS Synthetic Iron Sulfide Scale and Polymeric Scale Dissolvers, (March), 6–9.
- Haugen, I., Døssland, L., Brankovic, M., Osaland, E., Osugo, L., Technologies, Q., & Grødem, M. (2017). SPE-184758-MS Electric-Line Deployed Lightweight Intervention Technology for The Effective Removal of Barium Sulphate Scale Obstructions from Small Diameter Wellbores, 1–15.
- Heydrich, M., Hammami, A., Choudhary, S., Mockel, M., & Ratulowski, J. (2019, April 26). Impact of a Novel Coating on Inorganic Scale Deposit Growth and Adhesion. *Offshore Technology*

Conference. doi:10.4043/29218-MS

- Hinrichsen, C. J. (1998). Preventing scale deposition in oil production facilities: An industry review. Paper presented at the CORROSION 98.
- J. Leal, W. Nunez, S. Al-ismail, and J Ricardo Solares, “SPE 121404 Novel Mechanical Scale Clean-out Approach to Remove Iron Sulphide Scale from Tubulars in Vertical High Pressure and Temperature Deep Gas Producers : A Case History,” 2009.
- Jordan, M. M., Sjuræther, K., Collins, I. R., Feasey, N. D., & Emmons, D. (2001). Life Cycle Management of Scale Control within Subsea Fields and its Impact on Flow Assurance, Gulf of Mexico and the North Sea Basin. *Proceedings - SPE Annual Technical Conference and Exhibition*, 1971–1986. <https://doi.org/10.2118/71557-MS>
- Jordan, M., & Mackay, E. (2015). Predicting and Managing Inorganic Scale Associated With Produced Water from EOR Projects. *SPE Latin American and Caribbean Petroleum Engineering Conference*, 1–18. <https://doi.org/10.2118/177144-MS>
- Kamari, A., Gharagheizi, F., Bahadori, A., & Mohammadi, A. H. (2014). Rigorous modeling for prediction of barium sulfate (barite) deposition in oilfield brines. *Fluid Phase Equilibria*, 366, 117-126.
- Kan, A., & Tomson, M. (2012). Scale prediction for oil and gas production. *Spe Journal*, 17(02), 362-378.
- Kazemi Nia Korrani, A., Sepehrnoori, K., & Delshad, M. (2014). A Comprehensive Geochemical-Based Approach to Quantify the Scale Problems. Paper presented at the SPE International Symposium and Exhibition on Formation Damage Control.
- Kelland, M. A. (2014). *Production chemicals for the oil and gas industry*: CRC press.
- Kunanz, H., Wölfel, S., & Leoben, M. (2014). Working principle of ultrasonic cleaning Preparation of Samples, (May), 14–15.
- Wang, Q., Leal, J., Syafii, I., Mukhles, A. E., Chen, T., Chang, F., & Espinosa, M. (2016). Iron Sulfide and Removal in Scale Formation Sour Gas Wells. In *SPE International Oilfield Scale Conference and Exhibition held in Aberdeen, Scotland, UK, 11–12 May*
- Lewis, D. R., Aramco, S., Zainalabedin, K. A., Aramco, S., & Aramco, S. (2003). SPE 81569 Scale Mitigation Enhances Safety and Production, 1–8.
- Mackay, E. J., Jordan, M. M., & Torabi, F. (2003). Predicting Brine Mixing Deep Within the Reservoir and Its Impact on Scale Control in Marginal and Deepwater Developments. *SPE Production & Facilities*, 18(3), 210–220. <https://doi.org/10.2118/85104-PA>
- Mahmoud, M. A., Kamal, M. S., & Geri, B. S. B. (2015). Removal of Pyrite and Different Types of Iron Sulfide Scales in Oil and Gas Wells without H<sub>2</sub>S Generation. *International Petroleum Technology Conference Held in Doha, Qatar, 6–9 December*.
- Merdhah, A. B., & Yassin, A. (2008). Formation damage due to scale formation in porous media resulting water injection. system, 14, 15.
- Mirza, M. S., Prasad, V., & Company, O. (1999). SPE 53345 Scale Removal in Khuff Gas Wells.

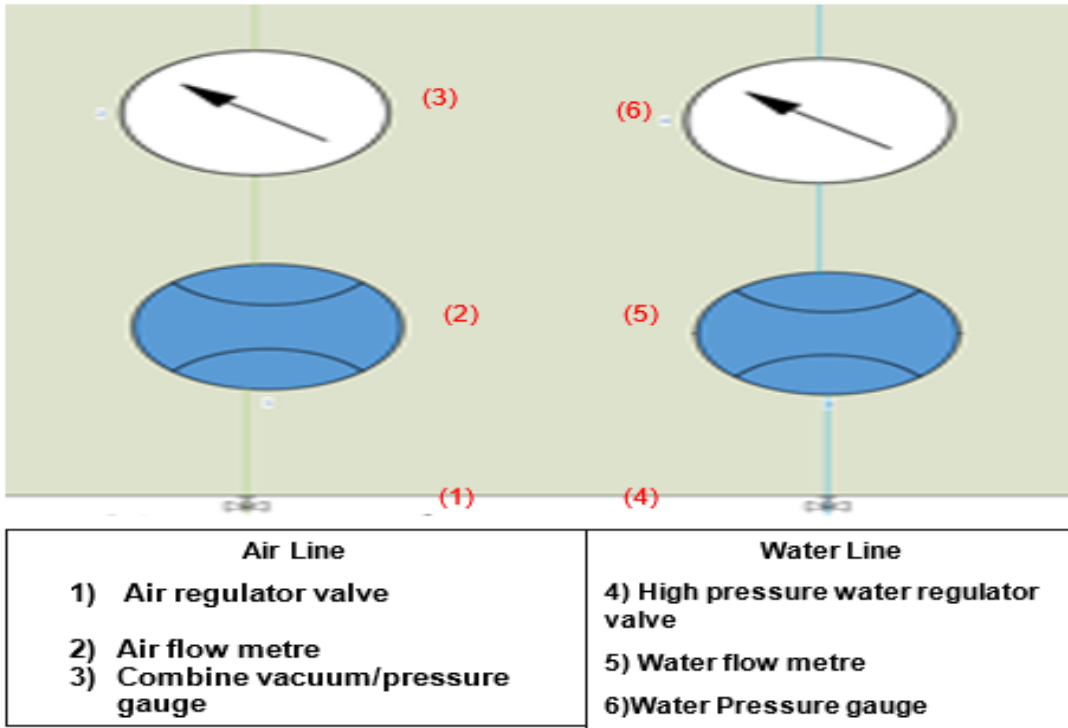
- Moghadasi, J., Jamialahmadi, M., Muller-Steinhagen, H., Sharif, a, Ghalambor, a, Izadpanah, M. R., & Motaie, E. (2003). Scale formation in Iranian oil reservoir and production equipment during water injection. *International Oilfield Scale Symposium and Exhibition*, 1–14. <https://doi.org/10.2118/80406-MS>
- Moradpour, M., Zamani, Z., & Moallemi, S. (2008). Controls on reservoir quality in the lower Triassic Kangan formation, southern Persian Gulf. *Journal of Petroleum Geology*, 31(4), 367-385.
- M. Qin, D. Y. Ju, and R. Oba, “Improvement on the process capability of water cavitation peening by aeration,” *Surf. Coatings Technol.*, vol. 200, no. 18–19, pp. 5364–5369, May 2006.
- Zongyi, “Investigation of the cavitation mechanism and erosion of submerged high pressure water jets,” University of Queensland, 2004.
- Mukhliss, A. E., Ogundare, T. M., Dashash, A. A., Malik, A. R., Aramco, S., Rivadeneira, E. V, & Molero, N. (2014). A Novel Non-damaging Approach to Isolate Open hole Lateral that Allowed Performing Mechanical Descaling in the Non-Monobore Cased Completion : A Case Study in Saudi Arabian Carbonate Reservoir, 1–9.
- Nasr-El-Din, H. A., Fadhel, B. A., Al-Humaidan, A. Y., Frenier, W. W., & Hill, D. (2000). An Experimental Study of Removing Iron Sulfide Scale from Well Tubulars. Paper presented at the International Symposium on Oilfield Scale, Aberdeen, United Kingdom. <https://doi.org/10.2118/60205-MS>
- Nasr, G. G., Enyi, G. G., El-Kamki, M. E., & Burby. (2012). Characterisation of Flat fan sprays for petroleum applications. *Institution of Liquid Atomization and Sprays Systems*, pp. 7–10.
- Nejad, A. M. and Karimi, M. S. (2017). “Investigation of the influence of scaling on corrosion behaviour of tubing in oil wells”, *Int. J. Sci. Tech. Res.* 6, 5, 109-113.
- Nourian, A. (2016). High Pressure Overlapping Flat Sprays Nozzles HIGH PRESSURE OVERLAPPING FLAT SPRAYS NOZZLES, (September 2010).
- Quiroga, M. H. V, Calmeto, J. C. N., Pinto, S. L., Assis, C. A. S., & Santos, I. (2003). SPE 89627 Hard Scale Mechanical Removal : A Solution for Brazilian Offshore Operations, (May), 1–6.
- Oddo, J., & Tomson, M. (1994). Why scale forms in the oil field and methods to predict it. *SPE Production & Facilities*, 9(01), 47-54.
- Okocha, C., & Sorbie, K. (2014). Sulphide Scale Co-Precipitation with Calcium Carbonate. Paper presented at the SPE International Symposium and Exhibition on Formation Damage Control.
- Peng, Y. and Guo, Z. (2017). “On the sweet corrosion of oil and gas wells”, *International Journal of Science and Engineering Investigations.* 6, 64, 25-27.
- Pinango, J. (2003). Design Simulation of a Presurized Test Facility and Application Of CFD. University of Salford,
- Q. Zongyi, “Investigation of the cavitation mechanism and erosion of submerged high-pressure water jets,” University of Queensland, 2004.

- Quiroga, M., Calmeto, J., Pinto, S., Assis, C., & Santos, I. (2004). Hard Scale Mechanical Removal: A Solution for Brazilian Offshore Operations. Paper presented at the SPE/ICoTA Coiled Tubing Conference and Exhibition.
- Onwusiri, H., Onwuzurike, C., Abiodun, A., & Uchendu, C. (2003). Rotating jetting nozzle adds value in the cleanup of horizontally gravel packed well-case histories from sandstone environment. Paper presented at the SPE European Formation Damage Conference.
- Ramachandran, S., Al-Muntasheri, G., Leal, J., & Wang, Q. (2015). Corrosion and Scale Formation in High Temperature Sour Gas Wells: Chemistry and Field Practice. *SPE International Symposium on Oilfield Chemistry*. <https://doi.org/10.2118/173713-MS>
- Ramones, M., Rachid, R., Flor, D., Gutierrez, L., & Milne, A. (2015). Removal of Organic and Inorganic Scale from Electric Submersible Pumps. *SPE Artificial Lift Conference — Latin America and Caribbean*, (May), 27–28. <https://doi.org/10.2118/173928-MS>
- Restivo, A., Brune, M., & International, O. (2016). Removing Marine Growth Using an ROV with Cavitation Technology, (May), 2–5.
- Shar, A. H., Ahmad, T., & Bregar, U. B. (2010). Scale buildup, its detection and removal in high temperature gas wells of miano field. Paper presented at the SPE Production and Operations Conference and Exhibition.
- Shepherd, A., Thomson, G., Westacott, R., Sorbie, K., Turner, M., & Smith, P. (2006). Analysis of organic field deposits: new types of calcium naphthenate scale or the effect of chemical treatment? Paper presented at the SPE International Oilfield Scale Symposium.
- Salami, A. R. Al, Monem, A. A., Development, Z., & Zadco, C. (2010). SPE 137906 Downhole and Topside Scale Challenge “ Removal , Prevention and Inhibition Strategy
- Smith, P. S., Jr, C. C. C., Amoco, B. P., Rojas, a M., & Instituto, E. (2000). SPE 60222 Combined Scale Removal and Scale Inhibition Treatments. *Adsorption Journal Of The International Adsorption Society*. <https://doi.org/10.2523/60222-MS>
- Schlumberger. (2018). Scale control: Remove and control scale buildup. Retrieved from [http://www.slb.com/services/completions/stimulation/sandstone/scale\\_control.aspx](http://www.slb.com/services/completions/stimulation/sandstone/scale_control.aspx)
- Sopngwi, J. S., Gauthreaux, A., Kiburz, D. E., Oil, M., Sonnier, B., Moghalu, D., & Smith, S. K. (2014). SPE 168255 Successful Mechanical Removal of Barium Sulfate Tubular Scale by Coiled Tubing : A Gulf of Mexico Case History of an Engineered Approach for Offshore Rigless Interventions.
- Spraying system, “Atomization droplet distribution,” 2018. [Online]. Available: <http://www.spraying system.co.uk/spray-nozzles/flat-fan-nozzles/air-actuated>. [Accessed: 18-Jun- 2018].
- Spraying system, “Specific gravity conversion graph,” 2018. [Online]. Available: <http://www.spraying system.co.uk/spray-nozzles/flat-fan-nozzles/air-actuated>. [Accessed: 19-Jun-2018].

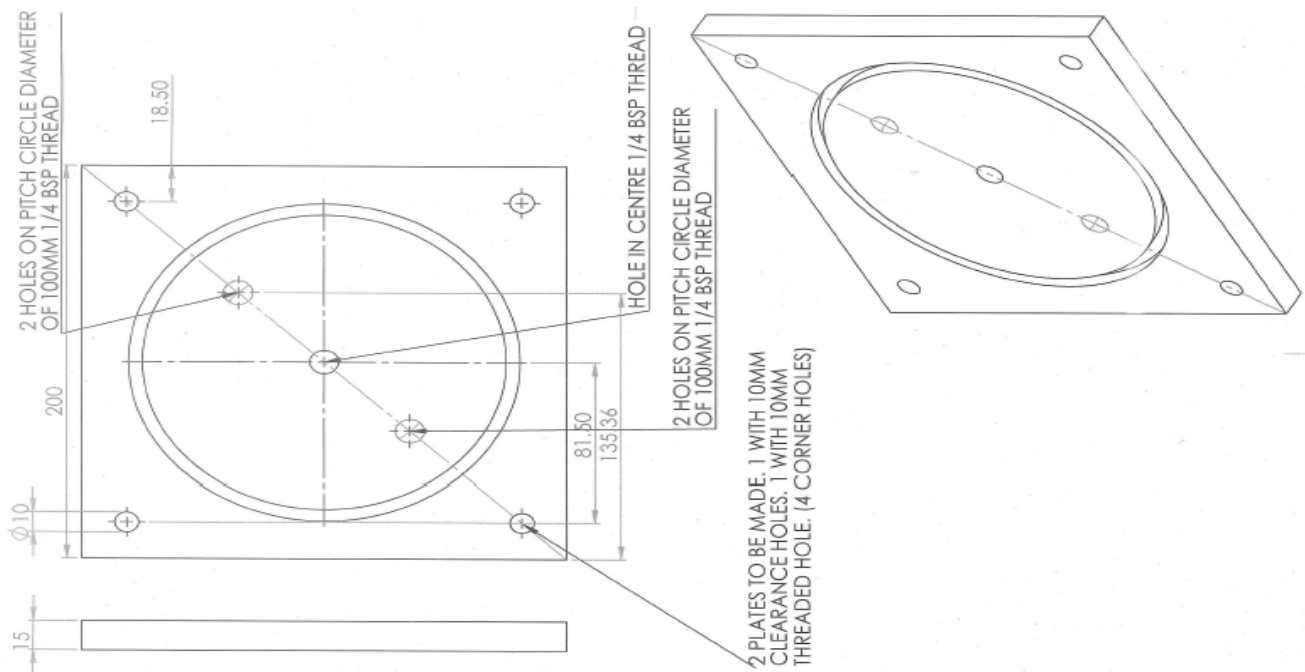
- Spraying system, "Relative droplet sizes by nozzles series," 2018. [Online]. Available: <http://www.spraying-system.co.uk/spray-nozzles/flat-fan-nozzles/air-actuated>. [Accessed: 19-Jun-2018].
- Stalker, R., Collins, I. R., & Graham, G. M. (2003). *The impact of chemical incompatibilities in commingled fluids on the efficiency of a produced water reinjection system: A North Sea example*. Paper presented at the International Symposium on Oilfield Chemistry.
- Sutherland, L., Johnston, C. J., & Taylor, W. (2013). *The influence of turbulence (or Hydrodynamic Effects) on barium sulphate scale formation and inhibitor performance*. Paper presented at the SPE International Symposium on Oilfield Chemistry.
- Spe, T. H. P., Fajt, J. R., Danilov, A. G., Swaco, M., Company, S., Spe, B. B., & Texas, A. (2013). SPE 163803 Aeration and Microfiltration for Solids Removal of Produced Waters from the Barnett Shale, (Marjani 2009).
- Taheri, A., Masoudi, R., Zahedzadeh, M., Ataei, A., & Fakhri, H. (2008). Simulation and experimental studies of mineral scale formation effects on performance of an Iranian carbonate oil reservoir under water injection. Paper presented at the SPE International Oilfield Scale Conference.
- Todd, A., & Yuan, M. (1992). Barium and strontium sulfate solid-solution scale
- Wang, Q., Leal, J., Syafii, I., Mukhles, A. E., Chen, T., Chang, F., & Espinosa, M. (2016). Iron Sulfide and Removal in Scale Formation Sour Gas Wells.
- Wang, X., Qu, Q., Berry, S., Cutler, J., & Hughes, B. (2013). SPE 165199 Iron Sulfide Removal : A Nonacidic Alternative to Hydrochloric Acid Treatment. *SPE European Formation Damage Conference & Exhibition*.
- Webb, P. J. C., Nistad, T. A., Knapstad, B., Ravenscroft, P. D., & Collins, I. R. (1999). Advantages of a New Chemical Delivery System for Fractured and Gravel- Packed Wells. *SPE Production & Facilities*, 14(03), 210-218. doi:10.2118/57421-PA
- Yuan, M., Jamieson, E., & Hammonds, P. (1998). Investigation of scaling and inhibition mechanisms and the influencing factors in static and dynamic inhibition tests. Paper presented at the CORROSION 98.
- Yusuf, A., Al-Hajiri, R.S., Al-Waheibi, Y.M., Jibril, B.Y., 2016b, 'In-situ upgrading of Omani Heavy Oil with Catalyst and Hydrogen Donor', *J Anal Appl Pyrol.*, 121.102-112
- Zhang, P., Allan, K., & Hugh, B. (2015). SPE-173747-MS Selection of Calcium Carbonate Scale Critical Values for Deepwater Production, 1–9.

# Appendices

## Appendix A

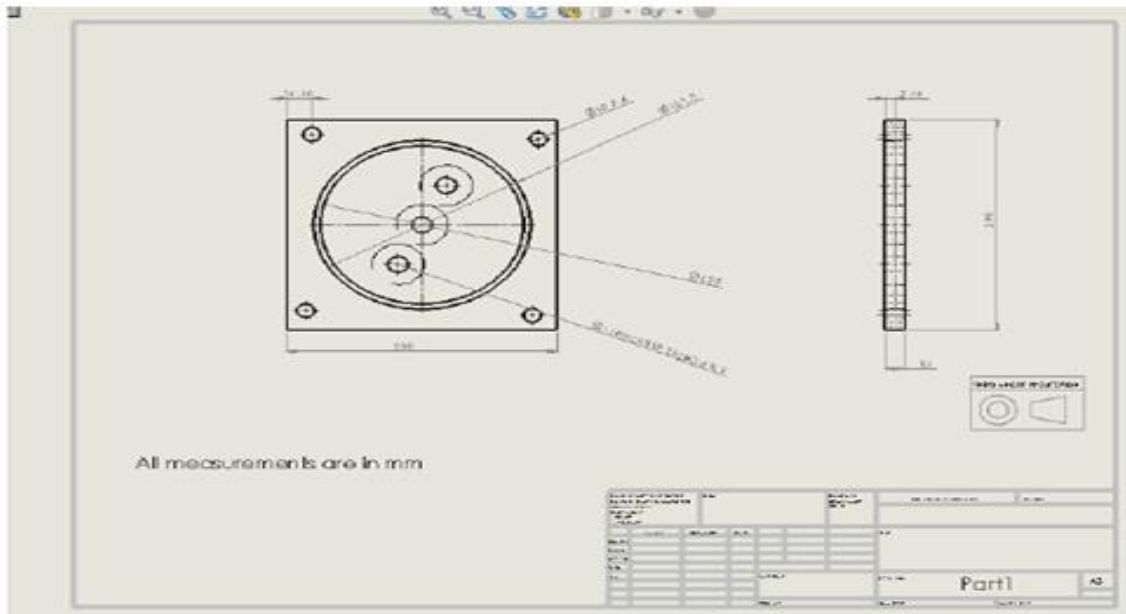


Appendix A 1: Schematic of the designed control board using Visio



Appendix A 2: 2D Design of metal plate using Solid works software





Appendix A 5: Bottom and Top metal plate 2D solid works design

Appendix A 6: Clear Acrylic tube (a) vendors specifications and (b) 2-meter length clear acrylic tube with a 2.25m measuring ruler

(a)

### MECHANICAL PROPERTIES

#### Extruded Acrylic Tube (Clear)

This data applies to the raw material used during production of our Extruded Acrylic Tube

PROPERTIES	UNIT	DIN No	Acrylic (PMMA)
Density	g/cm <sup>3</sup>	53 479	1.18
Impact Strength	KJ/m <sup>2</sup>	53 453	11
Notched Impact Strength	KJ/m <sup>2</sup>	53 453	2
Expansion	1/°C		
Refractive Index (20°C)	nD	53 491	1.49
Modulus of Elasticity	N/mm <sup>2</sup>	53 457	3300
Heat Distortion Temp (Vicat B)	°C	53 460	100
Constant Working Temp. (in air without mechanical force being applied)	°C		75
Flammability		4102 Part 1	82
Flammability (UL 94)			H0
Light Transmission	%		92

b



(a)

**OVERVIEW: WASHJET**

- High-impact sprays and high pressure operation ensure optimal cleaning – ideal for pressure washing
  - Long wear life – 400 series stainless steel material
  - Flat spray nozzles provide an even edge fan type spray pattern
  - Uniform spray distribution from 27 to 70 gpm (1.0 to 2.6 lpm) by using optional internal guide vane to stabilize liquid turbulence
  - Spray angles from 1° (solid stream) to 65° for MEG, MEG and MEG-SSTC; 4° to 80° for IEG
  - Operating pressures from 300 to 4000 psi (20 to 275 bar)
  - MEG-SSTC nozzles have tungsten carbide orifice inserts for maximum erosion resistance
  - IEG® versions are ideal for critical, demanding operations
- Features:
- Patented design that optimizes fluid dynamics by minimizing turbulence
  - Higher impact per unit area than MEG nozzles

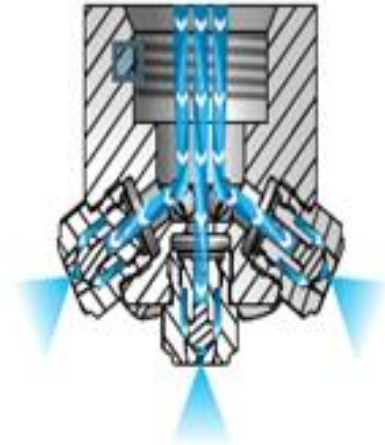


**WashJet Nozzles**  
As the liquid exits through the rounded lip shape of the orifice, it forms into a fan spray pattern. The distribution is even at pressures above 300 psi (20 bar).

(b)

**FogJet Nozzles**

The liquid passes through slots in the core component in each individual nozzle cap. The slots make the liquid spin in a circle at a very high speed. The energy from the spinning action causes the liquid to break up into very small droplets and form a hollow cone pattern as it exits the orifice.



Appendix A 7 : Wash jet operational crosssection (a) atomiser,(b) header over view

(a)



(b)

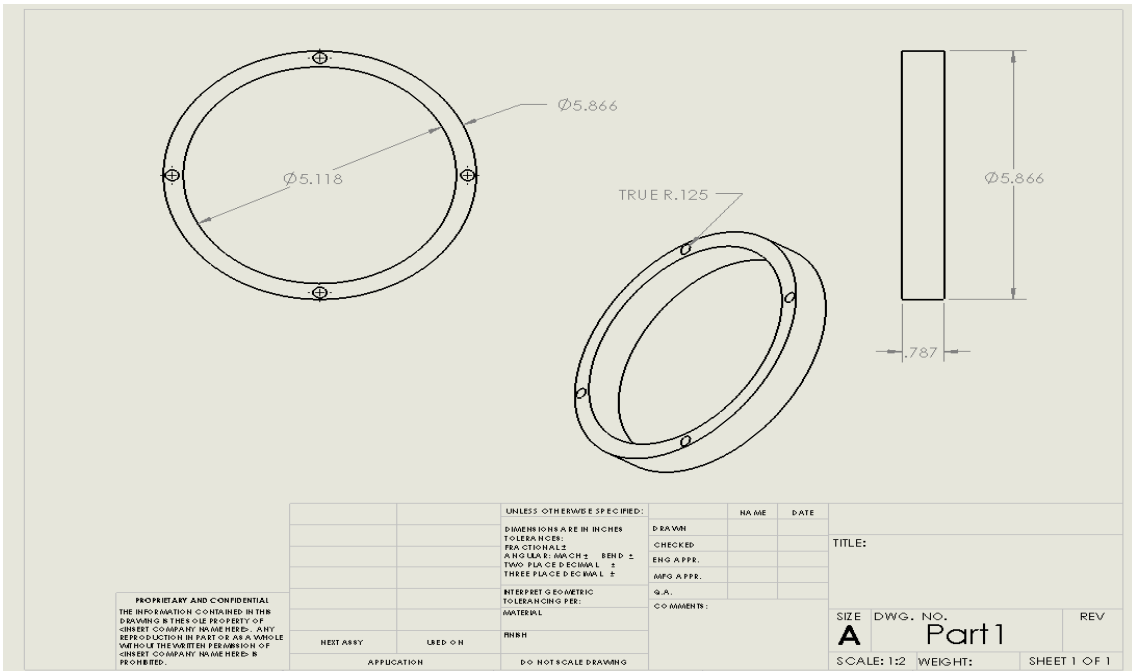


Appendix A 8: Picture of (a) replaced air mist nozzles and (b) blank plug

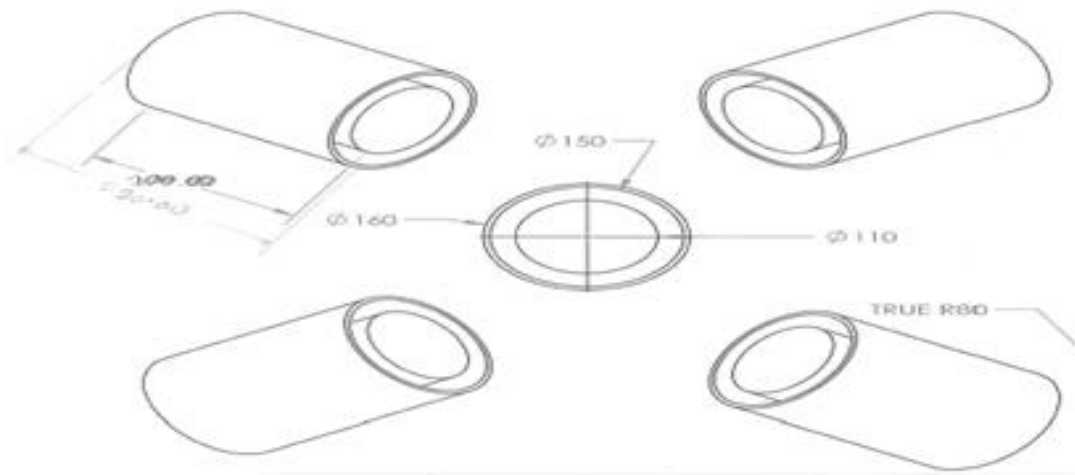


Appendix A 11 List of fittings used in assembling the chamber

S/N	Catalogue number	Discription	Quantity	Connection
1	SS-810-1-4RP	Male connector 1/2" OD X 1/4" BSPP	1	Main fog jet header connector
2	SS-400-R-6	Tube Fitting, Reducer, 1/4 in. x 3/8 in. Tube OD	1	Reducer from connector to tube
3	SS-600-1-16	Tube Fitting, Male Connector, 3/8 in. Tube OD x 1 in. Male NPT	1	Reducer to connector union
4	SS-810-1-16	Tube Fitting, Male Connector, 1/2 in. Tube OD x 1 in. Male NPT	1	1/2 inch tube to reducer
5	SS-400-1-4RP	Tube Fitting, Male Connector, 1/4 in. Tube OD x 1/4 in. Male ISO Parallel Thread	1	1/4 inch tube to reducer
6	SS-400-6	SS Swagelok Tube Fitting, Union, 1/4 in. Tube OD	3	Stand off distance adjustment for 1/4 inch tube
7	SS-810-6	Tube Fitting, Union, 1/2 in. Tube OD	3	Stand off distance adjustment for 1/2 inch tube.
8	CU-4-RP-2	Copper Gasket for 1/4 in. ISO Parallel Thread (RP) Fittings	10	1/4 inch tube seal for adjustment
9	CU-8-RP-2	Copper Gasket for 1/2 in. ISO Parallel Thread (RP) Fittings	10	1/2 inch tube seal for adjustment



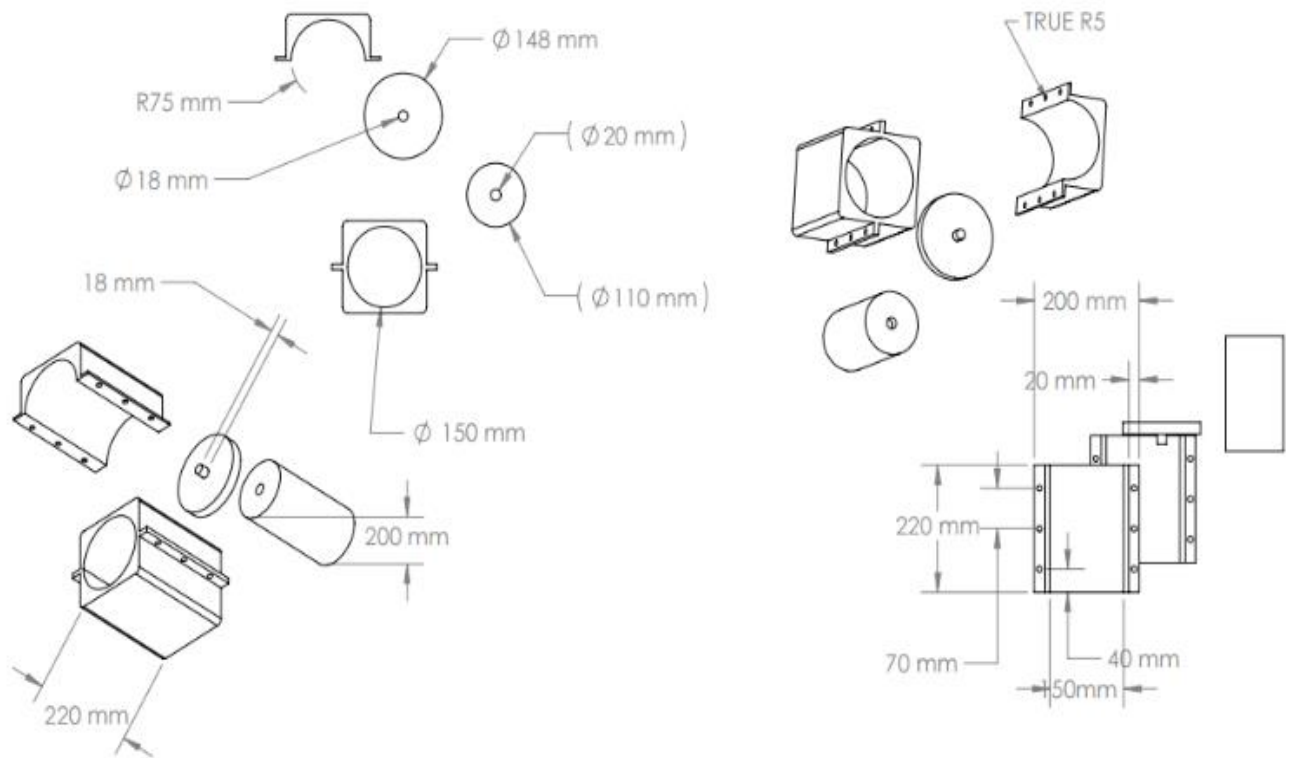
Appendix A 12: Wax holder solid works design



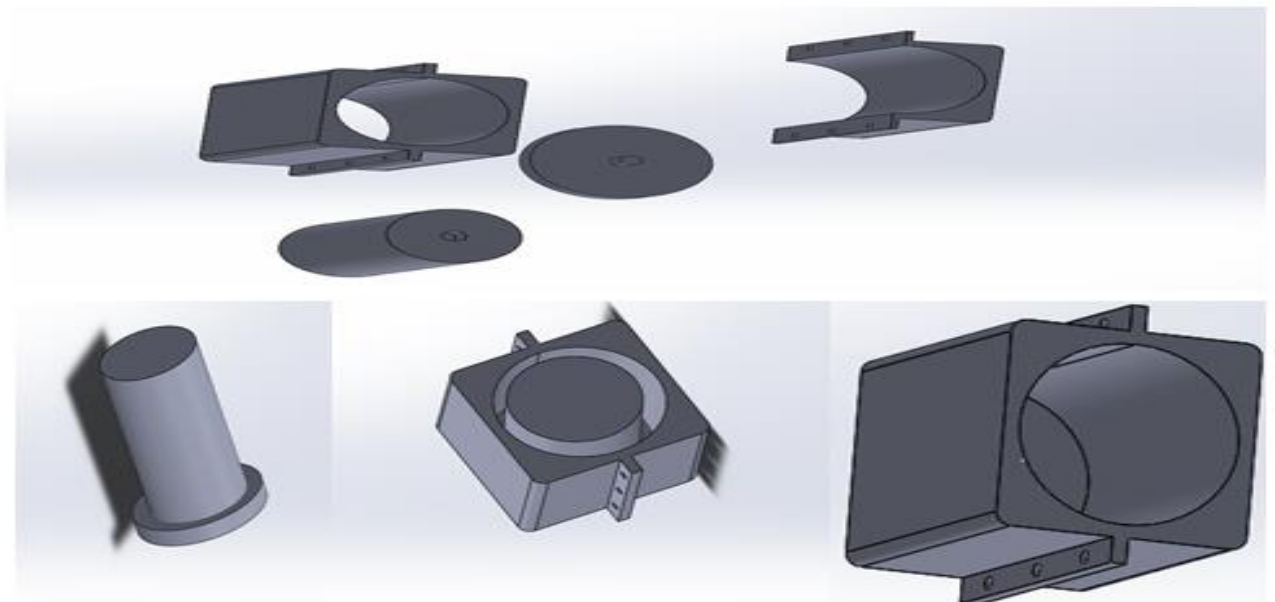
Appendix A 13: Scale moulder 2D solid works design



Appendix A 14 Scale moulder 3D solid works design



Appendix A 15: 3D scale mouler solid works design



Appendix A 16: 3D scale mouler design in solid works

## APPENDIX B

Appendix B 1: EDX quantitative result for sample A

kV:15.00	Tilt: 0.00	Take-off:34.61	AmpT:6.4			
Detector T	Resolution :133.78	Lsec :50				
EDAX ZAF Standardless						
Element Normalized						
SEC Table : User						
Element	Wt %	At %	K-Ratio	Z	A	F
C K	11.72	26.61	0.0174	1.1446	0.1293	1.0002
O K	29.88	50.92	0.08	1.1224	0.2386	1.0002
SrL	43.12	13.42	0.3574	0.8424	0.9819	1.0022
S K	8.7	7.4	0.0634	1.0627	0.6847	1.0006
CaK	0.73	0.5	0.0068	1.0394	0.8949	1.0034
BaL	5.85	1.16	0.0451	0.7702	1.0022	1
Total	100	100				
Element	Net Inte.	Bkgd Inte.	Inte. Error	P/B		
C K	41.24	8.38	2.61	4.92		
O K	332.64	14.38	0.81	23.13		
SrL	902.08	36.9	0.49	24.45		
S K	458.54	28.36	0.7	16.17		
CaK	16.04	21	6.72	0.76		
BaL	36.34	18.5	3.33	1.96		

Appendix B 2: Flow rate measurement

		During build-up		After build-up		
Number of nozzles	Pressure (MPa)	Average time (s)	Average mass of water (kg)	Time (s)	Average mass of water (kg)	Mass flow rate (kg/s)
5	4.8	21	14.81	120	52.09	0.434
	6	21	17.56	120	55.44	0.462
	10	23	15.79	120	91.81	0.765
4	4.8	5	3.58	120	45.22	0.377
	6	23	15.37	120	49.33	0.411
	10	31	15.00	120	72.90	0.608
3	4.8	22	11.63	120	36.77	0.306
	6	10	7.40	120	37.50	0.313
	10	61	18.79	120	42.41	0.353

## APPENDIX C



Appendix C 1: Descaling remark guide for hard and soft scale samples

Appendix C 2: Ambient descaling result for hollow samples

Number of nozzles	Injection pressure (MPa)	Mass flow rate (Kg/s)	Stand-off distance (mm)	Scale reference	Mass of scale before (kg)	Mass of scale after (Kg)	Mass of scale removed	Descaling time	Remark
5	4.8	0.434	25	18-SH	0.5415	0.5401	0.0014	3 min	Eroded
			50	1-SH	0.5383	0.5369	0.0014	3 min	Eroded
	6	0.462	25	20-SH	0.5399	0.5357	0.0042	3min	Eroded
			50	9- SH	0.4894	0.4872	0.0022	3min	Hole
	10	0.765	25	4- SH	0.5689	0.5106	0.0583	3 min	Hole
			50	19-SH	0.5469	0.4978	0.0491	3 min	Eroded
4	4.8	0.377	25	17-SH	0.5731	0.5714	0.0017	3 min	Eroded
			50	2- SH	0.534	0.5324	0.0016	3 min	Hole
	6	0.411	25	6- SH	0.5623	0.5396	0.0227	3 min	Hole
			50	8- SH	0.5321	0.5203	0.0118	3 min	Hole
	10	0.608	25	14- SH	0.5236	0.447	0.0766	3 min	Crack
			50	7- SH	0.6001	0.5298	0.0703	3 min	Hole
3	4.8	0.313	25	10- SH	0.5929	0.527	0.0659	3 min	Broken
			50	11- SH	0.5809	0.5181	0.0628	3 min	Broken
	6	0.306	25	15- SH	0.6597	0.526	0.1337	3 min	Broken
			50	13-SH	0.5807	0.4732	0.1075	3 min	Broken
	10	0.353	25	21-SH	0.5177	0.2639	0.2538	3 min	Broken
			50	12-SH	0.5535	0.3375	0.216	3 min	Broken

Appendix C 3: Ambient descaling result for solid scale samples

Number of nozzles	Injection pressure (MPa)	Mass flow rate (Kg/s)	Stand-off distance (mm)	Scale reference	Mass of scale before (kg)	Mass of scale after (Kg)	Mass of scale removed	Descaling time (s)	Remark
5	4.8	0.434	25	5-SS	0.6428	0.6421	0.0007	180	Eroded
			50	4-SS	0.6591	0.658	0.0011	180	Hole
	6	0.462	25	6-SS	0.5623	0.5604	0.0019	180	Hole
			50	11-SS	0.5258	0.5237	0.0021	180	Hole
	10	0.765	25	13-SS	0.581	0.568	0.013	180	Hole
			50	12-SS	0.5881	0.5682	0.0199	180	Hole
4	4.8	0.377	25	7-SS	0.5312	0.5304	0.0008	180	Hole
			50	14-SS	0.5339	0.5327	0.0012	180	Hole
	6	0.411	25	9-SS	0.6056	0.6035	0.0021	180	Hole
			50	8-SS	0.5689	0.5666	0.0023	180	Eroded
	10	0.608	25	16-SS	0.5308	0.5015	0.0293	180	Hole
			50	3-SS	0.6001	0.5537	0.0464	180	Hole
3	4.8	0.313	25	1-SS	0.4854	0.4845	0.0009	180	Eroded
			50	10-SS	0.5805	0.5792	0.0013	180	Eroded
	6	0.306	25	2-SS	0.5331	0.5307	0.0024	180	Eroded
			50	12-SS	0.6326	0.6298	0.0028	180	Hole
	10	0.353	25	18-SS	0.524	0.4733	0.0507	180	Hole
			50	15-SS	0.587	0.501	0.086	180	Hole

Appendix C 4: Ambient descaling results for SrSO<sub>4</sub> samples

Number of nozzles	Injection pressure (MPa)	Mass flow rate (Kg/s)	Stand-off distance (mm)	Scale reference	Mass of scale before (kg)	Mass of scale after (Kg)	Mass of scale removed (Kg)	Descaling time (S)	Remark
5	4.8	0.434	25	10-HSr	0.6104	0.6097	0.0007	180	Eroded
			50	1-HSr	0.4834	0.4826	0.0008	180	Eroded
	6	0.462	25	11-HSr	0.6082	0.6066	0.0016	180	Eroded
			50	8-HSr	0.6121	0.6104	0.0017	180	Eroded
	10	0.765	25	12-HSr	0.6081	0.6052	0.0029	180	Eroded
			50	5-HSr	0.4876	0.4844	0.0032	180	Eroded
4	4.8	0.377	25	13-HSr	0.6098	0.6089	0.0009	180	Eroded
			50	6-HSr	0.4844	0.4834	0.001	180	Eroded
	6	0.411	25	14-HSr	0.6083	0.6067	0.0016	180	Eroded
			50	4-HSr	0.5552	0.5534	0.0018	180	Eroded
	10	0.608	25	15-HSr	0.610	0.6059	0.0041	180	Eroded
			50	2-HSr	0.4829	0.478	0.0049	180	Broken
3	4.8	0.313	25	16-HSr	0.6124	0.6113	0.0011	180	Eroded
			50	9-HSr	0.6118	0.6105	0.0013	180	Eroded
	6	0.306	25	17-HSr	0.6092	0.6075	0.0017	180	Eroded
			50	7-HSr	0.612	0.61	0.002	180	Eroded
	10	0.353	25	18-HSr	0.611	0.6061	0.0049	180	Broken
			50	3-HSr	0.5614	0.5562	0.0052	180	Broken

Appendix C 5: Ambient descaling result for CaCO<sub>3</sub> samples

Number of nozzles	Injection pressure (MPa)	Mass flow rate (Kg/s)	Stand-off distance (mm)	Scale reference	Mass of scale before (kg)	Mass of scale after (Kg)	Mass of scale removed (Kg)	Descaling time (s)	Remark
5	4.8	0.434	25	10-HB <sub>a</sub>	0.4635	0.4631	0.0004	180	Eroded
			50	1-HB <sub>a</sub>	0.3534	0.3528	0.0006	180	Eroded
	6	0.462	25	11-HB <sub>a</sub>	0.3475	0.3467	0.0008	180	Eroded
			50	8-HB <sub>a</sub>	0.355	0.354	0.001	180	Eroded
	10	0.765	25	12-HB <sub>a</sub>	0.4450	0.4439	0.0011	180	Eroded
			50	7-HB <sub>a</sub>	0.3547	0.3536	0.0011	180	Eroded
4	4.8	0.377	25	13-HB <sub>a</sub>	0.4495	0.4489	0.0006	180	Eroded
			50	3-HB <sub>a</sub>	0.3483	0.3476	0.0007	180	Eroded
	6	0.411	25	14-HB <sub>a</sub>	0.3531	0.3521	0.001	180	Eroded
			50	9-HB <sub>a</sub>	0.4651	0.464	0.0011	180	Eroded
	10	0.608	25	15-HB <sub>a</sub>	0.4456	0.4433	0.0023	180	Eroded
			50	2-HB <sub>a</sub>	0.3526	0.3525	0.0028	180	Eroded
3	4.8	0.313	25	16-HB <sub>a</sub>	0.4645	0.4449	0.0007	180	Eroded
			50	5-HB <sub>a</sub>	0.3526	0.3517	0.0009	180	Eroded
	6	0.306	25	17-HB <sub>a</sub>	0.3484	0.3469	0.0015	180	Eroded
			50	6-HB <sub>a</sub>	0.3526	0.3526	0.0018	180	Eroded
	10	0.353	25	18-HB <sub>a</sub>	0.465	0.4619	0.0031	180	Eroded
			50	4-HB <sub>a</sub>	0.3526	0.3482	0.0044	180	Eroded

Appendix C 6: Compressed descaling results for hollow soft samples

Number of nozzles	Injection pressure (MPa)	Mass flow rate (kg/s)	Stand-off distance (mm)	Scale reference	Mass of scale before (kg)	Mass of scale after (Kg)	Mass of scale removed (Kg)	Descaling time (S)	Remark
5	4.8	4.8	25	1-SHA	0.5389	0.5338	0.0051	180	Eroded
			50	5-SHA	0.5193	0.514	0.0053	180	Hole
	6	6	25	2-SHA	0.51	0.5044	0.0056	180	Eroded
			50	4-SHA	0.5714	0.566	0.0054	180	Eroded
	10	10	25	3-SHA	0.5379	0.4716	0.0663	180	Broken
			50	9-SHA	0.5291	0.4707	0.0584	180	Hole Perf
4	4.8	4.8	25	10-SHA	0.5386	0.511	0.0276	180	Eroded
			50	8-SHA	0.5192	0.4918	0.0274	180	Eroded
	6	6	25	7-SHA	0.51	0.476	0.034	180	Hole Perf
			50	11-SHA	0.5713	0.5383	0.033	180	Hole
	10	10	25	6-SHA	0.5401	0.4037	0.1364	180	Broken
			50	12-SHA	0.5081	0.3999	0.1082	180	Broken
3	4.8	4.8	25	14-SHA	0.506	0.4496	0.0764	180	Hole
			50	18-SHA	0.5297	0.4537	0.076	180	Crack
	6	6	25	16-SHA	0.526	0.3476	0.1584	180	Eroded
			50	15-SHA	0.5161	0.5022	0.0139	180	Hole
	10	10	25	17-SHA	0.5912	0.293	0.2982	180	Hole
			50	13-SHA	0.5316	0.3034	0.2282	180	Broken

Appendix C 7: Compressed descaling results for solid soft samples

Number of nozzles	Injection pressure (MPa)	Mass flow rate (Kg/s)	Stand-off distance (mm)	Scale reference	Mass of scale before (kg)	Mass of scale after (Kg)	Mass of scale removed (Kg)	Descaling time (s)	Remark
5	4.8	0.434	25	8-SSA	0.531	0.5298	0.0012	180	Eroded
			50	5-SSA	0.5054	0.5041	0.0013	180	Eroded
	6.0	0.462	25	1-SSA	0.6142	0.6119	0.0023	180	Hole
			50	4-SSA	0.5395	0.537	0.0025	180	Hole
	10	0.765	25	15-SSA	0.5797	0.572	0.077	180	Hole
			50	10-SSA	0.592	0.5101	0.0819	180	Broken
4	4.8	0.377	25	17-SSA	0.552	0.5507	0.0013	180	Eroded
			50	7-SSA	0.5537	0.5523	0.0014	180	Eroded
	6.0	0.411	25	9-SSA	0.5604	0.5572	0.0032	180	Hole
			50	16-SSA	0.5534	0.5486	0.0048	180	Hole
	10	0.608	25	12-SSA	0.5535	0.4517	0.1018	180	Broken
			50	13-SSA	0.5807	0.4355	0.1452	180	Broken
3	4.8	0.313	25	2-SSA	0.5761	0.5671	0.0098	180	Eroded
			50	11-SSA	0.589	0.577	0.012	180	Hole
	6.0	0.306	25	18-SSA	0.531	0.473	0.058	180	Hole
			50	6-SSA	0.4573	0.3603	0.097	180	Broken
	10	0.353	25	3-SSA	0.6023	0.4062	0.1961	180	Broken
			50	14-SSA	0.523	0.3231	0.1999	180	Broken

Appendix C 8: Compressed descaling results for SrSO<sub>4</sub> samples

Number of nozzles	Injection pressure (MPa)	Mass flow rate (Kg/s)	Stand-off distance (mm)	Scale reference	Mass of scale before (kg)	Mass of scale after (Kg)	Mass of scale removed (Kg)	Descaling time (S)	Remark
5	4.8	0.434	25	10-SHA	0.4784	0.4772	0.0012	180	Eroded
			50	1-SHA	0.4773	0.4759	0.0014	180	Eroded
	6.0	0.462	25	11-HBA	0.6117	0.6089	0.0028	180	Eroded
			50	5-SHA	0.6192	0.6161	0.0031	180	Eroded
	10	0.765	25	12-SHA	0.6125	0.6088	0.0037	180	Eroded
			50	3-SHA	0.6175	0.6134	0.0041	180	Eroded
4	4.8	0.377	25	13-SHA	0.4782	0.4769	0.0013	180	Eroded
			50	2-SHA	0.6119	0.6104	0.0015	180	Eroded
	6.0	0.411	25	14-SHA	0.6128	0.6096	0.0032	180	Eroded
			50	2-SHA	0.4781	0.4745	0.0036	180	Eroded
	10	0.608	25	15-SHA	0.6118	0.6077	0.0041	180	Eroded
			50	6-SHA	0.6157	0.6114	0.0043	180	Eroded
3	4.8	0.313	25	16-SHA	0.4782	0.4765	0.0017	180	Eroded
			50	7-SHA	0.4781	0.4762	0.0019	180	Eroded
	6.0	0.306	25	17-SHA	0.6122	0.6087	0.0035	180	Eroded
			50	9-SHA	0.6121	0.6082	0.0039	180	Eroded
	10	0.353	25	18-SHA	0.6121	0.607	0.0051	180	Broken
			50	8-SHA	0.6123	0.6069	0.0054	180	Broken

Appendix C 9: Compressed descaling result for CaCO<sub>3</sub> samples

Number of nozzles	Injection pressure (MPa)	Mass flow rate (Kg/s)	Stand-off distance (mm)	Scale reference	Mass of scale before (kg)	Mass of scale after (Kg)	Mass of scale removed (Kg)	Descaling time (S)	Remark
5	4.8	0.434	25	10-HBA	0.466	0.3538	0.0011	180	Eroded
			50	6-HBA	0.3549	0.4647	0.0013	180	Eroded
	6.0	0.462	25	11-HBA	0.4523	0.3516	0.0024	180	Eroded
			50	5-HBA	0.354	0.4497	0.0026	180	Eroded
	10	0.765	25	12-HBA	0.3561	0.3529	0.0032	180	Eroded
			50	3-HBA	0.4503	0.4467	0.0036	180	Eroded
4	4.8	0.377	25	13-HBA	0.348	0.3538	0.0013	180	Eroded
			50	9-HBA	0.3551	0.3466	0.0014	180	Eroded
	6.0	0.411	25	14-HBA	0.4663	0.4636	0.0027	180	Eroded
			50	8-HBA	0.3551	0.3478	0.0032	180	Eroded
	10	0.608	25	15-HBA	0.4519	0.3523	0.0037	180	Eroded
			50	4-HBA	0.4512	0.4601	0.0041	180	Eroded
3	4.8	0.313	25	16-HBA	0.3561	0.3546	0.0015	180	Eroded
			50	7-HBA	0.3479	0.3462	0.0017	180	Eroded
	6.0	0.306	25	17-HBA	0.348	0.4606	0.0033	180	Eroded
			50	1-HBA	0.4639	0.3445	0.0035	180	Eroded
	10	0.353	25	18-HBA	0.356	0.448	0.0039	180	Eroded
			50	2-HBA	0.4642	0.4469	0.0043	180	Eroded

Appendix C 10: Vacuumed descaling results for hollow soft samples

Number of nozzles	Injection pressure (MPa)	Mass flow rate (Kg/s)	Stand-off distance (mm)	Scale reference	Mass of scale before (kg)	Mass of scale after (Kg)	Mass of scale removed (Kg)	Descaling time (S)	Remark
5	4.8	0.434	25	10-HBA	0.466	0.3538	0.0011	180	Eroded
			50	6-HBA	0.3549	0.4647	0.0013	180	Eroded
	6.0	0.462	25	11-HBA	0.4523	0.3516	0.0024	180	Eroded
			50	5-HBA	0.354	0.4497	0.0026	180	Eroded
	10	0.765	25	12-HBA	0.3561	0.3529	0.0032	180	Eroded
			50	3-HBA	0.4503	0.4467	0.0036	180	Eroded
4	4.8	0.377	25	13-HBA	0.348	0.3538	0.0013	180	Eroded
			50	9-HBA	0.3551	0.3466	0.0014	180	Eroded
	6.0	0.411	25	14-HBA	0.4663	0.4636	0.0027	180	Eroded
			50	8-HBA	0.3551	0.3478	0.0032	180	Eroded
	10	0.608	25	15-HBA	0.4519	0.3523	0.0037	180	Eroded
			50	4-HBA	0.4512	0.4601	0.0041	180	Eroded
3	4.8	0.313	25	16-HBA	0.3561	0.3546	0.0015	180	Eroded
			50	7-HBA	0.3479	0.3462	0.0017	180	Eroded
	6.0	0.306	25	17-HBA	0.348	0.4606	0.0033	180	Eroded
			50	1-HBA	0.4639	0.3445	0.0035	180	Eroded
	10	0.353	25	18-HBA	0.356	0.448	0.0039	180	Eroded
			50	2-HBA	0.4642	0.4469	0.0043	180	Eroded

Appendix C 11: Vacuumed descaling results for solid soft samples

Number of nozzles	Injection pressure (MPa)	Mass flow rate (Kg/s)	Stand-off distance (mm)	Scale reference	Mass of scale before (kg)	Mass of scale after (Kg)	Mass of scale removed (Kg)	Descaling time (S)	Remark
5	4.8	0.434	25	10-HBA	0.466	0.3538	0.0011	180	Eroded
			50	6-HBA	0.3549	0.4647	0.0013	180	Eroded
	6.0	0.462	25	11-HBA	0.4523	0.3516	0.0024	180	Eroded
			50	5-HBA	0.354	0.4497	0.0026	180	Eroded
	10	0.765	25	12-HBA	0.3561	0.3529	0.0032	180	Eroded
			50	3-HBA	0.4503	0.4467	0.0036	180	Eroded
4	4.8	0.377	25	13-HBA	0.348	0.3538	0.0013	180	Eroded
			50	9-HBA	0.3551	0.3466	0.0014	180	Eroded
	6.0	0.411	25	14-HBA	0.4663	0.4636	0.0027	180	Eroded
			50	8-HBA	0.3551	0.3478	0.0032	180	Eroded
	10	0.608	25	15-HBA	0.4519	0.3523	0.0037	180	Eroded
			50	4-HBA	0.4512	0.4601	0.0041	180	Eroded
3	4.8	0.313	25	16-HBA	0.3561	0.3546	0.0015	180	Eroded
			50	7-HBA	0.3479	0.3462	0.0017	180	Eroded
	6.0	0.306	25	17-HBA	0.348	0.4606	0.0033	180	Eroded
			50	1-HBA	0.4639	0.3445	0.0035	180	Eroded
	10	0.353	25	18-HBA	0.356	0.448	0.0039	180	Eroded
			50	2-HBA	0.4642	0.4469	0.0043	180	Eroded

Appendix C 12: Compressed descaling result for SrSO<sub>4</sub> samples

Number of nozzles	Injection pressure (MPa)	Mass flow rate (Kg/s)	Stand-off distance (mm)	Scale reference	Mass of scale before (kg)	Mass of scale after (Kg)	Mass of scale removed (Kg)	Descaling time (S)	Remark
5	4.8	0.434	25	10-HBA	0.466	0.3538	0.0011	180	Eroded
			50	6-HBA	0.3549	0.4647	0.0013	180	Eroded
	6.0	0.462	25	11-HBA	0.4523	0.3516	0.0024	180	Eroded
			50	5-HBA	0.354	0.4497	0.0026	180	Eroded
	10	0.765	25	12-HBA	0.3561	0.3529	0.0032	180	Eroded
			50	3-HBA	0.4503	0.4467	0.0036	180	Eroded
4	4.8	0.377	25	13-HBA	0.348	0.3538	0.0013	180	Eroded
			50	9-HBA	0.3551	0.3466	0.0014	180	Eroded
	6.0	0.411	25	14-HBA	0.4663	0.4636	0.0027	180	Eroded
			50	8-HBA	0.3551	0.3478	0.0032	180	Eroded
	10	0.608	25	15-HBA	0.4519	0.3523	0.0037	180	Eroded
			50	4-HBA	0.4512	0.4601	0.0041	180	Eroded
3	4.8	0.313	25	16-HBA	0.3561	0.3546	0.0015	180	Eroded
			50	7-HBA	0.3479	0.3462	0.0017	180	Eroded
	6.0	0.306	25	17-HBA	0.348	0.4606	0.0033	180	Eroded
			50	1-HBA	0.4639	0.3445	0.0035	180	Eroded
	10	0.353	25	18-HBA	0.356	0.448	0.0039	180	Eroded
			50	2-HBA	0.4642	0.4469	0.0043	180	Eroded

Appendix C 13: Vacuumed descaling result for CaCO<sub>3</sub> samples

Number of nozzles	Injection pressure (MPa)	Mass flow rate (Kg/s)	Stand-off distance (mm)	Scale reference	Mass of scale before (kg)	Mass of scale after (Kg)	Mass of scale removed (Kg)	Descaling time (S)	Remark
5	4.8	0.434	25	10-HBA	0.466	0.3538	0.0011	180	Eroded
			50	6-HBA	0.3549	0.4647	0.0013	180	Eroded
	6.0	0.462	25	11-HBA	0.4523	0.3516	0.0024	180	Eroded
			50	5-HBA	0.354	0.4497	0.0026	180	Eroded
	10	0.765	25	12-HBA	0.3561	0.3529	0.0032	180	Eroded
			50	3-HBA	0.4503	0.4467	0.0036	180	Eroded
4	4.8	0.377	25	13-HBA	0.348	0.3538	0.0013	180	Eroded
			50	9-HBA	0.3551	0.3466	0.0014	180	Eroded
	6.0	0.411	25	14-HBA	0.4663	0.4636	0.0027	180	Eroded
			50	8-HBA	0.3551	0.3478	0.0032	180	Eroded
	10	0.608	25	15-HBA	0.4519	0.3523	0.0037	180	Eroded
			50	4-HBA	0.4512	0.4601	0.0041	180	Eroded
3	4.8	0.313	25	16-HBA	0.3561	0.3546	0.0015	180	Eroded
			50	7-HBA	0.3479	0.3462	0.0017	180	Eroded
	6.0	0.306	25	17-HBA	0.348	0.4606	0.0033	180	Eroded
			50	1-HBA	0.4639	0.3445	0.0035	180	Eroded
	10	0.353	25	18-HBA	0.356	0.448	0.0039	180	Eroded
			50	2-HBA	0.4642	0.4469	0.0043	180	Eroded

## APPENDIX D

Appendix D 1: Ambient descaling efficiency for soft and hard scale samples

Nozzles	Pressure (MPa)	stand-off distance (mm)	Mass of water utilise (Kg)	Hallow		Solid	
				Mass of scale removed (Kg)	Descaling Efficiency (%)	Mass of scale removed (Kg)	Descaling Efficiency (%)
5	4.8	25	52.089	0.0014	0.0027	0.0007	0.0013
		50	52.089	0.0014	0.0027	0.0011	0.0021
	6	25	55.436	0.0042	0.0076	0.0019	0.0034
		50	55.436	0.0022	0.0040	0.0021	0.0038
	10	25	91.811	0.0583	0.0635	0.013	0.0142
		50	91.811	0.0491	0.0535	0.0199	0.0217
4	4.8	25	45.224	0.0017	0.0038	0.0008	0.0018
		50	45.224	0.0016	0.0035	0.0012	0.0027
	6	25	49.33	0.0227	0.0460	0.0021	0.0043
		50	49.33	0.0118	0.0239	0.0023	0.0047
	10	25	72.903	0.0766	0.1051	0.0293	0.0402
		50	72.903	0.0703	0.0964	0.0464	0.0636
3	4.8	25	37.5	0.0659	0.1757	0.0009	0.0024
		50	37.5	0.0628	0.1675	0.0007	0.0013
	6	25	36.771	0.1337	0.3636	0.0011	0.0021
		50	36.771	0.1075	0.2923	0.0019	0.0034
	10	25	42.412	0.2538	0.5984	0.0021	0.0038
		50	42.412	0.216	0.5093	0.013	0.0142

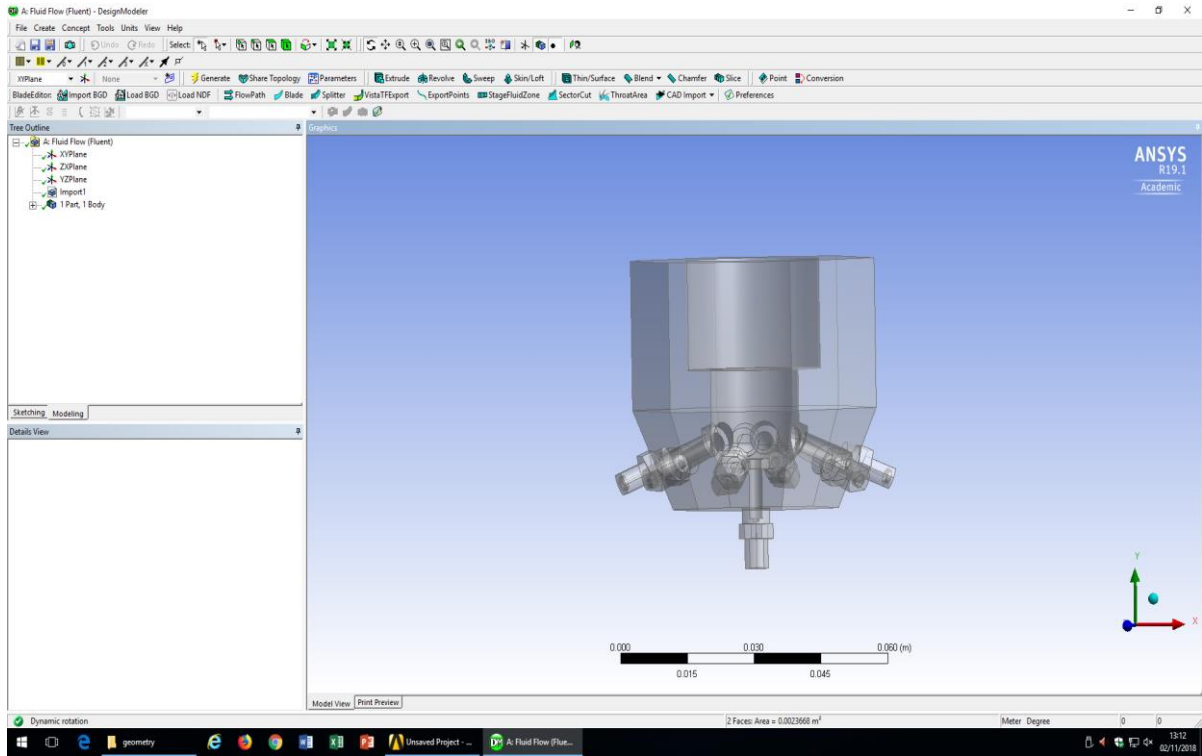
Appendix D 2: compressed descaling efficiency for soft and hard scale samples

Nozzles	Pressure (MPa)	stand-off distance (mm)	Mass of water utilise (Kg)	SrSO <sub>4</sub>		CaCO <sub>3</sub>	
				Mass of scale removed (Kg)	Descaling Efficiency (%)	Mass of scale removed (Kg)	Descaling Efficiency (%)
5	4.8	25	52.089	0.0007	0.0013	0.0004	0.0008
		50	52.089	0.0011	0.0021	0.0006	0.0012
	6	25	55.436	0.0019	0.0034	0.0008	0.0014
		50	55.436	0.0021	0.0038	0.001	0.0018
	10	25	91.811	0.013	0.0142	0.0011	0.0012
		50	91.811	0.0199	0.0217	0.0011	0.0012
4	4.8	25	45.224	0.0008	0.0018	0.0006	0.0013
		50	45.224	0.0012	0.0027	0.0007	0.0015
	6	25	49.33	0.0021	0.0043	0.001	0.0020
		50	49.33	0.0023	0.0047	0.0011	0.0022
	10	25	72.903	0.0293	0.0402	0.0023	0.0032
		50	72.903	0.0464	0.0636	0.0028	0.0038
3	4.8	25	37.5	0.0009	0.0024	0.0007	0.0019
		50	37.5	0.0013	0.0035	0.0009	0.0024
	6	25	36.771	0.0024	0.0065	0.0015	0.0041
		50	36.771	0.0028	0.0076	0.0018	0.0049
	10	25	42.412	0.0507	0.1195	0.0031	0.0073
		50	42.412	0.086	0.2028	0.0044	0.0104

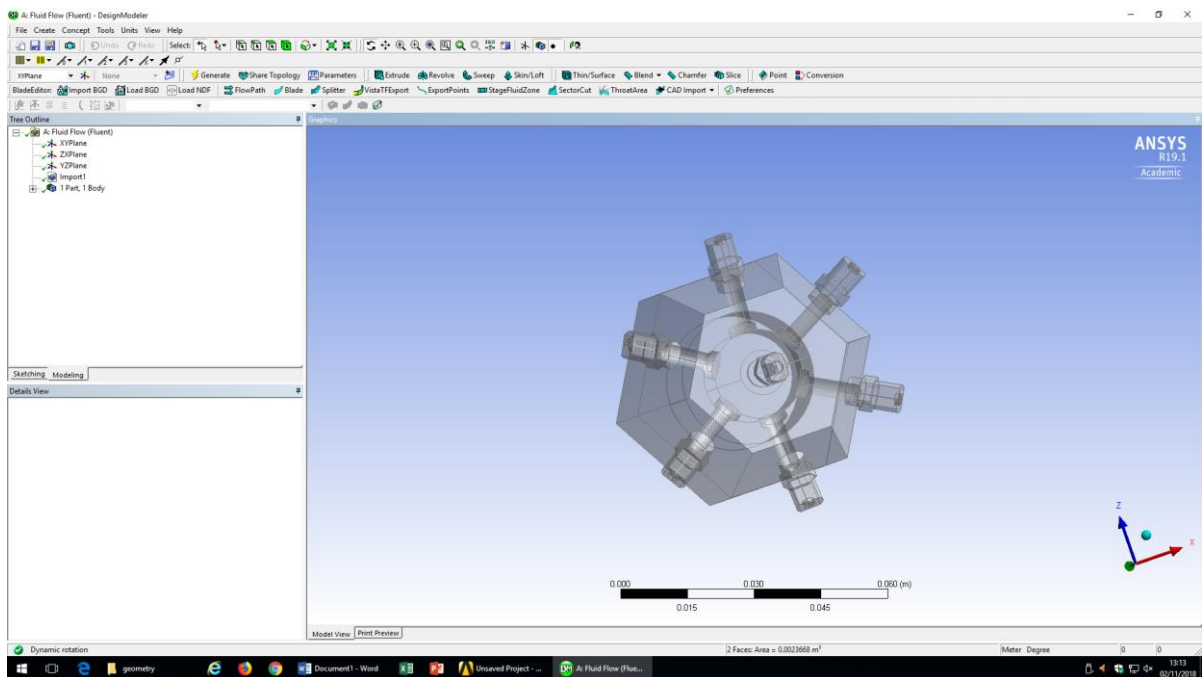
Appendix D 3: Vacuumed descaling efficiency for soft and hard scale samples

Nozzles	Pressure (MPa)	stand-off distance (mm)	Mass of water utilise (Kg)	Hollow		Solid	
				Mass of scale removed (Kg)	Descaling Efficiency (%)	Mass of scale removed (Kg)	Descaling Efficiency (%)
5	4.8	25	52.089	0.0051	0.0098	0.0012	0.0023
		50	52.089	0.0053	0.0102	0.0013	0.0025
	6	25	55.436	0.0056	0.0101	0.0023	0.0041
		50	55.436	0.0054	0.0097	0.0025	0.0045
	10	25	91.811	0.0663	0.0722	0.077	0.0839
		50	91.811	0.0584	0.0636	0.0819	0.0892
4	4.8	25	45.224	0.0276	0.0610	0.0013	0.0029
		50	45.224	0.0274	0.0606	0.0014	0.0031
	6	25	49.33	0.034	0.0689	0.0032	0.0065
		50	49.33	0.033	0.0669	0.0048	0.0097
	10	25	72.903	0.1364	0.1871	0.1018	0.1396
		50	72.903	0.1082	0.1484	0.1452	0.1992
3	4.8	25	37.5	0.0764	0.2037	0.0098	0.0261
		50	37.5	0.076	0.2027	0.012	0.0320
	6	25	36.771	0.1584	0.4308	0.058	0.1577
		50	36.771	0.0139	0.0378	0.097	0.2638
	10	25	42.412	0.2982	0.7031	0.1961	0.4624
		50	42.412	0.2282	0.5381	0.1999	0.4713

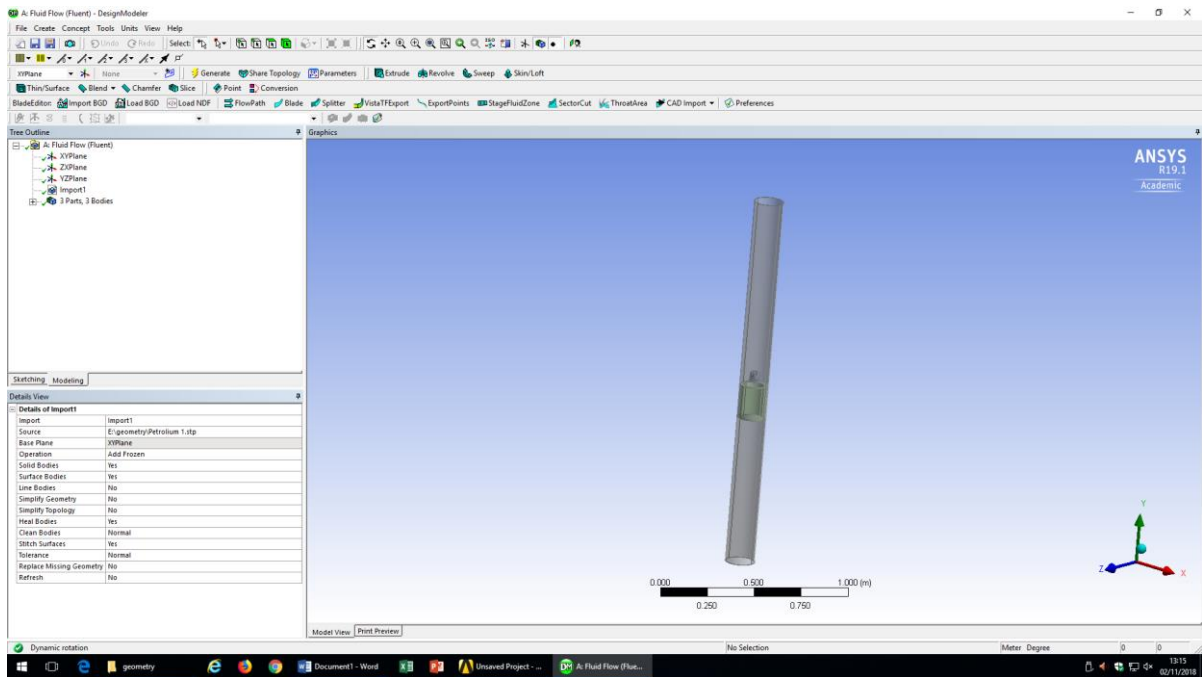
# APPENDIX E



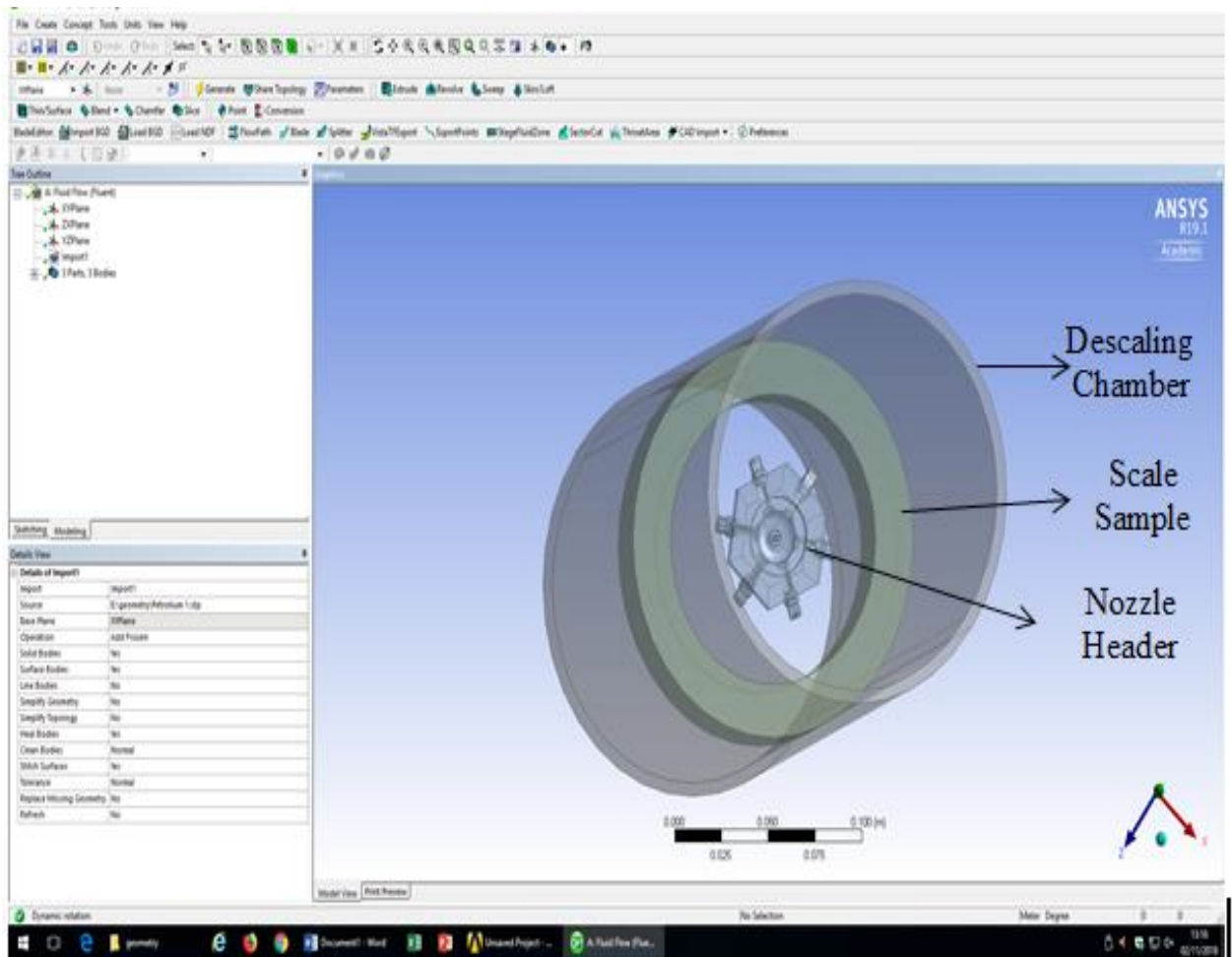
Appendix E 1: Side view of multiple nozzle header geometry



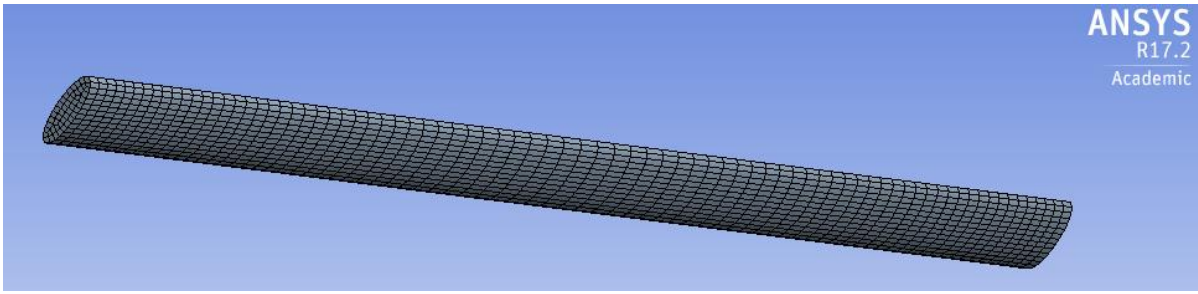
Appendix E 2: Arial view of multiple nozzle header



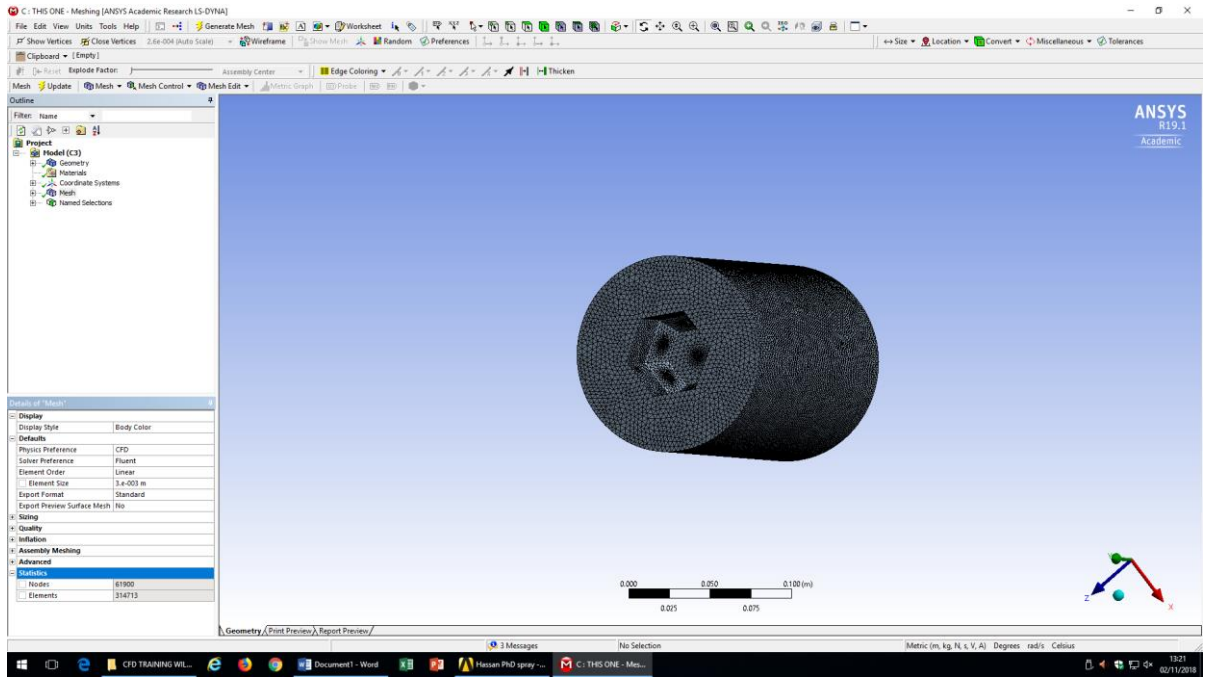
Appendix E 3: side view of the descaling rig



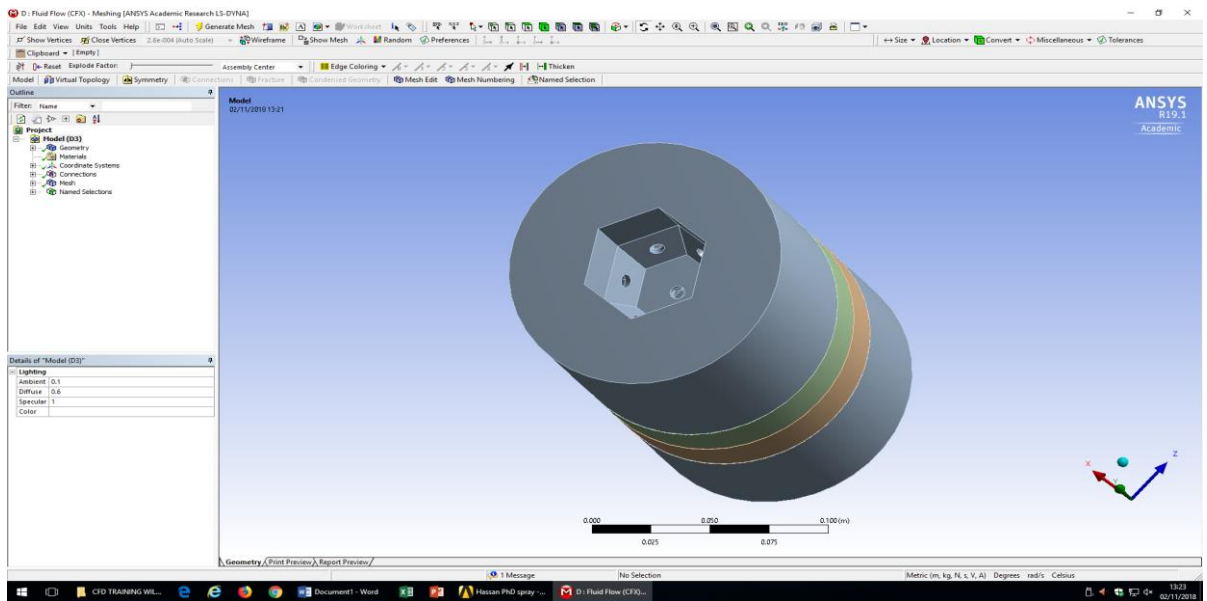
Appendix E 4: Arial view of the descaling rig



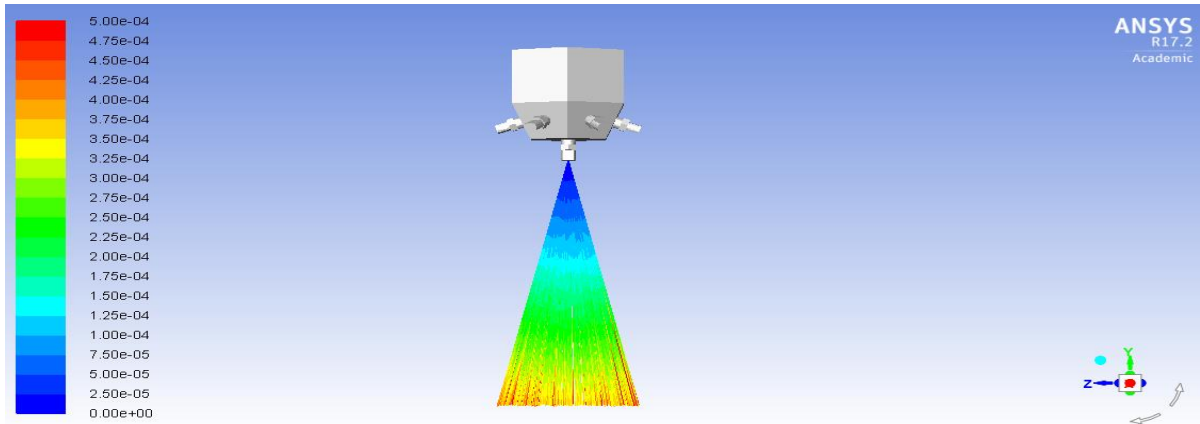
Appendix E 5: Meshed nozzle troughs CFD



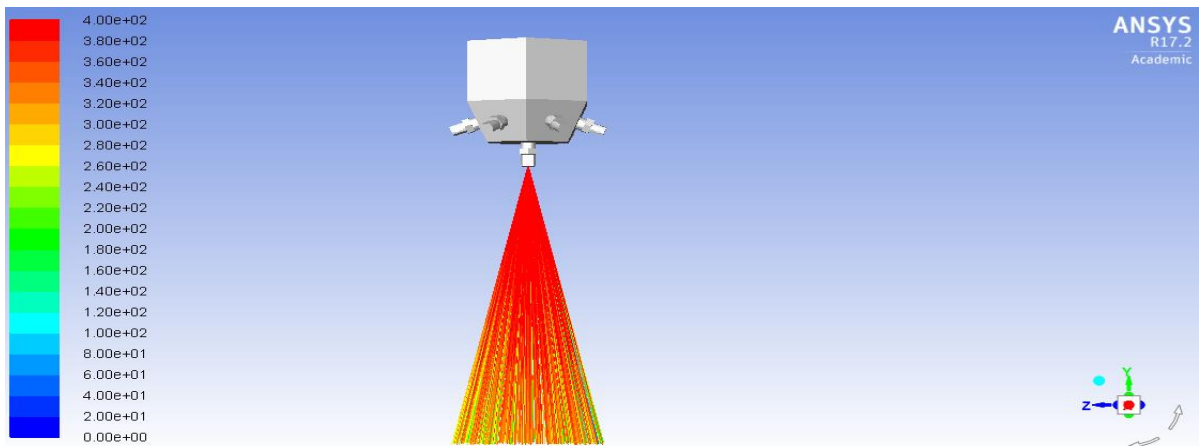
Appendix E 6: Meshed descaling rig



## Appendix E 7: descaling rig domain (stand-off distance)



## Appendix E 8: Particle residence time vector CFD



## Appendix E 9: Particle velocity CFD